



Ricerca di Sistema elettrico

## Dati Nucleari per la Sicurezza Reattore – PAR 2016: Attività di validazione librerie e code-package ANITA

M. Pescarini, R. Orsi, M. Frisoni

DATI NUCLEARI PER LA SICUREZZA REATTORE – PAR 2016: ATTIVITÀ DI VALIDAZIONE LIBRERIE E CODE-PACKAGE ANITA

M. Pescarini, R. Orsi, M. Frisoni (ENEA)

Settembre 2017

Report Ricerca di Sistema Elettrico

Accordo di Programma Ministero dello Sviluppo Economico - ENEA

Piano Annuale di Realizzazione 2016

Area: Generazione di energia elettrica con basse emissioni di carbonio

Progetto: Sviluppo competenze scientifiche nel campo della sicurezza nucleare e collaborazione ai programmi internazionali per il nucleare di IV generazione

Obiettivo: Progettazione di sistema e analisi di sicurezza

Responsabile del Progetto: Federico Rocchi, ENEA

Questo rapporto contiene i due seguenti Rapporti Tecnici ENEA:

- M. Pescarini, R. Orsi, Final Results of the BUGJEFF311.BOLIB Library Validation on the Iron-88 (Fe) Neutron Shielding Benchmark Experiment, ADPFISS-LP1-087
- M. Frisoni, ANITA-IEAF: an intermediate energy neutron activation system, ADPFISS-LP1-089

**Titolo**

## Final Results of the BUGJEFF311.BOLIB Library Validation on the Iron-88 (Fe) Neutron Shielding Benchmark Experiment

**Descrittori**

**Tipologia del documento:** Rapporto tecnico  
**Collocazione contrattuale:** Accordo di programma ENEA-MSE su sicurezza nucleare e reattori di IV generazione  
**Argomenti trattati:** Fisica nucleare, dati nucleari, fisica dei reattori nucleari

**Sommario**


Final results concerning the ENEA-Bologna BUGJEFF311.BOLIB working cross section library validation on the Iron-88 single material (iron) integral neutron shielding benchmark experiment are presented. The BUGJEFF311.BOLIB library is specifically dedicated to LWR shielding and pressure vessel dosimetry applications. It is a broad-group coupled (47 n + 20  $\gamma$ ) working library in FIDO-ANISN format, based on the OECD-NEADB JEFF-3.1.1 evaluated nuclear data library and with the same group structure as the ORNL BUGLE-96 similar library. The analysis of the Iron-88 Winfrith benchmark experiment was performed through 3D transport calculations in Cartesian geometry using the ORNL TORT-3.2 discrete ordinates ( $S_N$ ) code together with the BUGJEFF311.BOLIB library and the BUGLE-96 library as term of comparison. The activation cross sections for the Au-198(n, $\gamma$ )Au-198 dosimeters and the threshold activation cross sections for the Rh-103(n,n')Rh-103m, In-115(n,n')In-115m, S-32(n,p)P-32 and Al-27(n, $\alpha$ )Na-24 dosimeters were derived from the IAEA IRDF-2002 reactor dosimetry file.

**Note**

Authors: Massimo PESCARINI, Roberto ORSI

**Copia n.**
**In carico a:**

2			NOME			
			FIRMA			
1			NOME			
			FIRMA			
0	EMISSIONE	08/11/2017	NOME	M. Pescarini	F. Padoani	F. Rocchi
			FIRMA			
REV.	DESCRIZIONE	DATA	REDAZIONE	CONVALIDA	APPROVAZIONE	

 <b>Ricerca Sistema Elettrico</b>	<b>Sigla di identificazione</b>	<b>Rev.</b>	<b>Distrib.</b>	<b>Pag.</b>	<b>di</b>
	ADPFISS-LP1-087	0	L	2	92

## INDEX

1 - INTRODUCTION	p. 3
2 - THE IRON-88 NEUTRON SHIELDING BENCHMARK EXPERIMENT	p. 3
2.1 - The ASPIS Shielding Facility	p. 3
2.2 - The Iron-88 Benchmark Experimental Array	p. 4
2.3 - Activation Dosimeter Measurements	p. 9
2.4 - Source Description	p. 12
3 - TRANSPORT CALCULATIONS	p. 19
3.1 - The BUGJEFF311.BOLIB Library	p. 19
3.2 - Transport Calculation General Features	p. 24
3.2.1 - Activation Dosimeter Cross Sections	p. 30
3.2.2 - Neutron Source Normalization	p. 50
3.3 - Discussion of the Final Results	p. 51
4 - CONCLUSION	p. 88
REFERENCES	p. 90

# Final Results of the BUGJEFF311.BOLIB Library Validation on the Iron-88 (Fe) Neutron Shielding Benchmark Experiment

Massimo PESCARINI, Roberto ORSI

November 2017

## 1 - INTRODUCTION

The ENEA-Bologna Nuclear Data Group completed further validation of the ENEA-Bologna BUGJEFF311.BOLIB /1/ working cross section library for LWR shielding and pressure vessel dosimetry applications on the Iron-88 /2/ single material (iron) neutron shielding benchmark experiment (Winfrith, 1988, UK). Iron-88 is in particular included in the SINBAD REACTOR /3/ /4/ database of neutron shielding benchmark experiments, dedicated to nuclear fission reactors. The analysis of the Iron-88 benchmark experiment was performed through three-dimensional (3D) transport calculations using the ORNL TORT-3.2 /5/ discrete ordinates ( $S_N$ ) transport code and the BUGJEFF311.BOLIB library. The activation dosimeter cross sections for  $Au-198(n,\gamma)Au-198$  and the threshold activation cross sections for the  $Rh-103(n,n')Rh-103m$ ,  $In-115(n,n')In-115m$ ,  $S-32(n,p)P-32$  and  $Al-27(n,\alpha)Na-24$  dosimeters were derived from the IAEA IRDF-2002 /6/ reactor dosimetry file.

BUGJEFF311.BOLIB is in particular a broad-group coupled neutron/photon ( $47 n + 20 \gamma$ ) working cross section library in FIDO-ANISN /7/ format, based on the OECD-NEA Data Bank JEFF-3.1.1 /8/ (see also /9/) evaluated nuclear data library. It is characterized by the same group structure as the ORNL BUGLE-96 /10/ similar library, specifically recommended by the American National Standard /11/ of the American Nuclear Society “Neutron and Gamma-Ray Cross Sections for Nuclear Radiation Protection Calculations for Nuclear Power Plants” (ANSI/ANS-6.1.2-1999, R2009) for LWR shielding and radiation damage applications. A final comparison of the calculated and experimental reaction rates for the cited activation dosimeters used in the Iron-88 experiment is presented in this work while the preliminary results were already reported in reference /12/.

## 2 - THE IRON-88 NEUTRON SHIELDING BENCHMARK EXPERIMENT

The ASPIS shielding facility of the Winfrith NESTOR reactor, the Iron-88 benchmark experimental array, the activation dosimeter measurements and the fission plate neutron source are described, taking the relative information integrally from reference /2/ and from the document of the Iron-88 section of SINBAD REACTOR /3/, entitled “General Description of the Experiment”.

### 2.1 The ASPIS Shielding Facility

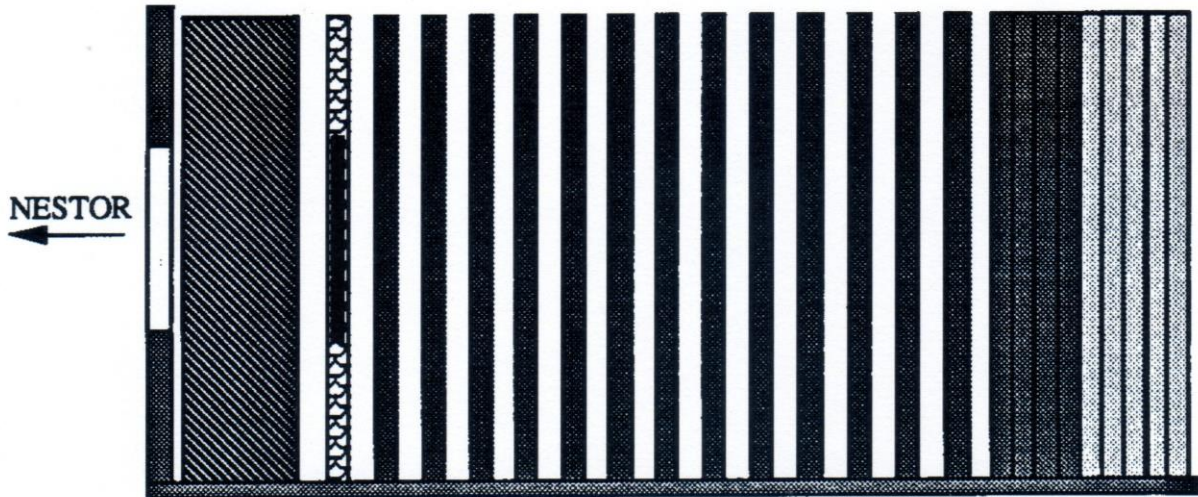
The ASPIS shielding facility was installed on the NESTOR reactor (presently dismantled) at Winfrith. NESTOR was a light water cooled, graphite and light water moderated reactor which operated at powers of up to 30 kW and was used as a source of neutrons for a wide

range of applications. The core of the reactor, which comprised 26 MTR (Materials Test Reactor) type fuel elements, was contained within an annulus formed by two concentric aluminium vessels through which water circulated. The inner vessel was filled with graphite to form an inner reflector. The outer tank was surrounded by an external graphite reflector in the form of a block having dimensions 182 cm × 182 cm × 122 cm which contained the control plate slots adjacent to the vessel wall. Leading off each of the four faces of the external reflector was an experiment cave which could be isolated from the reactor by shutters composed of boral or combinations of neutron/gamma-ray shield materials. ASPIS was located in the NESTOR cave C. Shield components, which were in the main slabs or tanks, were mounted vertically in a mobile tank which had an internal cross-sectional area of 1.8 m × 1.9 m and a length of 3.7 m. A fission plate was located within the experimental shield array. The loaded tank was moved into the cave where thermal neutrons leaking from the outer graphite reflector of NESTOR were used to drive the fission plate to provide a well defined neutron source for penetration measurements. The neutron flux levels within an ASPIS shield contained contributions from sources in the fission plate and from the NESTOR core and it was essential that the NESTOR contribution was subtracted from all measured responses to arrive at the response resulting from the fission plate sources.

## 2.2 - The Iron-88 Benchmark Experimental Array

The Iron-88 benchmark experimental array, irradiated in the ASPIS shielding facility, is shown schematically in side elevation in Figure 1. The array comprised three regions; the source region containing moderator and the fission plate, the shield made from 13 mild steel plates, each of approximately 5.1 cm thickness, and a deep backing shield manufactured from mild and stainless steel. To allow dosimeter access within the shield, 6 mm spacers were placed between each slab component. In practice the depth of the air gaps varied owing to positional uncertainties of the plates and their flatness. The 6 mm gap was therefore nominal and an average gap of 7.4 mm was measured for the experiment. The axial dimensions of the experimental components are given in Table 1. The outer boundaries of the experimental region were formed by the walls and floor of the ASPIS trolley and by the roof of the ASPIS cave. The floor and walls of the trolley were manufactured from 1.91 cm thick mild steel plate. The trolley base had a 25 cm high steel chassis in-filled with concrete. The structure of NESTOR surrounding the trolley comprised concrete bulk shielding blocks except on the NESTOR core side of the trolley front face where it was graphite. This graphite extended away from the trolley to the external graphite reflector of the reactor. Table 2 gives the compositions of the materials used in the experiment.

**Figure 1** Schematic side elevation of the shield in the iron 88 single material benchmark experiment



**KEY**

- Fuel
- Mild Steel
- Stainless Steel
- Fission Plate
- Graphite
- Aluminium


All components are 182.9cm wide by 191.0cm high

Not To Scale



**Table 1**
**Shield Dimensions of the Iron-88 Single Material Benchmark Experiment.**

Component	Mat.Thickness (cm)	Coordinate at End of Region (cm)	Mat. Reference Number
Trolley Face	3.18	-16.62	1 & 2
Void	0.52	-16.10	-
Graphite	15.00	-1.10	3
Void	1.10	0.00	-
Fission Plate	2.90	2.90	4 & 5
Void	0.74	3.64	-
Mild Steel	5.10	8.74	6
Void	0.74	9.48	-
Mild Steel	5.12	14.60	6
Void	0.74	15.34	-
Mild Steel	5.12	20.46	6
Void	0.74	21.20	-
Mild Steel	5.10	26.30	6
Void	0.74	27.04	-
Mild Steel	5.20	32.24	6
Void	0.74	32.98	-
Mild Steel	5.15	38.13	6
Void	0.74	38.87	-
Mild Steel	5.20	44.07	6
Void	0.74	44.81	-
Mild Steel	5.20	50.01	6
Void	0.74	50.75	-
Mild Steel	5.25	56.00	6
Void	0.74	56.74	-
Mild Steel	5.18	61.92	6
Void	0.74	62.66	-
Mild Steel	5.07	67.73	6
Void	0.74	68.47	-
Mild Steel	5.12	73.59	6
Void	0.74	74.33	-
Mild Steel	5.18	79.51	6
Void	0.74	80.25	-
Mild Steel	5.10	85.35	6
Mild Steel	5.25	90.60	6
Mild Steel	5.00	95.60	6
Mild Steel	4.67	100.27	6
Stainless Steel	22.41	122.68	7
Concrete	100.00	222.68	8

 <b>Ricerca Sistema Elettrico</b>	<b>Sigla di identificazione</b>	<b>Rev.</b>	<b>Distrib.</b>	<b>Pag.</b>	<b>di</b>
	ADPFISS-LP1-087	0	L	7	92

#### Notes

1. For material compositions see Table 2.
2. The trolley face is manufactured from mild steel with a central aluminium 'window' of radius 56.1 cm.
3. The construction of the fission plate is shown in Figure 5.
4. All slab components are 182.9 cm wide by 191.0 cm high and fill the full width and height of the ASPIS trolley.

**Table 2**
**Material Compositions in the Iron-88 Single Material Benchmark Experiment.**

Material	Material Ref. No.	Density (g/cm <sup>3</sup> )	Element	Weight Fraction
Mild Steel	1	7.835	Fe	0.9865
			Mn	0.0109
			C	0.0022
			Si	0.0004
Aluminium	2	2.700	Al	1.0000
Graphite	3	1.650	C	1.0000
Fuel	4	3.256	Al	0.7998
			U-235	0.1864
			U-238	0.0138
Aluminium	5	2.666	Fe	0.0056
			Si	0.0015
			Al	0.9929
Mild Steel	6	7.850	Fe	0.9903
			Mn	0.0074
			C	0.0023
Stainless Steel	7	7.917	Fe	0.6695
			Mn	0.0157
			Cr	0.1677
			Ni	0.1166
			C	0.0006
			Si	0.0050
			P	0.0003
			S	0.0002
			Mo	0.0244
Concrete	8	2.242	Fe	0.0141
			Si	0.3369
			Al	0.0340
			H	0.0100
			O	0.5290
			Ca	0.0379
			K	0.0200
			Na	0.0161

### 2.3 - Activation Dosimeter Measurements

The neutron distribution through the experimental shield was mapped using activation foils attached to thin aluminium carriers (0.5 mm thick by 9 cm wide) located between the slab components. The dosimeter set comprised activation foils to measure the epi-cadmium  $Au-197(n,\gamma)Au-198$  reaction rates and the  $S-32(n,p)P-32$ ,  $In-115(n,n')In-115m$ ,  $Rh-103(n,n')Rh-103m$  and  $Al-27(n,\alpha)Na-24$  threshold reaction rates. In particular the epi-cadmium activation reaction rate measurements were performed using cylindrical gold foils with a diameter of 12.7 mm, a thickness of 0.05 mm, a typical mass of 0.12 g - 0.13 g and a cadmium cover thickness of 50/1000 inches, equivalent to 1.27 mm. Penetration measurements were made along the nuclear centre line, which was the horizontal axis of the system passing through the centre of the fission plate. Lateral distributions were also measured at various positions in the shields, the foils being located at intervals of 25 cm up and down from the nuclear centre line. The labelling convention for the measurement locations is given in Figure 2.

A fraction of the neutrons present in the experimental array originated from leakage from the NESTOR core. To obtain a true comparison between measurement and a calculation using the fission plate source, the NESTOR core component must be subtracted from the measurement. There are two methods by which the background component can be estimated.

The best method is to repeat the measurement with the fissile content of the fission plate removed, i.e. an unfuelled measurement. This is a time consuming method as measurements have to be made twice at every point, once with the fuel and once without. The combination of low fluxes and low sensitivities of integral dosimeters can make foreground fuelled measurements difficult at deep penetration with the result that unfuelled measurements become impossible.

Background corrections of acceptable accuracy can be made for the high energy threshold reactions by a second method using the hydrogen filled proportional counters of the TNS system /13/ in integral mode. Here measurements of the neutron count-rates in the shield with the ASPIS shutter open and closed are required together with a measure of the shut-down ratio of the fission plate when the neutron shutter is closed. This technique was used for determining the background correction for the proportional counters; the correction was found to be around 2% throughout the shield and a value of 2% is recommended for the four threshold activation dosimeters at all positions in the shield.

The unfuelled technique for background correction was adopted for the gold measurements as there was a significant component of the low energy flux which did not arise from the fission plate particularly near the fission plate itself where the fuelled to unfuelled ratio could be as low as 3.

The reaction effective threshold energies for the  $Rh-103(n,n')$ ,  $In-115(n,n')$ ,  $S-32(n,p)$  and  $Al-27(n,\alpha)$  dosimeters, in a U-235 fission neutron spectrum similar to that of the Iron-88 experiment, are respectively 0.69 MeV, 1.30 MeV, 2.8 MeV and 7.30 MeV (see /14/). Nevertheless, since the effective threshold energy is not a completely satisfactory parameter for the characterization of the energy dependent cross section functions, the reported values give only a rough indication of the start of the response for the specific dosimeter.

If one wishes to characterize the dosimeter response energy range more accurately, the energy range corresponding to 90% of the response and the median energy of the response should be taken into account. The median energy is defined such that, in the specific spectrum, the responses below and above this energy numerical value are equal. Secondly, the definition of the energy range corresponding to 90% of the total response of a dosimeter implies that 5% of the response is below the lower boundary and 5% above the upper boundary of this energy range. A synthesis of these data for the four dosimeters used in the Iron-88 experiment was taken from reference /14/ and it is reported in Table 3 to give more specific detailed information addressed to obtain a more precise analysis in the comparison of the experimental and calculated dosimetric results.

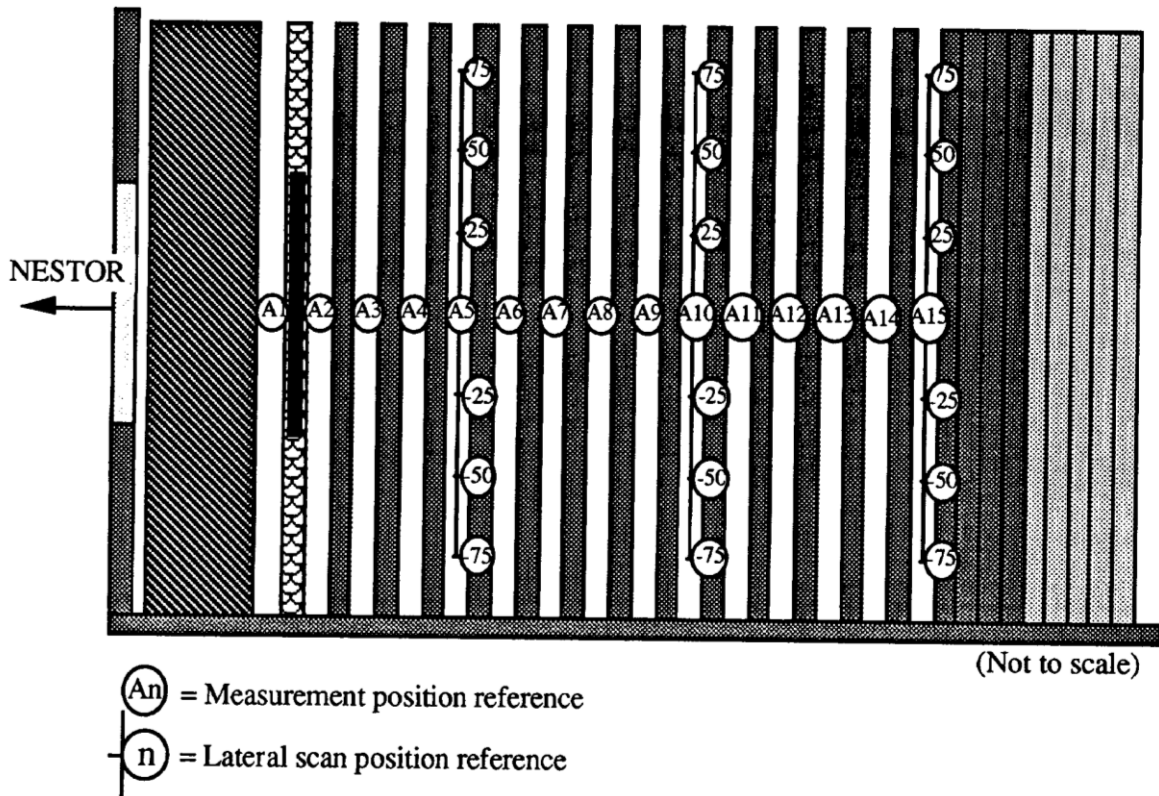
In practice the experimental results coming from Rh-103(n,n') and In-115(n,n') (see /15/) correspond to neutron fluxes above about 1.0 MeV and the experimental results from S-32(n,p) with neutron fluxes above about 3.0 MeV.

Table 3

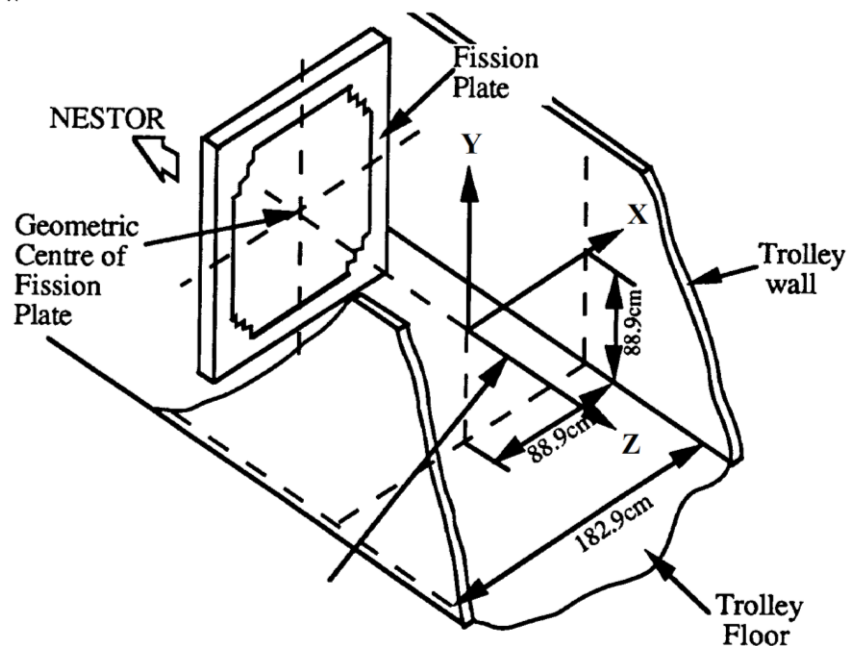
Iron-88 - Threshold Activation Dosimeter Parameters in a U-235 Fission Neutron Spectrum.

Dosimeter	Effective Threshold Energy [MeV]	90% Response Energy Range [MeV]	Median Energy [MeV]
Rh-103(n,n')	0.69	0.72 - 5.8	2.3
In-115(n,n')	1.30	1.1 - 5.9	2.6
S-32(n,p)	2.80	2.3 - 7.3	4.0
Al-27(n, $\alpha$ )	7.30	6.4 - 12.0	8.6

Figure 2 Measurement locations for the iron 88 single material benchmark experiment



Penetration measurements are located on the nuclear centre line as defined below



## 2.4 - Source Description

A schematic diagram of the fission plate is shown in Figure 3. It comprises an aluminium frame which fills the height and width of the ASPIS trolley. Located within the frame are 13 separate fuel elements. A schematic view of an individual fuel element is shown in Figure 4. Each element has two 12 mm thick aluminium cover plates which attach on either side of the top and bottom locating end pieces leaving a 5 mm separation in which U/Al alloy fuel strips are located. The fuel strips are 80% by weight aluminium and 20% by weight of uranium enriched to 93% having a density of 3.256 g/cm<sup>3</sup>. Each strip is nominally 30.5 mm wide and 1 mm thick and is fixed to the rear cover plate by M5 screws.

Three columns of fuel strips laid side by side fill the width of the element. There is depth for 4 fuel strips within each element leaving a 1 mm clearance gap next to the front cover plate. In the current configuration only the central two strips in each column contain U/Al alloy, the outer two are both blanks manufactured from aluminium. To approximate to a disc fission neutron source the axial fuel loading within each element has been arranged to the specification shown in Figure 5 by the substitution of aluminium blanks for fuel where necessary giving 4 mm of aluminium in the unfuelled regions.

The position of the fission plate is shown in Figure 2. The centre of the fuel is at a height of 889 mm from the floor of the trolley and at 889 mm from the right hand wall of the trolley when looking towards the NESTOR core. The measurements were made on this Z horizontal nuclear axis passing through the centre of the fission plate.

The approach taken to obtain the absolute power distribution within the fission plate is summarised as follows:

1. Mn-55(n, $\gamma$ )Mn-56 reaction-rates are measured over the front surface of the fission plate to define a thermal flux profile in X and Y.
2. The distribution of the U-235 content within the fuel is assessed.
3. 1. and 2. are combined to provide a relative fission-rate profile in X and Y.
4. The relative fission profile in the Z direction through the fuel is obtained from absolute measurements of fission-rate in the plate as described below.
5. The fission-rate profile is normalised to absolute measurements of the fission-rate per NESTOR Watt in the plate which are made by counting fission product decay rates in samples taken from the central strip of the central element at the centre, bottom and halfway between the centre and bottom of the fuel.
6. The neutron source distribution is obtained from the absolute fission-rate distribution.

The manganese reaction-rate measurements on the front face of the plate were input to the CRISP code /16/ to define the manganese reaction-rate surface covering the plate. From this surface the average manganese reaction-rate within the elements of any source mesh overlaid onto the fission plate can be defined. The fission-rate profile in X and Y is taken as the

manganese reaction-rate profile on the front face of the fuel plate. This has been normalised to give a plate power of 1 Watt and the resulting neutron source distribution is shown in Table 4. Constants of  $3.121\text{E}+10$  fissions per Watt and 2.437 neutrons per fission have been used in this derivation.

The absolute fission rate in the fuel was found to be between 5% and 16% higher in the strip nearer to NESTOR. This difference is caused by the attenuation of thermal neutrons from NESTOR through the 1 mm fuel strips. However, the attenuation of the neutrons produced by fission is small over this distance so an assumption of no Z dependence in the source strength has been made.

The absolute power in the fission plate, expressed as plate Watts per NESTOR Watt, has been determined by combining measurements of the absolute fission-rate at spot values, gained by fission product decay line counting, with the fission-rate profile data derived in CRISP. The analysis is rather involved and the result was an absolute plate power of  $5.68\text{E}-04$  Watts per NESTOR Watt. The uncertainty on the plate power is 8% at the two standard deviations ( $2\sigma$ ) level.



Table 4

## Source Distribution on the Fission Plate.

0	0	0	0	0	0	2.973	2.994	2.865	0	0	0	0	0	0
0	0	0	0	0	3.173	3.496	3.537	3.404	2.975	0	0	0	0	0
0	0	0	0	3.176	3.711	4.088	4.149	4.015	3.529	2.890	0	0	0	0
0	0	0	3.186	3.500	4.092	4.514	4.587	4.446	3.925	3.240	2.886	0	0	0
0	0	3.249	3.635	3.999	4.696	5.197	5.286	5.130	4.555	3.807	3.422	3.009	0	0
0	3.150	3.575	4.003	4.412	5.202	5.770	5.870	5.699	5.080	4.282	3.873	3.431	2.970	0
3.040	3.322	3.769	4.223	4.660	5.505	6.110	6.215	6.034	5.387	4.559	4.133	3.673	3.188	2.850
3.132	3.427	3.893	4.364	4.815	5.684	6.304	6.412	6.227	5.563	4.710	4.270	3.792	3.287	2.932
3.026	3.325	3.784	4.239	4.669	5.491	6.079	6.183	6.009	5.364	4.523	4.084	3.607	3.103	2.751
0	3.136	3.574	4.001	4.400	5.157	5.701	5.802	5.643	5.031	4.221	3.795	3.331	2.843	0
0	0	3.182	3.562	3.912	4.572	5.053	5.149	5.013	4.461	3.713	3.317	2.887	0	0
0	0	0	3.004	3.299	3.855	4.267	4.357	4.247	3.766	3.101	2.748	0	0	0
0	0	0	0	2.896	3.396	3.770	3.855	3.758	3.320	2.712	0	0	0	0
0	0	0	0	0	2.745	3.072	3.150	3.067	2.685	0	0	0	0	0
0	0	0	0	0	0	2.458	2.525	2.448	0	0	0	0	0	0

Units are neutrons  $\times \text{cm}^{-3} \times \text{second}^{-1} \times 1.0\text{E}+07$ .  
 The plate power for this distribution is 1 Watt.

Coordinate boundaries for source distribution.  
 Units are cm.

X	-52.25	-49.08	-45.92	-39.58	-36.42	-30.08	-14.25	-4.75
	4.75	14.25	30.08	36.42	39.58	45.92	49.08	52.25
Y	-51.44	-47.63	-40.64	-35.56	-31.75	-19.69	-15.88	-5.29
	5.29	15.88	19.69	31.75	35.56	40.64	47.63	51.44

Figure 3 Schematic diagram of fission plate

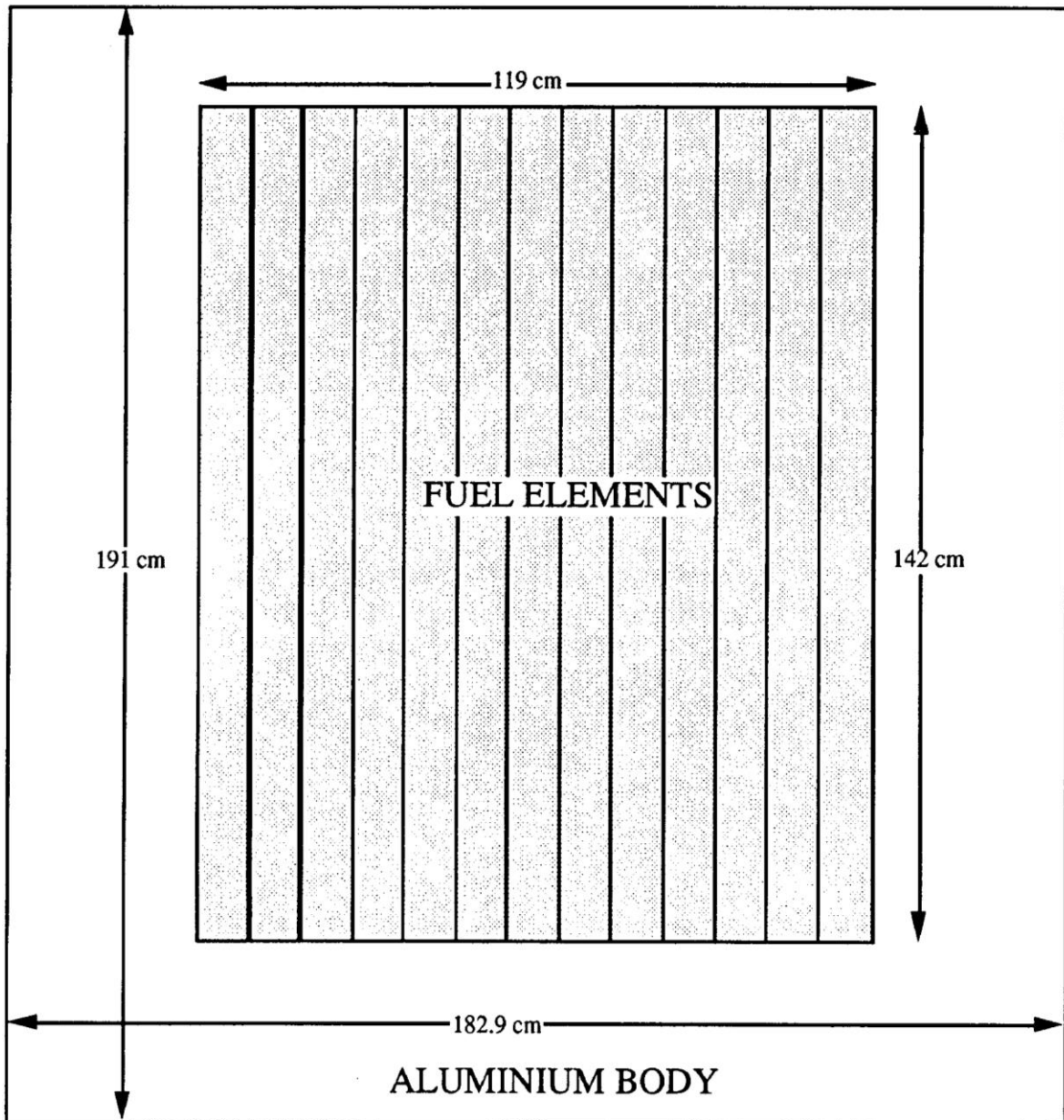


**Figure 4** Diagram of fuel element

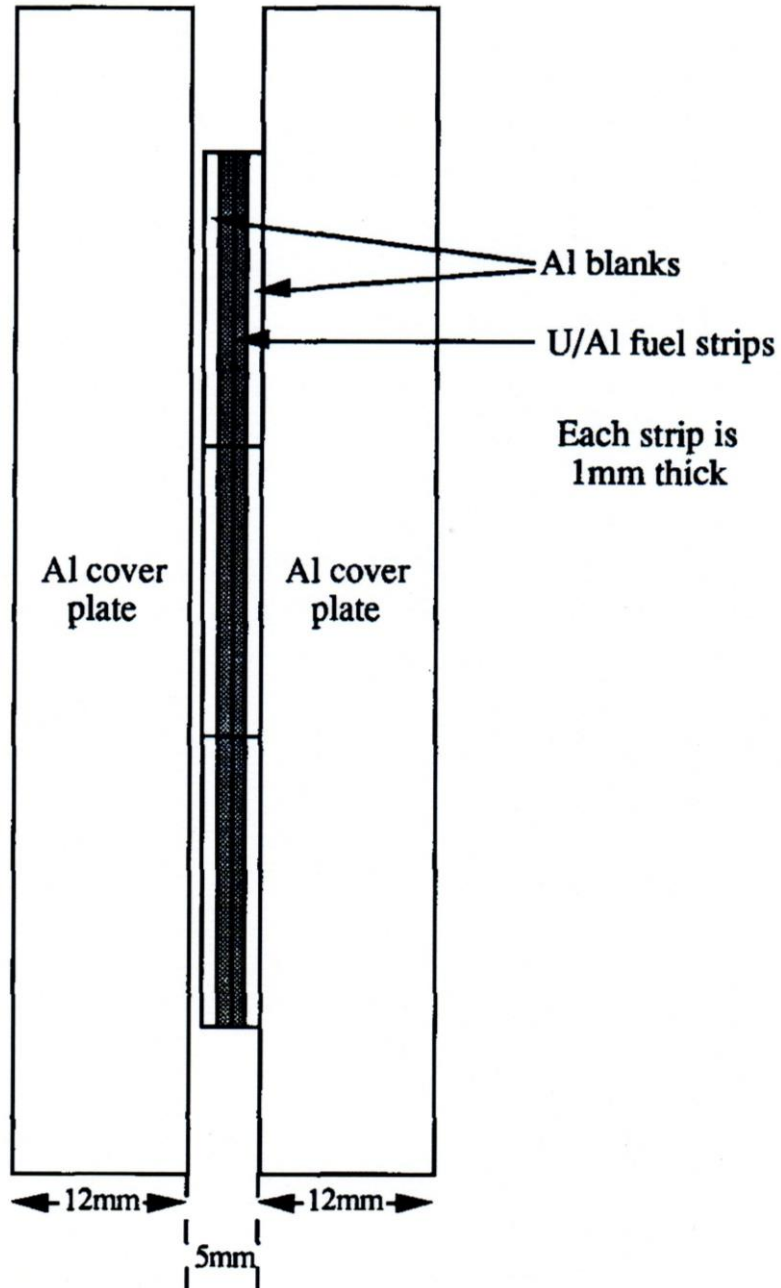


Figure 5 Disposition of fuel in fission plate

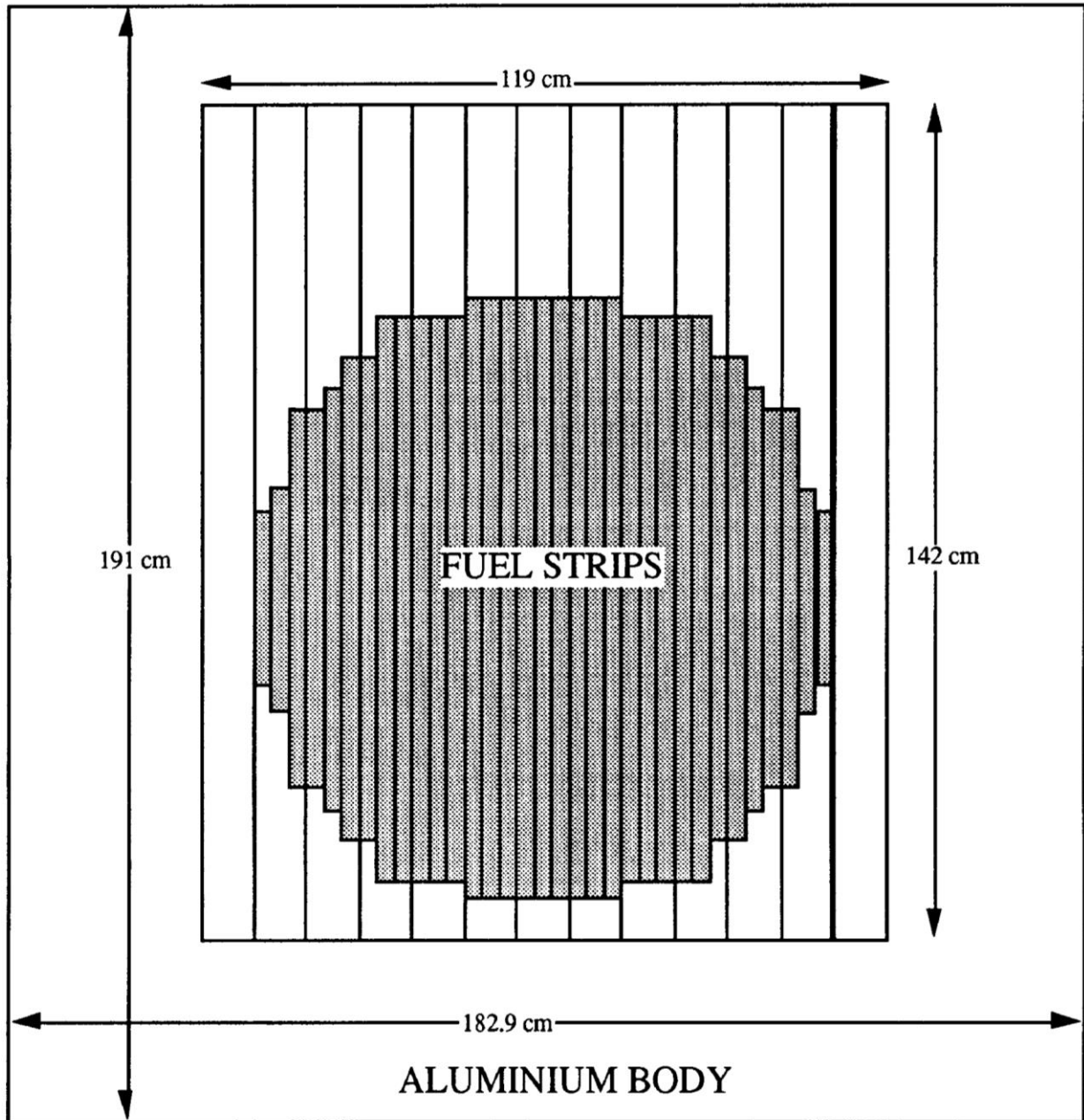


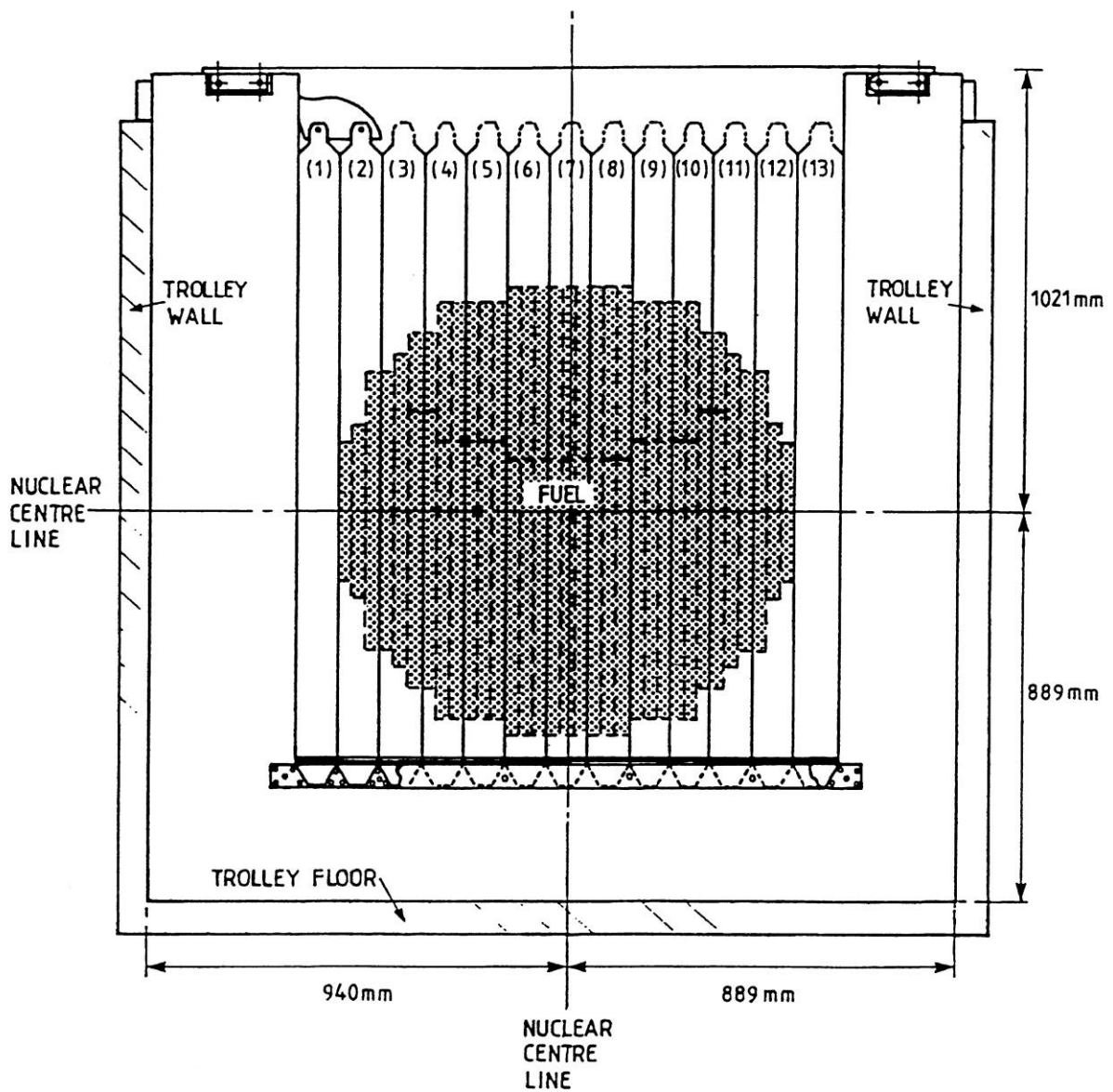
Figure 6

Section Normal to the Z Horizontal Axis at the Fission Plate Centre.

Position of the Fission Plate with respect to the ASPIS Trolley.

THE FISSION PLATE

Details of the fuel loading pattern when viewed looking towards the NESTOR core



### 3.0 - TRANSPORT CALCULATIONS

#### 3.1 - The BUGJEFF311.BOLIB Library

The ENEA-Bologna BUGJEFF311.BOLIB /1/ is a broad-group coupled neutron/photon working cross section library in FIDO-ANISN /7/ format with parameterized cross section sets of problem-dependent self-shielded neutron cross sections, dedicated to the previously cited LWR radiation shielding and radiation damage applications and, in particular, to the reactor pressure vessel (RPV) dosimetry analyses. The BUGJEFF311.BOLIB library adopts (see Tables 5 and 6) the neutron and photon energy group structures (47 neutron groups + 20 photon groups) of the similar ORNL BUGLE-96 /10/ broad-group working library in FIDO-ANISN format, specifically conceived for the same previously cited applications in LWRs. BUGLE-96 was derived in particular from the ORNL VITAMIN-B6 /10/ library in AMPX format, based on the ENDF/B-VI.3 /17/ evaluated data library. It is underlined that BUGJEFF311.BOLIB is the first BUGLE-type multi-group working library, based on OECD-NEADB JEFF nuclear data, freely released by OECD-NEADB and ORNL-RSICC at international level.

BUGJEFF311.BOLIB was obtained through problem-dependent cross section collapsing from the ENEA-Bologna VITJEFF311.BOLIB /18/ fine-group coupled neutron/photon cross section library for nuclear fission applications, based on the JEFF-3.1.1 /8/ (see also /9/) evaluated nuclear data library and on the Bondarenko /19/ (f-factor) method for the treatment of neutron resonance self-shielding and temperature effects. The VITJEFF311.BOLIB library is a “pseudo-problem-independent” library in AMPX format, i.e., a fine-group library prepared with enough detail in energy, temperatures and neutron resonance self-shielding so as to be applicable to a wide range of physical systems. VITJEFF311.BOLIB is characterized in particular by the same neutron and photon energy group structures (199 neutron groups + 42 photon groups) as VITAMIN-B6.

Concerning the BUGJEFF311.BOLIB library validation on integral neutron shielding benchmark experiments, a limited preliminary testing was successfully performed with the 3D TORT-3.2 discrete ordinates transport code on the PCA-Replica 12/13 /20/ /21/ (Winfrith, UK) and VENUS-3 /22/ (Mol, Belgium) engineering neutron shielding benchmark integral experiments, whose compositional and geometrical specifications were taken from the fission reactor shielding section of the ORNL-RSICC/OECD-NEADB SINBAD REACTOR /3/ international database of shielding benchmark experiments.

The two cited engineering integral neutron shielding benchmark experiments are specifically dedicated to test the accuracy of nuclear data and transport codes employed, in particular, in the PWR shielding and pressure vessel dosimetry.

The PCA-Replica 12/13 low-flux engineering neutron shielding benchmark experiment is a water/iron benchmark experiment including PWR thermal shield and pressure vessel simulators. The source of neutrons was a thin fission plate of highly enriched uranium (93.0 w% in U-235), irradiated by the NESTOR low-power experimental reactor through a graphite thermal column (total thickness 43.91 cm). Beyond the fission plate, the PCA-Replica shielding array (12/13 experimental configuration with two water gaps of about 12 cm and 13 cm) was arranged in a large parallelepiped steel tank filled with water. After a first water gap (12.1 cm), there was the stainless steel thermal shield simulator (5.9 cm), the second water

gap (12.7 cm), the mild steel pressure vessel simulator (thickness  $T = 22.5$  cm) and a wide box made of a thin layer of aluminium simulating the air cavity between the pressure vessel and the biological shield in a real PWR.

The VENUS-3 low-flux engineering neutron shielding benchmark experiment is closely related to PWR pressure vessel safety. It was designed to test the accuracy of the nuclear data and transport codes in the calculation of the neutron radiation damage parameters in stainless steel reactor components, in a context of great precision of the experimental results. Among the available experiments, the VENUS-3 configuration offers the exceptional advantage of exhibiting a realistic radial core shape and a typical PWR neutron spectrum. Typical “17x17” PWR fuel assemblies were employed and a mock-up of the pressure vessel internals, representative of a three-loop Westinghouse power plant, was prepared. VENUS-3 was conceived taking into account that, for some early built reactors, it was proposed to reduce the lead factor at the level of the PV horizontal welding by loading Partial Length Shielded Assemblies (PLSA) at the most critical corners of the core periphery (the shielded part was obtained by replacing part of the fuel length by a stainless steel rod). VENUS-3 was addressed to test this improvement, introducing a PLSA region in the core, and to permit the validation of the analytical methods needed to predict the azimuthal variation of the fluence in the pressure vessel. The core has a cruciform-shaped configuration. The core consisted of three types of fuel pins: 1) stainless-steel-clad  $UO_2$  rods (typical of a “15x15” lattice of the early Generation I reactors of Westinghouse plants) containing 4% enriched U-235, 2) zircaloy-clad  $UO_2$  rods containing 3.3% enriched U-235 and 3) zircaloy-clad  $UO_2$  rods containing 3.3% enriched U-235 over the upper half of their height and zircaloy-clad steel rods over the lower half. The first two types of fuel pins were of uniform composition over their complete height. The 4% enriched rods were positioned in the inner part of the core while the 3.3% enriched rods were located in the arms of the cross configuration together with the PLSA-modified rods.

Starting from the centre, the core quadrant between  $0^\circ$  and  $90^\circ$  may be divided in the following 10 horizontal radial regions:

- the CENTRAL HOLE (water);
- the INNER BAFFLE (stainless steel thickness: 2.858 cm);
- the 4/0 FUEL REGION: 4% enriched uranium fuel rods and 11 pyrex control rods, typical of PWR poison clusters;
- the 3/0 FUEL REGION: 3.3% enriched uranium fuel rods and PLSA rods;
- the OUTER BAFFLE (stainless steel thickness. 2.858 cm);
- the REFLECTOR (water minimum thickness: 2.169 cm);
- the BARREL (stainless steel thickness: 4.99 cm);
- the WATER GAP (water thickness: 5.80 cm);
- the NEUTRON PAD (stainless steel average thickness: 6.72 cm);
- the VENUS environment, i.e., the jacket (air filled), the reactor vessel (stainless steel) and the reactor room (air).

In the present ENEA-Bologna Nuclear Data Group program of cross section testing activities for BUGLE-type libraries it was decided to add the analysis of another important neutron shielding benchmark experiment, dedicated to the validation of BUGJEFF311.BOLIB.

Sigla di identificazione	Rev.	Distrib.	Pag.	di
ADPFISS-LP1-087	0	L	21	92

In particular BUGJEFF311.BOLIB was used in three-dimensional transport analyses dedicated to a single-material (iron) benchmark experiment named Iron-88 /2/. This experiment permits to verify the neutron deep penetration (about six decades of neutron flux attenuation) through a mild steel layer of about 67 cm and is complementary with respect to the two previously cited engineering benchmark shielding experiments. It is underlined that the performance of the iron nuclear data are obviously essential for any fission reactor applications. It is well known in fact that the LWR pressure vessels and the so-called internals are made of different types of steels where in any case the iron cross sections, and in particular those of Fe-56, with an isotopic abundance of about 92% in natural iron, play a crucial role in the accurate prediction of the EoL (End-of-Life) neutron fluence of the steel reactor components as the reactor pressure vessel.



Table 5

Neutron Group Energy and Lethargy Boundaries for the BUGJEFF311.BOLIB Library.

Group	Upper Energy [eV]	Upper Lethargy
1	1.7332E+07	-5.4997E-01
2	1.4191E+07	-3.5002E-01
3	1.2214E+07	-2.0000E-01
4	1.0000E+07	0.
5	8.6071E+06	1.5000E-01
6	7.4082E+06	3.0000E-01
7	6.0653E+06	5.0000E-01
8	4.9659E+06	7.0000E-01
9	3.6788E+06	1.0000E-00
10	3.0119E+06	1.2000E+00
11	2.7253E+06	1.3000E+00
12	2.4660E+06	1.4000E+00
13	2.3653E+06	1.4417E+00
14	2.3457E+06	1.4500E+00
15	2.2313E+06	1.5000E+00
16	1.9205E+06	1.6500E+00
17	1.6530E+06	1.8000E+00
18	1.3534E+06	2.0000E+00
19	1.0026E+06	2.3000E+00
20	8.2085E+05	2.5000E+00
21	7.4274E+05	2.6000E+00
22	6.0810E+05	2.8000E+00
23	4.9787E+05	3.0000E+00
24	3.6883E+05	3.3000E+00
25	2.9721E+05	3.5159E+00
26	1.8316E+05	4.0000E+00
27	1.1109E+05	4.5000E+00
28	6.7379E+04	5.0000E+00
29	4.0868E+04	5.5000E+00
30	3.1828E+04	5.7500E+00
31	2.6058E+04	5.9500E+00
32	2.4176E+04	6.0250E+00
33	2.1875E+04	6.1250E+00
34	1.5034E+04	6.5000E+00
35	7.1017E+03	7.2500E+00
36	3.3546E+03	8.0000E+00
37	1.5846E+03	8.7500E+00
38	4.5400E+02	1.0000E+01
39	2.1445E+02	1.0750E+01
40	1.0130E+02	1.1500E+01
41	3.7266E+01	1.2500E+01
42	1.0677E+01	1.3750E+01
43	5.0435E+00	1.4500E+01
44	1.8554E+00	1.5500E+01
45	8.7643E-01	1.6250E+01
46	4.1399E-01	1.7000E+01
47	1.0000E-01	1.8421E+01
	1.0000E-05	2.7631E+01

Table 6

Photon Group Energy Boundaries for the BUGJEFF311.BOLIB Library.

Group	Upper Energy [eV]
1	1.4000E+07
2	1.0000E+07
3	8.0000E+06
4	7.0000E+06
5	6.0000E+06
6	5.0000E+06
7	4.0000E+06
8	3.0000E+06
9	2.0000E+06
10	1.5000E+06
11	1.0000E+06
12	8.0000E+05
13	7.0000E+05
14	6.0000E+05
15	4.0000E+05
16	2.0000E+05
17	1.0000E+05
18	6.0000E+04
19	3.0000E+04
20	2.0000E+04
	1.0000E+04

### 3.2 - Transport Calculation General Features

Fixed source transport calculations in Cartesian geometry were performed for the Iron-88 neutron shielding benchmark experiment using the ORNL TORT-3.2 /5/ three-dimensional discrete ordinates ( $S_N$ ) code included in the ORNL DOORS-3.2 /23/ system of deterministic transport codes. The whole Iron-88 experimental array (see /2/ and 2.2) was reproduced with the TORT-3.2 code using the realistic inhomogeneous fission neutron source (see 2.4 and Table 4) emitted by the fission plate.

The TORT-3.2 code was used on a personal computer (CPU: INTEL PENTIUM D 3.40 GHz, 3.10 GB of RAM) under Linux openSUSE 10.2 (i586) operating system with FORTRAN-77 compiler g77, version 3.3.5-38.

The automatic generation of the spatial mesh grid and the graphical verification of the Iron-88 benchmark experiment geometrical model for TORT-3.2 were performed through the ENEA-Bologna BOT3P-5.3 /24/ (see also /25/, /26/ and /27/) pre/post-processor system.

The reference system adopted in the present calculations has its origin on the Z horizontal axis passing through the centre of the fission plate (see Figures 2 and 6) and normal to it. It is underlined that the centre of the fission plate is not aligned with the centre of the trolley face. In fact the centre of the trolley face is shifted by -2.55 cm in the X horizontal axis direction and by +6.6 cm in the Y vertical axis direction.

The whole three-dimensional Iron-88 experimental array was reproduced in the (X,Y,Z) Cartesian geometry and adopted in all the calculations in order to assure a proper detailed description (see Figure 7) of the spatial inhomogeneity of the neutron source (see Table 4) emitted by the fission plate. In particular it was described a parallelepiped geometry with a 69X×86Y×278Z fine spatial mesh grid, being Z the horizontal nuclear axis (see Figure 2) where the dosimetric measurement positions were located. Volumetric meshes with sides always inferior to 1.0 cm were described along the Z axis, in correspondence of the measurement region, to obtain the best calculated result accuracy. Volumetric meshes with sides always inferior to 0.25 cm were used in the measurement positions along the Z axis, i.e. in the 0.74 cm air gaps between each mild steel slab component.

The horizontal section (at the vertical axis position  $Y = 0.0$  cm) of the Iron-88 compositional and geometrical model, reproduced in all the TORT-3.2 (X,Y,Z) calculations, is reported in Figure 8 together with the dosimeter locations (×). A detail of the Figure 8 is represented in the Figure 9, representing an enlargement of the compositional and geometrical model in the measurement region where it is possible to see better the 0.74 cm thick air gaps between the various mild steel slab components and the related dosimeter measurement locations.

The mild steel floor, the roof and the trolley lateral walls with 1.91 cm thickness (see 2.2) were simulated in the TORT calculations since they were originally represented in the input data of the Monte Carlo MCBEND /28/ code calculation example, reported in the Iron-88 benchmark experiment section of reference /3/.

The adopted calculation model includes a 1.0 m long graphite region (see Figure 8) to represent the region of the NESTOR reactor behind the trolley face and the fission plate

(i.e. towards NESTOR reactor from the fission plate), not contained in Table 1, where only the regions behind the fission plate up to the end of the trolley are indicated. As confirmed in the Iron-88 report (see /2/, page 4), the realistic presence of the graphite zone will permit to obtain more accurate Au-197(n, $\gamma$ )Au-198 calculated reaction rate results, particularly in the first five measurement positions (see Figure 2). Concerning this, it was decided to introduce the previously cited additional graphite region in all the calculations (producing in particular the gold reaction rate results) to compare all the reaction rate results in a consistent way.

The ENEA-Bologna ADEFTA-4.1 /29/ program was employed in the calculation of the atomic densities of the isotopes involved in the compositional model on the basis of the atomic abundances reported in the BNL-NNDC database /30/ included in ADEFTA. The Iron-88 atomic densities were calculated using the densities and the weight fractions reported in the Table 2 of reference /2/.

The ENEA-Bologna BUGJEFF311.BOLIB /1/ (JEFF-3.1.1 /8/ /9/ data) working library was used in the transport calculations with TORT-3.2, in alternative to the ORNL BUGLE-96 /10/ (ENDF/B-VI.3 /17/ data) similar working library considered a well tested reference library.

The calculations of the Au-197(n, $\gamma$ )Au-198 activation dosimeter reaction rates were performed (see more detail in 3.2.1) using the first 44 neutron groups (see Table 5) of the BUGLE-type libraries. This implicitly assumes 0.876 eV as the nearer energy value, in the BUGLE-type neutron energy structure, to the 0.73 eV epi-cadmium cutoff thermal neutron energy, corresponding to the cadmium cover thickness of 1.27 mm used in the reaction rate measurements with gold dosimeters in the Iron-88 benchmark experiment.

All the reaction rate calculations for the Rh-103(n,n')Rh-103m, In-115(n,n')In-115m, S-32(n,p)P-32 and Al-27(n, $\alpha$ )Na-24 threshold activation dosimeters were performed only with the first 29 neutron groups (see Table 5), above 3.1828E+04 eV, since all the neutron threshold energies of the four employed dosimeters are above this neutron energy value.

Both infinite dilution and self-shielded neutron cross sections were selected. Proper self-shielded cross sections from the BUGJEFF311.BOLIB and BUGLE-96 library packages were used when available. In particular it is underlined that the mild steel and stainless steel regions of Iron-88 are characterized by atomic densities quite similar to those used to calculate the background cross sections, employed in the self-shielding of the BUGJEFF311.BOLIB and BUGLE-96 neutron cross sections. Group-organized files of macroscopic cross sections, requested by TORT-3.2 and derived from the BUGJEFF311.BOLIB and BUGLE-96 working libraries in FIDO-ANISN format, were prepared through the ORNL GIP (see /16/) program, specifically dedicated to the discrete ordinates transport codes (ANISN-ORNL, DORT, TORT) of the DOORS system. The ENEA-Bologna ADEFTA-4.1 program was used not only to calculate the atomic densities for the benchmark experiment compositional model but also to handle them properly in order to automatically prepare the macroscopic cross section sets of the compositional model material mixtures in the format required by GIP.

Fixed source transport calculations with one source (outer) iteration and 60 inner iterations were performed using fully symmetrical discrete ordinates directional quadrature sets for the flux solution. The P<sub>3</sub>-S<sub>8</sub> approximation was adopted as the standard reference in all the

calculations with the BUGJEFF311.BOLIB and BUGLE-96 libraries.  $P_N$  corresponds to the order of the expansion in Legendre polynomials of the scattering cross section matrix and  $S_N$  represents the order of the flux angular discretization. It is underlined that the  $P_3-S_8$  approximation is the most widely used option in the fixed source calculations dedicated to LWR safety analyses.

The theta-weighted difference approximation was selected for the flux extrapolation model. In all the calculations the same numerical value (1.0E-03) for the point-wise flux convergence criterion was employed.

The vacuum boundary condition was selected at the left, right, inside, outside, bottom and top geometrical boundaries.

The calculated reaction rates were obtained in all the experimental dosimeter positions in the 0.74 cm air gaps (see Figures 2, 8 and 9) between each mild steel slab component.

Figure 7

Iron-88 - Vertical Section of the Fission Plate Neutron Source Distribution  
Described in the TORT-3.2 (X,Y,X) Calculations.

Vertical Section at Z = 1.5 cm.  
69X×86Y×278Z Spatial Meshes.

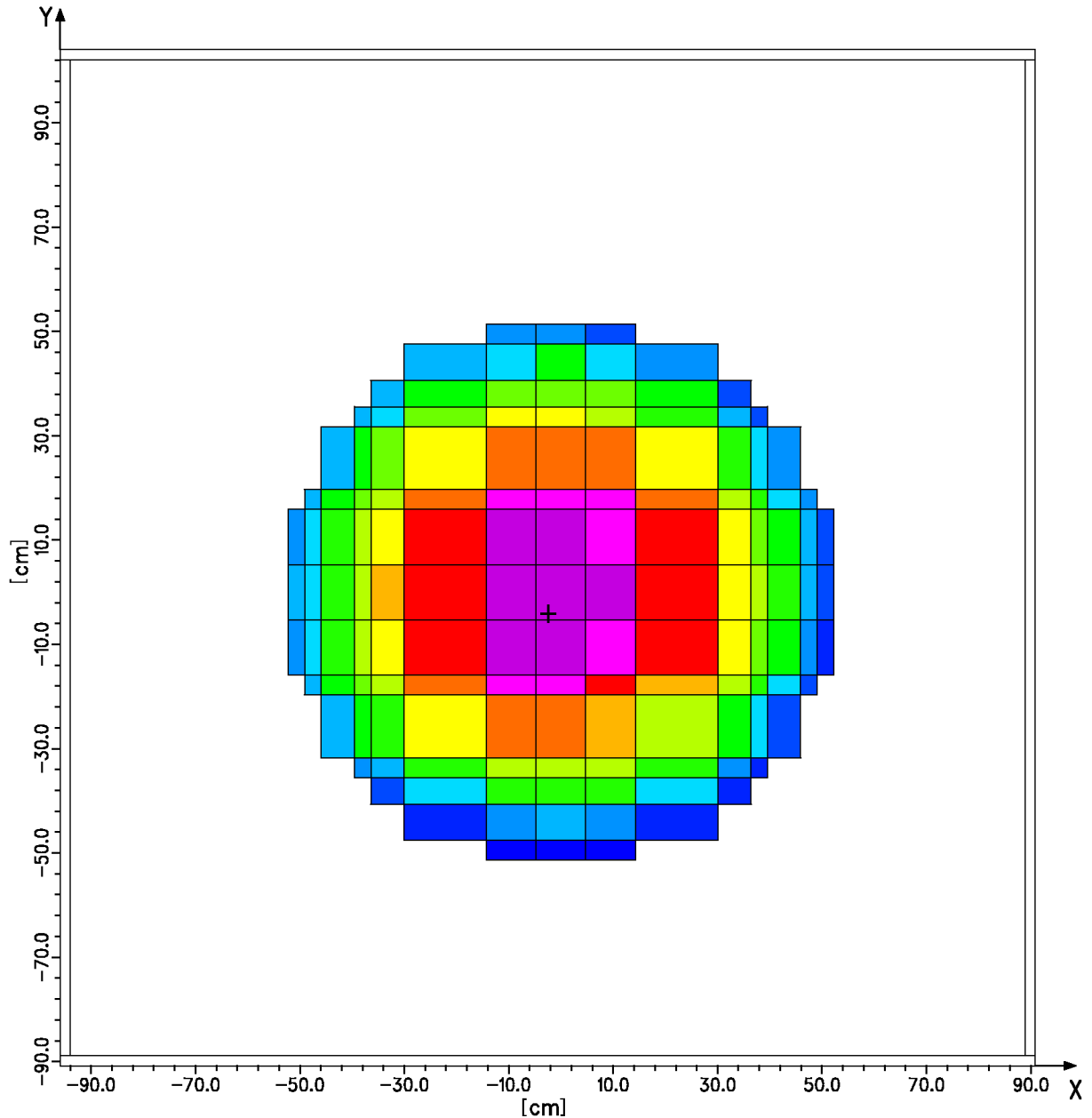
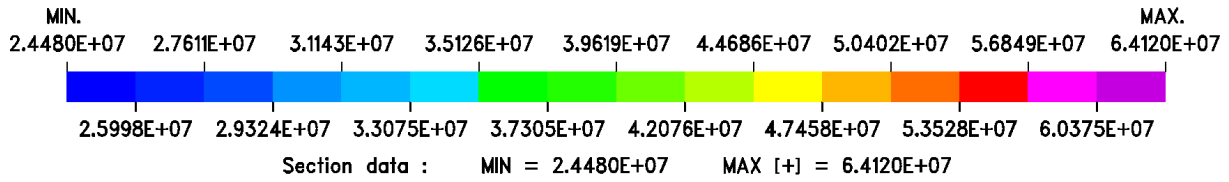


Figure 8

Iron-88 - Compositional and Geometrical Model in the TORT-3.2 (X,Y,Z) Calculations.

Horizontal Section at Y = 0.0 cm.  
Dosimeter Locations “x”, 69X×86Y×278Z Spatial Meshes.

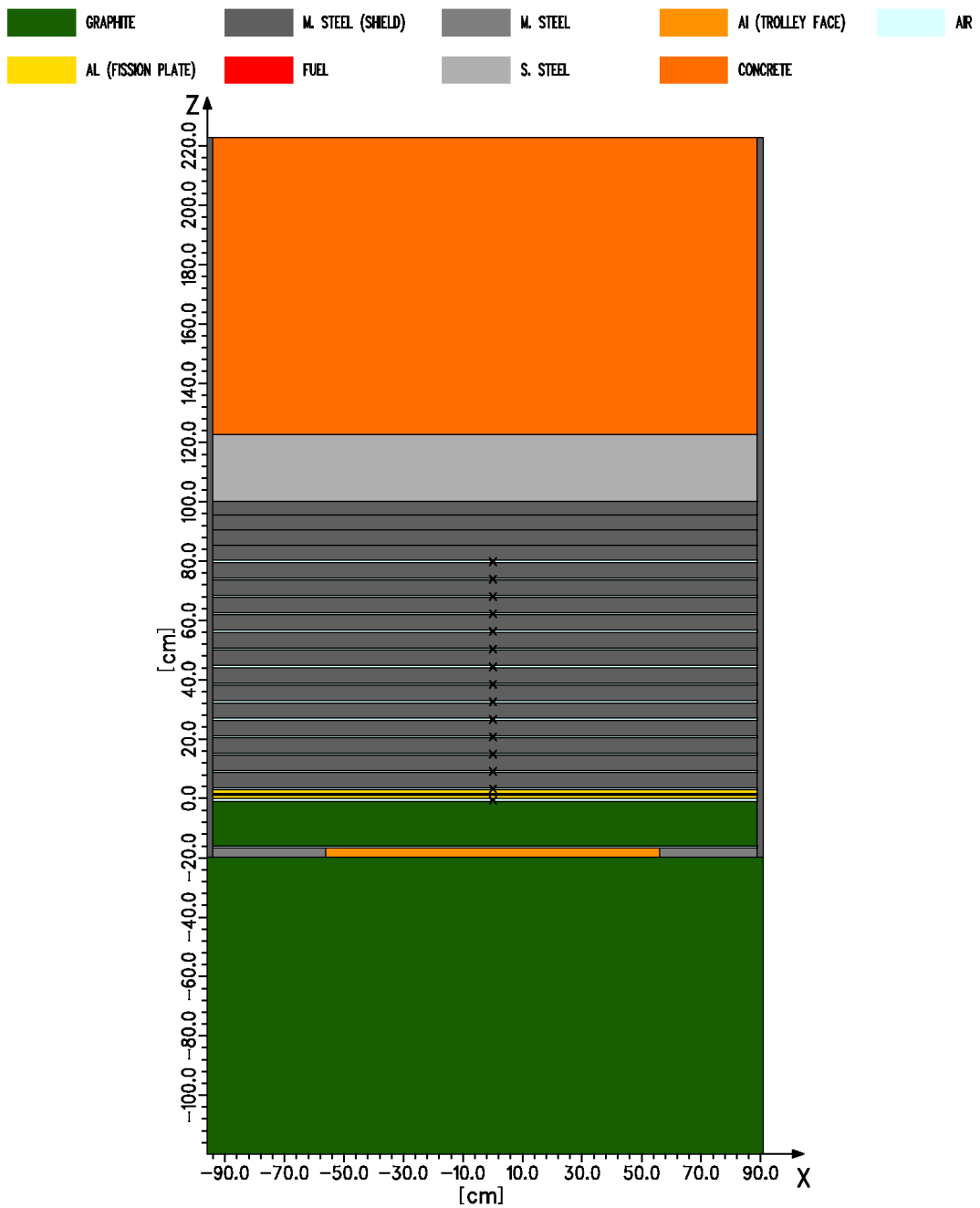
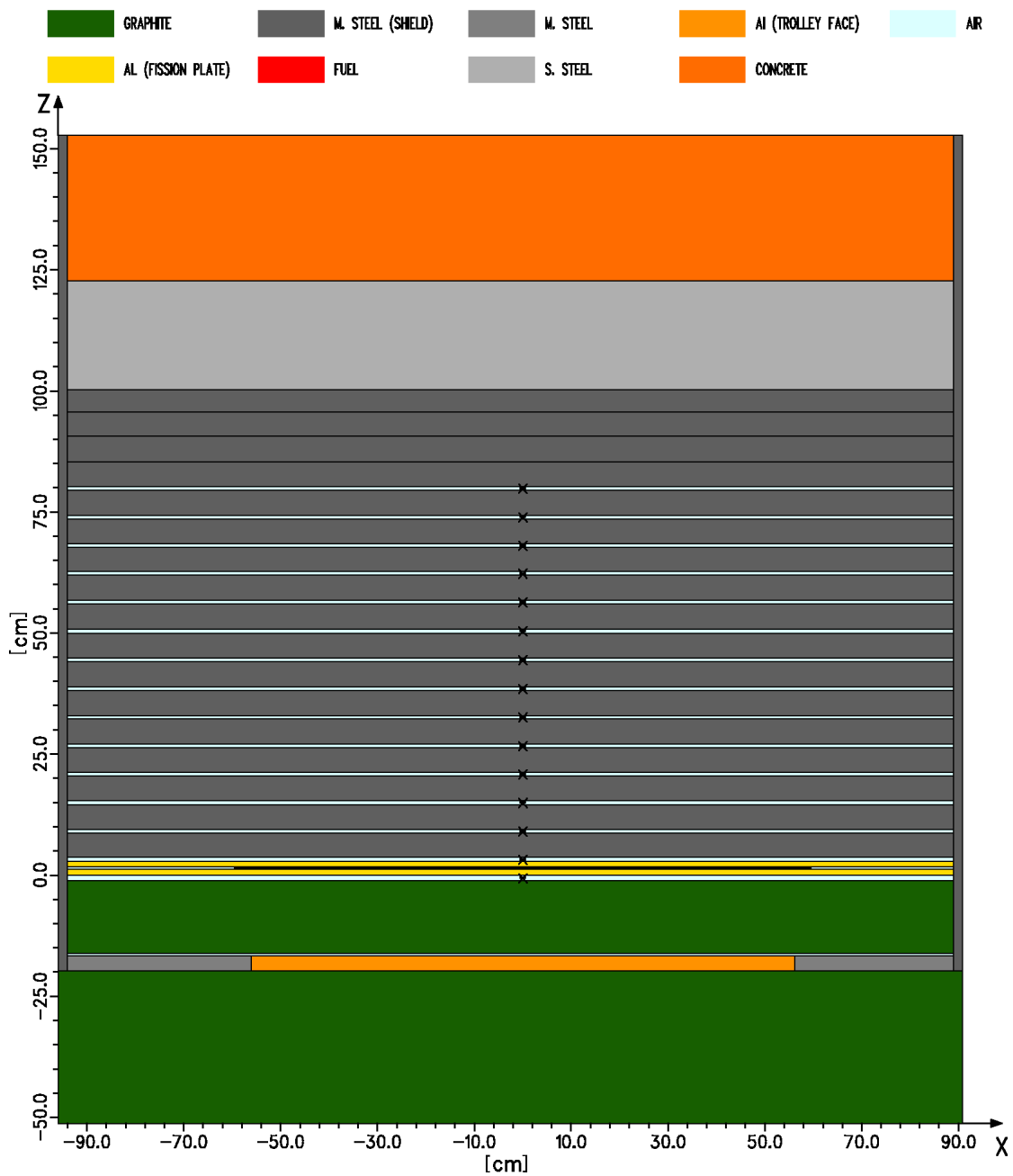


Figure 9

Iron-88 - Compositional and Geometrical Model in the TORT-3.2 (X,Y,Z) Calculations.

Enlargement of the Measurement Region, Horizontal Section at Y = 0.0 cm.  
Dosimeter Locations “x”, 69X×86Y×278Z Spatial Meshes.





### 3.2.1 - Activation Dosimeter Cross Sections

The activation dosimeter cross sections for the Au-197(n, $\gamma$ )Au-198 nuclear reactions (see Figures 10÷16) and the threshold activation dosimeter cross sections for the Rh-103(n,n')Rh-103m (see Figures 17 and 18), In-115(n,n')In-115m (see Figures 19 and 20), S-32(n,p)P-32 (see Figures 21 and 22) and Al-27(n, $\alpha$ )Na-24 (see Figures 23÷26) nuclear reactions, used in the present Iron-88 transport analysis, were derived (see /1/ and /31/) from the IAEA IRDF-2002 /6/ International Reactor Dosimetry File.

The nuclear reaction cross sections for the Au-197(n, $\gamma$ )Au-198, Rh-103(n,n')Rh-103m, In-115(n,n')In-115m, S-32(n,p)P-32 and Al-27(n, $\alpha$ )Na-24 activation dosimeters were obtained in the 47-group neutron energy structure (see Table 5) typical of the BUGJEFF311.BOLIB and BUGLE-96 libraries.

The dosimeter cross sections for the BUGJEFF311.BOLIB and BUGLE-96 calculations were obtained from IRDF-2002, through the GROUPIE module of the PREPRO /32/ nuclear data processing system. Two types of neutron weighting spectra in the 199-group neutron energy structure, typical of the VITJEFF311.BOLIB and VITAMIN-B6 mother libraries of the BUGJEFF311.BOLIB and BUGLE-96 libraries, were used in GROUPIE to generate the 47-group dosimeter cross sections: the flat weighting and the 1/4 T PV weighting. As flat neutron weighting spectrum, the constant numerical value of unity was attributed to all the neutron groups of the 199-group flat neutron spectrum in GROUPIE and the generated flat weighting dosimeter cross sections could be obviously used by both the BUGJEFF311.BOLIB and BUGLE-96 libraries.

On the contrary, the 1/4 T PV neutron weighting spectrum, used to generate the dosimeter cross sections employed in the BUGJEFF311.BOLIB calculations, was obtained (see /1/ and /31/) through a fixed source one-dimensional transport calculation using the VITJEFF311.BOLIB /18/ fine-group mother library, describing the in-vessel and ex-vessel radial geometry of a PWR. In particular this 1/4 T PV neutron weighting spectrum was calculated in a steel zone, the reactor pressure vessel (RPV) of a PWR, at a spatial position corresponding to one quarter of the thickness (T) of the reactor pressure vessel (1/4 T PV).

Concerning the 1/4 T PV weighting dosimeter cross sections, used in the transport calculations with BUGLE-96, they were obtained in ENEA-Bologna, for the present transport analysis, with the same PREPRO calculation procedure previously cited, using in this case, in GROUPIE, the original 1/4 T PV neutron weighting spectrum calculated at ORNL with the VITAMIN-B6 fine-group mother library of BUGLE-96 in the same RPV spatial position.

The 47-group dosimeter cross sections, obtained with both the flat weighting and the 1/4 T PV weighting neutron spectra, were in general employed in all the calculations but, for this type of transport analysis dedicated to the Iron-88 single material (iron) neutron shielding benchmark experiment, the dosimeter cross sections obtained with the 1/4 T PV weighting were considered more proper since this neutron weighting spectrum, obtained within an iron region, is obviously more similar to the neutron spectra in the Iron-88 experimental region made of iron.

It is underlined that a unique flat weighting cross section set in the 47-group neutron energy structure for each specific dosimeter nuclear reaction was employed in the transport calculations using BUGJEFF311.BOLIB and BUGLE-96, as already previously reported.

On the contrary, for each specific dosimeter nuclear reaction, the corresponding group numerical values of the two 1/4 T PV weighting cross section sets, respectively used in the BUGJEFF311.BOLIB and BUGLE-96 calculations, are slightly different. In fact the 1/4 T PV weighting dosimeter cross section sets, respectively used in the calculations with BUGJEFF311.BOLIB and BUGLE-96, were obtained through GROUPIE, using separately two slightly different 199-group 1/4 T PV neutron weighting spectra. The cited neutron spectra, previously calculated using the VITJEFF311.BOLIB and VITAMIN-B6 mother libraries, based respectively on JEFF-3.1.1 and ENDF/B-VI.3 nuclear data, are in particular slightly different since they were obtained from calculations using different nuclear data.

The Au-197(n, $\gamma$ )Au-198 activation cross sections were properly self-shielded (see in particular Figure 10 for the flat weighting cross sections and Figures 13 and 14, respectively for the 1/4 T PV weighting cross sections used with the BUGJEFF311.BOLIB and BUGLE-96 libraries) through the GROUPIE module of the PREPRO /32/ nuclear data processing system using a background cross section  $\sigma_0$  equal to 1695.0 barns to take into account in particular the neutron self-shielding in the resolved resonance energy region. The reported numerical value of the background cross section  $\sigma_0$  was obtained assuming that the total background cross section for a lump with finite dimensions is given by (see /33/, pages 9-41 and 9-42) the sum of a first component given by the background cross section depending on the dilution rate of a specific nuclide in the isotopic material mixture of the lump plus a second component given by an escape cross section from the lump. For the gold foils, composed by a monoisotopic material, the first component is a negligible quantity equal to 0.0 or 1.0E-06 barns, as commonly assumed in the data processing procedures. The second component is calculated herewith and can be considered equivalent to the total background cross section, used to self-shield properly the gold cross sections, since the first component is negligible.

For a lump of resonance material (gold foil) embedded in a large moderating region, escapes from the lump also increase the background cross section and the Wigner rational approximation is used to obtain an effective escape cross section "sigmaescape". This additional escape cross section is given by:

$$\text{sigmaescape} = 1/(N \times \langle \ell \rangle),$$

where the mean chord length of the lump is given by  $\langle \ell \rangle = 4V/S$  where:

S = Total area of the surface of the cylindrical gold foil (lump);

V = Total volume of the cylindrical gold foil (lump);

N = Atomic density of gold.

Therefore  $4V/S = 4 \times \pi r^2 h / 2\pi r^2 = 2h$ , where h (0.005 cm) is the thickness (or height) of the cylindrical gold foils used in the Iron-88 experiment, expressed in cm.

So we have  $4V/S = 2 \times 0.005 = 0.01$  cm = mean chord length of the cylindrical lump ( $\langle \ell \rangle$  gold foil), considering negligible the area of the lateral cylindrical surface of the gold foils.

Then we have:

$$\text{sigmaescape} = S/4V \times 1/N = 1/2h \times 1/N.$$

Taking into account that  $N(\text{Au-197}) = \text{gold density} \times \text{Avogadro constant} / \text{gold gram atomic weight}$ , we have:

$$N(\text{Au-197}) = 19.3 \times 0.602214129 / 196.967 = 5.9\text{E-}02 \text{ atoms}/(\text{barns} \times \text{cm})$$

where:

gold density = 19.3 g/cm<sup>3</sup>;

Avogadro constant = 0.602214129 × 1.0E+24 atoms/mol;

gold gram atomic weight = 196.967 gram-atom.

Finally we have:

$$\text{sigmaescape} = 1/0.01 \times 1/5.9\text{E-}02 = 100 \times 169.949 = 1695.0 \text{ barns}$$

The epi-cadmium measurements with gold dosimeters were performed using gold foils inserted in cadmium covers able to absorb the thermal neutrons below a cutoff energy depending on the cadmium cover thickness.

Taking into account that the cadmium cover thickness for the gold dosimeters employed in Iron-88 was equal to 50/1000 inches (1.27 mm), the cadmium cutoff energy for a thin 1/v neutron absorber, as a gold dosimeter, is about 0.73 eV, as can be deduced from reference /34/ (specifically from Figure 12.2.5 at page 276). The identification of an energy value for the effective experimental cadmium cutoff energy is necessary to decide how many neutron groups of the 47-group BUGLE-type neutron energy structure must be excluded to calculate correctly the total gold activation reaction rates for the Iron-88 benchmark experiment.

Eliminating in particular, in the calculations with the BUGLE-type libraries, the two last neutron groups No. 46 and No. 47 of the BUGLE-type neutron energy structure (see Table 5), the effective cadmium cutoff energy is implicitly assumed at the classical 0.414 eV upper thermal threshold energy. Eliminating an additional neutron group, i.e. the neutron group No. 45, the effective cadmium cutoff energy is implicitly assumed at 0.876 eV, the upper energy limit of the neutron group No. 45.

Probably the most correct choice, adopted in the present work, is to eliminate from the calculations the gold reaction rate contributions of the three previously cited last neutron groups. In fact the energy value nearer to 0.73 eV, i.e. the effective cadmium cutoff energy corresponding to a cadmium cover thickness of 1.27 mm, is 0.876 eV, the upper energy limit of the neutron group No. 45 in a BUGLE-type neutron energy structure.

Figure 10

Comparison of Flat Weighting Au-197(n, $\gamma$ )Au-198 Neutron Self-Shielded and not Self-Shielded Cross Sections

Used with the BUGJEFF311.BOLIB and BUGLE-96 Libraries.

47-Group Neutron Energy Structure Typical of the BUGLE-Type Libraries.

Self-Shielding Calculated Assuming a Background Cross Section  $\sigma_0 = 1695.0$  barns.

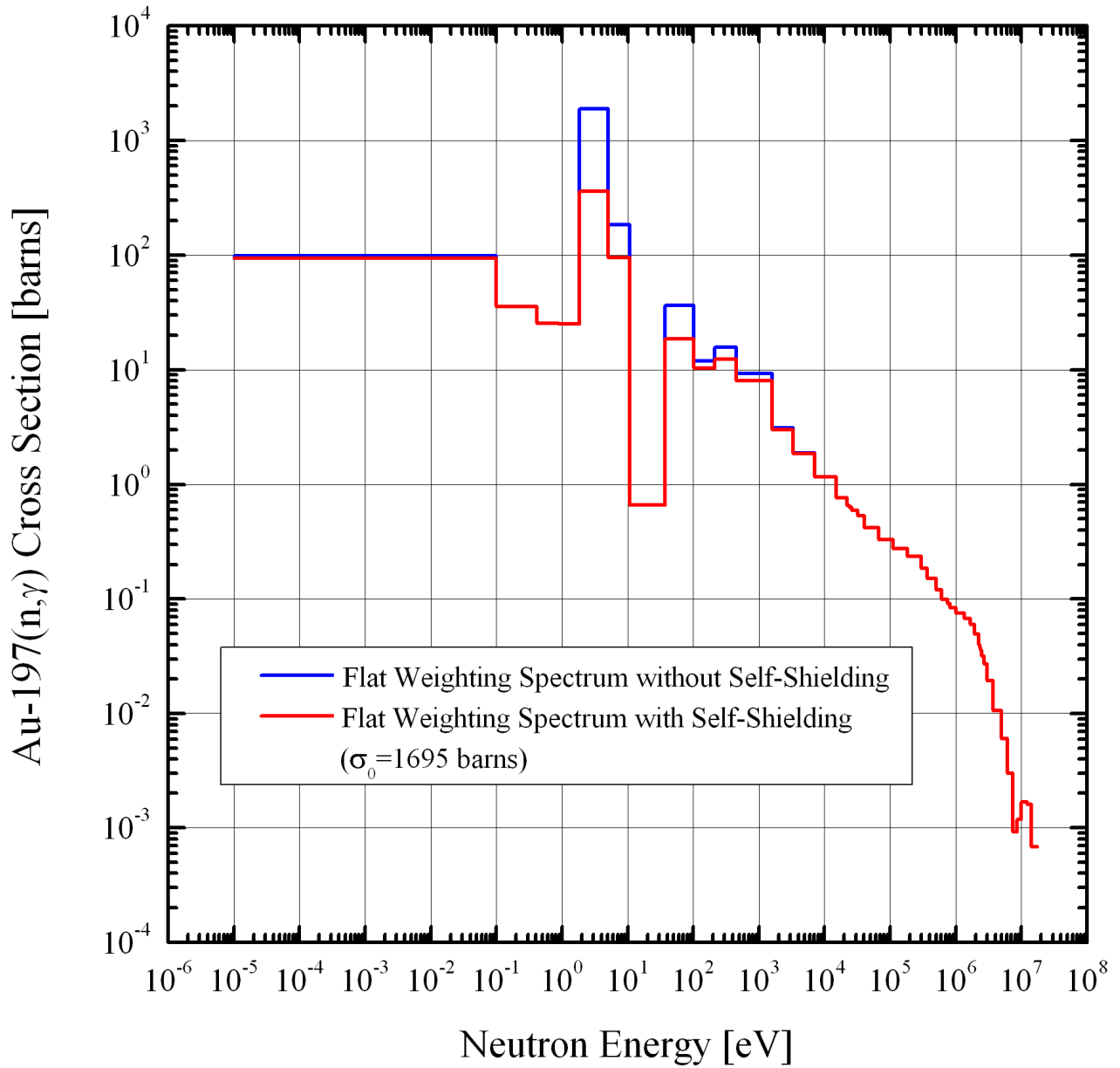


Figure 11

Comparison of 1/4 T PV Weighting Au-197(n, $\gamma$ )Au-198 Neutron Self-Shielded and not Self-Shielded Cross Sections Used with the BUGJEFF311.BOLIB Library.

47-Group Neutron Energy Structure Typical of the BUGLE-Type Libraries.

Self-Shielding Calculated Assuming a Background Cross Section  $\sigma_0 = 1695.0$  barns.

1/4 T PV Weighting Au-197(n, $\gamma$ )Au-198 Neutron Cross Sections Obtained through Data Processing Using the 199-Group Neutron Spectrum Calculated in the 1/4 T PV Position with the VITJEFF311.BOLIB Library.

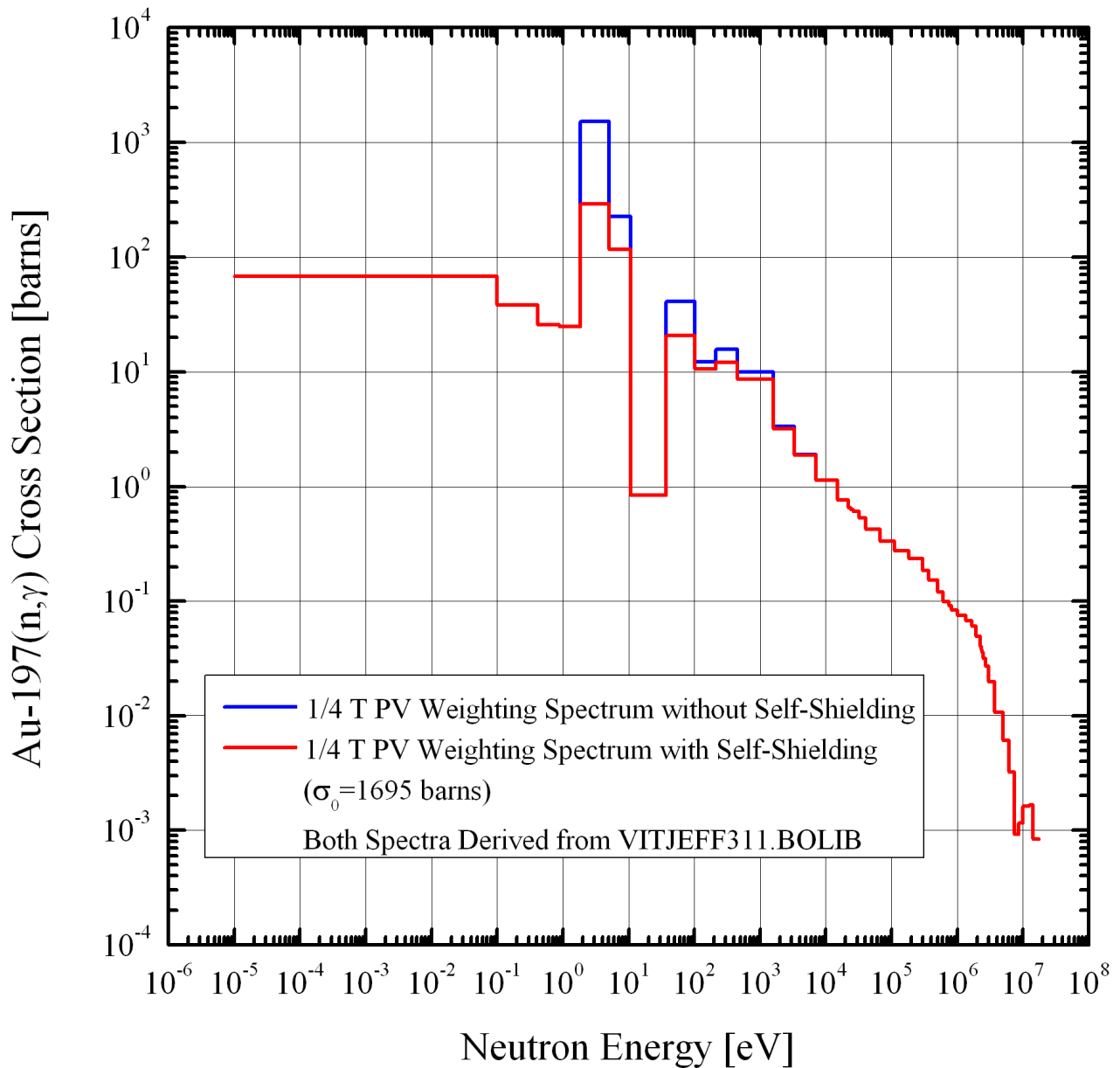


Figure 12

Comparison of 1/4 T PV Weighting Au-197(n,γ)Au-198 Neutron Self-Shielded and not Self-Shielded Cross Sections Used with the BUGLE-96 Library.

47-Group Neutron Energy Structure Typical of the BUGLE-Type Libraries.

Self-Shielding Calculated Assuming a Background Cross Section  $\sigma_0 = 1695.0$  barns.

1/4 T PV Weighting Au-197(n,γ)Au-198 Neutron Cross Sections Obtained through Data Processing Using the 199-Group Neutron Spectrum Calculated in the 1/4 T PV Position with the VITAMIN-B6 Library.

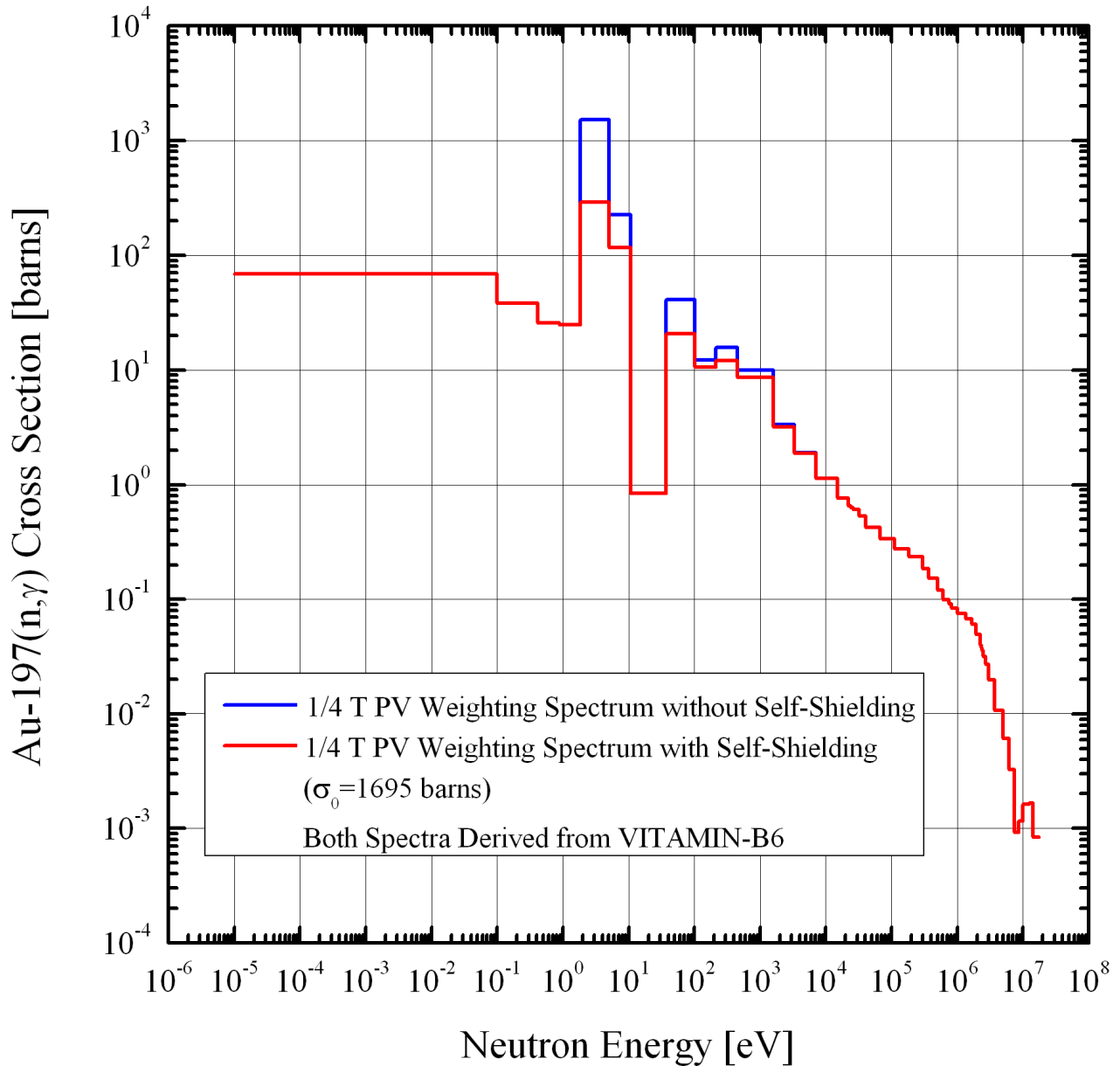


Figure 13

Comparison of Flat Weighting and 1/4 T PV Weighting Au-197(n, $\gamma$ )Au-198 Neutron Self-Shielded Cross Sections Used with the BUGJEFF311.BOLIB Library.

47-Group Neutron Energy Structure Typical of the BUGLE-Type Libraries.

Self-Shielding Calculated Assuming a Background Cross Section  $\sigma_0 = 1695.0$  barns.

1/4 T PV Weighting Au-197(n, $\gamma$ )Au-198 Neutron Self-Shielded Cross Sections Obtained through Data Processing Using the 199-Group Neutron Spectrum Calculated in the 1/4 T PV Position with the VITJEFF311.BOLIB Library.

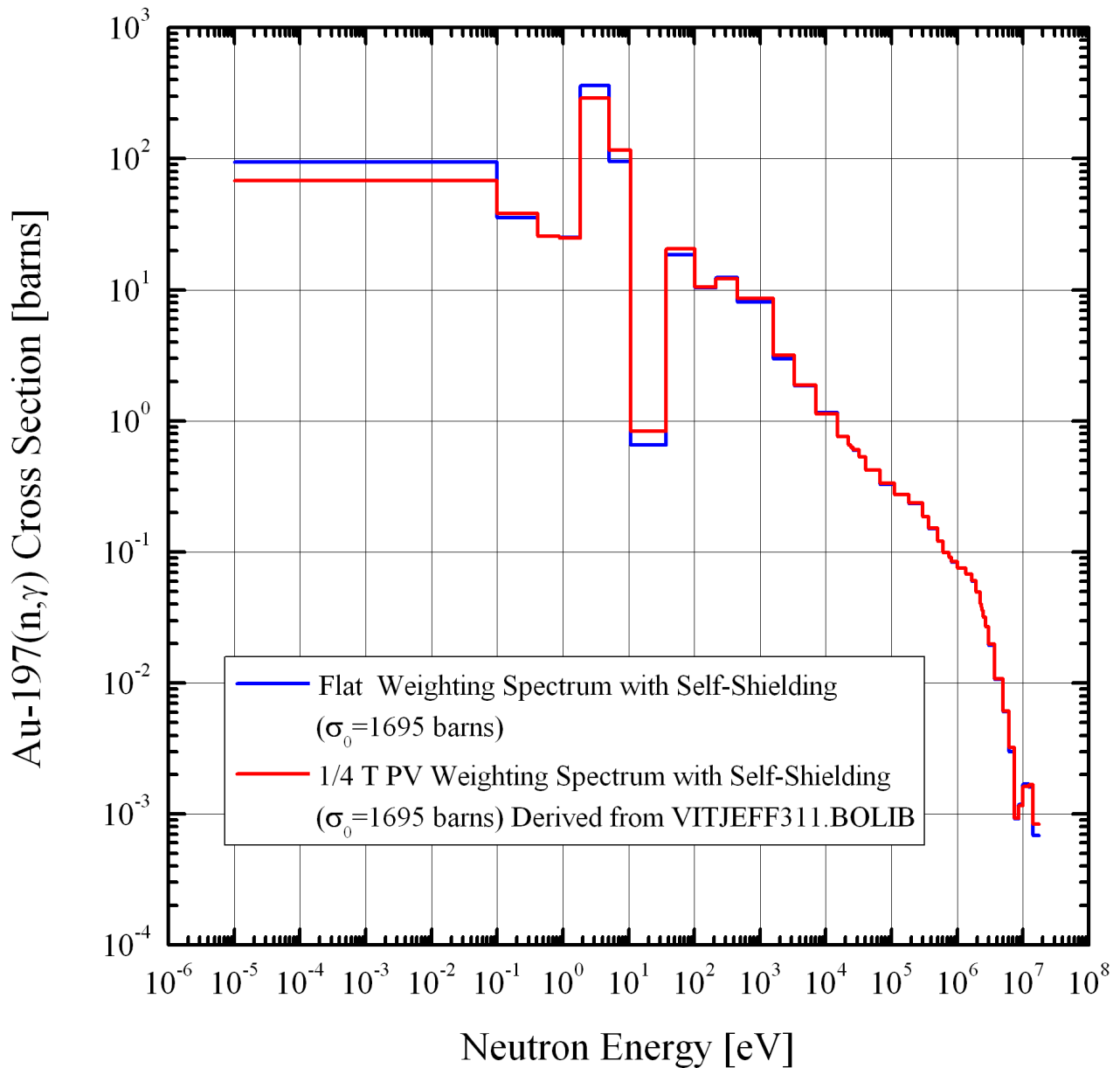


Figure 14

Comparison of Flat Weighting and 1/4 T PV Weighting Au-197(n,γ)Au-198 Neutron Self-Shielded Cross Sections Used with the BUGLE-96 Library.

47-Group Neutron Energy Structure Typical of the BUGLE-Type Libraries.

Self-Shielding Calculated Assuming a Background Cross Section  $\sigma_0 = 1695.0$  barns.

1/4 T PV Weighting Au-197(n,γ)Au-198 Neutron Self-Shielded Cross Sections Obtained through Data Processing Using the 199-Group Neutron Spectrum Calculated in the 1/4 T PV Position with the VITAMIN-B6 Library.

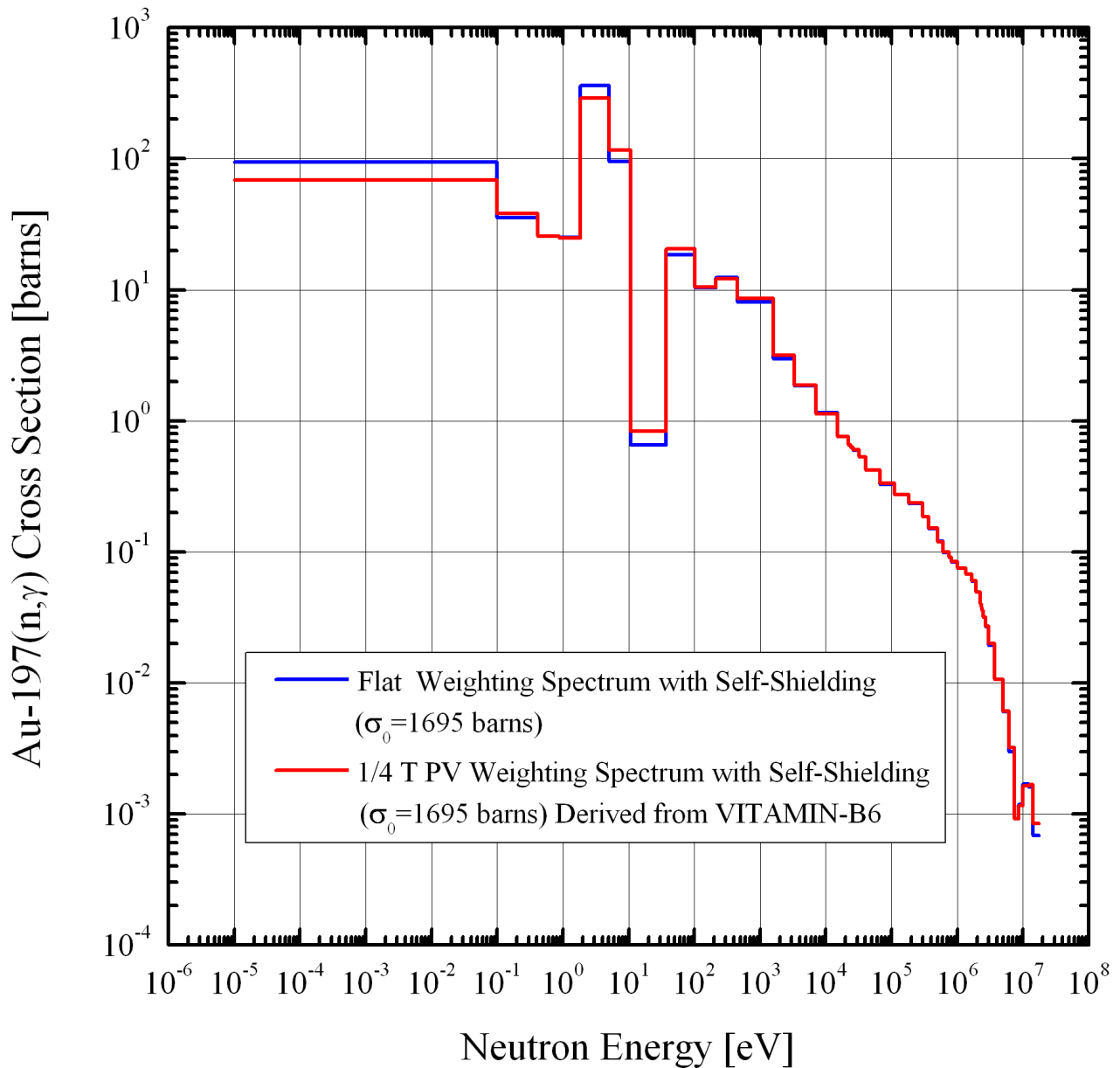




Figure 15

Ratio (1/4 T PV Weighting / Flat Weighting) of the Au-197(n, $\gamma$ )Au-198 Neutron Self-Shielded Cross Sections Used with the BUGJEFF311.BOLIB Library.

47-Group Neutron Energy Structure Typical of the BUGLE-Type Libraries.

1/4 T PV Weighting Au-197(n, $\gamma$ )Au-198 Neutron Cross Sections  
 Obtained through Data Processing Using the 199-Group Neutron Spectrum  
 Calculated in the 1/4 T PV Position with the VITJEFF311.BOLIB Library.

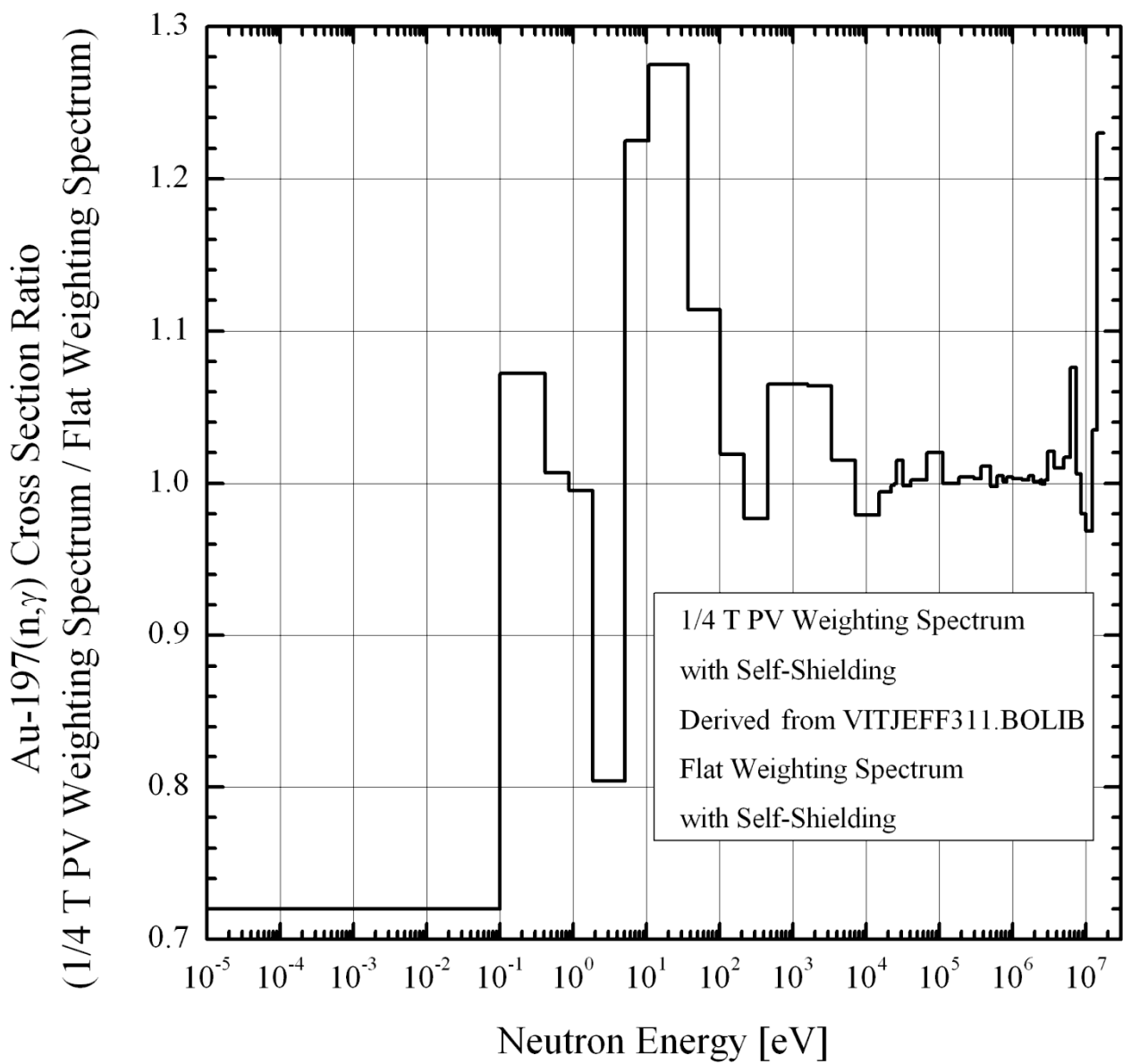


Figure 16

Ratio (1/4 T PV Weighting / Flat Weighting) of the Au-197(n, $\gamma$ )Au-198 Neutron Self-Shielded Cross Sections Used with the BUGLE-96 Library.

47-Group Neutron Energy Structure Typical of the BUGLE-Type Cross Section Libraries.

1/4 T PV Weighting Au-197(n, $\gamma$ )Au-198 Neutron Self-Shielded Cross Sections Obtained through Data Processing Using the 199-Group Neutron Spectrum Calculated in the 1/4 T PV Position with the VITAMIN-B6 Library.

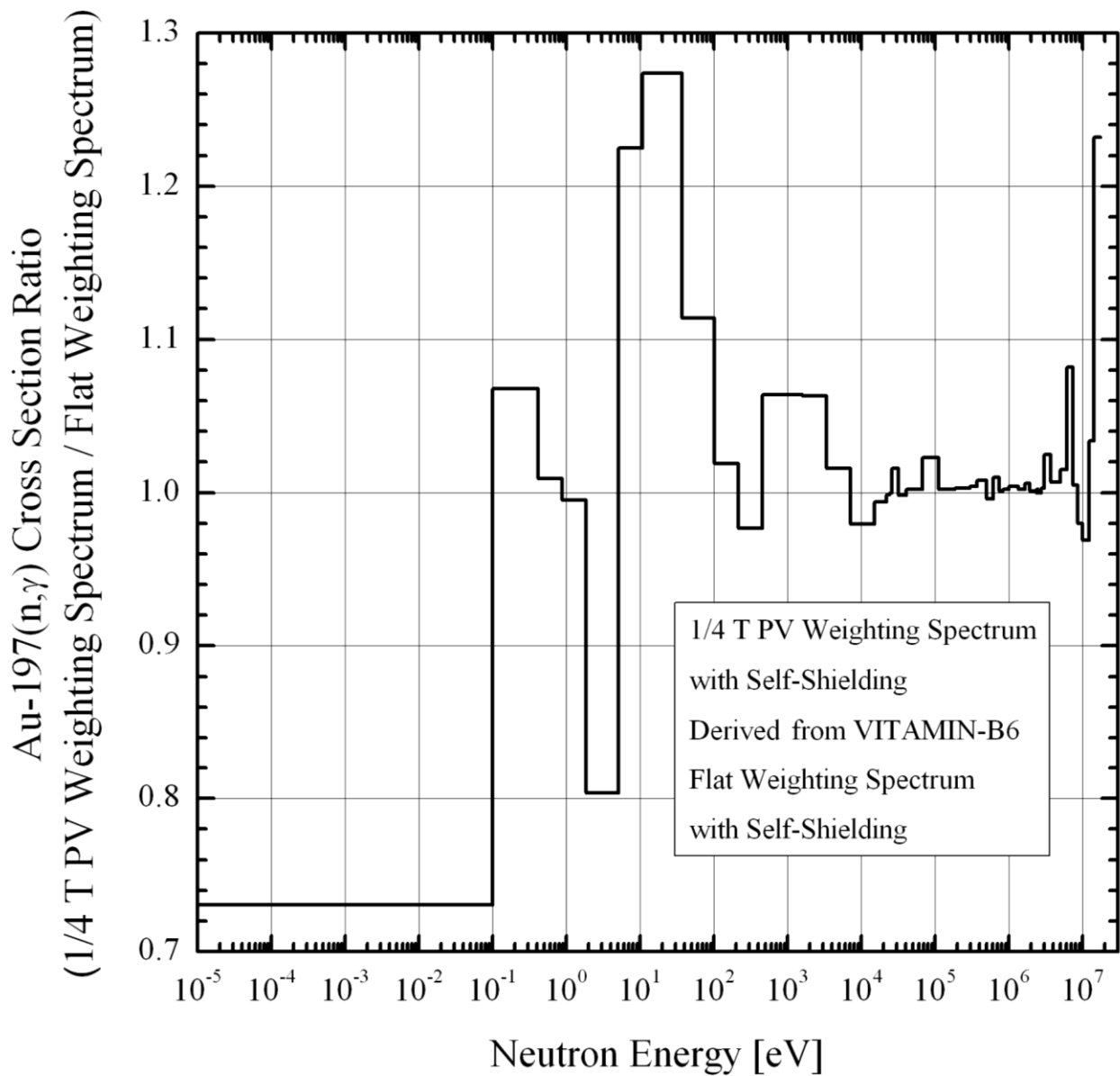


Figure 17

Comparison of the IRDF-2002 Flat Weighting and 1/4 T PV Weighting  
 Rh-103(n,n')Rh-103m Dosimeter Cross Sections  
 Used with the BUGJEFF311.BOLIB Library.

47-Group Neutron Energy Structure Typical of the BUGLE-Type Libraries.

1/4 T PV Weighting Rh-103(n,n')Rh-103m Neutron Cross Sections  
 Obtained through Data Processing Using the 199-Group Neutron Spectrum  
 Calculated in the 1/4 T PV Position with the VITJEFF311.BOLIB Library.

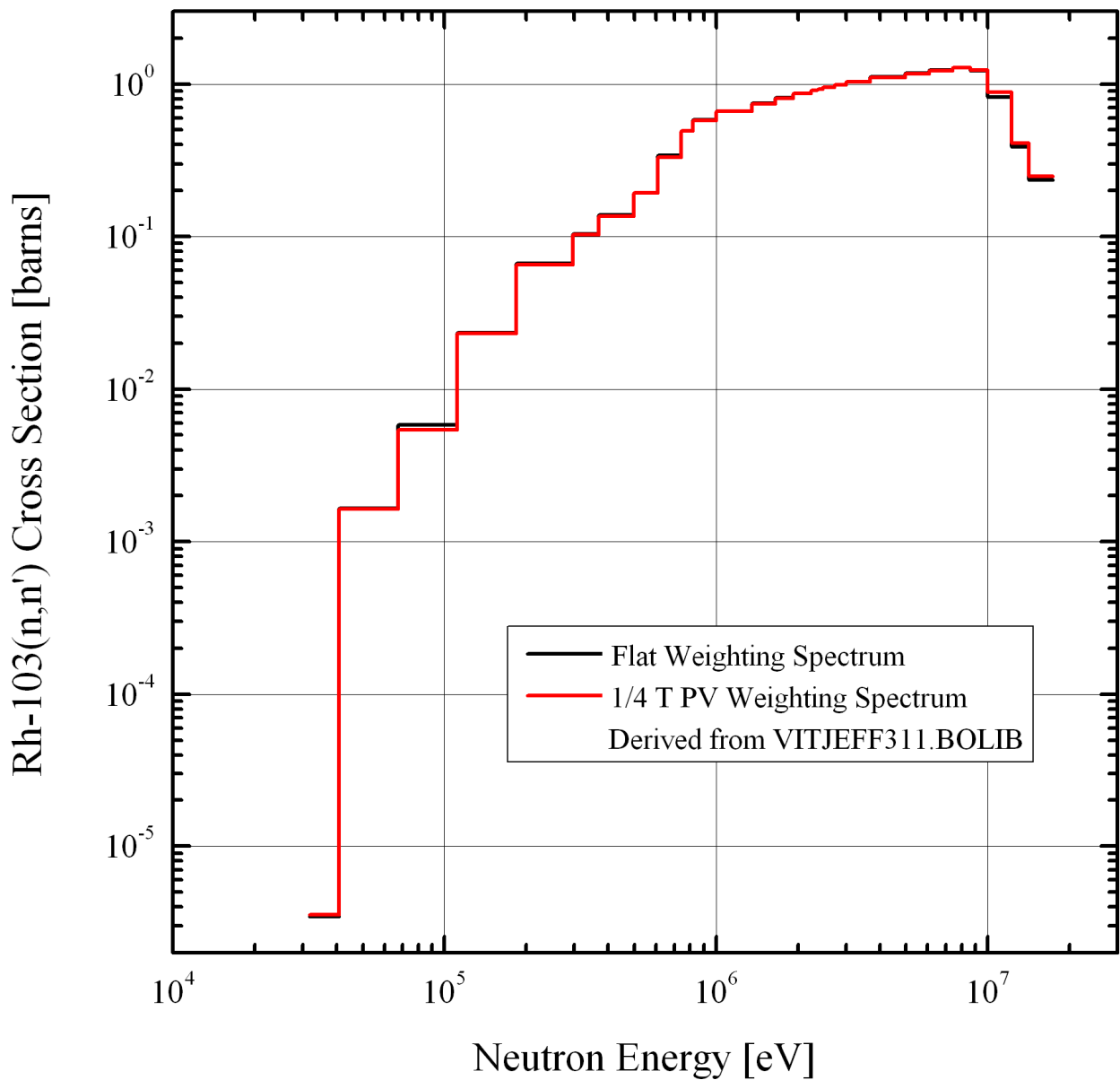


Figure 18

Comparison of the IRDF-2002 Flat Weighting and 1/4 T PV Weighting  
 Rh-103(n,n')Rh-103m Dosimeter Cross Sections  
 Used with the BUGLE-96 library

47-Group Neutron Energy Structure Typical of the BUGLE-Type Libraries.

1/4 T PV Weighting Rh-103(n,n')Rh-103m Neutron Cross Sections  
 Obtained through Data Processing Using the 199-Group Neutron Spectrum  
 Calculated in the 1/4 T PV Position with the VITAMIN-B6 Library.

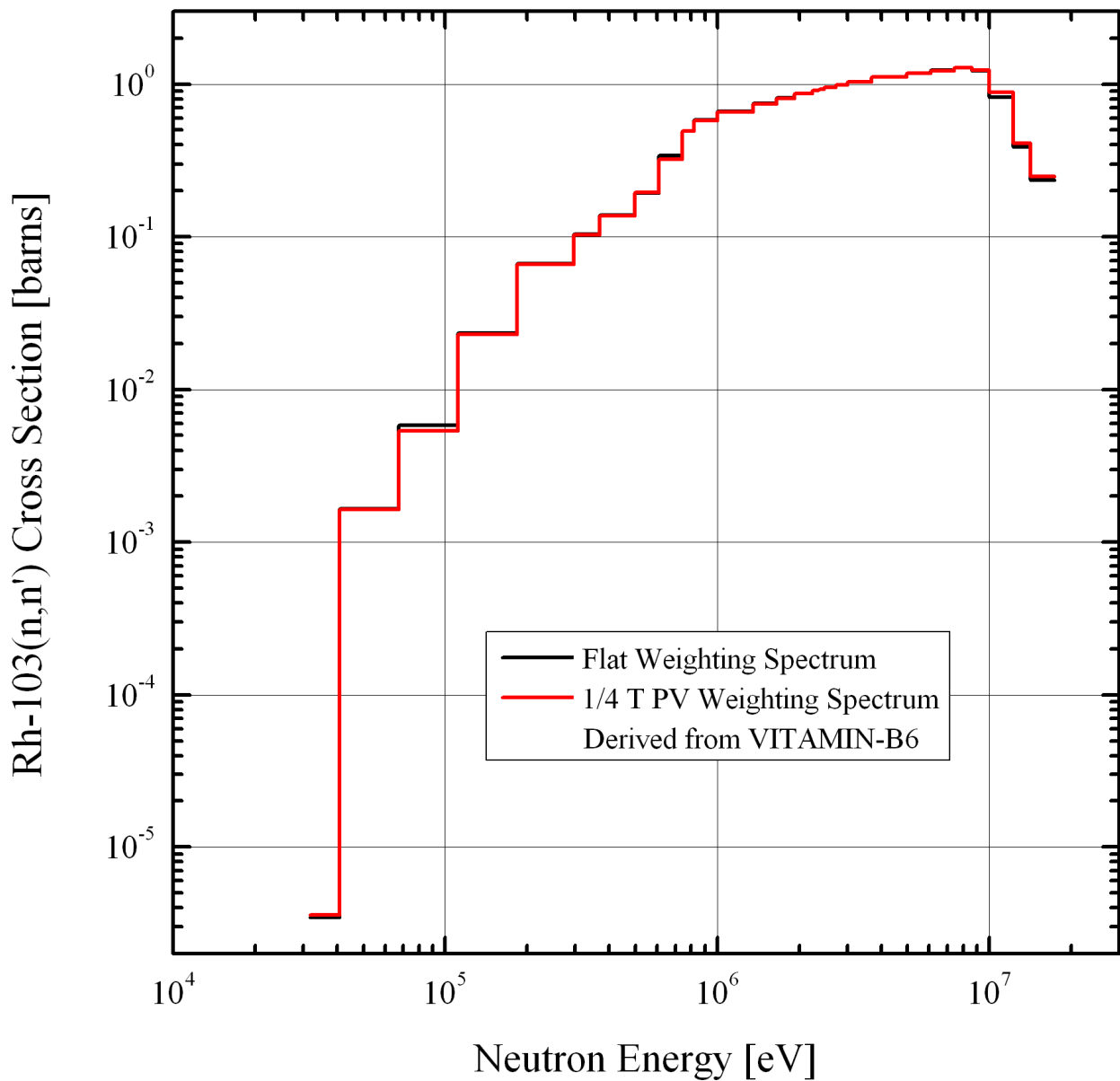


Figure 19

Comparison of the IRDF-2002 Flat Weighting and 1/4 T PV Weighting  
 In-115(n,n')In-115m Dosimeter Cross Sections  
 Used with the BUGJEFF311.BOLIB Library.

47-Group Neutron Energy Structure Typical of the BUGLE-Type Libraries.

1/4 T PV Weighting In-115(n,n')In-115m Neutron Cross Sections  
 Obtained through Data Processing Using the 199-Group Neutron Spectrum  
 Calculated in the 1/4 T PV Position with the VITJEFF311.BOLIB Library.

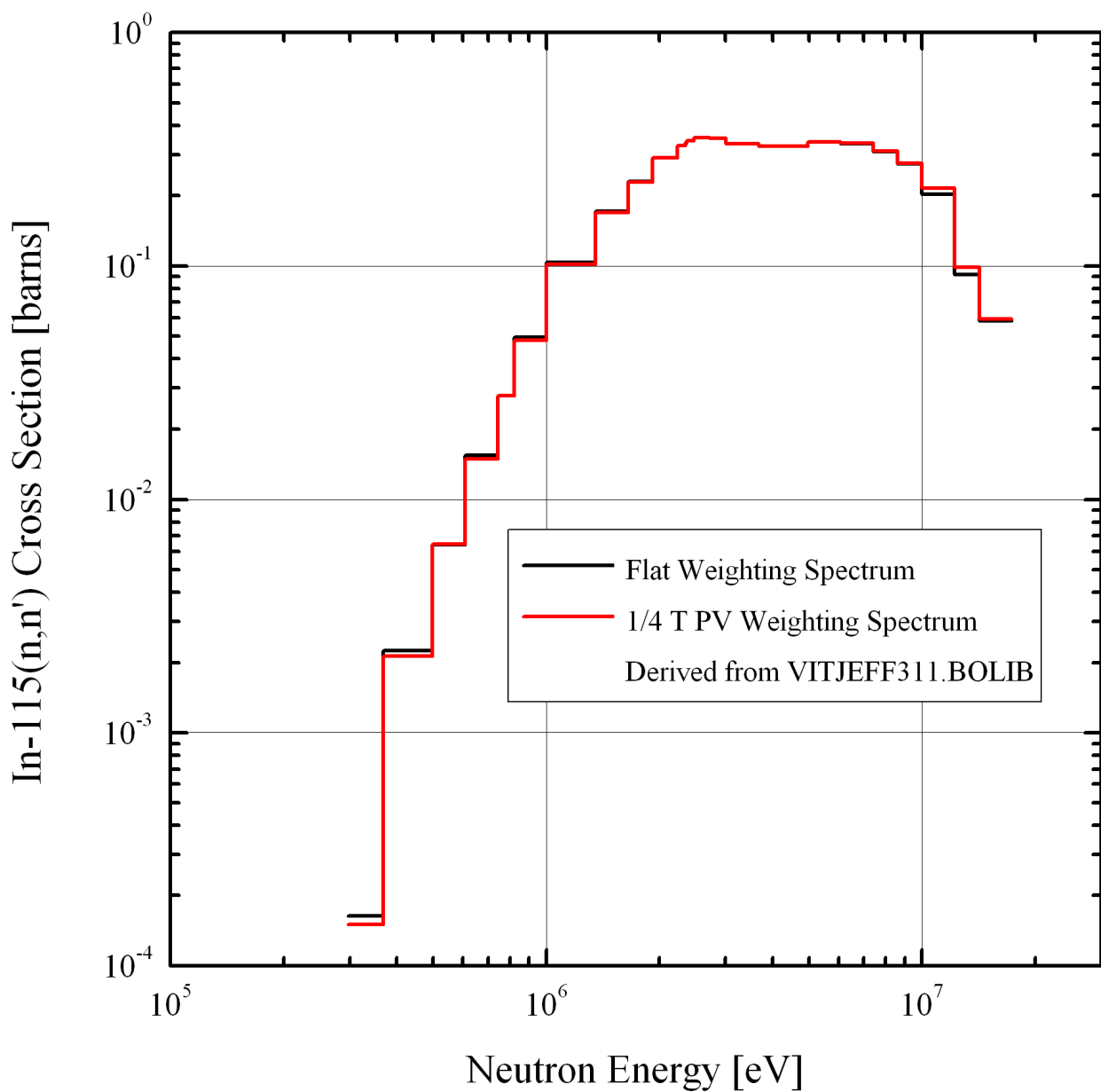


Figure 20

Comparison of the IRDF-2002 Flat Weighting and 1/4 T PV Weighting  
 In-115(n,n')In-115m Dosimeter Cross Sections  
 Used with the BUGLE-96 Library.

47-Group Neutron Energy Structure Typical of the BUGLE-Type Libraries.

1/4 T PV Weighting In-115(n,n')In-115m Neutron Cross Sections  
 Obtained through Data Processing Using the 199-Group Neutron Spectrum  
 Calculated in the 1/4 T PV Position with the VITAMIN-B6 Library.

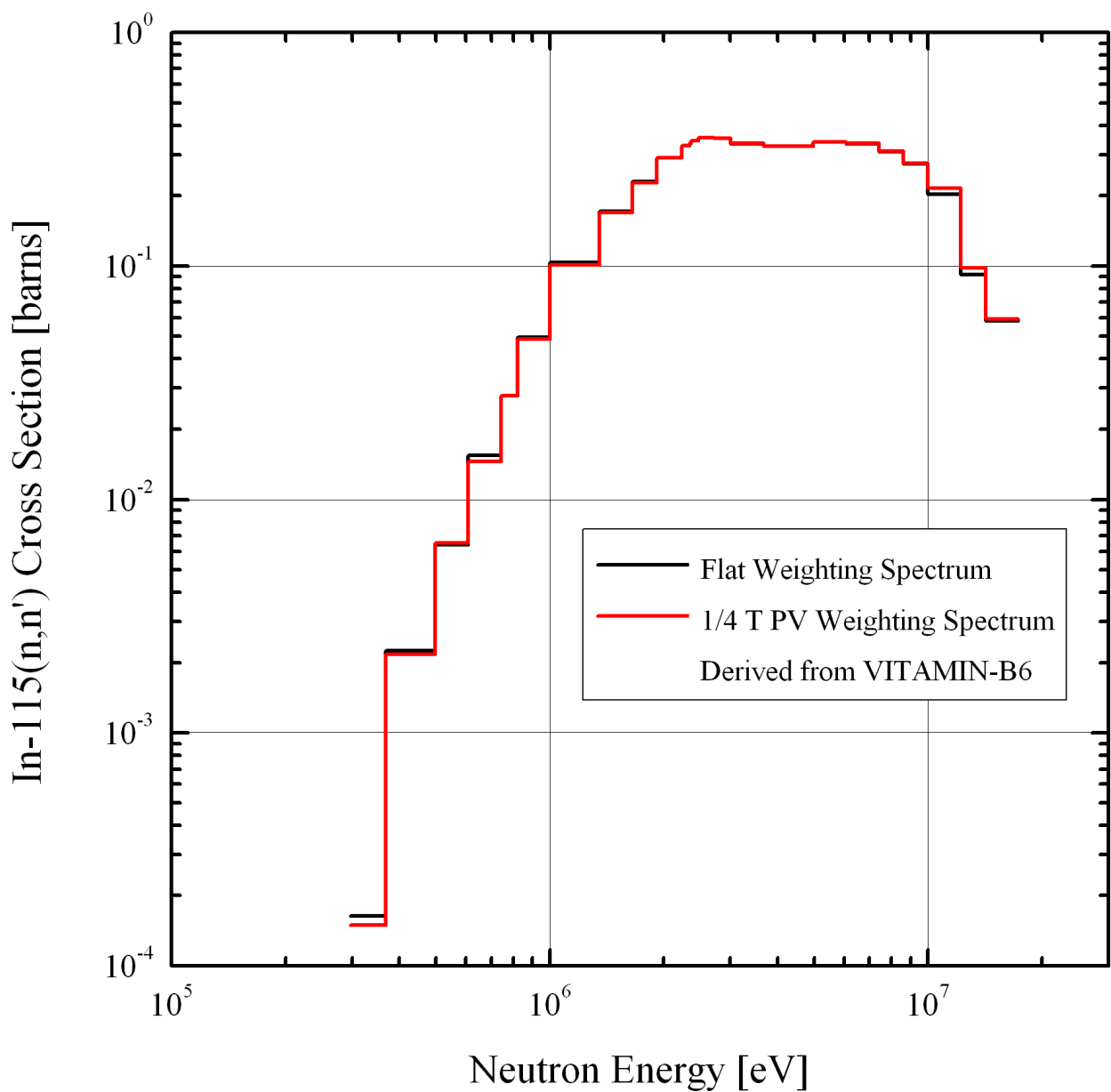


Figure 21

Comparison of the IRDF-2002 Flat Weighting and 1/4 T PV Weighting  
 S-32(n,p)P-32 Dosimeter Cross Sections  
 Used with the BUGJEFF311.BOLIB Library.

47-Group Neutron Energy Structure Typical of the BUGLE-Type Libraries.

1/4 T PV Weighting S-32(n,p)P-32 Neutron Cross Sections  
 Obtained through Data Processing Using the 199-Group Neutron Spectrum  
 Calculated in the 1/4 T PV Position with the VITJEFF311.BOLIB Library.

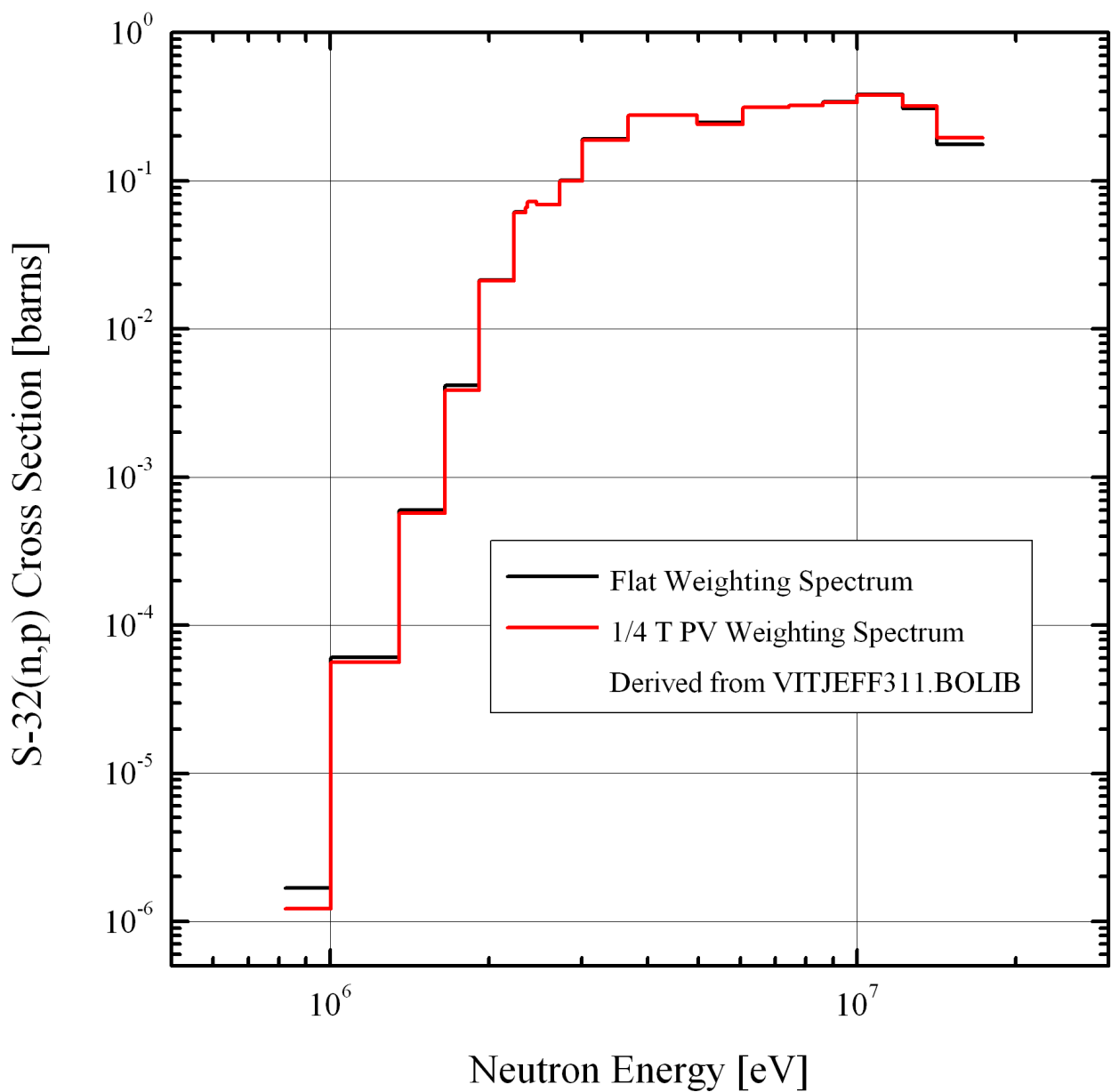


Figure 22

Comparison of the IRDF-2002 Flat Weighting and 1/4 T PV Weighting  
 S-32(n,p)P-32 Dosimeter Cross Sections  
 Used with the BUGLE-96 Library.

47-Group Neutron Energy Structure Typical of the BUGLE-Type Libraries.

1/4 T PV Weighting S-32(n,p)P-32 Neutron Cross Sections  
 Obtained through Data Processing Using the 199-Group Neutron Spectrum  
 Calculated in the 1/4 T PV Position with the VITAMIN-B6 Library.

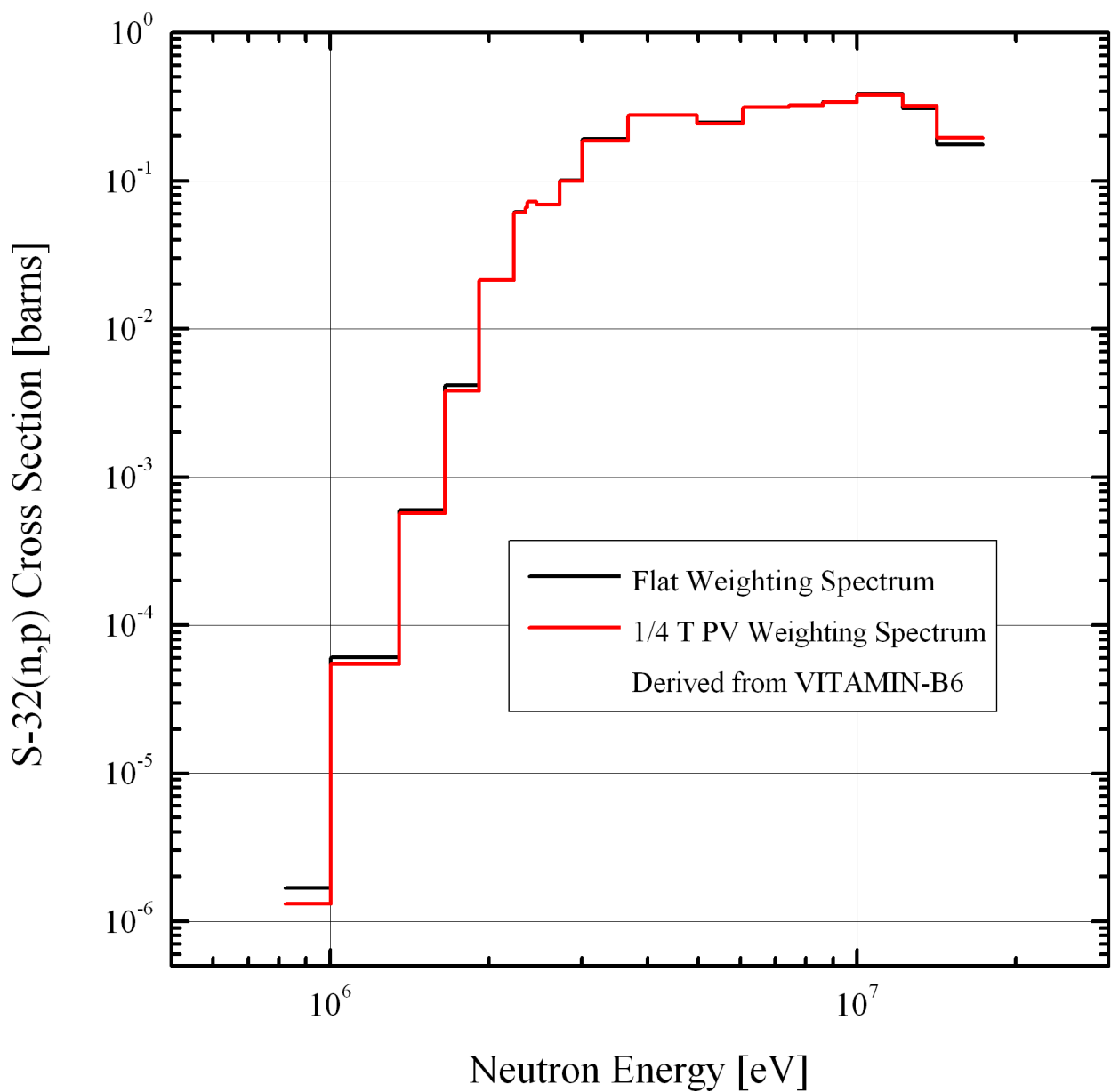




Figure 23

Comparison of the IRDF-2002 Flat Weighting and 1/4 T PV Weighting  
 Al-27(n, $\alpha$ )Na-24 Dosimeter Cross Sections  
 Used with the BUGJEFF311.BOLIB Library.

47-Group Neutron Energy Structure Typical of the BUGLE-Type Libraries.

1/4 T PV Weighting Al-27(n, $\alpha$ )Na-24 Neutron Cross Sections  
 Obtained through Data Processing Using the 199-Group Neutron Spectrum  
 Calculated in the 1/4 T PV Position with the VITJEFF311.BOLIB Library.

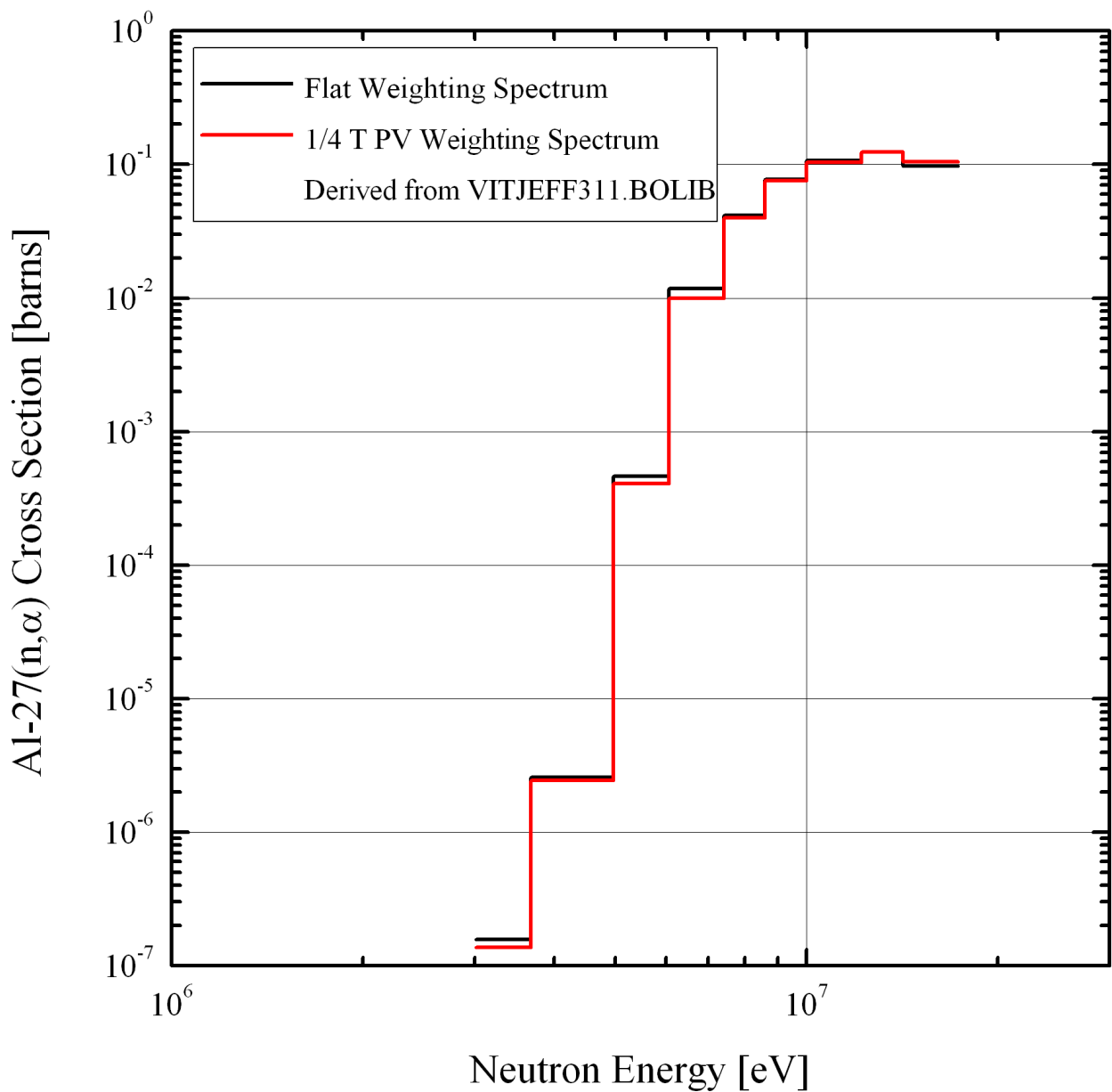


Figure 24

Comparison of the IRDF-2002 Flat Weighting and 1/4 T PV Weighting  
 Al-27(n, $\alpha$ )Na-24 Dosimeter Cross Sections  
 Used with the BUGLE-96 Library.

47-Group Neutron Energy Structure Typical of the BUGLE-Type Libraries.

1/4 T PV Weighting Al-27(n, $\alpha$ )Na-24 Neutron Cross Sections  
 Obtained through Data Processing Using the 199-Group Neutron Spectrum  
 Calculated in the 1/4 T PV Position with the VITAMIN-B6 Library.

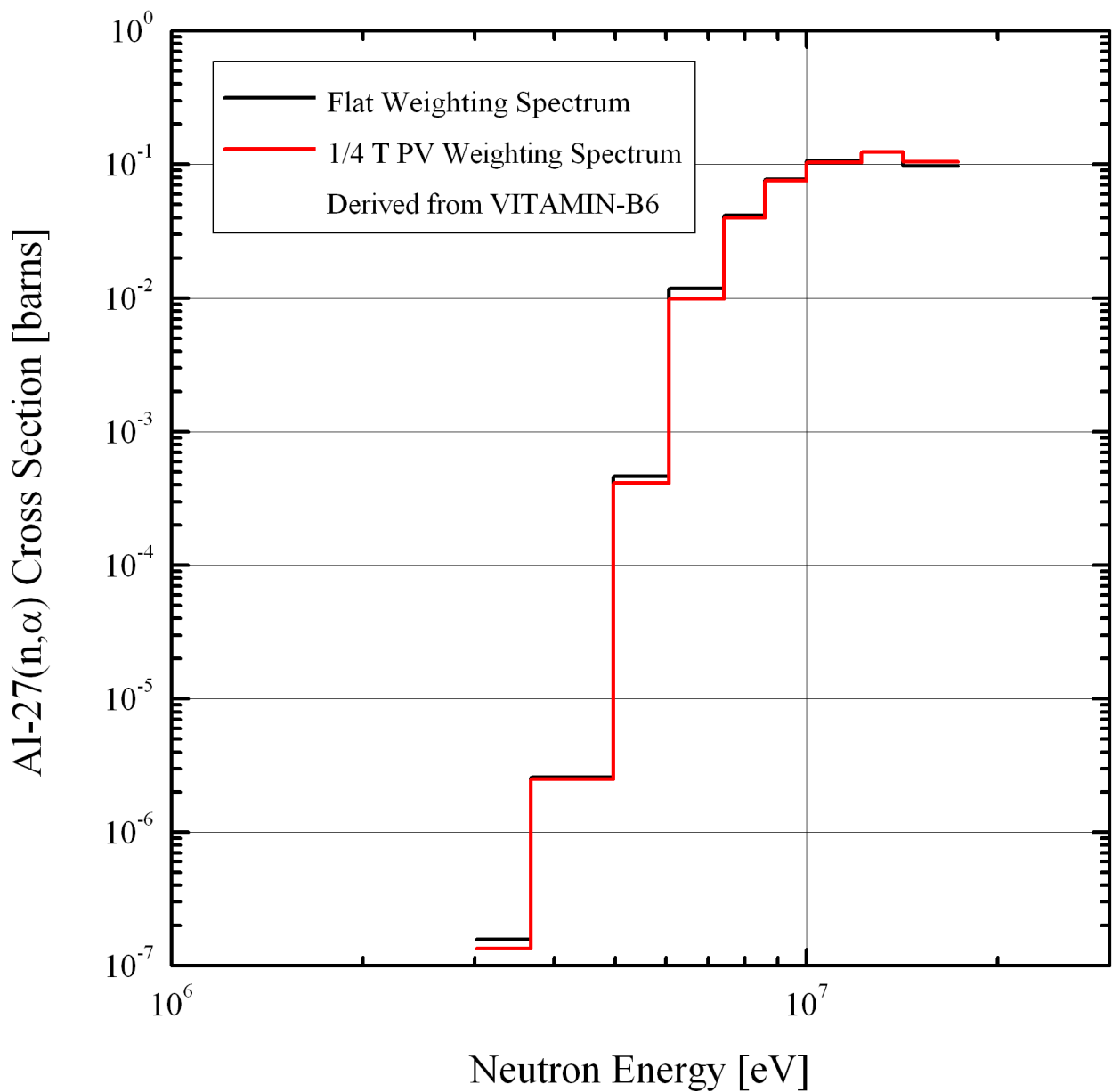


Figure 25

Ratio (1/4 T PV Weighting / Flat Weighting)  
of the Al-27(n, $\alpha$ )Na-24 Neutron Cross Sections  
Used with the BUGJEFF311.BOLIB Library.

47-Group Neutron Energy Structure Typical of the BUGLE-Type Libraries.

1/4 T PV Weighting Al-27(n, $\alpha$ )Na-24 Neutron Cross Sections  
Obtained through Data Processing Using the 199-Group Neutron Spectrum  
Calculated in the 1/4 T PV Position with the VITJEFF311.BOLIB Library.

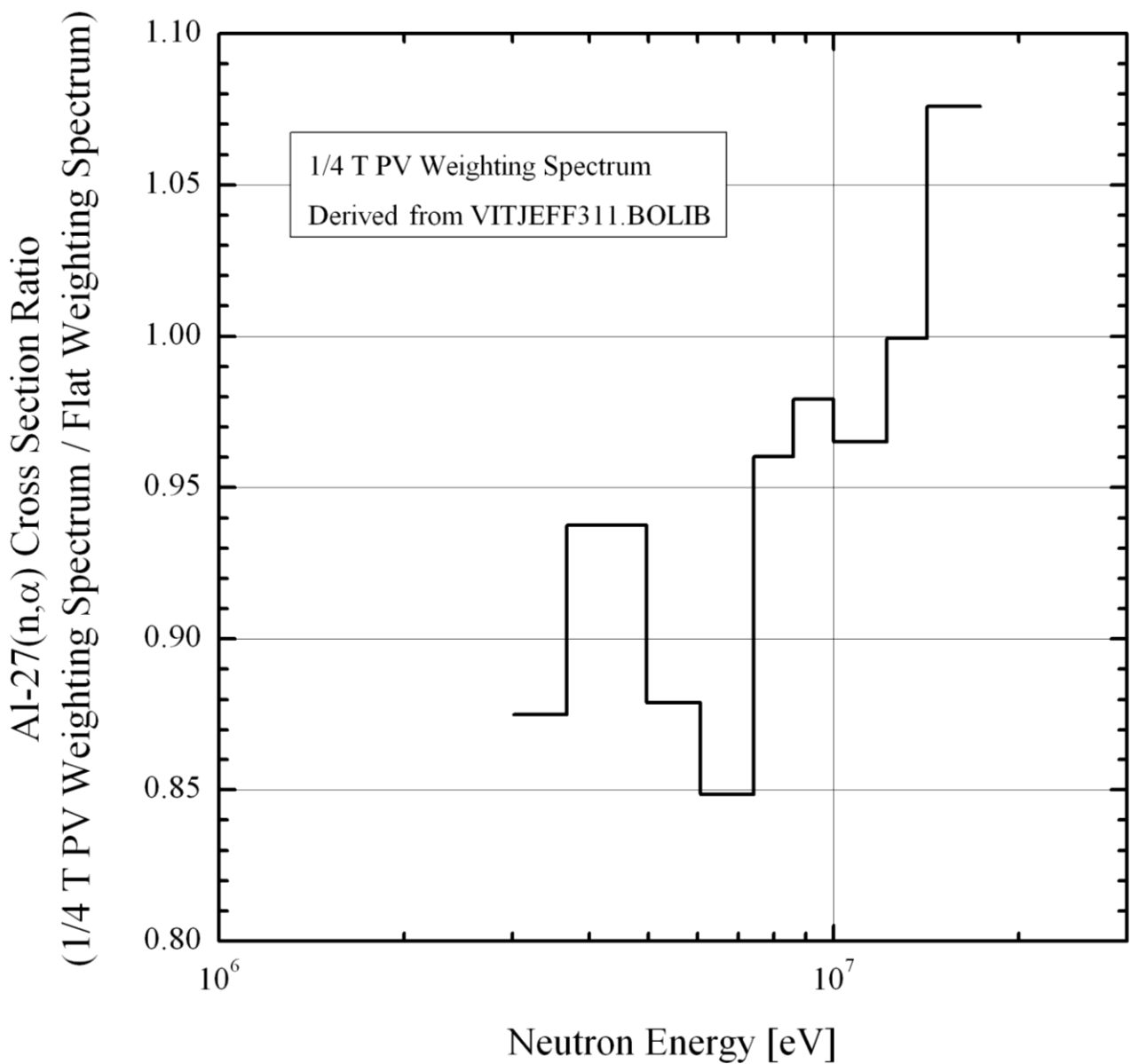
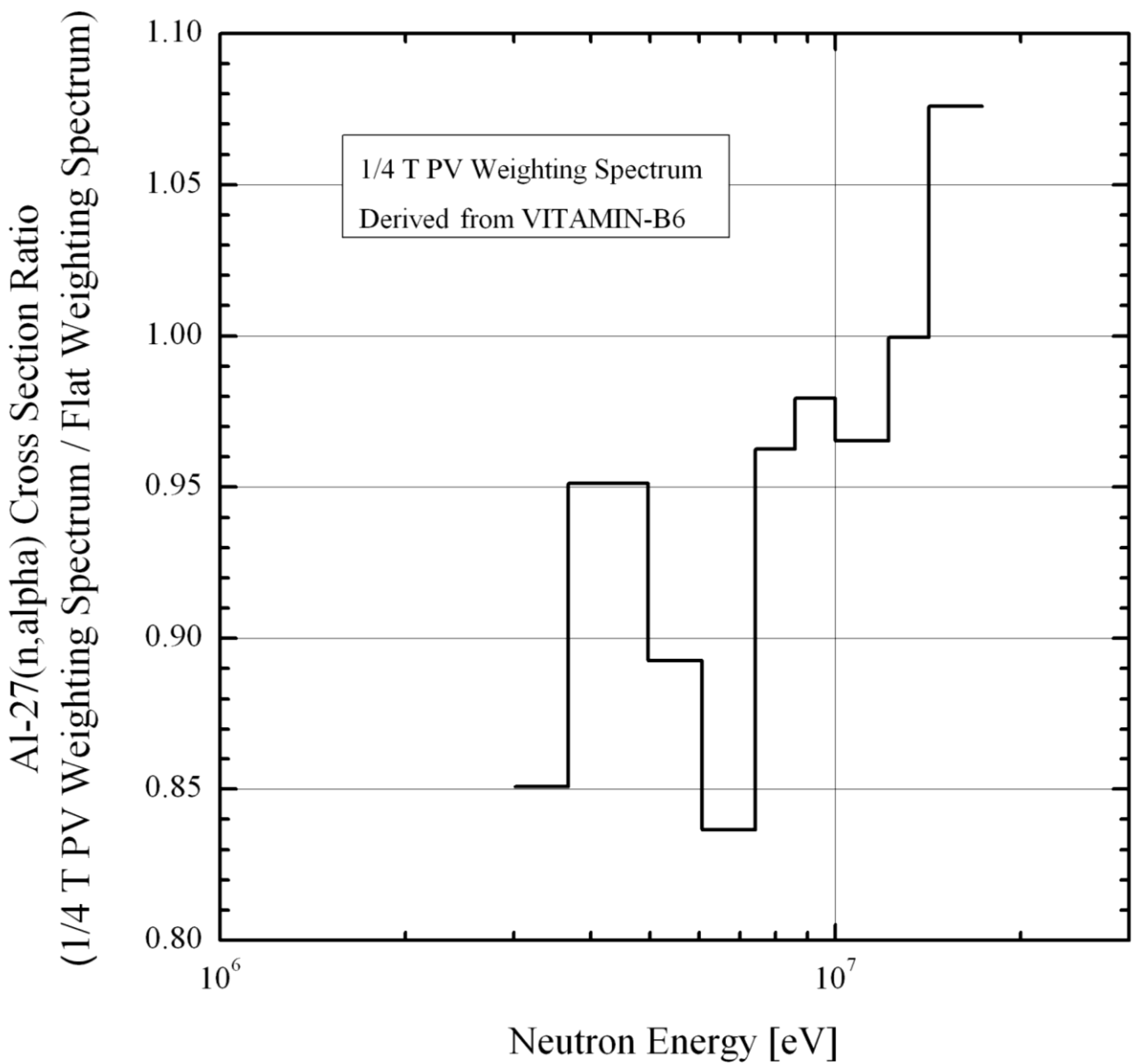



Figure 26

Ratio (1/4 T PV Weighting / Flat Weighting)  
of the Al-27(n, $\alpha$ )Na-24 Neutron Cross Sections  
Used with the BUGLE-96 Library.

47-Group Neutron Energy Structure Typical of the BUGLE-Type Libraries.

1/4 T PV Weighting Al-27(n, $\alpha$ )Na-24 Neutron Cross Sections  
Obtained through Data Processing Using the 199-Group Neutron Spectrum  
Calculated in the 1/4 T PV Position with the VITAMIN-B6 Library.



 <b>Ricerca Sistema Elettrico</b>	<b>Sigla di identificazione</b>	<b>Rev.</b>	<b>Distrib.</b>	<b>Pag.</b>	<b>di</b>
	ADPFISS-LP1-087	0	L	50	92

### 3.2.2 - Neutron Source Normalization

The following approach was adopted with respect to the fission neutron source normalization. Taking into account that the fission plate neutron source is given in units of neutrons  $\times \text{cm}^{-3} \times \text{second}^{-1} \times 1.0\text{E}+07$  (see Table 4), corresponding to 1 Watt of fission plate power, the “xnf” normalization factor in TORT-3.2 is given by:

$$\text{xfn} = 5.68\text{E}-04 \times 3.0\text{E}+04 \times 1.0\text{E}-24 = 1.704\text{E}-25$$

where

5.68E-04 (see /2/) are the fission plate Watts per NESTOR reactor Watt,

3.0E+04 Watts (see /2/) is the NESTOR reactor power and

1.0E-24 is a conversion factor taking into account that the atomic densities introduced in TORT-3.2 were expressed in atoms  $\times \text{barn}^{-1} \times \text{cm}^{-1}$ .

### 3.3 - Discussion of the Results

The Iron-88 reaction rates for the Au-197(n, $\gamma$ )Au-198 activation dosimeters and for the Rh-103(n,n')Rh-103m, In-115(n,n')In-115m, S-32(n,p)P-32 and Al-27(n, $\alpha$ )Na-24 threshold activation dosimeters (see 2.3), calculated using the BUGJEFF311.BOLIB and BUGLE-96 libraries, were compared with the corresponding experimental results.

The experimental dosimetric results were obtained in Iron-88 with five activation dosimeters located (see Figure 2, Tables 8÷12 and 2.3) in fourteen measurement positions. In particular the Au-197(n, $\gamma$ )Au-198 and S-32(n,p)P-32 dosimeters were positioned in all the fourteen measurement positions located in the air gaps between the mild steel slab components, the Rh-103(n,n')Rh-103m dosimeters in thirteen positions, the In-115(n,n')In-115m dosimeters in ten positions and the Al-27(n, $\alpha$ )Na-24 dosimeters only in four positions.

The calculated reaction rate results obtained with flat weighting and 1/4 T PV weighting dosimeter cross sections are reported in Tables 7 and 8 for Au-197(n, $\gamma$ )Au-198, in Table 9 for Rh-103(n,n')Rh-103m, in Table 10 for In-115(n,n')In-115m, in Table 11 for S-32(n,p)P-32 and in Table 12 for Al-27(n, $\alpha$ )Na-24.

The dosimeter total experimental uncertainties at the specific measurement positions and at the confidence level of one standard deviation ( $1\sigma$ ) were taken from the “General Description of the Experiment” document, included in the Iron-88 section of the SINBAD REACTOR /3/ database.

The experimental reaction rates for all the five activation dosimeters were respectively taken from the Table 8 of reference /2/ for sulphur dosimeters, from the Table 9 for indium dosimeters, from the Table 10 for rhodium dosimeters, from the Table 11 for gold dosimeters and from the Table 12 for aluminium dosimeters. It is underlined that the experimental results for the gold dosimeters, presented in the Table 11 of reference /2/, take into account a correction for the NESTOR core neutron leakage background whilst, on the contrary, the “as measured” experimental reaction rates for the other four threshold activation dosimeters, reported in the previously cited tables of reference /2/, contain a contribution from the NESTOR core neutron leakage background (see 2.3). Consequently, since the Calculated (C) reaction rates refer only to the neutrons produced in the fission plate, the “as measured” Experimental (E) reaction rate values in the C/E ratios, reported in the Tables 9÷12 of the present work, are reduced by 2% to eliminate the NESTOR reactor background component in all the measurement positions for all the four threshold activation dosimeters, as recommended at page 2 of reference /2/. All the calculated results shown in the previously cited Tables 7÷12 were obtained using the BUGJEFF311.BOLIB and the BUGLE-96 libraries together with the TORT-3.2 code in P<sub>3</sub>-S<sub>8</sub> approximation.

The Figures 27÷36 show the comparisons of the results of the calculations with the BUGJEFF311.BOLIB and BUGLE-96 libraries using alternatively flat weighting or 1/4 T PV weighting dosimeter cross sections. In particular the Figures 27 and 28 for the gold dosimeters correspond to Table 8, the Figures 29 and 30 for the rhodium dosimeters to Table 9, the Figures 31 and 32 for the indium dosimeters to Table 10, the Figures 33 and 34 for the sulphur dosimeters to Table 11, and finally the Figures 35 and 36 for the aluminium dosimeters to Table 12.

The calculations using the BUGJEFF311.BOLIB library give the following results.

The Au-197(n, $\gamma$ )Au-198 calculated reaction rates using 1/4 T PV weighting dosimeter cross sections, corresponding to epi-cadmium measurements, present deviations (see Table 8 and Figure 27) from the corresponding experimental results contained within  $\pm 15\%$  and a systematic trend to overestimate the experimental results. When flat weighting dosimeter cross sections are employed, the deviations (see Table 8 and Figure 28) of the calculated epi-cadmium reaction rates are within an increased  $\pm 25\%$ . Meaningful differences between the results obtained with flat weighting dosimeter cross sections and those calculated with 1/4 T PV weighting dosimeter cross sections are found. In fact, with flat weighting dosimeter cross sections, the deviations from the corresponding experimental results are systematically overestimated between about 6% and 10% with respect to the corresponding results obtained with 1/4 T PV weighting dosimeter cross sections which permit to have calculated results significantly more in agreement with the corresponding experimental results. The Figures 15 and 16, referring to the Au-197(n, $\gamma$ )Au-198 neutron cross sections, respectively used in the calculations with the BUGJEFF311.BOLIB and BUGLE-96 libraries, show group cross section ratios which permit in particular to appreciate the differences between flat weighting and 1/4 T PV weighting self-shielded cross sections.

The Rh-103(n,n')Rh-103m calculated reaction rates present deviations (see Table 9 and Figures 29 and 30) from the corresponding experimental results contained within  $\pm 20\%$  and are characterized by a trend to overestimation, independently of the use of flat weighting or 1/4 T PV weighting dosimeter cross sections.

The In-115(n,n')In-115m calculated reaction rates show deviations (see Table 10 and Figures 31 and 32) from the corresponding experimental results contained within  $\pm 15\text{-}20\%$  and present a trend to underestimation with increasing neutron penetration depth, independently of the use of flat weighting or 1/4 T PV weighting dosimeter cross sections.

Concerning the S-32(n,p)P-32 calculated reaction rates, the results obtained with flat weighting and 1/4 T PV weighting dosimeter cross sections give deviations (see Table 11 and Figures 33 and 34) from the corresponding experimental results within  $\pm 15\text{-}20\%$  and show a systematic trend to underestimation.

Finally for the Al-27(n, $\alpha$ )Na-24 calculated reaction rates obtained with 1/4 T PV weighting dosimeter cross sections, systematic overestimated deviations (see Table 12 and Figure 35) from the corresponding experimental results up to +30% are noted. It is underlined that only for these threshold activation dosimeters, with the highest effective threshold energy of 7.30 MeV, there are meaningful differences between the results obtained with flat weighting dosimeter cross sections and those calculated with 1/4 T PV weighting dosimeter cross sections.

In fact with flat weighting dosimeter cross sections, the deviations from the corresponding experimental results are systematically overestimated (see Table 12 and Figure 36) by about 8%, with respect to the corresponding results obtained with 1/4 T PV weighting dosimeter cross sections. The Figures 25 and 26, referring to the Al-27(n, $\alpha$ )Na-24 neutron cross sections respectively used in the calculations with the BUGJEFF311.BOLIB and BUGLE-96 libraries, show group cross section ratios which permit in particular to appreciate the differences between the flat weighting and the 1/4 T PV weighting dosimeter cross sections.

Concerning the BUGLE-96 results, it is noted that for the Au-197(n, $\gamma$ )Au-198 (see Table 8 and Figures 27 and 28) activation dosimeters and for the three Rh-103(n,n')Rh-103m (see Table 9 and Figures 29 and 30), In-115(n,n')In-115m (see Table 10 and Figures 31 and 32) and S-32(n,p)P-32 (see Table 11 and Figures 33 and 34) activation dosimeters with lower effective threshold energy, the BUGLE-96 results are systematically lower with respect to the corresponding BUGJEFF311.BOLIB results. On the contrary, for the Al-27(n, $\alpha$ )Na-24 (see Table 12 and Figures 35 and 36) dosimeters with the highest effective threshold energy, the BUGLE-96 reaction rate results are higher with respect to the corresponding BUGJEFF311.BOLIB results.

Table 7 shows the differences in the gold calculated reaction rates obtained through transport calculations using alternatively the first 44 or the first 45 neutron groups of the BUGLE-type neutron energy structure (see Table 5) of the BUGJEFF311.BOLIB library. It was intended in this way to verify the impact of different cadmium cutoff energies (0.876 eV with the 44-group calculation or 0.414 eV with the 45-group calculation), for the upper thermal threshold energy (see 3.2.1), on the corresponding calculated reaction rates.

Taking into account the experimental cadmium cutoff energy of 0.73 eV, corresponding to the cadmium cover thickness of 1.27 mm, used for the gold dosimeters employed in the Iron-88 benchmark experiment, it was decided to assume the 44-group calculations (corresponding to a cadmium cutoff energy of 0.876 eV) with both the BUGJEFF311.BOLIB and BUGLE-96 libraries as the most proper reference choice (see Table 8 and Figures 27 and 28). In this way it was obtained better agreement with the gold experimental reaction rates. On the other hand it was verified and it is underlined that, summing up alternatively the contributions of the first 44 or 45 neutron groups (see Table 5) in the Iron-88 calculations using the BUGJEFF311.BOLIB library, the total gold reaction rate difference in each dosimeter position between the two calculations is limited to few percents (see Table 7).

Figures 37÷46 show the comparisons of the results of the calculations with flat weighting and 1/4 T PV weighting dosimeter cross sections using alternatively the BUGJEFF311.BOLIB or the BUGLE-96 library. In particular Figures 37 and 38 for the gold dosimeters correspond to Table 8, Figures 39 and 40 for the rhodium dosimeters to Table 9, Figures 41 and 42 for the indium dosimeters to Table 10, Figures 43 and 44 for the sulphur dosimeters to Table 11 and, finally, Figures 45 and 46 for the aluminium dosimeters to Table 12.

The absolute values of the experimental and calculated reaction rates for the Au-197(n, $\gamma$ )Au-198, Rh-103(n,n')Rh-103m, In-115(n,n')In-115m, S-32(n,p)P-32 and Al-27(n, $\alpha$ )Na-24 activation dosimeters are respectively shown in Figures 47÷51 where subjective trend lines for the experimental reaction rates are represented. These trend lines connect in particular all the experimental reaction rates for the cited dosimeters and the experimental reaction rates are compared with the corresponding calculated reaction rates obtained using the BUGJEFF311.BOLIB library.

The spatial distributions of the neutron fluxes, the spatial distributions of the dosimeter reaction rates and the calculated neutron spectra in different measurement positions, obtained using the BUGJEFF311.BOLIB library and the TORT-3.2 code in P<sub>3</sub>-S<sub>8</sub> approximation, are respectively reported in Figures 52÷56 for the neutron fluxes, in Figures 57÷61 for the dosimeter reaction rates and in Figures 62÷63 for the calculated neutron spectra.



The spatial distributions of the neutron fluxes for neutron energies above 0.414 eV, 0.1 MeV, 1.0 MeV, 3.0 MeV and 8.0 MeV are respectively presented in Figures 52÷56 in the Iron-88 horizontal section at  $Y = 0.0$  cm (see Figure 8).

The spatial distributions of the reaction rates for the Au-197(n, $\gamma$ )Au-198, Rh-103(n,n')Rh-103m, In-115(n,n')In-115m, S-32(n,p)P-32 and Al-27(n, $\alpha$ )Na-24 activation dosimeters are shown respectively in Figures 57÷61 in the Iron-88 horizontal section at  $Y = 0.0$  cm (see Figure 8).

It is underlined that, in practice, the reaction rate results coming from Au-197(n, $\gamma$ )Au-198 correspond to neutron fluxes above about 0.414 eV, the results coming from Rh-103(n,n')Rh-103m correspond to neutron fluxes above about 0.1 MeV, the results coming from In-115(n,n')In-115m to neutron fluxes above about 1.0 MeV, the results coming from S-32(n,p)P-32 to neutron fluxes above about 3.0 MeV and, finally, the results coming from Al-27(n, $\alpha$ )Na-24 to neutron fluxes above about 8.0 MeV (see also 3.2.1 and Table 3).

Finally, a comparison of the calculated neutron spectra above 0.414 eV at various Iron-88 measurement positions (A2, A4, A8, A12 and A15) is shown in Figure 62. An enlargement of the previous figure is reported in Figure 63 for neutron energies above 0.1 MeV. The different black and red colours in the previously cited figures are here alternatively used only to distinguish better the different spectral trends.

In conclusion, the BUGJEFF311.BOLIB library permitted to obtain calculated results, for the Au-197(n, $\gamma$ )Au-198 activation dosimeters and for the three Rh-103(n,n')Rh-103m, In-115(n,n')In-115m and S-32(n,p)P-32 activation dosimeters with lower effective threshold energy, characterized by deviations of  $\pm 15$ -20% from the corresponding experimental results. Only the calculations with the Al-27(n, $\alpha$ )Na-24 dosimeter cross sections gave systematically results excessively overestimated (from 20% up to about 30%) with respect to the corresponding experimental results.

Taking into account the total experimental uncertainties at the confidence level of one standard deviation ( $1\sigma$ ) of the Au-197(n, $\gamma$ )Au-198, Rh-103(n,n')Rh-103m, In-115(n,n')In-115m and S-32(n,p)P-32 dosimeters, the corresponding calculated reaction rate results presented in this work exhibit good statistical consistency with the corresponding measurements. On the contrary, the calculated reaction rates for the Al-27(n, $\alpha$ )Na-24 dosimeters are always excessively overestimated with respect to the corresponding experimental results, taking into account their related uncertainties at the confidence level of one standard deviation ( $1\sigma$ ).

Table 7

Iron-88 - Comparison of the Au-197(n, $\gamma$ )Au-198 epi-Cadmium Reaction Rate Ratios (Calculated/Experimental) in 44-Group and 45-Group Calculations.

P<sub>3</sub>-S<sub>8</sub> Calculations Using the BUGJEFF311.BOLIB Library with Flat Weighting and 1/4 T PV Weighting Dosimeter Cross Sections.

**Au-197(n, $\gamma$ ) Flat Weighting**

Position	Shield Thickness [cm]	Experiment RR <sup>a,b</sup> (E)	Total Error (1 $\sigma$ ) [%]	44-Group Calculation RR <sup>a</sup> (C)	C/E	45-Group Calculation RR <sup>a</sup> (C)	C/E
A2	0.00	1.05E-14	4.2	1.31370E-14	1.25	1.34822E-14	1.28
A3	5.10	6.24E-15	4.2	7.55178E-15	1.21	7.65235E-15	1.23
A4	10.22	4.19E-15	4.2	4.89977E-15	1.17	4.94665E-15	1.18
A5	15.34	2.97E-15	4.2	3.40712E-15	1.15	3.43609E-15	1.16
A6	20.44	2.19E-15	4.2	2.51225E-15	1.15	2.53259E-15	1.16
A7	25.64	1.70E-15	4.2	1.93419E-15	1.14	1.94938E-15	1.15
A8	30.79	1.35E-15	4.2	1.54726E-15	1.15	1.55917E-15	1.15
A9	35.99	1.11E-15	4.2	1.26321E-15	1.14	1.27282E-15	1.15
A10	41.19	9.10E-16	4.2	1.04319E-15	1.15	1.05108E-15	1.16
A11	46.44	7.67E-16	4.2	8.63161E-16	1.13	8.69683E-16	1.13
A12	51.62	6.55E-16	4.2	7.15482E-16	1.09	7.20898E-16	1.10
A13	56.69	5.44E-16	4.2	5.94104E-16	1.09	5.98616E-16	1.10
A14	61.81	4.62E-16	4.2	4.91605E-16	1.06	4.95355E-16	1.07
A15	66.99	3.99E-16	4.2	4.06232E-16	1.02	4.09343E-16	1.03

<sup>a</sup> RR = Reaction Rates in units of reactions per second per atom at the NESTOR reactor maximum power (30 kW).

<sup>b</sup> The reported RR were already corrected for the NESTOR reactor background component. These data were used to obtain the C/E ratios.

**Au-197(n, $\gamma$ ) 1/4 T PV Weighting**

Position	Shield Thickness [cm]	Experiment RR <sup>a,b</sup> (E)	Total Error (1 $\sigma$ ) [%]	44-Group Calculation RR <sup>a</sup> (C)	C/E	45-Group Calculation RR <sup>a</sup> (C)	C/E
A2	0.00	1.05E-14	4.2	1.19920E-14	1.14	1.23396E-14	1.18
A3	5.10	6.24E-15	4.2	7.01968E-15	1.12	7.12096E-15	1.14
A4	10.22	4.19E-15	4.2	4.58651E-15	1.09	4.63372E-15	1.11
A5	15.34	2.97E-15	4.2	3.19971E-15	1.08	3.22889E-15	1.09
A6	20.44	2.19E-15	4.2	2.36461E-15	1.08	2.38509E-15	1.09
A7	25.64	1.70E-15	4.2	1.82371E-15	1.07	1.83901E-15	1.08
A8	30.79	1.35E-15	4.2	1.46064E-15	1.08	1.47263E-15	1.09
A9	35.99	1.11E-15	4.2	1.19334E-15	1.08	1.20302E-15	1.08
A10	41.19	9.10E-16	4.2	9.85801E-16	1.08	9.93749E-16	1.09
A11	46.44	7.67E-16	4.2	8.15704E-16	1.06	8.22273E-16	1.07
A12	51.62	6.55E-16	4.2	6.76052E-16	1.03	6.81506E-16	1.04
A13	56.69	5.44E-16	4.2	5.61227E-16	1.03	5.65771E-16	1.04
A14	61.81	4.62E-16	4.2	4.64256E-16	1.00	4.68032E-16	1.01
A15	66.99	3.99E-16	4.2	3.83510E-16	0.96	3.86643E-16	0.97

<sup>a</sup> RR = Reaction Rates in units of reactions per second per atom at the NESTOR reactor maximum power (30 kW).

<sup>b</sup> The reported RR were already corrected for the NESTOR reactor background component. These data were used to obtain the C/E ratios.

Table 8

Iron-88 - Summary of Experimental (E) and Calculated (C)  
 Au-197(n, $\gamma$ )Au-198 epi-Cadmium Reaction Rates along the Z Horizontal Axis

P<sub>3</sub>-S<sub>8</sub> Calculations Using the BUGJEFF311.BOLIB and BUGLE-96 Libraries  
 with Flat Weighting and 1/4 T PV Weighting Dosimeter Cross Sections.

**Au-197(n, $\gamma$ ) Flat Weighting**

Position	Shield Thickness [cm]	Experiment RR <sup>a,b</sup> (E)	Total Error (1 $\sigma$ ) [%]	BUGJEFF311 Calculation RR <sup>a</sup> (C)	C/E	BUGLE-96 Calculation RR <sup>a</sup> (C)	C/E
A2	0.00	1.05E-14	4.2	1.31370E-14	1.25	1.28366E-14	1.22
A3	5.10	6.24E-15	4.2	7.55178E-15	1.21	7.24905E-15	1.16
A4	10.22	4.19E-15	4.2	4.89977E-15	1.17	4.72741E-15	1.13
A5	15.34	2.97E-15	4.2	3.40712E-15	1.15	3.31582E-15	1.12
A6	20.44	2.19E-15	4.2	2.51225E-15	1.15	2.46337E-15	1.12
A7	25.64	1.70E-15	4.2	1.93419E-15	1.14	1.90554E-15	1.12
A8	30.79	1.35E-15	4.2	1.54726E-15	1.15	1.52590E-15	1.13
A9	35.99	1.11E-15	4.2	1.26321E-15	1.14	1.24277E-15	1.12
A10	41.19	9.10E-16	4.2	1.04319E-15	1.15	1.02108E-15	1.12
A11	46.44	7.67E-16	4.2	8.63161E-16	1.13	8.38866E-16	1.09
A12	51.62	6.55E-16	4.2	7.15482E-16	1.09	6.89519E-16	1.05
A13	56.69	5.44E-16	4.2	5.94104E-16	1.09	5.67253E-16	1.04
A14	61.81	4.62E-16	4.2	4.91605E-16	1.06	4.64550E-16	1.01
A15	66.99	3.99E-16	4.2	4.06232E-16	1.02	3.79452E-16	0.95

<sup>a</sup> RR = Reaction Rates in units of reactions per second per atom at the NESTOR reactor maximum power (30 kW).

<sup>b</sup> The reported RR were already corrected for the NESTOR reactor background component. These data were used to obtain the C/E ratios.

**Au-197(n, $\gamma$ ) 1/4 T PV Weighting**

Position	Shield Thickness [cm]	Experiment RR <sup>a,b</sup> (E)	Total Error (1 $\sigma$ ) [%]	BUGJEFF311 Calculation RR <sup>a</sup> (C)	C/E	BUGLE-96 Calculation RR <sup>a</sup> (C)	C/E
A2	0.00	1.05E-14	4.2	1.19920E-14	1.14	1.17502E-14	1.12
A3	5.10	6.24E-15	4.2	7.01968E-15	1.12	6.77962E-15	1.09
A4	10.22	4.19E-15	4.2	4.58651E-15	1.09	4.45462E-15	1.06
A5	15.34	2.97E-15	4.2	3.19971E-15	1.08	3.13459E-15	1.06
A6	20.44	2.19E-15	4.2	2.36461E-15	1.08	2.33373E-15	1.07
A7	25.64	1.70E-15	4.2	1.82371E-15	1.07	1.80817E-15	1.06
A8	30.79	1.35E-15	4.2	1.46064E-15	1.08	1.44946E-15	1.07
A9	35.99	1.11E-15	4.2	1.19334E-15	1.08	1.18122E-15	1.06
A10	41.19	9.10E-16	4.2	9.85801E-16	1.08	9.70733E-16	1.07
A11	46.44	7.67E-16	4.2	8.15704E-16	1.06	7.97499E-16	1.04
A12	51.62	6.55E-16	4.2	6.76052E-16	1.03	6.55411E-16	1.00
A13	56.69	5.44E-16	4.2	5.61227E-16	1.03	5.39060E-16	0.99
A14	61.81	4.62E-16	4.2	4.64256E-16	1.00	4.41326E-16	0.96
A15	66.99	3.99E-16	4.2	3.83510E-16	0.96	3.60374E-16	0.90

<sup>a</sup> RR = Reaction Rates in units of reactions per second per atom at the NESTOR reactor maximum power (30 kW).

<sup>b</sup> The reported RR were already corrected for the NESTOR reactor background component. These data were used to obtain the C/E ratios.

Table 9

 Iron-88 - Summary of Experimental (E) and Calculated (C)  
 Rh-103(n,n')Rh-103m Reaction Rates along the Horizontal Z Axis.

## Rh-103(n,n') Flat Weighting

Position	Shield Thickness [cm]	Exp. RR <sup>a</sup> as Measured	Total Error (1σ) [%]	Exp. RR <sup>a,b</sup> without Background (E)	BUGJEFF311 Calculation RR <sup>a</sup> (C)	C/E	BUGLE-96 Calculation RR <sup>a</sup> (C)	C/E
A2	0.00	3.35E-16	5.1	3.28E-16	3.41610E-16	1.04	3.42973E-16	1.04
A3	5.10	1.42E-16	5.2	1.39E-16	1.50060E-16	1.08	1.49423E-16	1.07
A4	10.22	7.78E-17	5.1	7.62E-17	8.67702E-17	1.14	8.58214E-17	1.13
A5	15.34	4.70E-17	5.1	4.61E-17	5.27376E-17	1.14	5.18212E-17	1.13
A6	20.44	2.86E-17	5.2	2.80E-17	3.32228E-17	1.19	3.24300E-17	1.16
A7	25.64	1.82E-17	5.1	1.78E-17	2.12622E-17	1.19	2.06113E-17	1.16
A8	30.79	1.20E-17	5.1	1.18E-17	1.39108E-17	1.18	1.33901E-17	1.14
A9	35.99	7.97E-18	5.2	7.81E-18	9.18976E-18	1.18	8.78199E-18	1.12
A10	41.19	5.48E-18	5.2	5.37E-18	6.13757E-18	1.14	5.82288E-18	1.08
A11	46.44	3.84E-18	5.2	3.76E-18	4.11633E-18	1.09	3.87668E-18	1.03
A12	51.62	2.68E-18	5.1	2.63E-18	2.79215E-18	1.06	2.61051E-18	0.99
A13	56.69	1.89E-18	5.2	1.85E-18	1.91861E-18	1.04	1.78095E-18	0.96
A14	61.81	1.34E-18	5.1	1.31E-18	1.31908E-18	1.00	1.21543E-18	0.93
A15	66.99	-	-	-	-	-	-	-

<sup>a</sup> RR = Reaction Rates in units of reactions per second per atom at the NESTOR reactor maximum power (30 kW).

<sup>b</sup> RR "without background" are the experimental reaction rates reduced by 2% to eliminate the NESTOR reactor background component. These data are used to obtain the C/E ratios.

## Rh-103(n,n') 1/4 T PV Weighting

Position	Shield Thickness [cm]	Exp. RR <sup>a</sup> as Measured	Total Error (1σ) [%]	Exp. RR <sup>a,b</sup> without Background (E)	BUGJEFF311 Calculation RR <sup>a</sup> (C)	C/E	BUGLE-96 Calculation RR <sup>a</sup> (C)	C/E
A2	0.00	3.35E-16	5.1	3.28E-16	3.40180E-16	1.04	3.41214E-16	1.04
A3	5.10	1.42E-16	5.2	1.39E-16	1.49111E-16	1.07	1.48200E-16	1.06
A4	10.22	7.78E-17	5.1	7.62E-17	8.61097E-17	1.13	8.49630E-17	1.11
A5	15.34	4.70E-17	5.1	4.61E-17	5.22841E-17	1.14	5.12326E-17	1.11
A6	20.44	2.86E-17	5.2	2.80E-17	3.29125E-17	1.17	3.20303E-17	1.14
A7	25.64	1.82E-17	5.1	1.78E-17	2.10523E-17	1.18	2.03440E-17	1.14
A8	30.79	1.20E-17	5.1	1.18E-17	1.37686E-17	1.17	1.32114E-17	1.12
A9	35.99	7.97E-18	5.2	7.81E-18	9.09382E-18	1.16	8.66324E-18	1.11
A10	41.19	5.48E-18	5.2	5.37E-18	6.07277E-18	1.13	5.74394E-18	1.07
A11	46.44	3.84E-18	5.2	3.76E-18	4.07266E-18	1.08	3.82434E-18	1.02
A12	51.62	2.68E-18	5.1	2.63E-18	2.76251E-18	1.05	2.57555E-18	0.98
A13	56.69	1.89E-18	5.2	1.85E-18	1.89828E-18	1.02	1.75733E-18	0.95
A14	61.81	1.34E-18	5.1	1.31E-18	1.30516E-18	0.99	1.19947E-18	0.91
A15	66.99	-	-	-	-	-	-	-

<sup>a</sup> RR = Reaction Rates in units of reactions per second per atom at the NESTOR reactor maximum power (30 kW).

<sup>b</sup> RR "without background" are the experimental reaction rates reduced by 2% to eliminate the NESTOR reactor background component. These data are used to obtain the C/E ratios.

Table 10

Iron-88 - Summary of Experimental (E) and Calculated (C)  
In-115(n,n')In-115m Reaction Rates along the Horizontal Z Axis.

## In-115(n,n') Flat Weighting

Position	Shield Thickness [cm]	Exp. RR <sup>a</sup> as Measured	Total Error (1σ) [%]	Exp. RR <sup>a,b</sup> without Background (E)	BUGJEFF311 Calculation RR <sup>a</sup> (C)	C/E	BUGLE-96 Calculation RR <sup>a</sup> (C)	C/E
A2	0.00	7.02E-17	4.5	6.88E-17	7.15052E-17	1.04	7.17707E-17	1.04
A3	5.10	2.40E-17	4.5	2.35E-17	2.27472E-17	0.97	2.26078E-17	0.96
A4	10.22	1.06E-17	4.5	1.04E-17	1.02723E-17	0.99	1.01409E-17	0.98
A5	15.34	5.14E-18	4.5	5.04E-18	4.89770E-18	0.97	4.80992E-18	0.95
A6	20.44	2.53E-18	4.5	2.48E-18	2.43008E-18	0.98	2.37515E-18	0.96
A7	25.64	1.32E-18	4.5	1.29E-18	1.22881E-18	0.95	1.19474E-18	0.92
A8	30.79	7.21E-19	4.5	7.07E-19	6.43201E-19	0.91	6.21436E-19	0.88
A9	35.99	3.93E-19	4.6	3.85E-19	3.43725E-19	0.89	3.29522E-19	0.86
A10	41.19	2.21E-19	4.6	2.17E-19	1.88652E-19	0.87	1.79248E-19	0.83
A11	46.44	1.28E-19	4.7	1.25E-19	1.05383E-19	0.84	9.91191E-20	0.79
A12	51.62	-	-	-	-	-	-	-
A13	56.69	-	-	-	-	-	-	-
A14	61.81	-	-	-	-	-	-	-
A15	66.99	-	-	-	-	-	-	-

<sup>a</sup> RR = Reaction Rates in units of reactions per second per atom at the NESTOR reactor maximum power (30 kW).

<sup>b</sup> RR "without background" are the experimental reaction rates reduced by 2% to eliminate the NESTOR reactor background component. These data are used to obtain the C/E ratios.

## In-115(n,n') 1/4 T PV Weighting

Position	Shield Thickness [cm]	Exp. RR <sup>a</sup> as Measured	Total Error (1σ) [%]	Exp. RR <sup>a,b</sup> without Background (E)	BUGJEFF311 Calculation RR <sup>a</sup> (C)	C/E	BUGLE-96 Calculation RR <sup>a</sup> (C)	C/E
A2	0.00	7.02E-17	4.5	6.88E-17	7.11248E-17	1.03	7.13646E-17	1.04
A3	5.10	2.40E-17	4.5	2.35E-17	2.25498E-17	0.96	2.23923E-17	0.95
A4	10.22	1.06E-17	4.5	1.04E-17	1.01599E-17	0.98	1.00171E-17	0.96
A5	15.34	5.14E-18	4.5	5.04E-18	4.83372E-18	0.96	4.73912E-18	0.94
A6	20.44	2.53E-18	4.5	2.48E-18	2.39330E-18	0.97	2.33429E-18	0.94
A7	25.64	1.32E-18	4.5	1.29E-18	1.20770E-18	0.93	1.17123E-18	0.91
A8	30.79	7.21E-19	4.5	7.07E-19	6.30919E-19	0.89	6.07748E-19	0.86
A9	35.99	3.93E-19	4.6	3.85E-19	3.36548E-19	0.87	3.21528E-19	0.83
A10	41.19	2.21E-19	4.6	2.17E-19	1.84412E-19	0.85	1.74534E-19	0.81
A11	46.44	1.28E-19	4.7	1.25E-19	1.02867E-19	0.82	9.63309E-20	0.77
A12	51.62	-	-	-	-	-	-	-
A13	56.69	-	-	-	-	-	-	-
A14	61.81	-	-	-	-	-	-	-
A15	66.99	-	-	-	-	-	-	-

<sup>a</sup> RR = Reaction Rates in units of reactions per second per atom at the NESTOR reactor maximum power (30 kW).

<sup>b</sup> RR "without background" are the experimental reaction rates reduced by 2% to eliminate the NESTOR reactor background component. These data are used to obtain the C/E ratios.

Table 11

 Iron-88 - Summary of Experimental (E) and Calculated (C)  
 S-32(n,p)P-32 Reaction Rates along the Horizontal Z Axis.

## S-32 (n,p) Flat Weighting

Position	Shield Thickness [cm]	Exp. RR <sup>a</sup> as Measured	Total Error (1σ) [%]	Exp. RR <sup>a,b</sup> without Background (E)	BUGJEFF311 Calculation RR <sup>a</sup> (C)	C/E	BUGLE-96 Calculation RR <sup>a</sup> (C)	C/E
A2	0.00	2.02E-17	6.5	1.98E-17	1.83602E-17	0.93	1.84440E-17	0.93
A3	5.10	4.29E-18	6.5	4.20E-18	3.74140E-18	0.89	3.68026E-18	0.88
A4	10.22	1.40E-18	6.5	1.37E-18	1.26967E-18	0.93	1.22978E-18	0.90
A5	15.34	5.12E-19	6.5	5.02E-19	4.65183E-19	0.93	4.45076E-19	0.89
A6	20.44	1.91E-19	6.5	1.87E-19	1.74899E-19	0.93	1.65574E-19	0.88
A7	25.64	7.13E-20	6.5	6.99E-20	6.55344E-20	0.94	6.14629E-20	0.88
A8	30.79	2.70E-20	6.6	2.65E-20	2.48779E-20	0.94	2.31380E-20	0.87
A9	35.99	1.03E-20	6.5	1.01E-20	9.35837E-21	0.93	8.63658E-21	0.86
A10	41.19	3.93E-21	6.5	3.85E-21	3.53309E-21	0.92	3.23855E-21	0.84
A11	46.44	1.49E-21	6.5	1.46E-21	1.32126E-21	0.90	1.20369E-21	0.82
A12	51.62	5.73E-22	6.5	5.62E-22	5.01085E-22	0.89	4.54099E-22	0.81
A13	56.69	2.27E-22	6.9	2.22E-22	1.94247E-22	0.87	1.75282E-22	0.79
A14	61.81	8.53E-23	8.6	8.36E-23	7.47260E-23	0.89	6.72015E-23	0.80
A15	66.99	3.50E-23	21.	3.43E-23	2.84802E-23	0.83	2.55487E-23	0.74

<sup>a</sup> RR = Reaction Rates in units of reactions per second per atom at the NESTOR reactor maximum power (30 kW).

<sup>b</sup> RR "without background" are the experimental reaction rates reduced by 2% to eliminate the NESTOR reactor background component. These data are used to obtain the C/E ratios.

## S-32 (n,p) 1/4 T PV Weighting

Position	Shield Thickness [cm]	Exp. RR <sup>a</sup> as Measured	Total Error (1σ) [%]	Exp. RR <sup>a,b</sup> without Background (E)	BUGJEFF311 Calculation RR <sup>a</sup> (C)	C/E	BUGLE-96 Calculation RR <sup>a</sup> (C)	C/E
A2	0.00	2.02E-17	6.5	1.98E-17	1.82053E-17	0.92	1.82829E-17	0.92
A3	5.10	4.29E-18	6.5	4.20E-18	3.70835E-18	0.88	3.64734E-18	0.87
A4	10.22	1.40E-18	6.5	1.37E-18	1.25807E-18	0.92	1.21856E-18	0.89
A5	15.34	5.12E-19	6.5	5.02E-19	4.60796E-19	0.92	4.40926E-19	0.88
A6	20.44	1.91E-19	6.5	1.87E-19	1.73197E-19	0.93	1.63992E-19	0.88
A7	25.64	7.13E-20	6.5	6.99E-20	6.48755E-20	0.93	6.08590E-20	0.87
A8	30.79	2.70E-20	6.6	2.65E-20	2.46191E-20	0.93	2.29034E-20	0.87
A9	35.99	1.03E-20	6.5	1.01E-20	9.25741E-21	0.92	8.54577E-21	0.85
A10	41.19	3.93E-21	6.5	3.85E-21	3.49346E-21	0.91	3.20308E-21	0.83
A11	46.44	1.49E-21	6.5	1.46E-21	1.30580E-21	0.89	1.18989E-21	0.81
A12	51.62	5.73E-22	6.5	5.62E-22	4.94951E-22	0.88	4.48620E-22	0.80
A13	56.69	2.27E-22	6.9	2.22E-22	1.91752E-22	0.86	1.73047E-22	0.78
A14	61.81	8.53E-23	8.6	8.36E-23	7.37139E-23	0.88	6.62906E-23	0.79
A15	66.99	3.50E-23	21.	3.43E-23	2.80710E-23	0.82	2.51778E-23	0.73

<sup>a</sup> RR = Reaction Rates in units of reactions per second per atom at the NESTOR reactor maximum power (30 kW).

<sup>b</sup> RR "without background" are the experimental reaction rates reduced by 2% to eliminate the NESTOR reactor background component. These data are used to obtain the C/E ratios.

Table 12

 Iron-88 - Summary of Experimental (E) and Calculated (C)  
 Al-27(n, $\alpha$ )Na-24 Reaction Rates along the Horizontal Z Axis.

 Al-27(n, $\alpha$ ) Flat Weighting

Position	Shield Thickness [cm]	Exp. RR <sup>a</sup> as Measured	Total Error (1 $\sigma$ ) [%]	Exp. RR <sup>a,b</sup> without Background (E)	BUGJEFF311 Calculation RR <sup>a</sup> (C)	C/E	BUGLE-96 Calculation RR <sup>a</sup> (C)	C/E
A2	0.00	-	-	-	-	-	-	-
A3	5.10	2.23E-20	4.7	2.19E-20	2.88891E-20	1.32	2.92900E-20	1.34
A4	10.22	-	-	-	-	-	-	-
A5	15.34	2.55E-21	4.7	2.50E-21	3.27233E-21	1.31	3.35773E-21	1.34
A6	20.44	9.56E-22	4.7	9.37E-22	1.23792E-21	1.32	1.27643E-21	1.36
A7	25.64	3.56E-22	4.7	3.49E-22	4.76262E-22	1.37	4.92905E-22	1.41
A8	30.79	-	-	-	-	-	-	-
A9	35.99	-	-	-	-	-	-	-
A10	41.19	-	-	-	-	-	-	-
A11	46.44	-	-	-	-	-	-	-
A12	51.62	-	-	-	-	-	-	-
A13	56.69	-	-	-	-	-	-	-
A14	61.81	-	-	-	-	-	-	-
A15	66.99	-	-	-	-	-	-	-

<sup>a</sup> RR = Reaction Rates in units of reactions per second per atom at the NESTOR reactor maximum power (30 kW).

<sup>b</sup> RR "without background" are the experimental reaction rates reduced by 2% to eliminate the NESTOR reactor background component. These data are used to obtain the C/E ratios.

 Al-27(n, $\alpha$ ) 1/4 T PV Weighting

Position	Shield Thickness [cm]	Exp. RR <sup>a</sup> as Measured	Total Error (1 $\sigma$ ) [%]	Exp. RR <sup>a,b</sup> without Background (E)	BUGJEFF311 Calculation RR <sup>a</sup> (C)	C/E	BUGLE-96 Calculation RR <sup>a</sup> (C)	C/E
A2	0.00	-	-	-	-	-	-	-
A3	5.10	2.23E-20	4.7	2.19E-20	2.71400E-20	1.24	2.74629E-20	1.26
A4	10.22	-	-	-	-	-	-	-
A5	15.34	2.55E-21	4.7	2.50E-21	3.08155E-21	1.23	3.15582E-21	1.26
A6	20.44	9.56E-22	4.7	9.37E-22	1.16749E-21	1.25	1.20151E-21	1.28
A7	25.64	3.56E-22	4.7	3.49E-22	4.49935E-22	1.29	4.64792E-22	1.33
A8	30.79	-	-	-	-	-	-	-
A9	35.99	-	-	-	-	-	-	-
A10	41.19	-	-	-	-	-	-	-
A11	46.44	-	-	-	-	-	-	-
A12	51.62	-	-	-	-	-	-	-
A13	56.69	-	-	-	-	-	-	-
A14	61.81	-	-	-	-	-	-	-
A15	66.99	-	-	-	-	-	-	-

<sup>a</sup> RR = Reaction Rates in units of reactions per second per atom at the NESTOR reactor maximum power (30 kW).

<sup>b</sup> RR "without background" are the experimental reaction rates reduced by 2% to eliminate the NESTOR reactor background component. These data are used to obtain the C/E ratios.

Figure 27

Iron-88 - Au-197(n, $\gamma$ )Au-198 epi-Cadmium Reaction Rate Ratios (Calculated/Experimental)  
 Calculated Using the BUGJEFF311.BOLIB and BUGLE-96 Libraries  
 with 1/4 T PV Weighting Dosimeter Cross Sections.

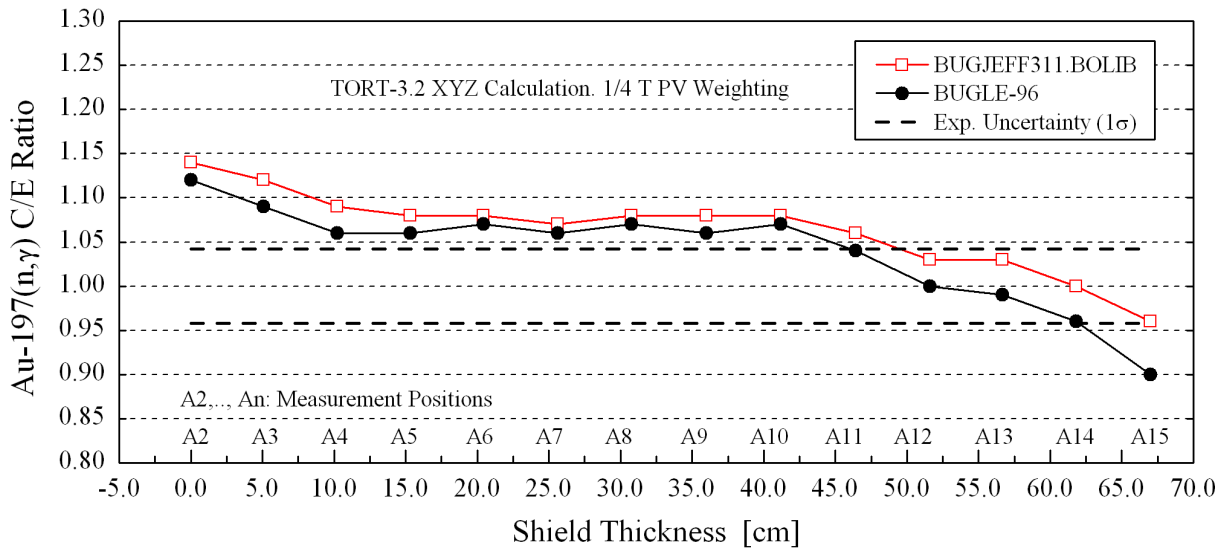


Figure 28

Iron-88 - Au-197(n, $\gamma$ )Au-198 epi-Cadmium Reaction Rate Ratios (Calculated/Experimental)  
 Calculated Using the BUGJEFF311.BOLIB and BUGLE-96 Libraries  
 with Flat Weighting Dosimeter Cross Sections.

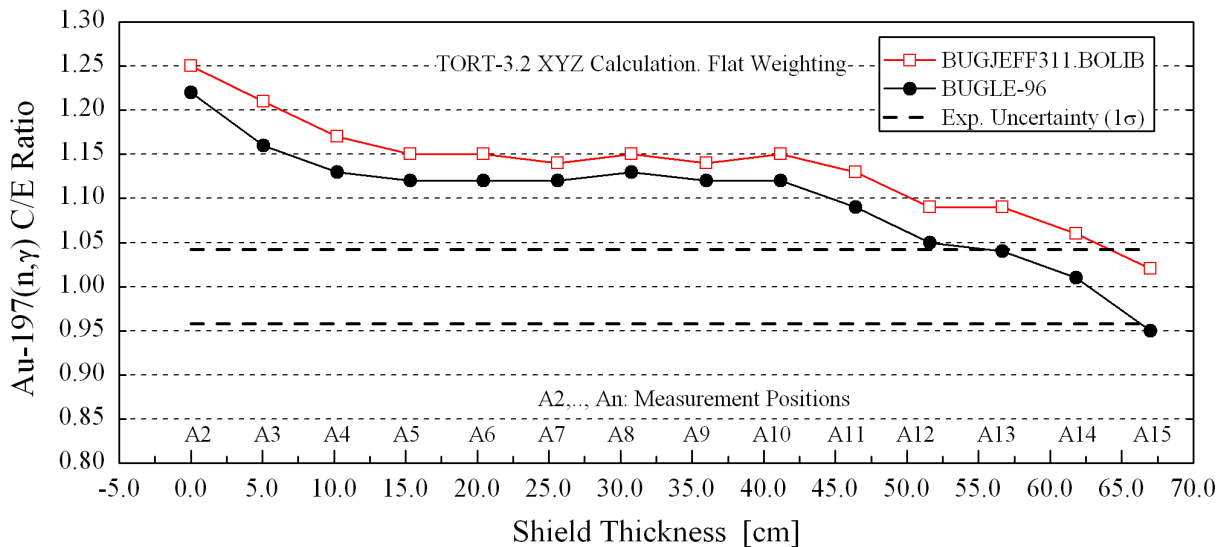




Figure 29

Iron-88 - Rh-103(n,n')Rh-103m Reaction Rate Ratios (Calculated/Experimental)  
 Calculated Using the BUGJEFF311.BOLIB and BUGLE-96 Libraries  
 with 1/4 T PV Weighting Dosimeter Cross Sections.

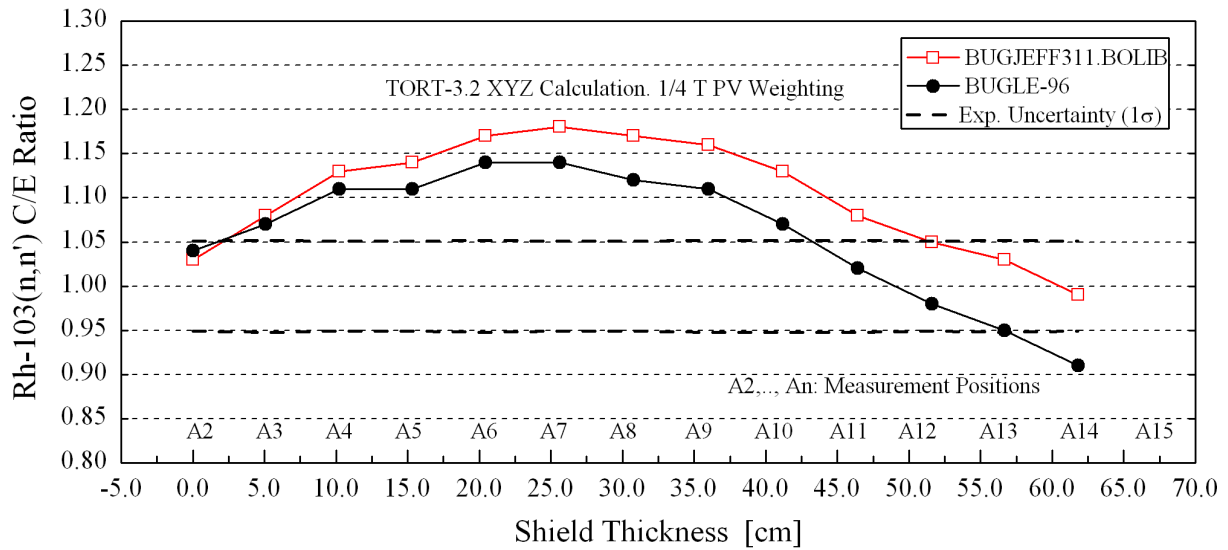


Figure 30

Iron-88 - Rh-103(n,n')Rh-103m Reaction Rate Ratios (Calculated/Experimental)  
 Calculated Using the BUGJEFF311.BOLIB and BUGLE-96 Libraries  
 with Flat Weighting Dosimeter Cross Sections.

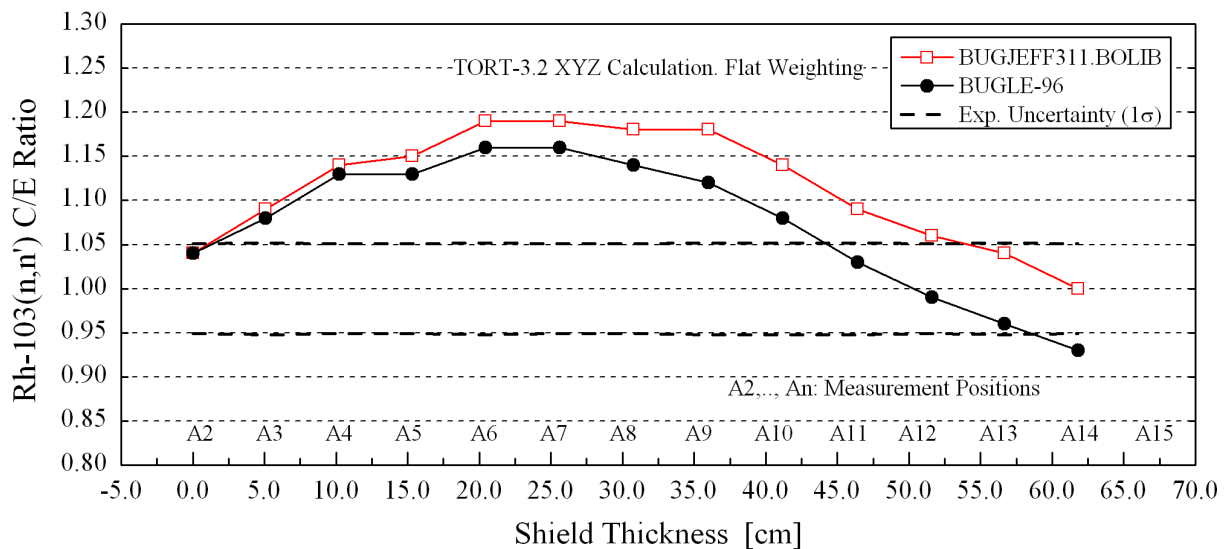


Figure 31

Iron-88 - In-115(n,n')In-115m Reaction Rate Ratios (Calculated/Experimental)  
 Calculated Using the BUGJEFF311.BOLIB and BUGLE-96 Libraries  
 with 1/4 T PV Weighting Dosimeter Cross Sections.

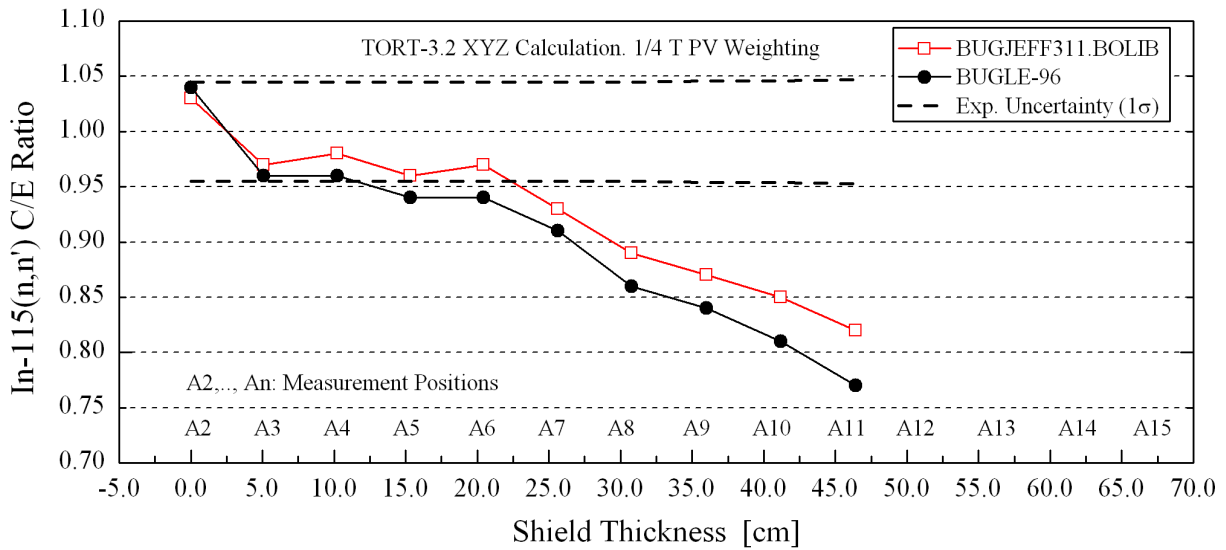


Figure 32

Iron-88 - In-115(n,n')In-115m Reaction Rate Ratios (Calculated/Experimental)  
 Calculated Using the BUGJEFF311.BOLIB and BUGLE-96 Libraries  
 with Flat Weighting Dosimeter Cross Sections.

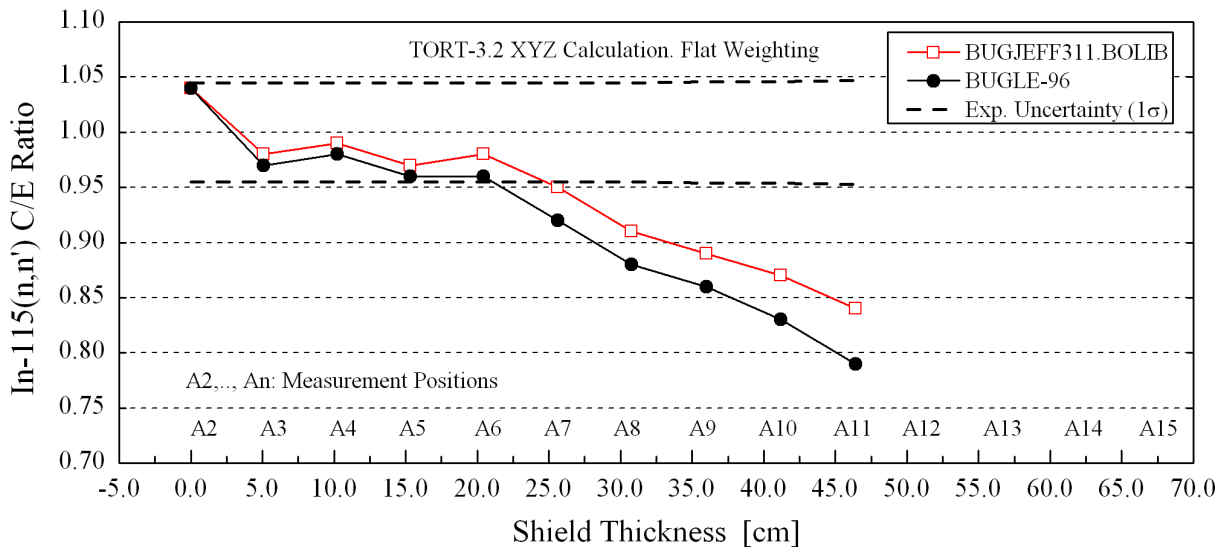


Figure 33

Iron-88 - S-32(n,p)P-32 Reaction Rate Ratios (Calculated/Experimental)  
 Calculated Using the BUGJEFF311.BOLIB and BUGLE-96 Libraries  
 with 1/4 T PV Weighting Dosimeter Cross Sections.

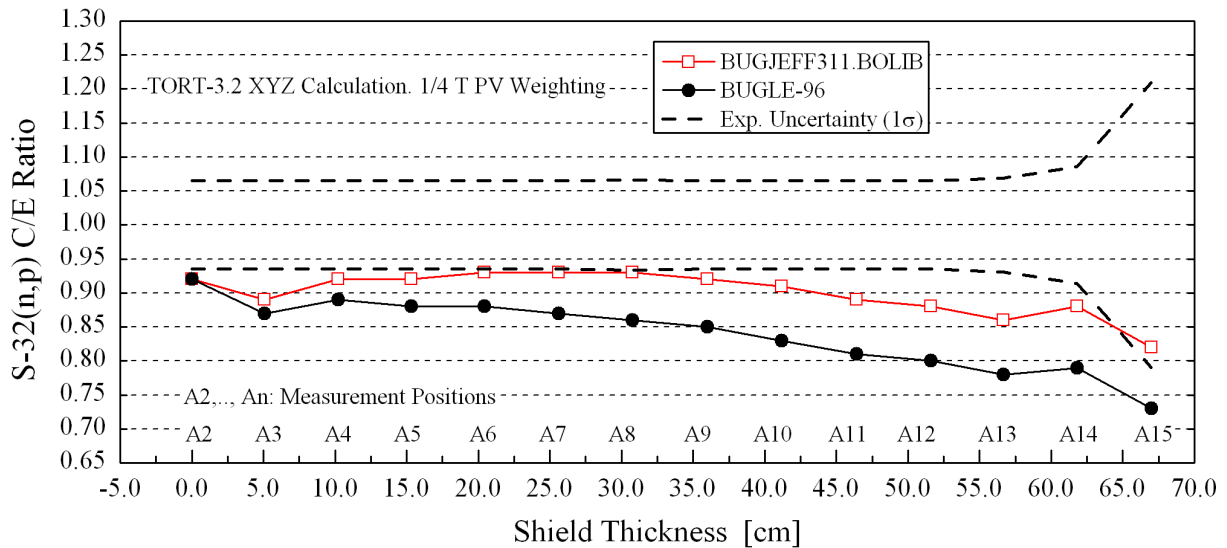


Figure 34

Iron-88 - S-32(n,p)P-32 Reaction Rate Ratios (Calculated/Experimental)  
 Calculated Using the BUGJEFF311.BOLIB and BUGLE-96 Libraries  
 with Flat Weighting Dosimeter Cross Sections.

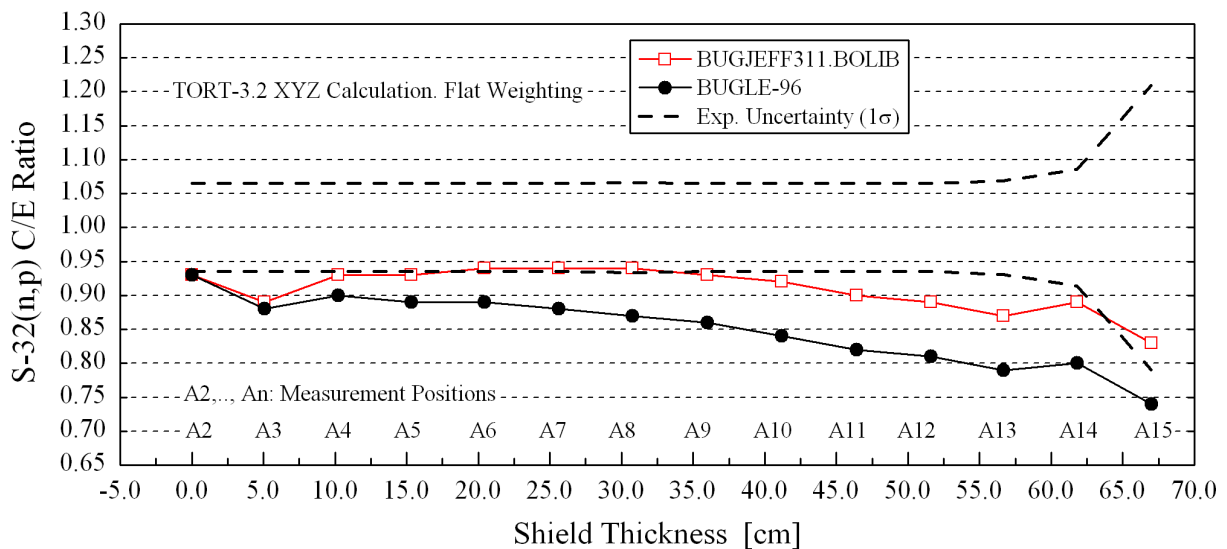


Figure 35

Iron-88 - Al-27(n, $\alpha$ )Na-24 Reaction Rate Ratios (Calculated/Experimental)  
 Calculated Using the BUGJEFF311.BOLIB and BUGLE-96 Libraries  
 with 1/4 T PV Weighting Dosimeter Cross Sections.

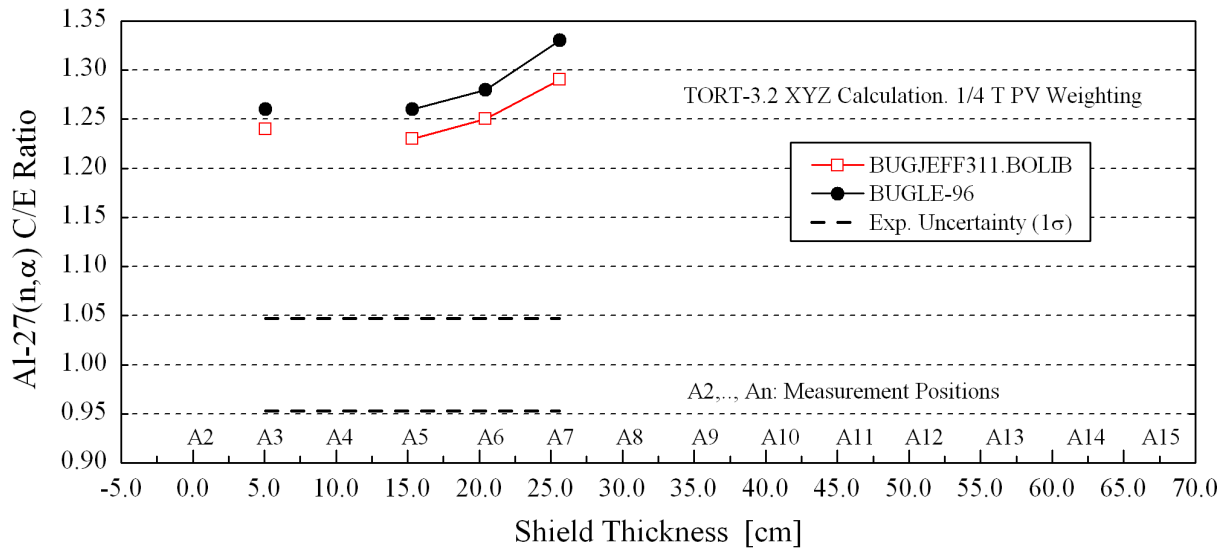


Figure 36

Iron-88 - Al-27(n, $\alpha$ )Na-24 Reaction Rate Ratios (Calculated/Experimental)  
 Calculated Using the BUGJEFF311.BOLIB and BUGLE-96 Libraries  
 with Flat Weighting Dosimeter Cross Sections.

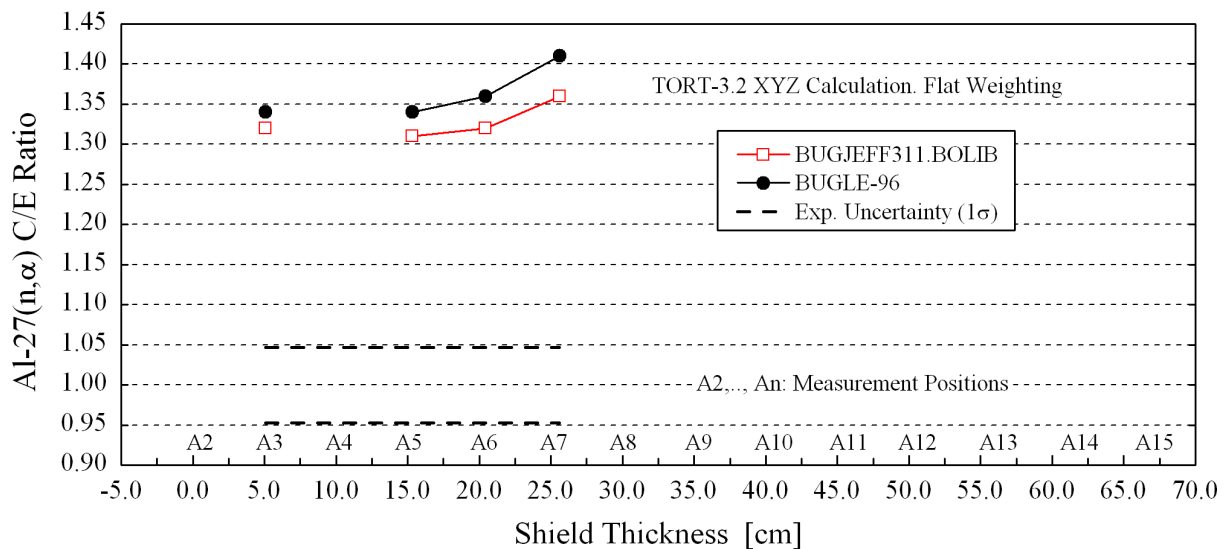


Figure 37

Iron-88 - Au-197(n, $\gamma$ )Au-198 epi-Cadmium Reaction Rate Ratios (Calculated/Experimental)  
 Calculated Using the BUGJEFF311.BOLIB Library and Dosimeter Cross Sections  
 with Flat Weighting and 1/4 T PV Weighting.

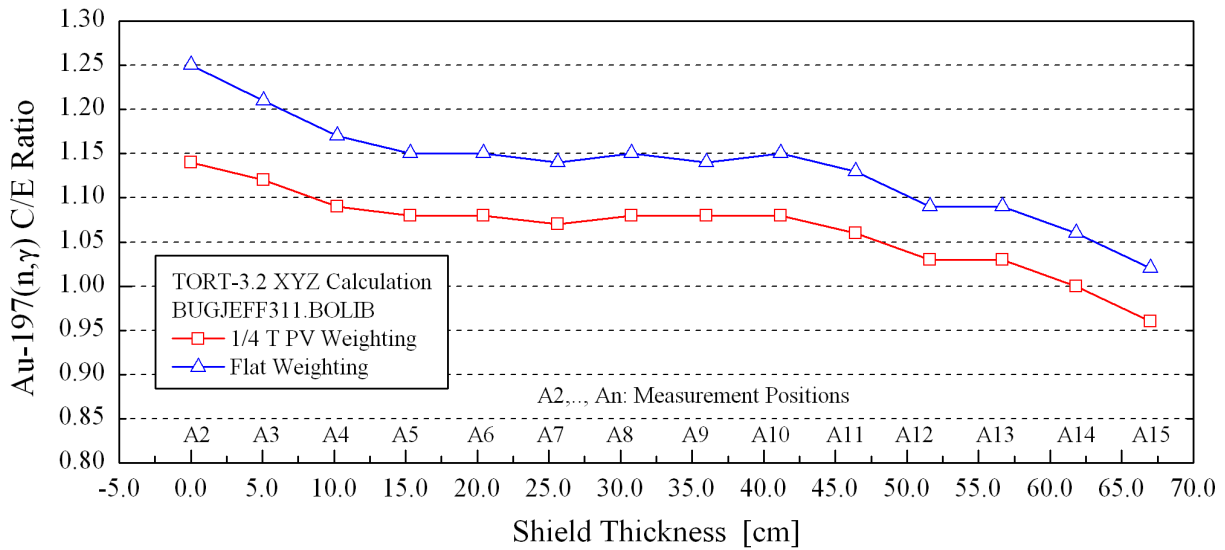


Figure 38

Iron-88 - Au-197(n, $\gamma$ )Au-198 epi-Cadmium Reaction Rate Ratios (Calculated/Experimental)  
 Calculated Using the BUGLE-96 Library and Dosimeter Cross Sections  
 with Flat Weighting and 1/4 T PV Weighting.

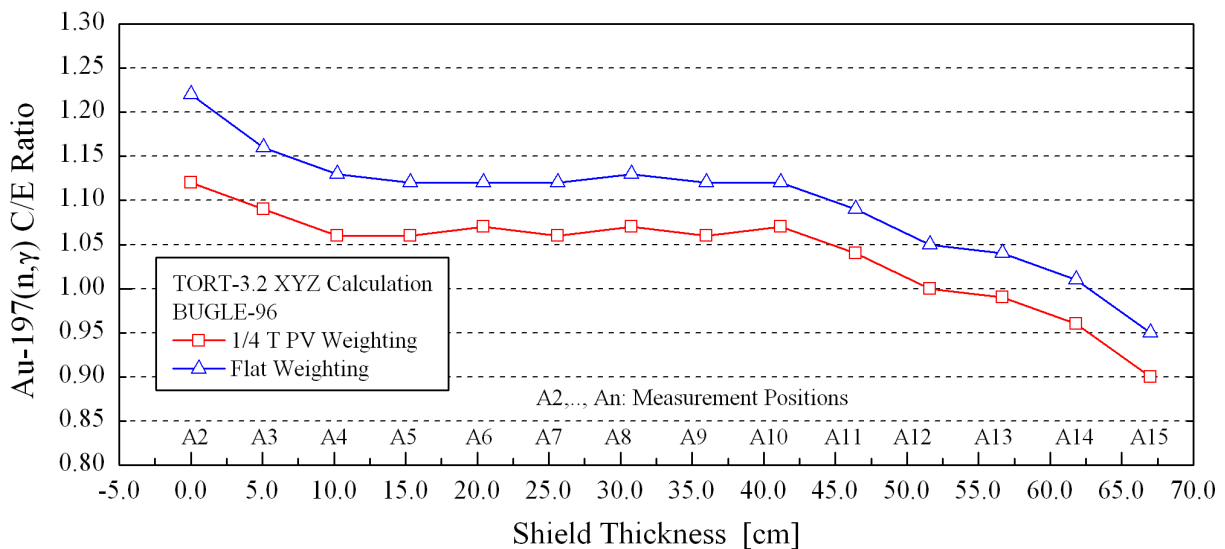


Figure 39

Iron-88 - Rh-103(n,n')Rh-103m Reaction Rate Ratios (Calculated/Experimental)  
 Calculated Using the BUGJEFF311.BOLIB Library and Dosimeter Cross Sections  
 with Flat Weighting and 1/4 T PV Weighting.

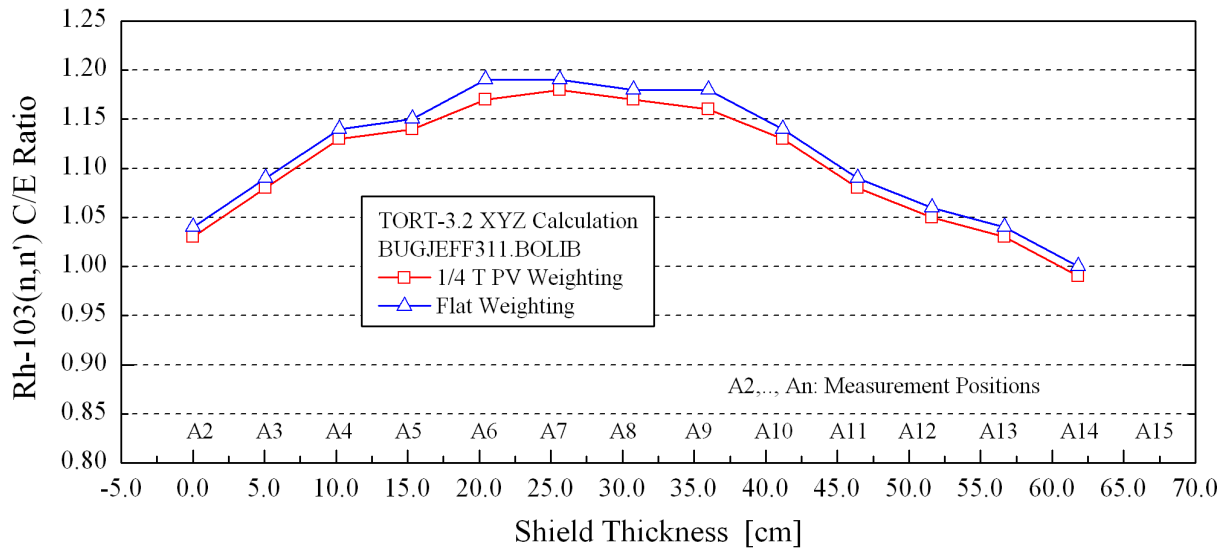


Figure 40

Iron-88 - Rh-103(n,n')Rh-103m Reaction Rate Ratios (Calculated/Experimental)  
 Calculated Using the BUGLE-96 Library and Dosimeter Cross Sections  
 with Flat Weighting and 1/4 T PV Weighting.

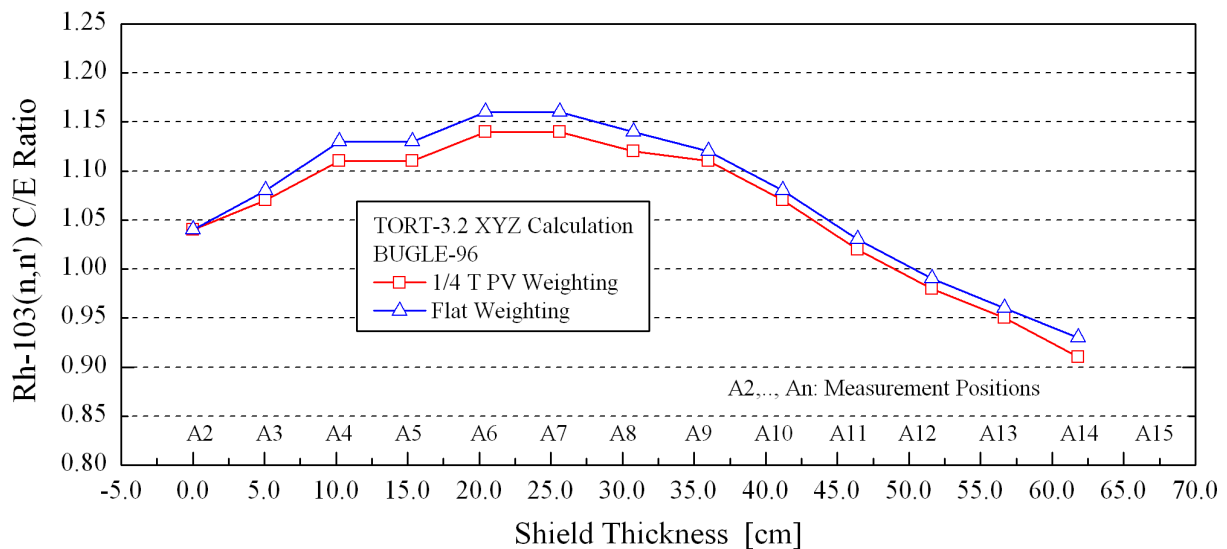


Figure 41

Iron-88 - In-115(n,n')In-115m Reaction Rate Ratios (Calculated/Experimental)  
Calculated Using the BUGJEFF311.BOLIB Library and Dosimeter Cross Sections  
with Flat Weighting and 1/4 T PV Weighting.

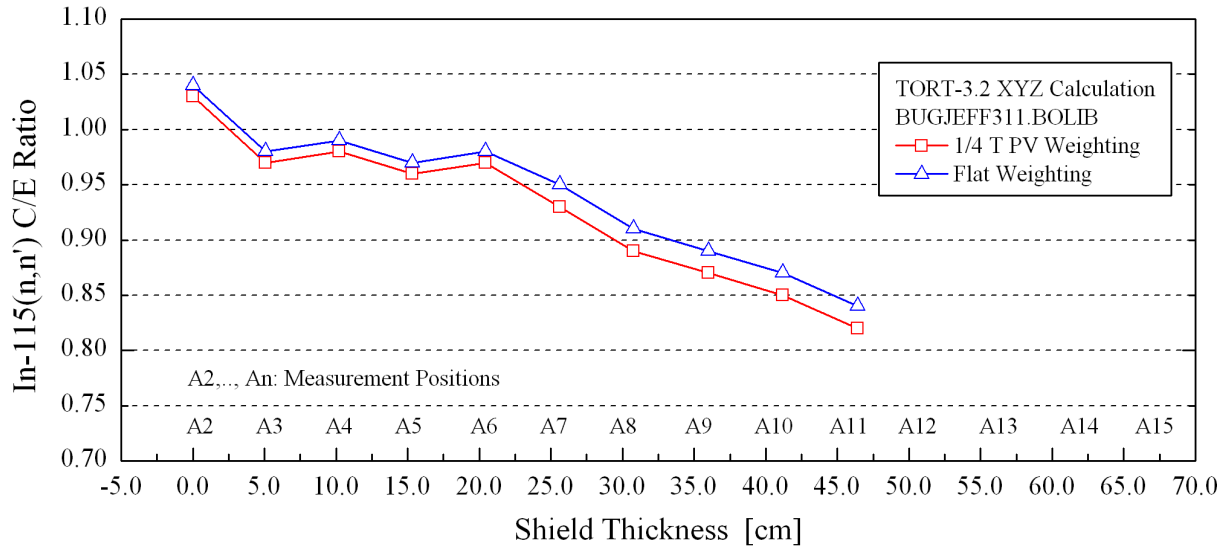


Figure 42

Iron-88 - In-115(n,n')In-115m Reaction Rate Ratios (Calculated/Experimental)  
Calculated Using the BUGLE-96 Library and Dosimeter Cross Sections  
with Flat Weighting and 1/4 T PV Weighting.

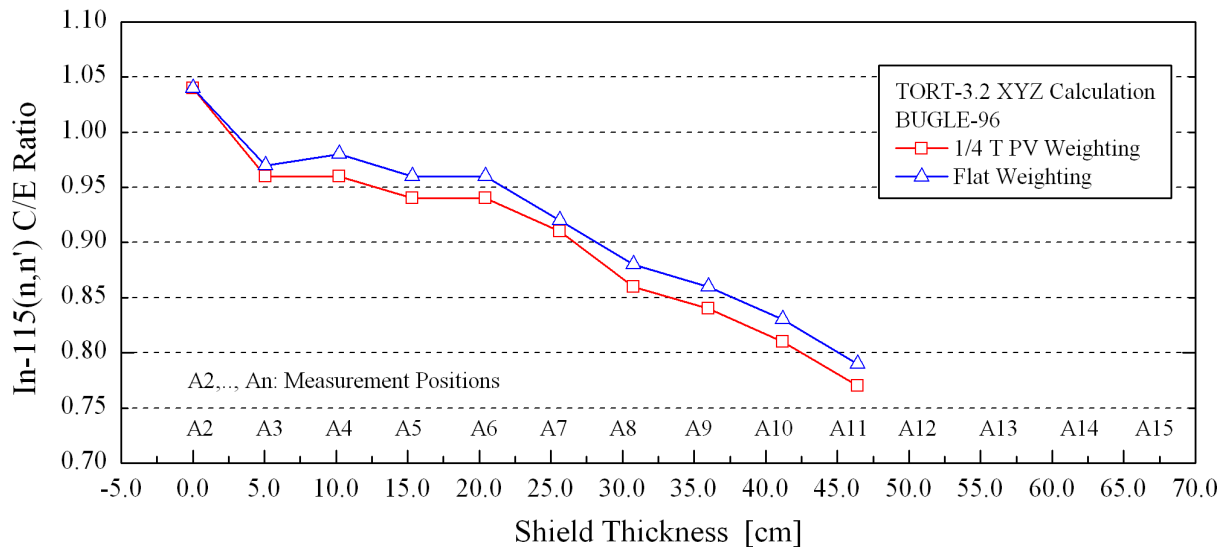


Figure 43

Iron-88 - S-32(n,p)P-32 Reaction Rate Ratios (Calculated/Experimental)  
 Calculated Using the BUGJEFF311.BOLIB Library and Dosimeter Cross Sections  
 with Flat Weighting and 1/4 T PV Weighting.

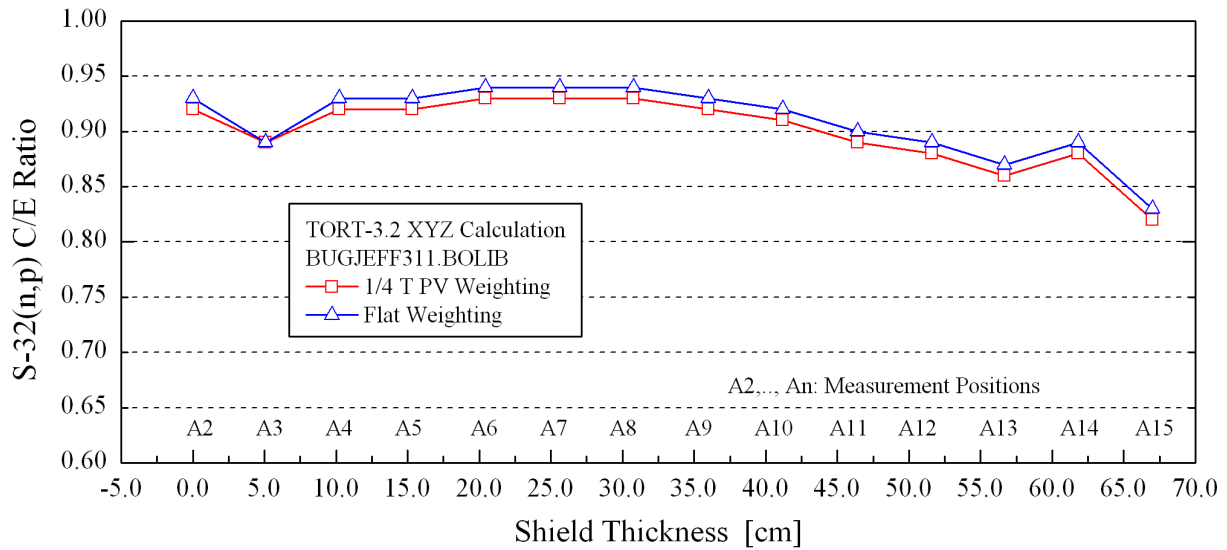


Figure 44

Iron-88 - S-32(n,p)P-32 Reaction Rate Ratios (Calculated/Experimental)  
 Calculated Using the BUGLE-96 Library and Dosimeter Cross Sections  
 with Flat Weighting and 1/4 T PV Weighting.

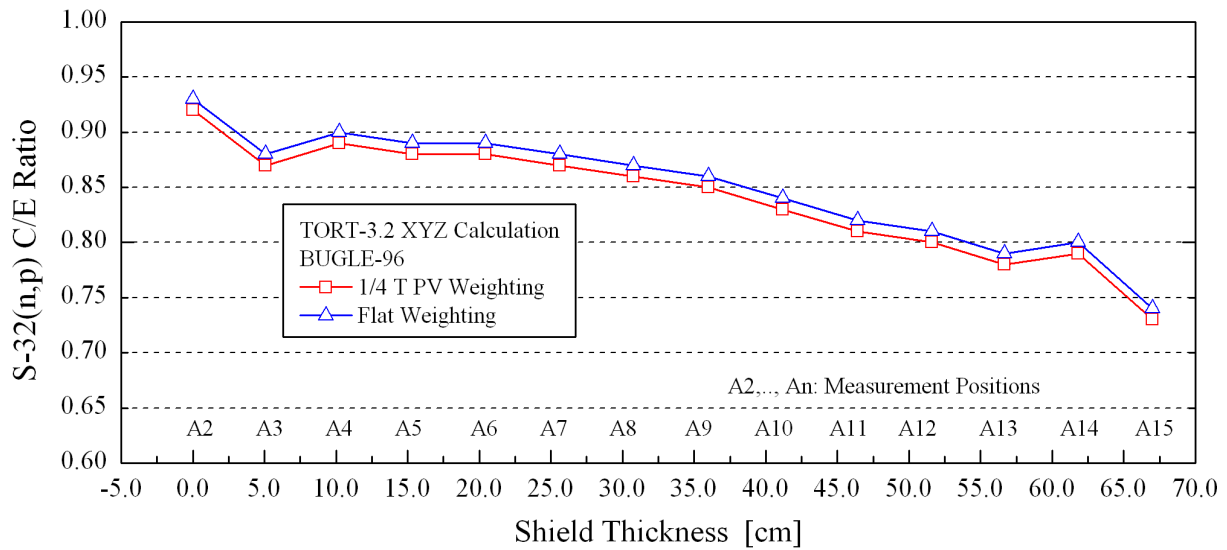




Figure 45

Iron-88 - Al-27(n, $\alpha$ )Na-24 Reaction Rate Ratios (Calculated/Experimental)  
Calculated Using the BUGJEFF311.BOLIB Library and Dosimeter Cross Sections  
with Flat Weighting and 1/4 T PV Weighting.

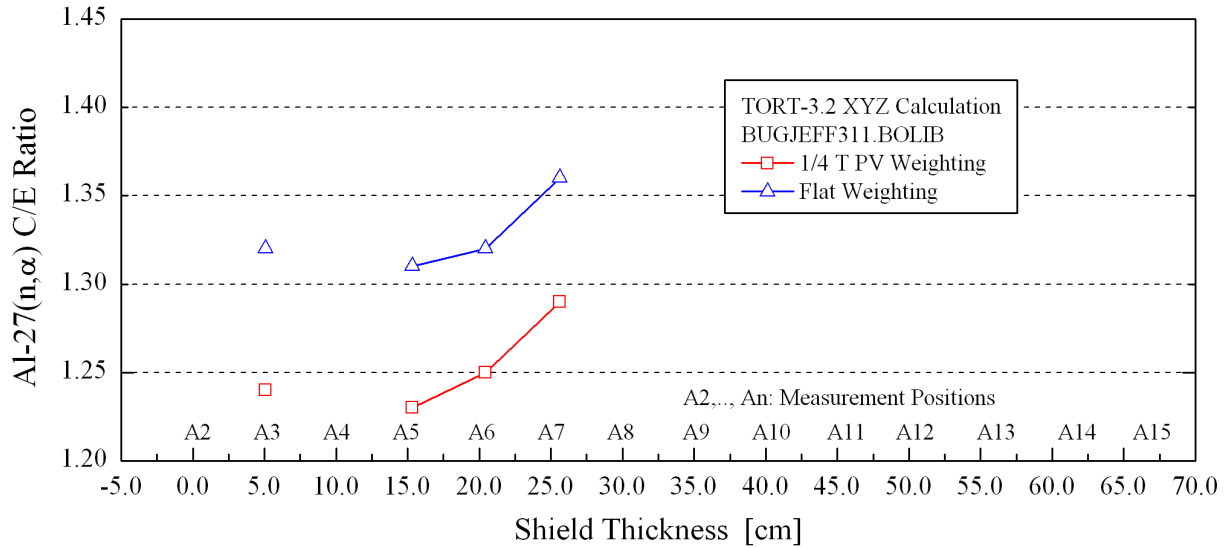


Figure 46

Iron-88 - Al-27(n, $\alpha$ )Na-24 Reaction Rate Ratios (Calculated/Experimental)  
Calculated Using the BUGLE-96 Library and Dosimeter Cross Sections  
with Flat Weighting and 1/4 T PV Weighting.

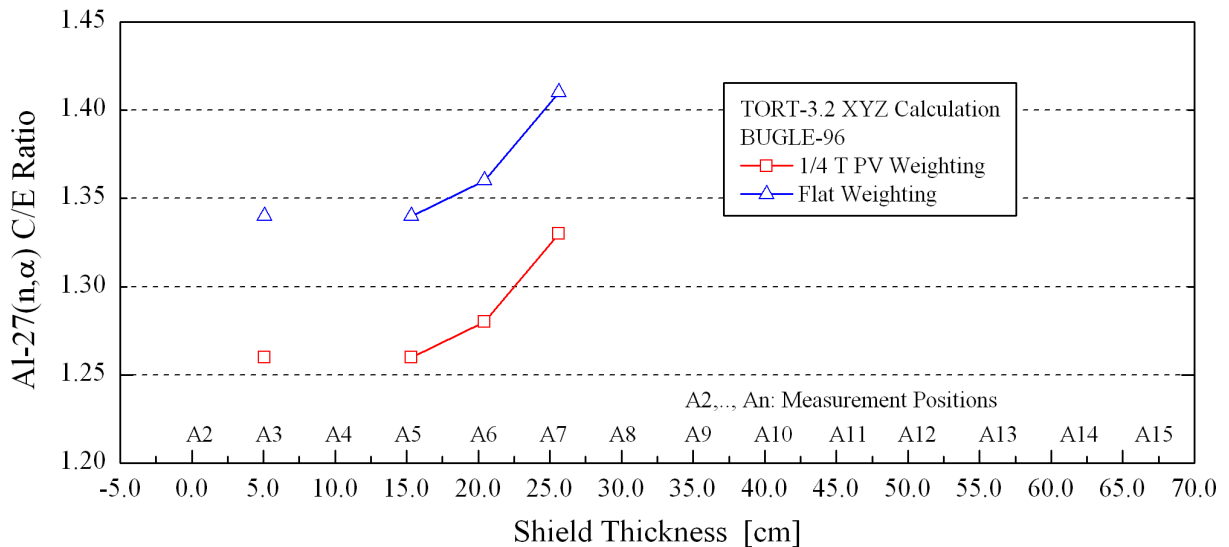


Figure 47

Iron-88 - Au-197(n, $\gamma$ )Au-198 epi-Cadmium Reaction Rates  
 at the NESTOR Reactor Maximum Power (30 kW)  
 on the Z Horizontal Axis.  
 [reactions  $\times$  s<sup>-1</sup>  $\times$  atom<sup>-1</sup>]

Comparison of Experimental and Calculated Reaction Rates.

P<sub>3</sub>-S<sub>8</sub> Calculation Using the BUGJEFF311.BOLIB Library  
 and 1/4 T PV Weighting Dosimeter Cross Sections.

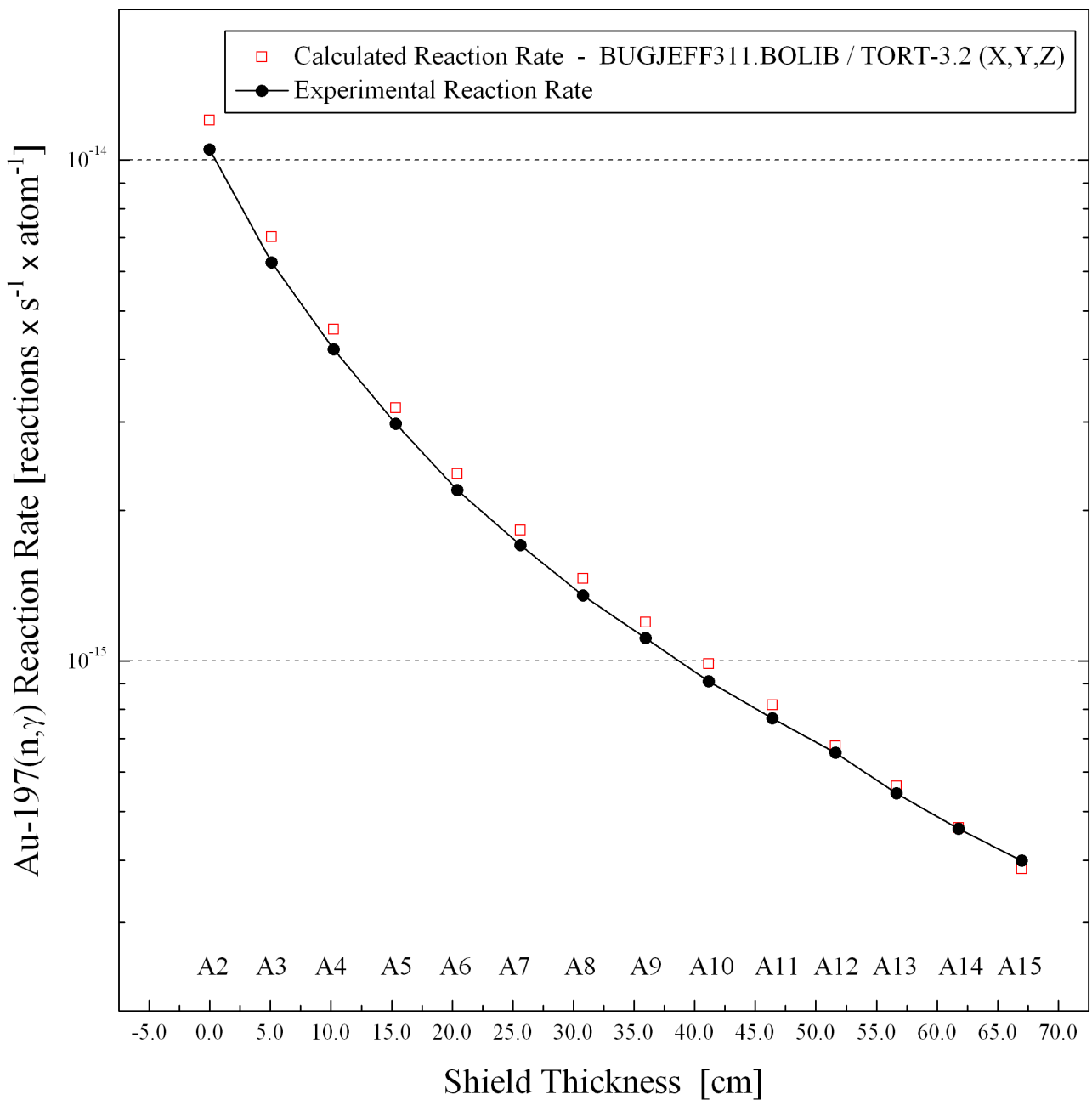


Figure 48

Iron-88 - Rh-103(n,n')Rh-103m Reaction Rates  
at the NESTOR Reactor Maximum Power (30 kW)  
on the Z Horizontal Axis.  
[reactions  $\times$  s<sup>-1</sup>  $\times$  atom<sup>-1</sup>]

Comparison of Experimental and Calculated Reaction Rates.

P<sub>3</sub>-S<sub>8</sub> Calculation Using the BUGJEFF311.BOLIB Library  
and 1/4 T PV Weighting Dosimeter Cross Sections.

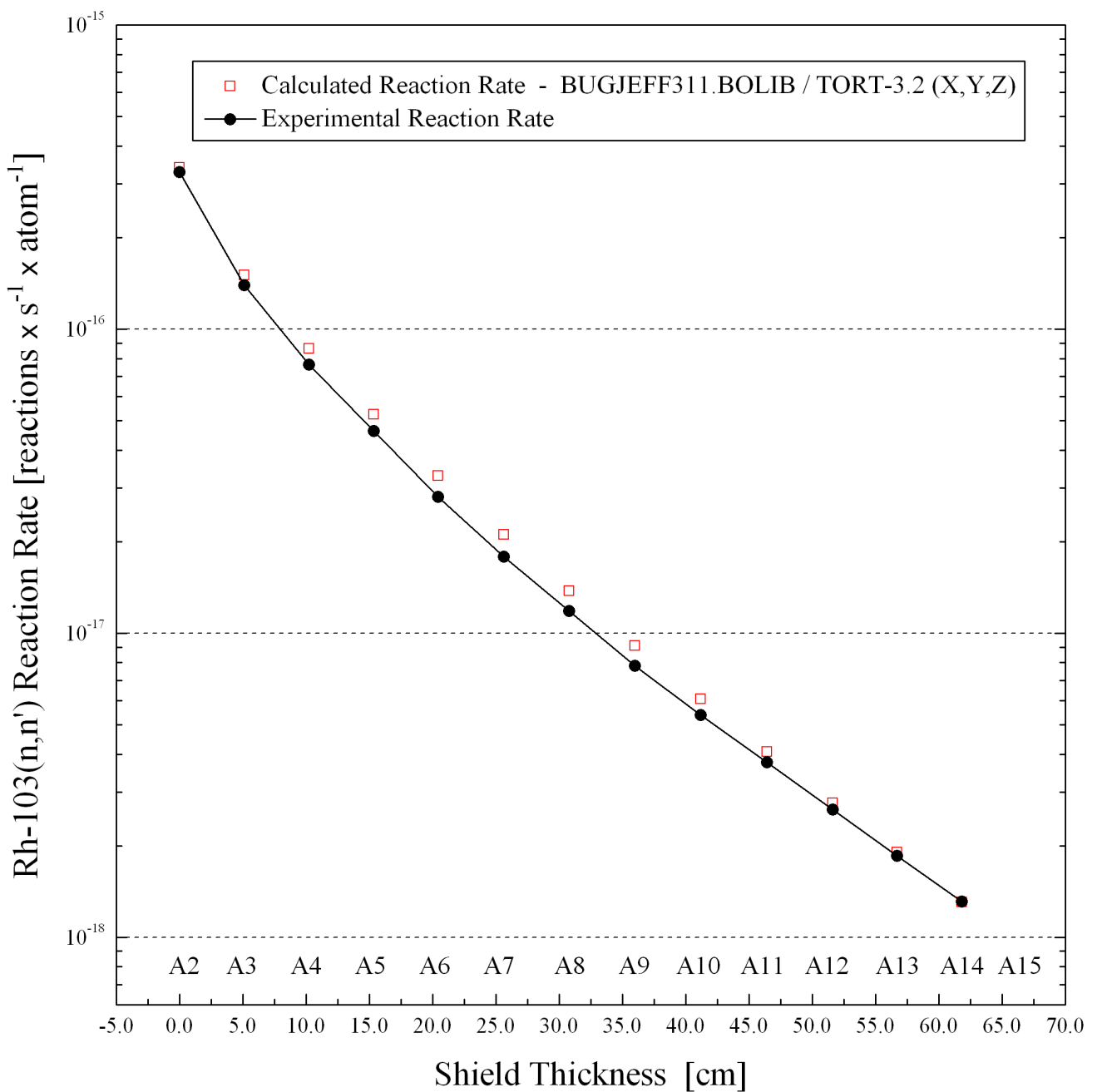


Figure 49

Iron-88 - In-115(n,n')In-115m Reaction Rates  
at the NESTOR Reactor Maximum Power (30 kW)  
on the Z Horizontal Axis.  
[reactions  $\times$  s<sup>-1</sup>  $\times$  atom<sup>-1</sup>]

Comparison of Experimental and Calculated Reaction Rates.

P<sub>3</sub>-S<sub>8</sub> Calculation Using the BUGJEFF311.BOLIB Library  
and 1/4 T PV Weighting Dosimeter Cross Sections.

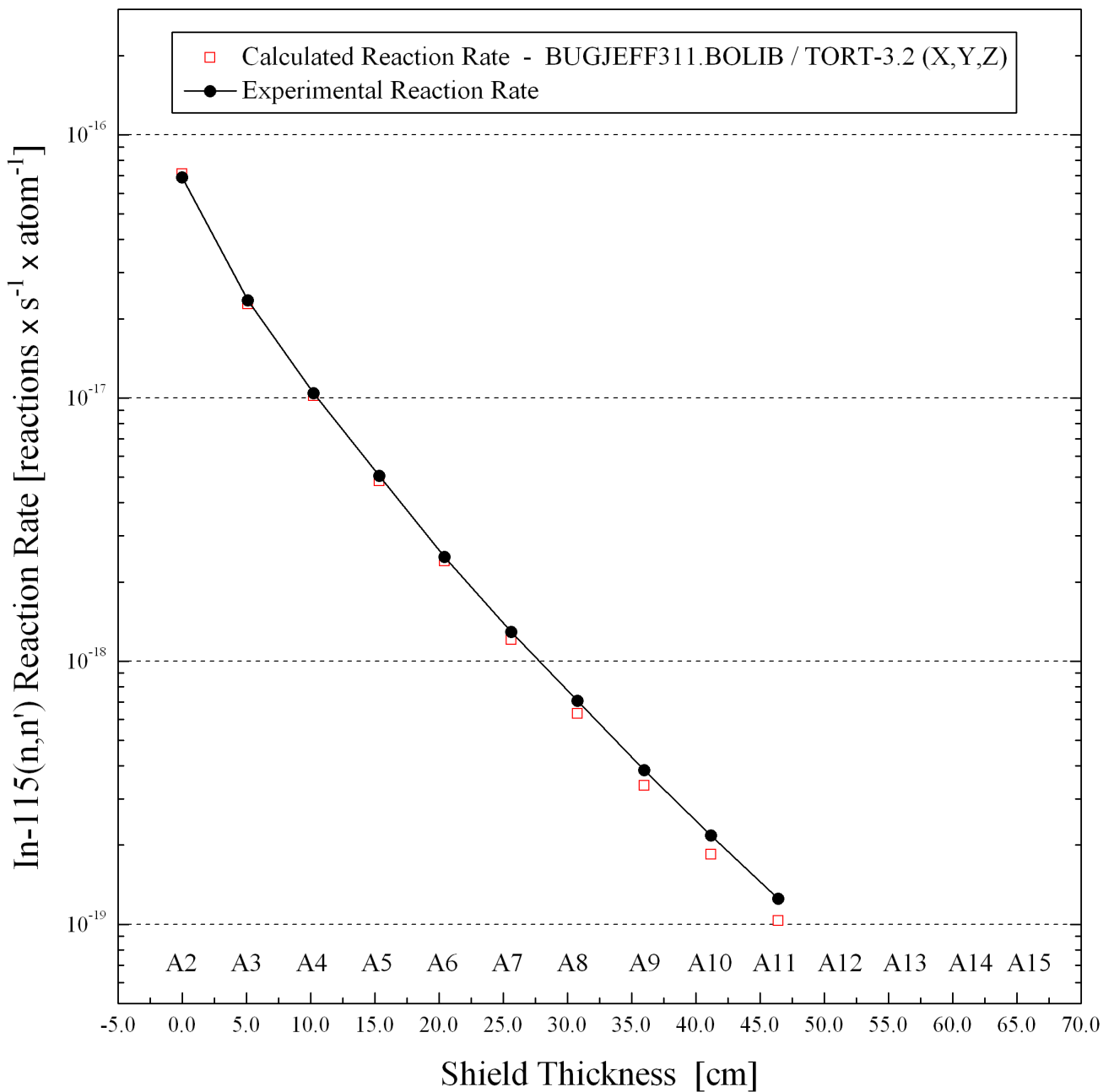


Figure 50

Iron-88 - S-32(n,p)P-32 Reaction Rates  
 at the NESTOR Reactor Maximum Power (30 kW)  
 on the Z Horizontal Axis.  
 [reactions  $\times$  s<sup>-1</sup>  $\times$  atom<sup>-1</sup>]

Comparison of Experimental and Calculated Reaction Rates.

P<sub>3</sub>-S<sub>8</sub> Calculation Using the BUGJEFF311.BOLIB Library  
 and 1/4 T PV Weighting Dosimeter Cross Sections.

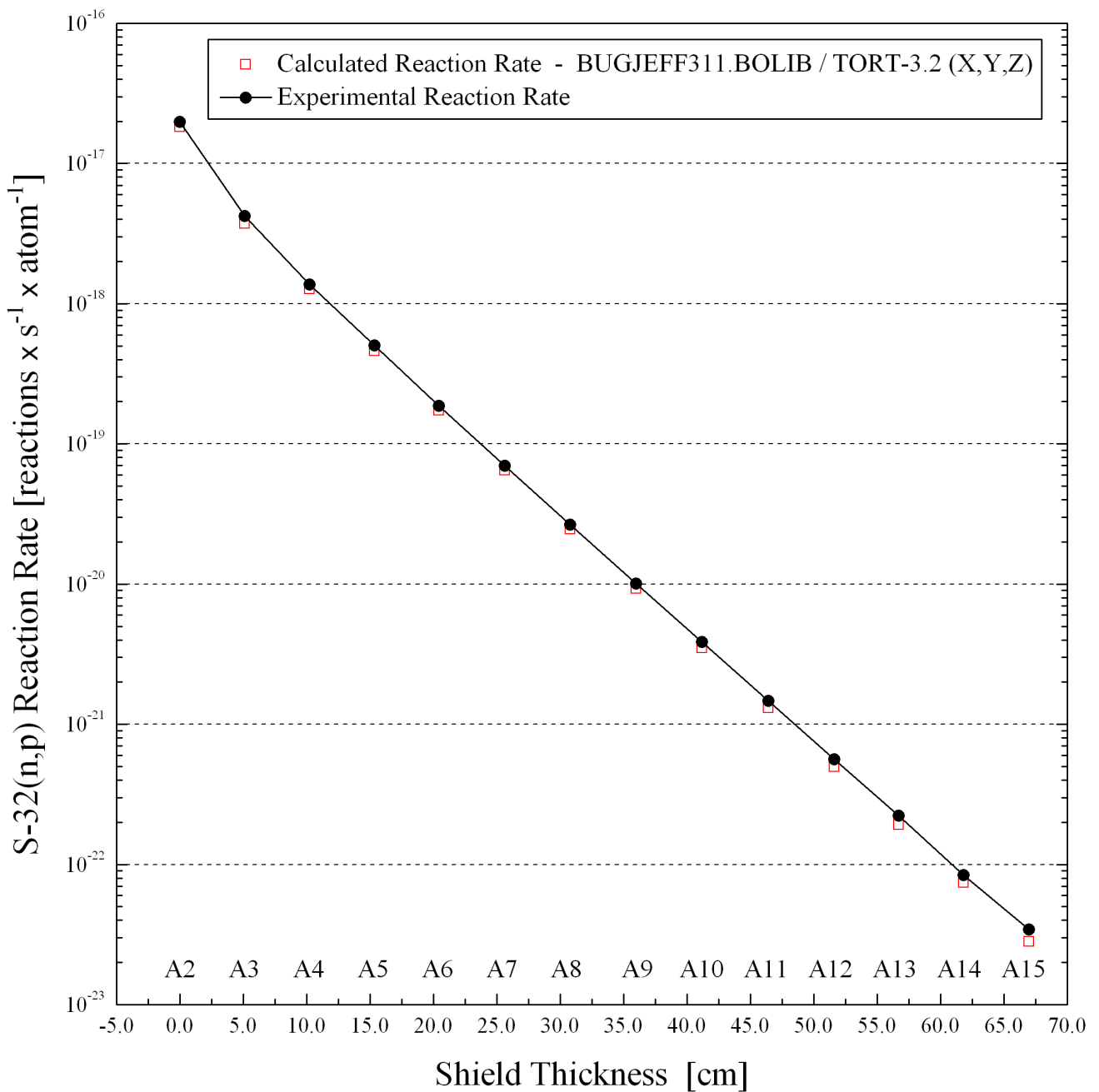


Figure 51

Iron-88 - Al-27(n, $\alpha$ )Na-24 Reaction Rates  
at the NESTOR Reactor Maximum Power (30 kW)  
on the Z Horizontal Axis.  
[reactions  $\times$  s<sup>-1</sup>  $\times$  atom<sup>-1</sup>]

Comparison of Experimental and Calculated Reaction Rates.

P<sub>3</sub>-S<sub>8</sub> Calculation Using the BUGJEFF311.BOLIB Library  
and 1/4 T PV Weighting Dosimeter Cross Sections.

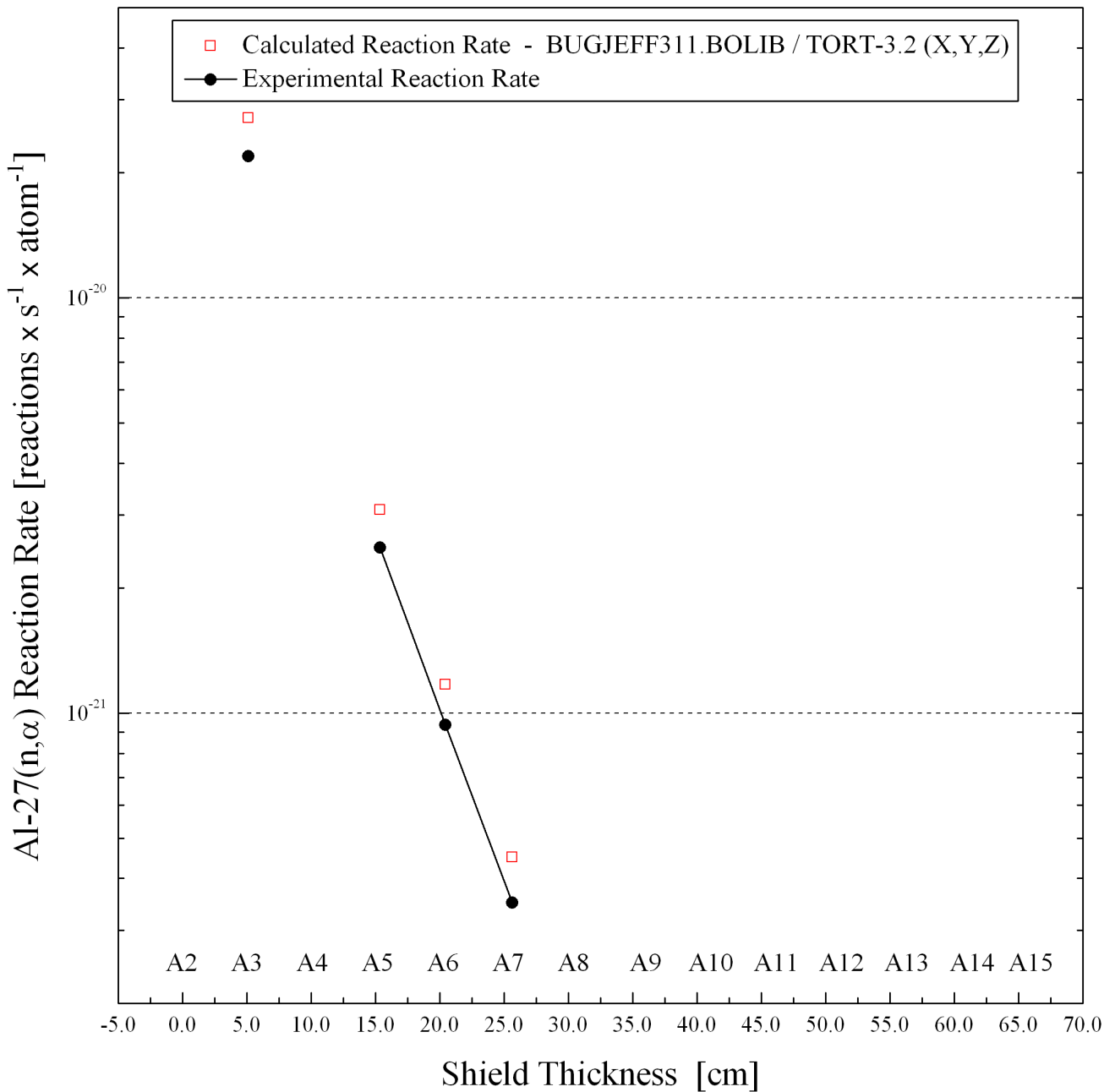


Figure 52

Iron-88 - Spatial Distribution of the Neutron Fluxes at the NESTOR Reactor  
 Maximum Power (30 kW) for Neutron Energy > 0.414 eV.  
 [neutrons × barn<sup>-1</sup> × s<sup>-1</sup>]

Horizontal Section at Y = 0.0 cm.  
 Dosimeter Locations “x”, 73X×79Y×278Z Spatial Meshes.

P<sub>3</sub>-S<sub>8</sub> Calculation Using the BUGJEFF311.BOLIB Library.

IRON-88 Distribution of Neutron Flux [n·barns<sup>-1</sup>·s<sup>-1</sup>] > 0.414 eV.  
 Meshes: 73X, 79Y, 278Z Section at Y = 0.00 cm

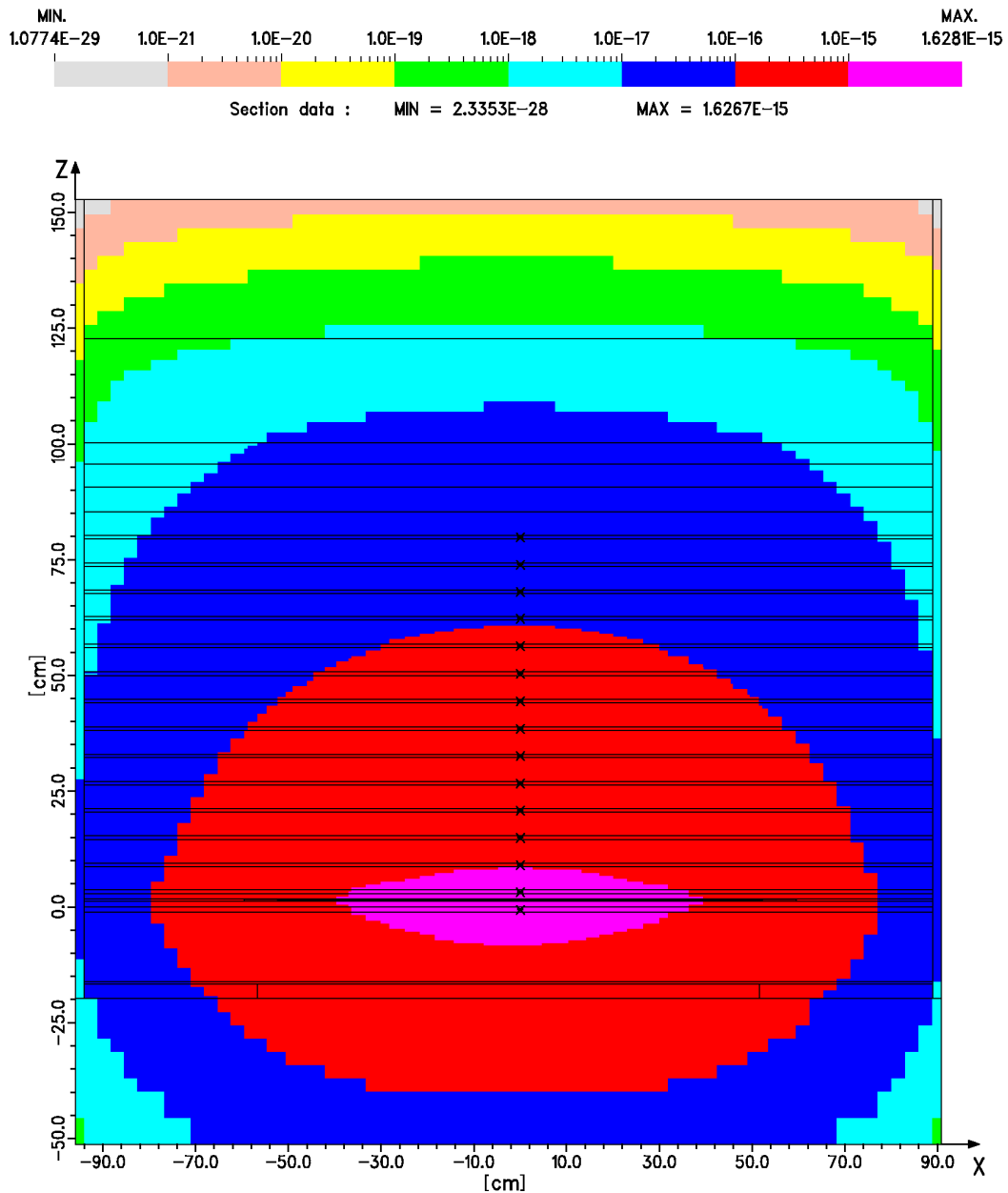


Figure 53

Iron-88 - Spatial Distribution of the Neutron Fluxes at the NESTOR Reactor  
 Maximum Power (30 kW) for Neutron Energy > 0.1 MeV.  
 [neutrons × barn<sup>-1</sup> × s<sup>-1</sup>]

Horizontal Section at Y = 0.0 cm.  
 Dosimeter Locations “x”, 73X×79Y×278Z Spatial Meshes.

P<sub>3</sub>-S<sub>8</sub> Calculation Using the BUGJEFF311.BOLIB Library.

IRON-88 Distribution of Neutron Flux [n·barns<sup>-1</sup>·s<sup>-1</sup>] > 0.1 MeV.

Meshes: 73X, 79Y, 278Z Section at Y = 0.00 cm

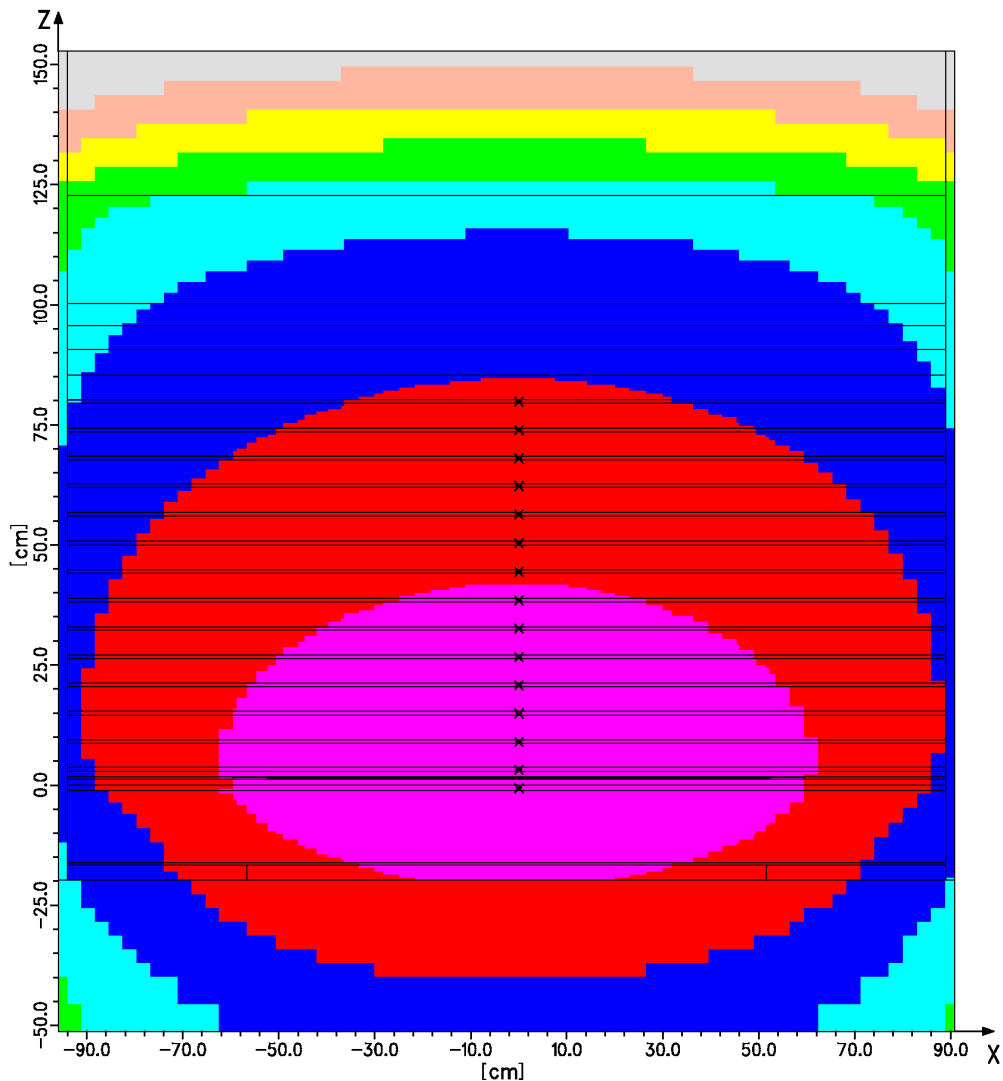
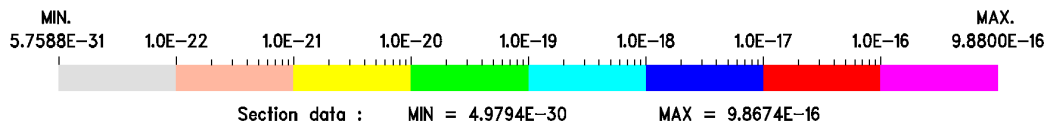




Figure 54

Iron-88 - Spatial Distribution of the Neutron Fluxes at the NESTOR Reactor  
 Maximum Power (30 kW) for Neutron Energy > 1.0 MeV.  
 [neutrons × barn<sup>-1</sup> × s<sup>-1</sup>]

Horizontal Section at Y = 0.0 cm.  
 Dosimeter Locations “×”, 73X×79Y×278Z Spatial Meshes.

P<sub>3</sub>-S<sub>8</sub> Calculation Using the BUGJEFF311.BOLIB Library.

IRON-88 Distribution of Neutron Flux [n·barns<sup>-1</sup>·s<sup>-1</sup>] > 1 MeV.

Meshes: 73X, 79Y, 278Z Section at Y = 0.00 cm

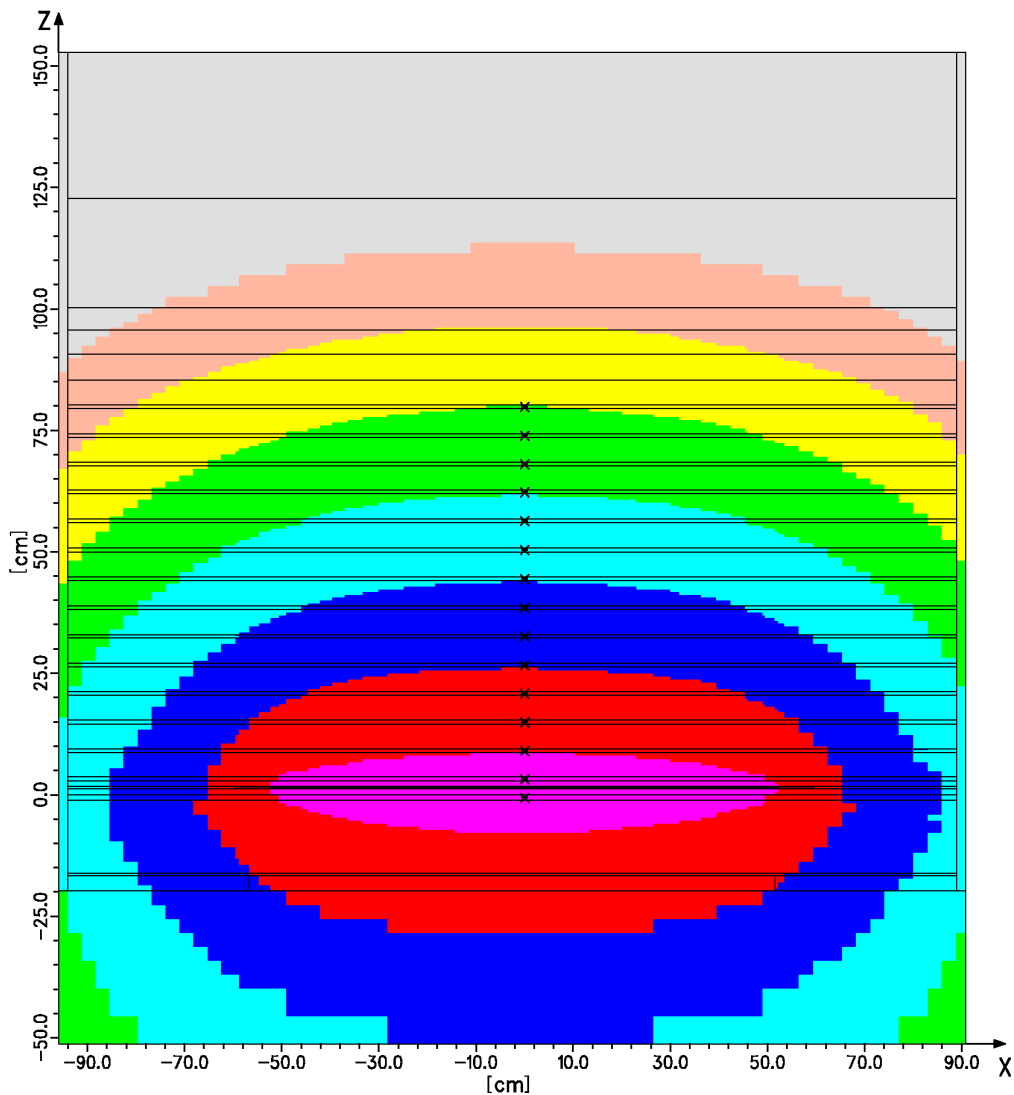
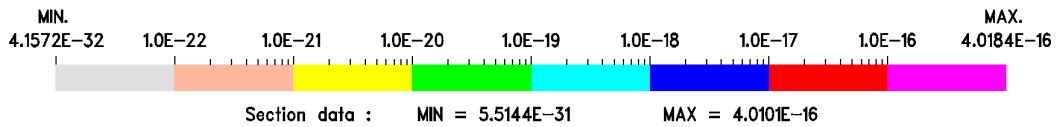


Figure 55

Iron-88 - Spatial Distribution of the Neutron Fluxes at the NESTOR Reactor  
 Maximum Power (30 kW) for Neutron Energy > 3.0 MeV.  
 [neutrons × barn<sup>-1</sup> × s<sup>-1</sup>]

Horizontal Section at Y = 0.0 cm.  
 Dosimeter Locations “×”, 73X×79Y×278Z Spatial Meshes.

P<sub>3</sub>-S<sub>8</sub> Calculation Using the BUGJEFF311.BOLIB Library.

IRON-88 Distribution of Neutron Flux [n·barns<sup>-1</sup>·s<sup>-1</sup>] > 3 MeV.

Meshes: 73X, 79Y, 278Z Section at Y = 0.00 cm

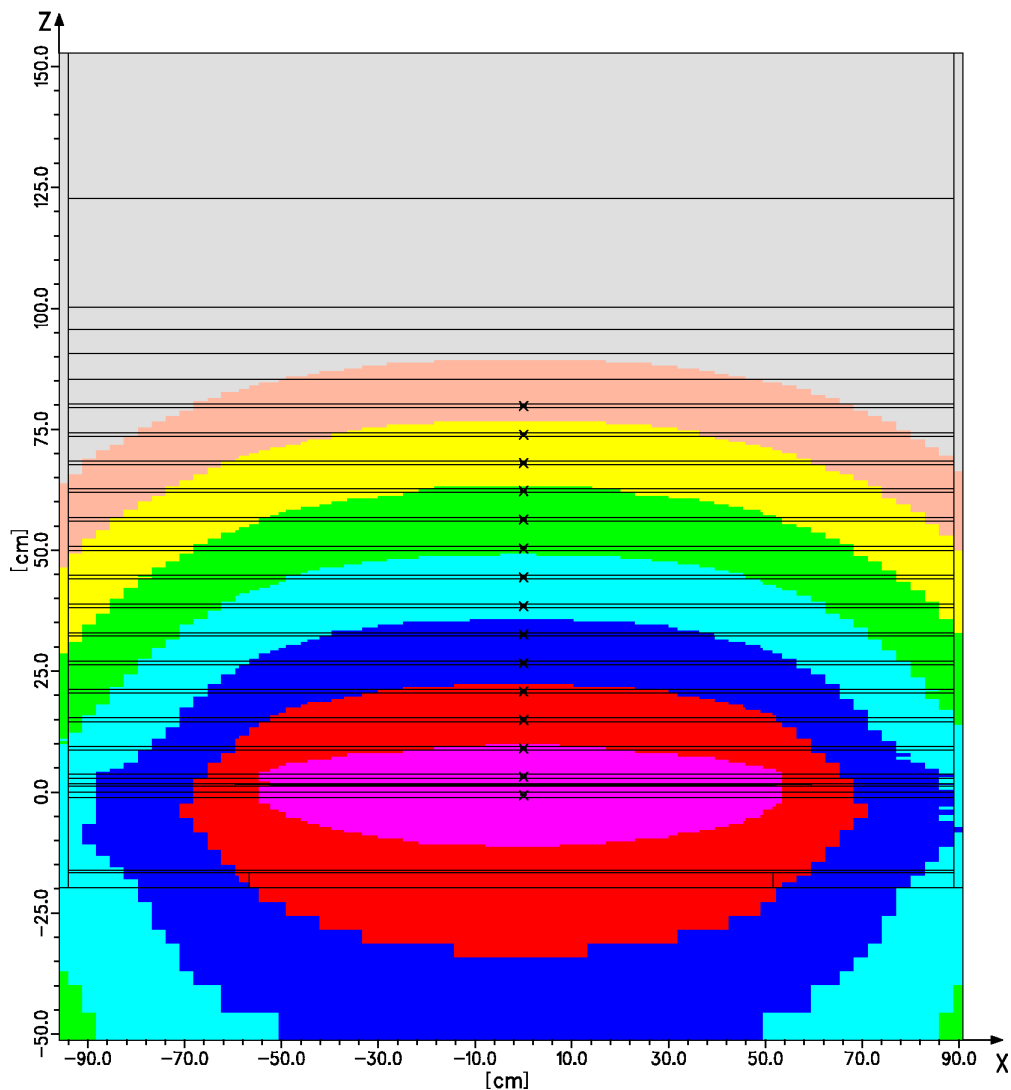
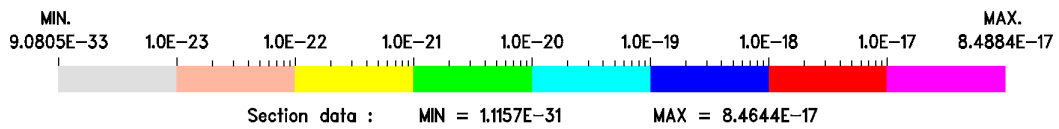


Figure 56

Iron-88 - Spatial Distribution of the Neutron Fluxes at the NESTOR Reactor  
Maximum Power (30 kW) for Neutron Energy > 8.0 MeV.  
[neutrons × barn<sup>-1</sup> × s<sup>-1</sup>]

Horizontal Section at Y = 0.0 cm.  
Dosimeter Locations “x”, 73X×79Y×278Z Spatial Meshes.

P<sub>3</sub>-S<sub>8</sub> Calculation Using the BUGJEFF311.BOLIB Library.

IRON-88 Distribution of Neutron Flux [n·barns<sup>-1</sup>·s<sup>-1</sup>] > 8 MeV.

Meshes: 73X, 79Y, 278Z Section at Y = 0.00 cm

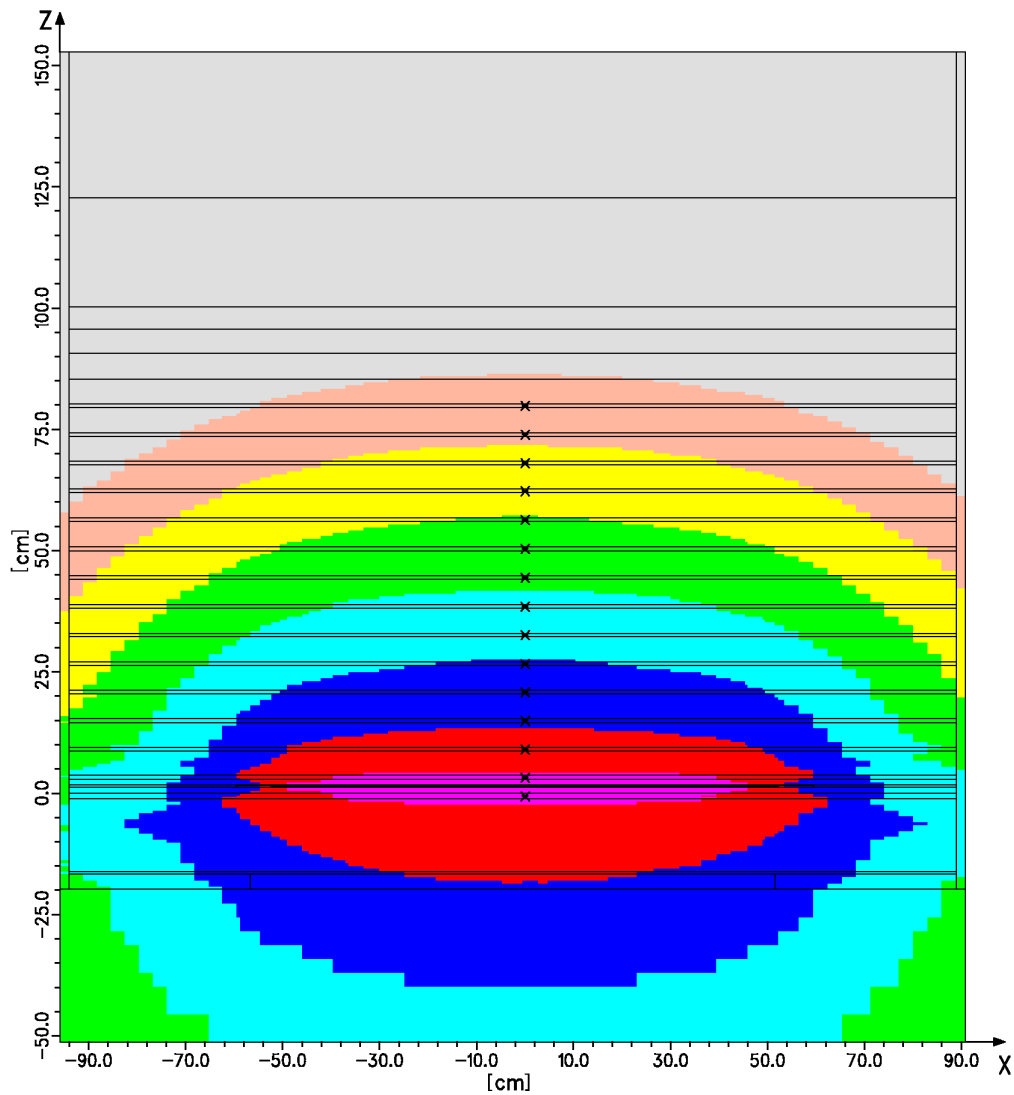
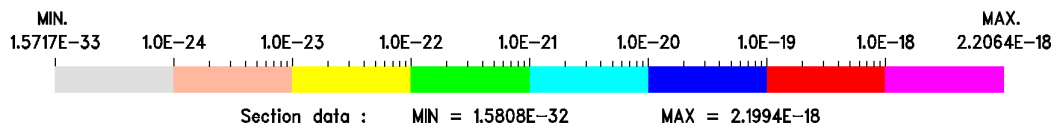


Figure 57

Iron-88 - Spatial Distribution of the Au-197(n, $\gamma$ )Au-198 epi-Cadmium Reaction Rates at the NESTOR Reactor Maximum Power (30 kW).  
[reactions  $\times$  s<sup>-1</sup>  $\times$  atom<sup>-1</sup>]

Horizontal Section at Y = 0.0 cm.  
Dosimeter Locations “x”, 73X $\times$ 79Y $\times$ 278Z Spatial Meshes.

P<sub>3</sub>-S<sub>8</sub> Calculation Using the BUGJEFF311.BOLIB Library and 1/4 T PV Weighting Dosimeter Cross Sections.

IRON-88 Au-197(n,g) Reaction Rates (BUGJEFF311.BOLIB, 1/4 T PV, 44grp).

Meshes: 73X, 79Y, 278Z Section at Y = 0.00 cm

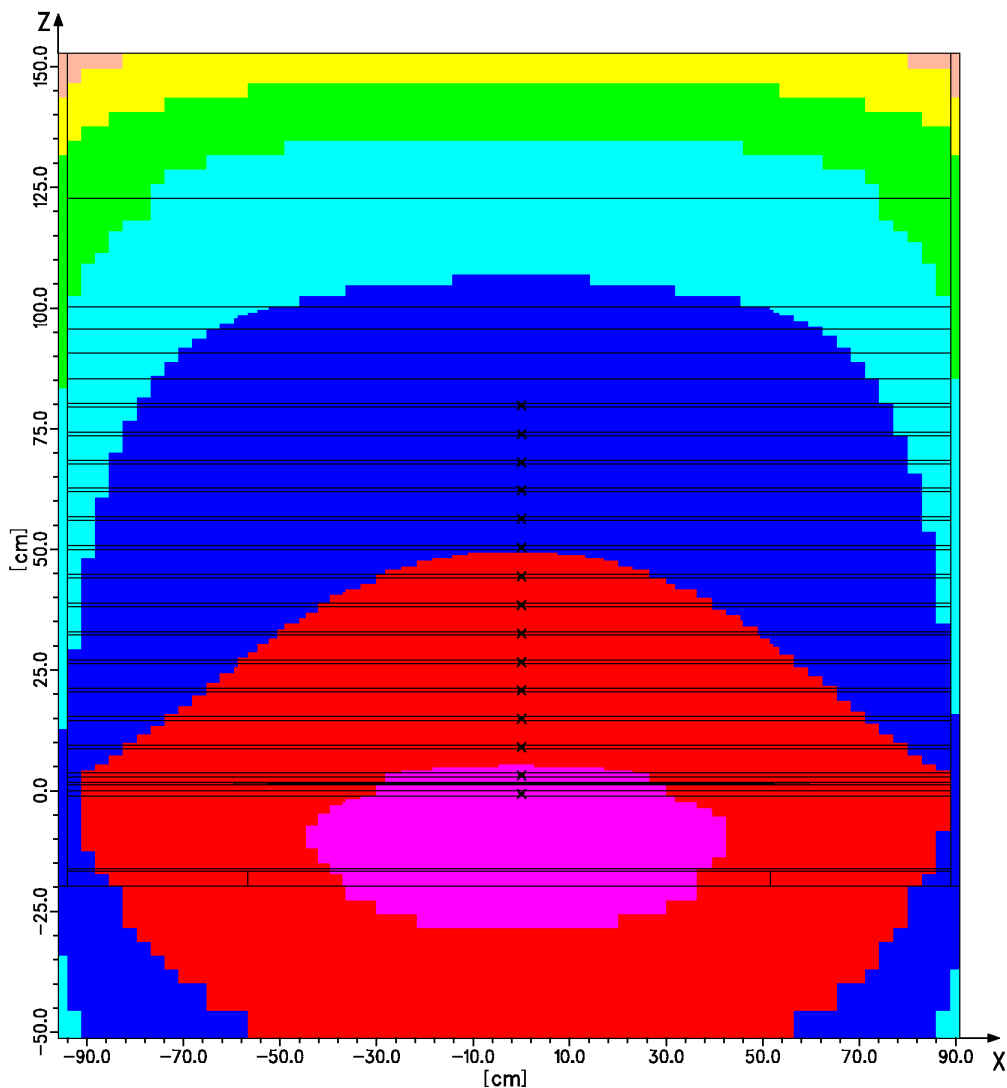
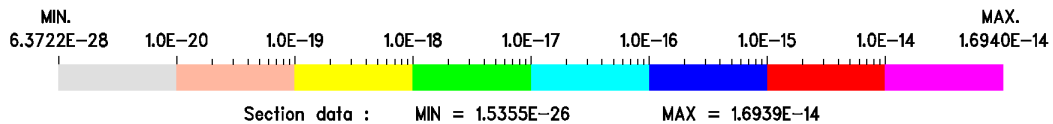


Figure 58

Iron-88 - Spatial Distribution of the Rh-103(n,n')Rh-103m Reaction Rates at the NESTOR Reactor Maximum Power (30 kW).  
[reactions  $\times$  s<sup>-1</sup>  $\times$  atom<sup>-1</sup>]

Horizontal Section at Y = 0.0 cm.  
Dosimeter Locations "x", 73X $\times$ 79Y $\times$ 278Z Spatial Meshes.

P<sub>3</sub>-S<sub>8</sub> Calculation Using the BUGJEFF311.BOLIB Library and 1/4 T PV Weighting Dosimeter Cross Sections.

IRON-88 Rh-103(n,n') Reaction Rates (BUGJEFF311.BOLIB, 1/4 T PV).

Meshes: 73X, 79Y, 278Z Section at Y = 0.00 cm

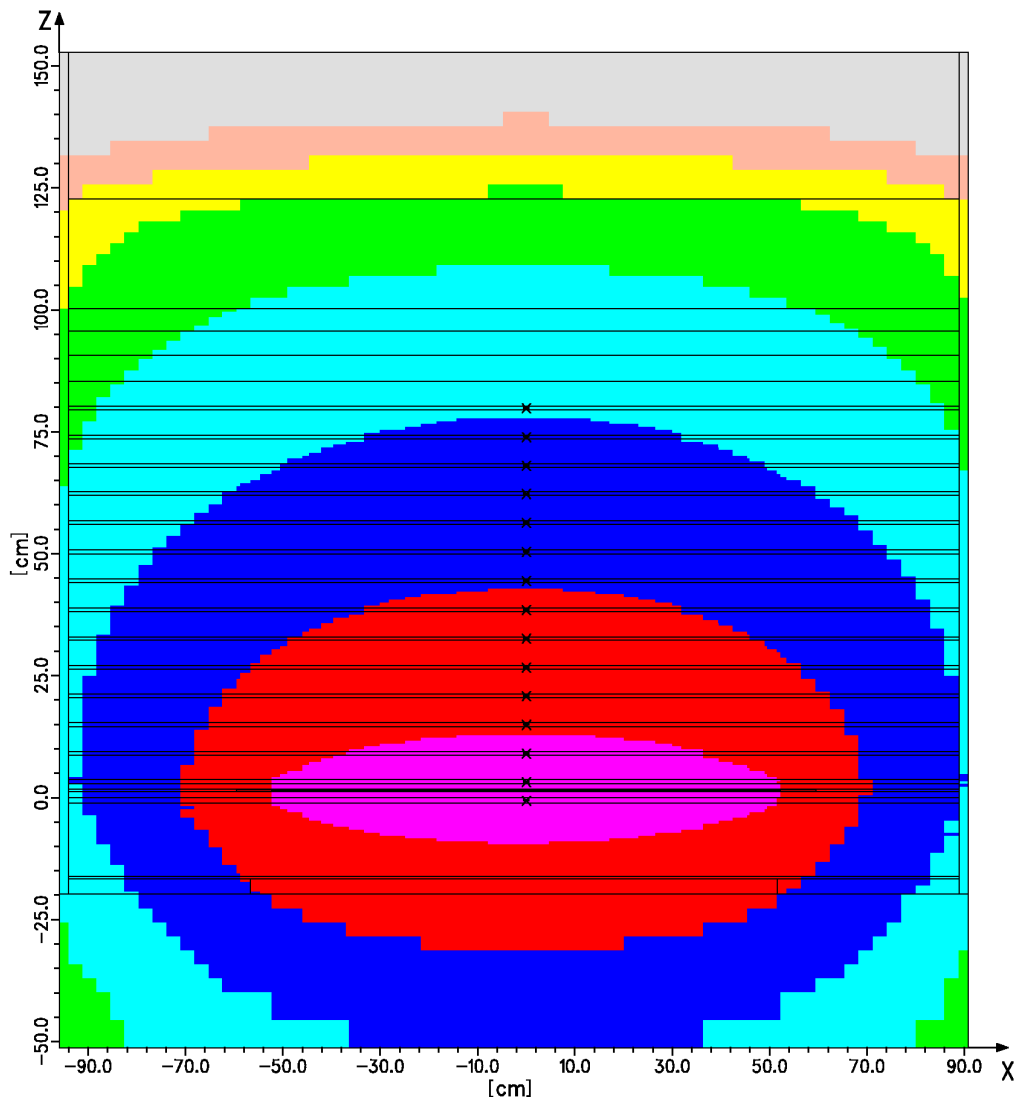
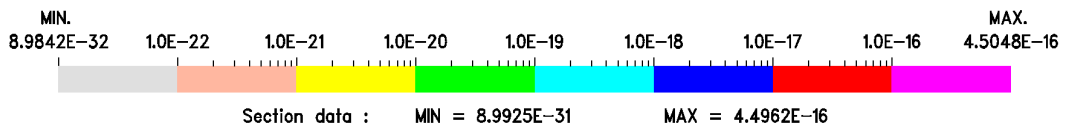


Figure 59

Iron-88 - Spatial Distribution of the In-115(n,n')In-115m Reaction Rates at the NESTOR Reactor Maximum Power (30 kW).  
[reactions  $\times$  s<sup>-1</sup>  $\times$  atom<sup>-1</sup>]

Horizontal Section at Y = 0.0 cm.  
Dosimeter Locations "x", 73X $\times$ 79Y $\times$ 278Z Spatial Meshes.

P<sub>3</sub>-S<sub>8</sub> Calculation Using the BUGJEFF311.BOLIB Library and 1/4 T PV Weighting Dosimeter Cross Sections.

IRON-88 In-115(n,n') Reaction Rates (BUGJEFF311.BOLIB, 1/4 T PV).

Meshes: 73X, 79Y, 278Z Section at Y = 0.00 cm

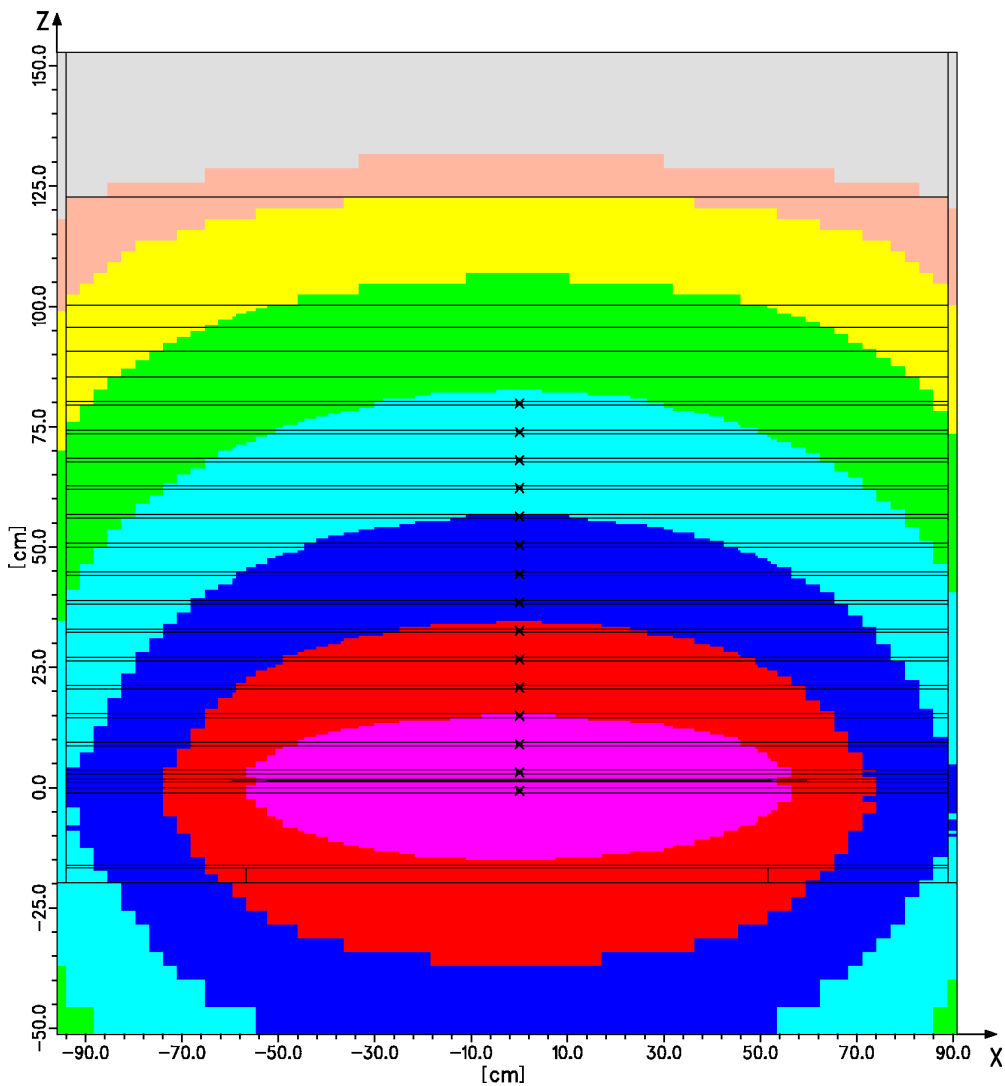
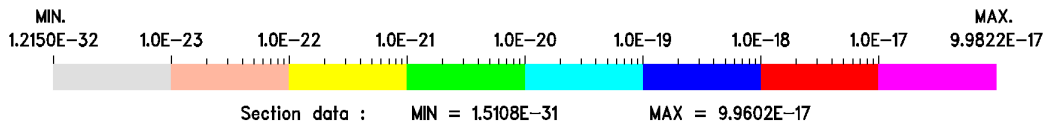


Figure 60

Iron-88 - Spatial Distribution of the S-32(n,p)P-32 Reaction Rates at the NESTOR Reactor Maximum Power (30 kW).  
[reactions  $\times$  s<sup>-1</sup>  $\times$  atom<sup>-1</sup>]

Horizontal Section at Y = 0.0 cm.  
Dosimeter Locations "x", 73X $\times$ 79Y $\times$ 278Z Spatial Meshes.

P<sub>3</sub>-S<sub>8</sub> Calculation Using the BUGJEFF311.BOLIB Library and 1/4 T PV Weighting Dosimeter Cross Sections.

IRON-88 S-32(n,p) Reaction Rates (BUGJEFF311.BOLIB, 1/4 T PV).

Meshes: 73X, 79Y, 278Z Section at Y = 0.00 cm

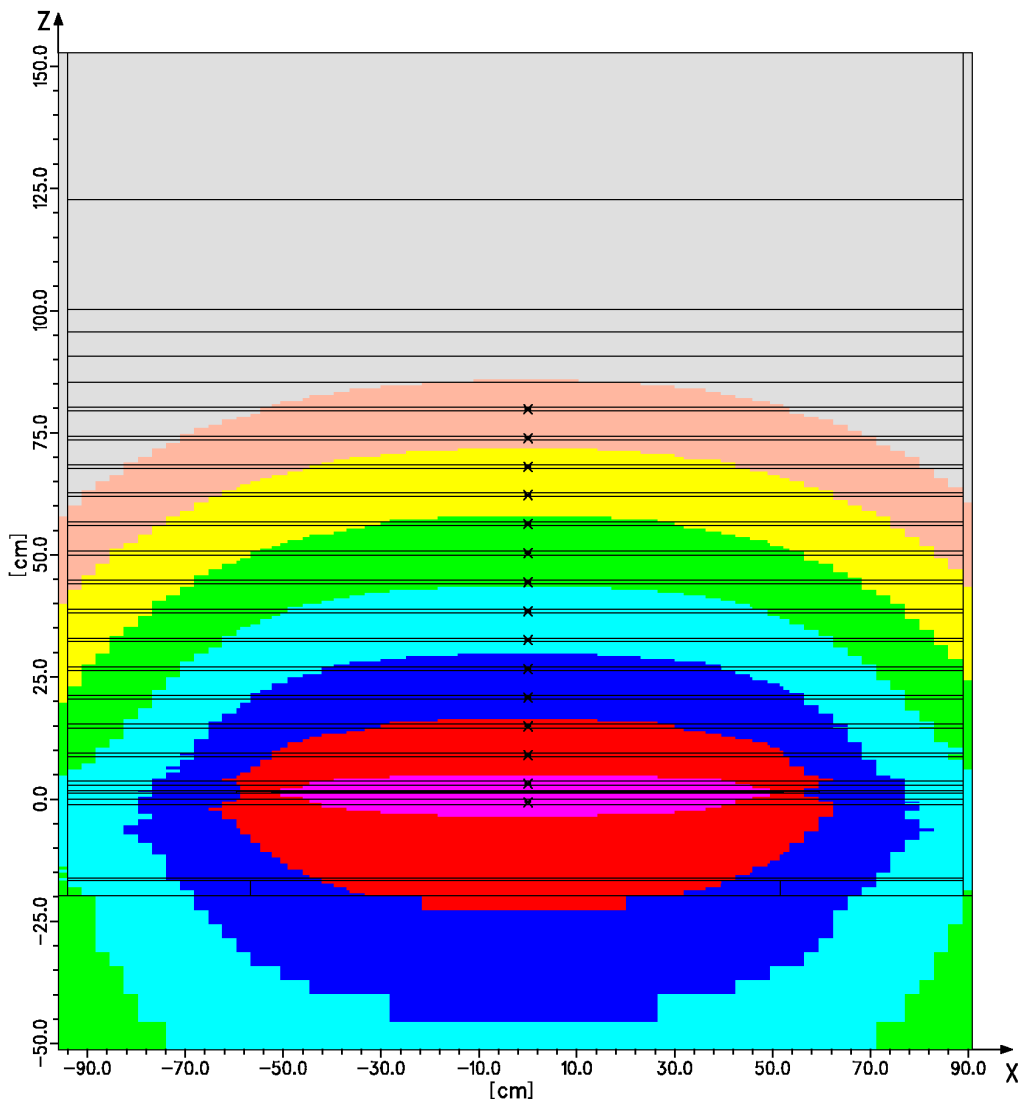
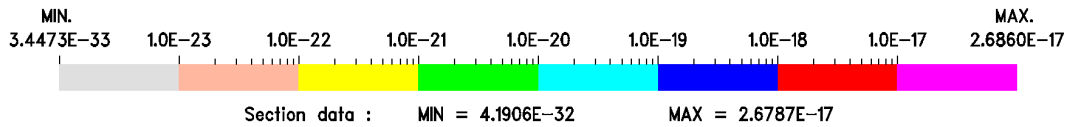


Figure 61

Iron-88 - Spatial Distribution of the Al-27(n, $\alpha$ )Na-24 Reaction Rates at the NESTOR Reactor Maximum Power (30 kW).  
[reactions  $\times$  s<sup>-1</sup>  $\times$  atom<sup>-1</sup>]

Horizontal Section at Y = 0.0 cm.  
Dosimeter Locations "x", 73X $\times$ 79Y $\times$ 278Z Spatial Meshes.

P<sub>3</sub>-S<sub>8</sub> Calculation Using the BUGJEFF311.BOLIB Library and 1/4 T PV Weighting Dosimeter Cross Sections.

IRON-88 Al-27(n, $\alpha$ ) Reaction Rates (BUGJEFF311.BOLIB, 1/4 T PV).

Meshes: 73X, 79Y, 278Z Section at Y = 0.00 cm

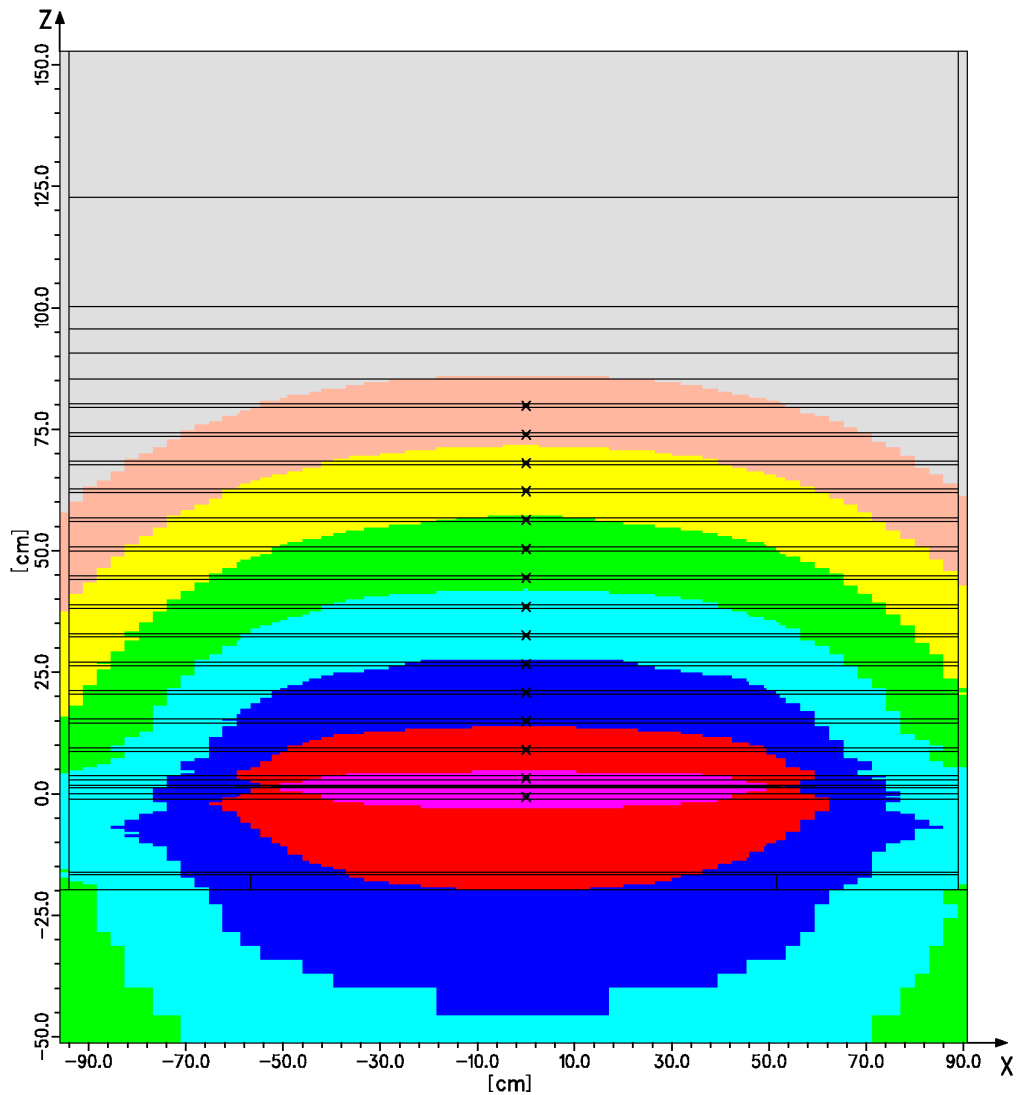
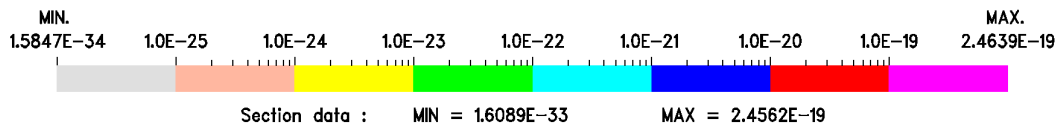




Figure 62

Iron-88 - Calculated Neutron Spectra in Mild Steel at the A2, A4, A8, A12 and A15 Measurement Positions for Neutron Energy > 0.414 eV.

P<sub>3</sub>-S<sub>8</sub> Calculation Using the BUGJEFF311.BOLIB Library.

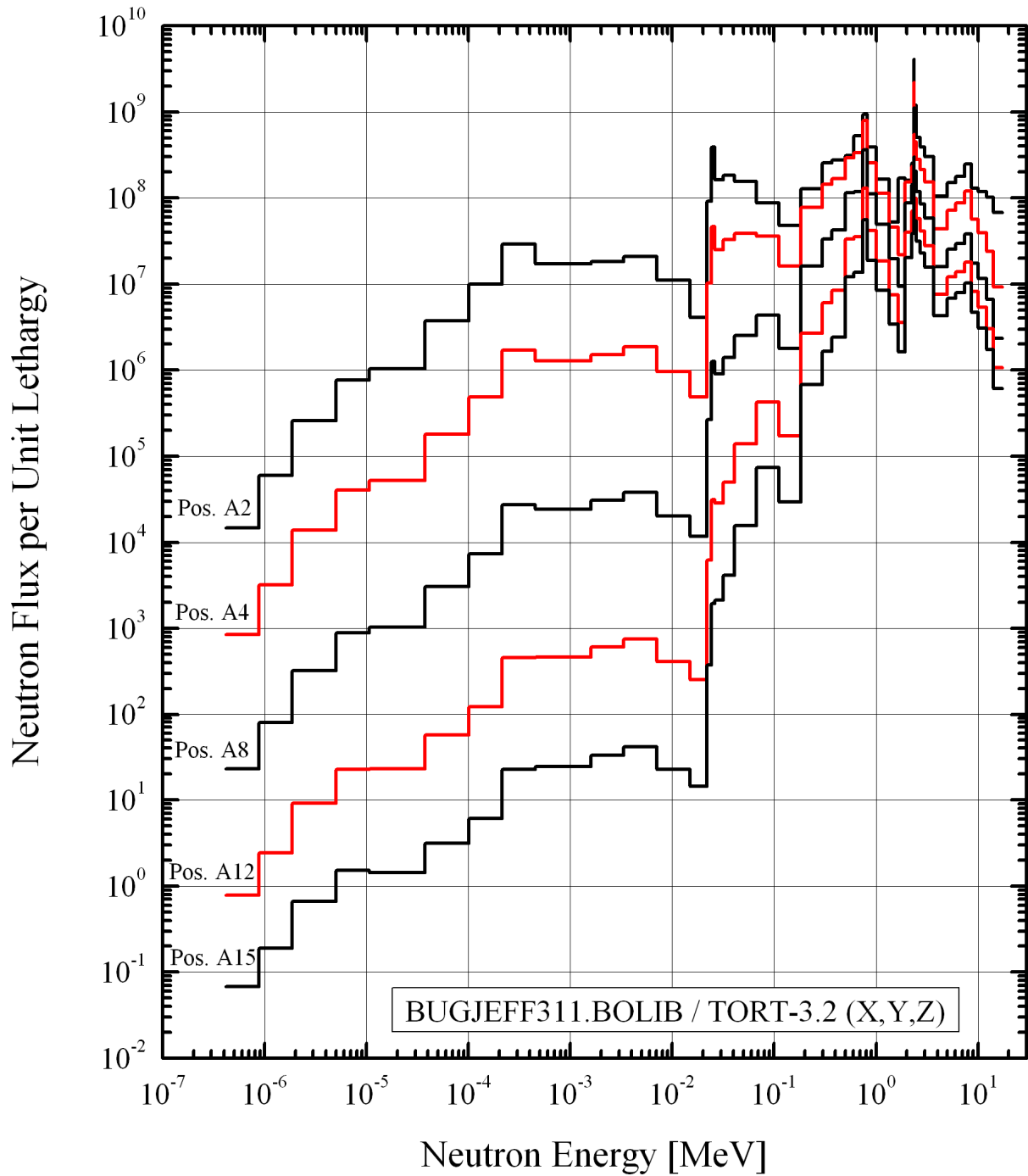
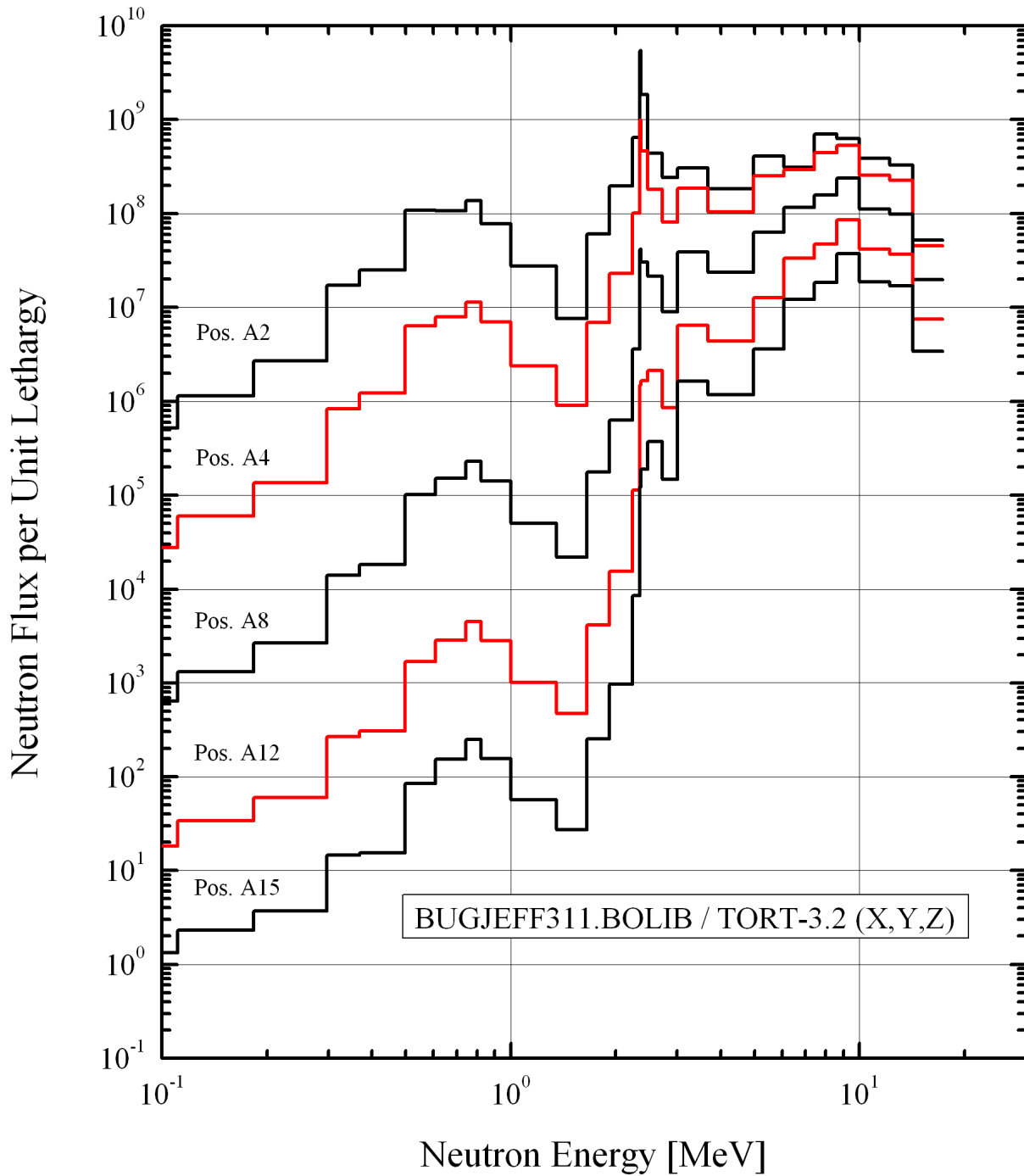


Figure 63

Iron-88 - Calculated Neutron Spectra in Mild Steel at the A2, A4, A8, A12 and A15 Measurement Positions for Neutron Energy > 0.1 MeV.

P<sub>3</sub>-S<sub>8</sub> Calculation Using the BUGJEFF311.BOLIB Library.



#### 4 - CONCLUSION

The ENEA-Bologna BUGJEFF311.BOLIB (JEFF-3.1.1 data) broad-group coupled ( $47 n + 20 \gamma$ ) working cross section library in FIDO-ANISN format, specifically conceived for LWR shielding and pressure vessel dosimetry applications, was validated on the Iron-88 single material (iron) neutron shielding benchmark experiment, included in the SINBAD REACTOR international database. This library validation was performed through three-dimensional fixed source transport calculations in Cartesian (X,Y,Z) geometry using the ORNL TORT-3.2 discrete ordinates ( $S_N$ ) code. The calculated reaction rates for the five activation dosimeters (Au-197(n, $\gamma$ )Au-198, Rh-103(n,n')Rh-103m, In-115(n,n')In-115m, S-32(n,p)P-32 and Al-27(n, $\alpha$ )Na-24) used in the Iron-88 experiment were obtained through the corresponding dosimeter cross section sets, derived from the IAEA IRDF-2002 dosimetry file, and were compared with the corresponding experimental results.

The BUGJEFF311.BOLIB library gives calculated results, corresponding to epi-cadmium measurements with the Au-197(n, $\gamma$ )Au-198 activation dosimeters, characterized by deviations from the corresponding experimental results contained within  $\pm 15\%$ .

For the three activation dosimeters Rh-103(n,n')Rh-103m, In-115(n,n')In-115m and S-32(n,p)P-32 with lower effective threshold energy, the BUGJEFF311.BOLIB library gives calculated results characterized by deviations of  $\pm 15-20\%$  from the corresponding experimental results. Only the calculations for the Al-27(n, $\alpha$ )Na-24 dosimeters with the highest effective threshold energy produce results systematically and excessively overestimated (from 20% up to about 30%) with respect to the corresponding experimental results.

Taking into account the total experimental uncertainties at the confidence level of one standard deviation ( $1\sigma$ ) of the Au-197(n, $\gamma$ )Au-198, Rh-103(n,n')Rh-103m, In-115(n,n')In-115m and S-32(n,p)P-32 dosimeters, the corresponding calculated reaction rate results presented in this work exhibit good statistical consistency with the corresponding measurements. On the contrary, the calculated reaction rates for the Al-27(n, $\alpha$ )Na-24 dosimeters are always excessively overestimated with respect to the corresponding experimental results, taking into account their related uncertainties at the confidence level of one standard deviation ( $1\sigma$ ).

The reaction rate results obtained using the BUGLE-96 reference library are systematically underestimated with respect to the corresponding calculated results obtained with the BUGJEFF311.BOLIB library for the Au-197(n, $\gamma$ )Au-198 activation dosimeters and the three Rh-103(n,n')Rh-103m, In-115(n,n')In-115m and S-32(n,p)P-32 threshold activation dosimeters with lower effective threshold energy. On the contrary, for the Al-27(n, $\alpha$ )Na-24 dosimeters with the highest effective threshold energy, the BUGLE-96 reaction rate results are systematically overestimated with respect to the corresponding BUGJEFF311.BOLIB calculated results.

All the cited calculated results at the various Iron-88 measurement positions in mild steel refer to those obtained using 1/4 T PV weighting dosimeter cross sections, obtained using a neutron spectrum properly calculated in iron, at one quarter of the thickness of a PWR pressure vessel (1/4 T PV). The preferable use of 1/4 T PV weighting dosimeter cross sections is obviously due to the similar main material (iron) involved in the dosimeter cross section weighting and

in the Iron-88 experimental reaction rate measurements. This is confirmed by the fact that, using 1/4 T PV weighting dosimeter cross sections, the calculated reaction rate results are always systematically more adherent to the Iron-88 corresponding experimental results. It is underlined that, in the case of the Au-197(n, $\gamma$ )Au-198 and Al-27(n, $\alpha$ )Na-24 calculated reaction rates, the differences in the results obtained using 1/4 T PV weighting dosimeter cross sections are particularly relevant with respect to those obtained using flat weighting dosimeter cross sections: the overestimated reaction rate results are in fact systematically reduced by 6% up to 10% when 1/4 T PV weighting dosimeter cross sections are used.

## REFERENCES

- /1/ M. Pescarini, V. Sinita, R. Orsi, M. Frisoni, BUGJEFF311.BOLIB - A JEFF-3.1.1 Broad-Group Coupled ( $47 n + 20 \gamma$ ) Cross Section Library in FIDO-ANISN Format for LWR Shielding and Pressure Vessel Dosimetry Applications, ENEA-Bologna Technical Report UTFISSM-P9H6-002, May 12, 2011. ENEA-Bologna Technical Report UTFISSM-P9H6-002 Revision 1 published on March 14, 2013. Available from OECD-NEA Data Bank as NEA-1866/02 ZZ BUGJEFF311.BOLIB.
- /2/ G.A. Wright, M.J. Grimstone, Benchmark Testing of JEF-2.2 Data for Shielding Applications: Analysis of the Winfrith Iron-88 Benchmark Experiment, AEA Report AEA-RS-1231, March 1993.
- /3/ Radiation Shielding Integral Benchmark Archive Database (SINBAD), OECD-NEA Data Bank/ ORNL-RSICC, SINBAD REACTOR, NEA-1517, 2009 Edition.
- /4/ I. Kodeli, E. Sartori, B. Kirk, SINBAD Shielding Benchmark Experiments Status and Planned Activities, The American Society's 14<sup>th</sup> Biennial Topical Meeting of the Radiation Protection and Shielding Division, Carlsbad, New Mexico, USA, April 3-6, 2006.
- /5/ W.A. Rhoades, D.B. Simpson, The TORT Three-Dimensional Discrete Ordinates Neutron/Photon Transport Code (TORT Version 3), Oak Ridge, ORNL Report ORNL/TM-13221, October 1997.
- /6/ O.Bersillon, L.R. Greenwood, P.J. Griffin, W. Mannhart, H.J. Nolthenius, R. Paviotti-Corcuera, K.I. Zolotarev, E.M. Zsolnay, International Reactor Dosimetry File 2002 (IRDF-2002), IAEA, Vienna, Austria, Technical Reports Series No. 452, 2006.
- /7/ W.W. Engle, Jr., A Users Manual for ANISN, A One Dimensional Discrete Ordinates Transport Code with Anisotropic Scattering, ORNL K-1693, Updated June 6, 1973. Available from OECD-NEA Data Bank as CCC-254 ANISN-ORNL.
- /8/ The JEFF-3.1.1 Nuclear Data Library, JEFF Report 22, OECD-NEA Data Bank, 2009.
- /9/ The JEFF-3.1 Nuclear Data Library, JEFF Report 21, OECD-NEA Data Bank, 2006.
- /10/ J.E. White, D.T. Ingersoll, R.Q. Wright, H.T. Hunter, C.O. Slater, N.M. Greene, R.E. MacFarlane, R.W. Roussin, Production and Testing of the Revised VITAMIN-B6 Fine-Group and the BUGLE-96 Broad-Group Neutron/Photon Cross-Section Libraries Derived from ENDF/B-VI.3 Nuclear Data, Oak Ridge, ORNL Report ORNL-6795/R1, NUREG/CR-6214, Revision 1, January 1995. VITAMIN-B6 library available from OECD-NEA Data Bank as DLC-0184 ZZ VITAMIN-B6. BUGLE-96 library available from OECD-NEA Data Bank as DLC-0185 ZZ BUGLE-96.
- /11/ American National Standard, American Nuclear Society, Neutron and Gamma-Ray Cross Sections for Nuclear Radiation Protection Calculations for Nuclear Power Plants, ANSI/ANS-6.1.2-1999 (R2009).
- /12/ M. Pescarini, R. Orsi, Preliminary Results of the BUGJEFF311.BOLIB Library Validation on the Iron-88 (Fe) Neutron Shielding Benchmark Experiment, ENEA-Bologna Technical Report ADPFISS-LP1-064, June 28, 2016.

- 13/ M.J. Armishaw, J. Butler, M.D. Carter, I.J. Curl, A.K. McCracken, A transportable Neutron Spectrometer (TNS) for radiological applications, AEEW-M2365, 1986.
- /14/ J.H. Baard, W.L. Zijp, H.J. Nolthenius, Nuclear Data Guide for Reactor Neutron Metrology, Kluwer Academic Publishers, 1989.
- /15/ G. Hehn, A. Sohn, M. Mattes, G. Pfister, IKE Calculations of the OECD/NEA Benchmarks VENUS-1 and VENUS-3 for Computing Radiation Dose to Reactor Pressure Vessel and Internals, Universität Stuttgart, Institut für Kernenergetik und Energiesysteme, IKE 6 NEA 2, December 1997.
- /16/ I.J. Curl, CRISP - A Computer Code to Define Fission Plate Source Profiles, RPD/IJC/934.
- /17/ P.F. Rose, ENDF/B-VI Summary Documentation, Brookhaven National Laboratory, BNL-NCS-17541 (ENDF-201) 4<sup>th</sup> Edition, October 1991.
- /18/ M. Pescarini, V. Sinitza, R. Orsi, VITJEFF311.BOLIB - A JEFF-3.1.1 Multigroup Coupled (199 n + 42  $\gamma$ ) Cross Section Library in AMPX Format for Nuclear Fission Applications, ENEA-Bologna Technical Report UTFISSM-P9H6-003, November 10, 2011. ENEA-Bologna Technical Report UTFISSM-P9H6-003 Revision 1 published on March 14, 2013. Available from OECD-NEA Data Bank as NEA-1869/01 ZZ VITJEFF311.BOLIB.
- /19/ I.I. Bondarenko, M.N. Nikolaev, L.P. Abagyan, N.O. Bazaziants, Group Constants for Nuclear Reactors Calculations, Consultants Bureau, New York, 1964.
- /20/ J. Butler, M.D. Carter, I.J. Curl, M.R. March, A.K. McCracken, M.F. Murphy, A. Packwood, The PCA-Replica Experiment Part I Winfrith Measurements and Calculations, UKAEA, AEE Winfrith Report AEEW-R 1736, January 1984.
- /21/ J. Butler, The NESTOR Shielding and Dosimetry Improvement Programme NESDIP for PWR Applications, PRPWG/P (82)5, Internal UKAEA Document, November 1982.
- /22/ L. Leenders, LWR-PVS Benchmark Experiment VENUS-3 (with Partial Shielded Assemblies) - Core Description and Qualification, Mol, SCK/CEN Report FCP/VEN/01, September 1, 1988.
- /23/ DOORS3.1: One-, Two- and Three-Dimensional Discrete Ordinates Neutron/Photon Transport Code System, ORNL, RSIC Computer Code Collection CCC-650, August 1996. Available from OECD/NEA Data Bank as CCC-0650/04 DOORS-3.2A.
- /24/ R. Orsi, BOT3P Version 5.3: A Pre/Post-Processor System for Transport Analysis, ENEA-Bologna Technical Report FPN-P9H6-011, October 22, 2008. Available from OECD-NEA Data Bank as NEA-1678/09 BOT3P-5.3.
- /25/ R. Orsi, The ENEA-Bologna pre-post-Processor Package BOT3P for the DORT and TORT Transport Codes (Version 1.0 - December 1999), JEF/DOC-828, JEFF Working Group Meeting on Benchmark Testing, Data Processing and Evaluations, OECD-NEA Data Bank, Issy-les-Moulineaux, France, May 22-24, 2000.

- /26/ R. Orsi, BOT3P: Bologna Transport Analysis Pre-Post-Processors Version 1.0, Nuclear Science and Engineering, Technical Note, Volume 142, pp. 349-354, 2002.
- /27/ R. Orsi, BOT3P: Bologna Transport Analysis Pre-Post-Processors Version 3.0, Nuclear Science and Engineering, Technical Note, Volume 146, pp. 248-255, 2004.
- /28/ MCBEND User Guide to Version 7, ANSWERS/MCBEND(91)7.
- /29/ R. Orsi, ADEFTA Version 4.1: A Program to Calculate the Atomic Densities of a Compositional Model for Transport Analysis, ENEA-Bologna Technical Report FPN-P9H6-010, May 20, 2008. Available from OECD-NEA Data Bank as NEA-1708/06 ADEFTA 4.1.
- /30/ J.K. Tuli, Nuclear Wallet Cards (6<sup>th</sup> Edition), National Nuclear Data Centre, Brookhaven National Laboratory, Upton, New York 11973-5000, USA, January 2000.
- /31/ R. Orsi, M. Pescarini, V. Sinitsa, Dosimetry Cross Section Processing from IRDF-2002 in the BUGLE-96 (47 n) Neutron Group Structure Using Flat and Updated Problem Dependent Neutron Spectra, ENEA-Bologna Technical Report UTFISSM-P9H6-006, May 9, 2012.
- /32/ D.E. Cullen, PREPRO 2007: 2007 ENDF/B Pre-processing Codes (ENDF/B-VII Tested), LLNL, owned, maintained and distributed by IAEA-NDS, Vienna, Austria, IAEA Report IAEA-NDS-39, Rev. 13, March 17, 2007. Available from OECD-NEA Data Bank as IAEA-1379 PREPRO-2007.
- /33/ N.M. Greene, J.L. Lucius, L.M. Petrie, W.E. Ford III, J.E. White and R.Q. Wright, AMPX: A Modular Code System for Generating Coupled Multigroup Neutron-Gamma Libraries from ENDF/B, Oak Ridge, ORNL Report ORNL/TM-3706, March 1976, informally revised to level of AMPX-II in December 1978. See in particular Chapter 9.12: BONAMI -AMPX Module to Perform Bondarenko Resonance Self-Shielding.
- /34/ K.H. Beckurts and K. Wirtz, Neutron Physics, Springer Verlag, 1964.

**Titolo**

**ANITA-IEAF :  
 an intermediate energy neutron activation system**

**Descrittori**

**Tipologia del documento:** Rapporto tecnico  
**Collocazione contrattuale:** Accordo di programma ENEA-MSE su sicurezza nucleare e reattori di IV generazione  
**Argomenti trattati:** Fisica nucleare, dati nucleari, librerie di dati di decadimento,

**Sommario**

ANITA-IEAF is an activation package (code and libraries) developed in ENEA-Bologna in order to assess the activation of materials exposed to neutrons with energies up to 55 MeV. It is suitable to be applied to the study of the irradiation effects on materials in facilities like the International Fusion Materials Irradiation Facility (IFMIF) and, more recently, the DEMO Oriented Neutron Source (DONES), in which a considerable amount of neutrons with energies above 20 MeV is produced. The package provides: a) the activation code ANITA-IEAF, b) the activation cross section library, file "eaf2010\_lib", based on the EAF-2010 group-wise neutron activation cross section library "eaf\_n\_gxs\_211\_ft\_20010" in the VITAMIN-J+ (211 energy group structure) up to 55 MeV, c) the Decay, Hazard and Clearance data library (file "fl1") containing the quantities describing the decay properties of unstable nuclides and d) the Gamma library (file "fl2") containing the gamma ray spectra emitted by the radioactive nuclei. The data contained in the fl1 and fl2 files are based on the JEFF-3.1.1 Radioactive Decay Data Library. Three test cases (both input and output files) are included in the code package. In this report the main characteristics of the code and the libraries, together with the description of the input and output files, are given. It can be used as the ANITA-IEAF "user's manual". The validation effort related to the comparison between the code predictions and the activity measurements obtained from the Karlsruhe Isochronous Cyclotron is also presented.


**Note**

Author: Manuela Frisoni

**Copia n.**
**In carico a:**

2			NOME			
			FIRMA			
1			NOME			
			FIRMA			
0	EMISSIONE	09/11/2017	NOME	M. Frisoni	F. Padoani	F. Rocchi
			FIRMA	<i>Manuela Frisoni</i>	<i>F. Padoani</i>	<i>F. Rocchi</i>
REV.	DESCRIZIONE	DATA	REDAZIONE	CONVALIDA	APPROVAZIONE	



 <b>Ricerca Sistema Elettrico</b>	<b>Sigla di identificazione</b>	<b>Rev.</b>	<b>Distrib.</b>	<b>Pag.</b>	<b>di</b>
	ADPFISS-LP1-089	0	L	2	67

## CONTENTS


1	INTRODUCTION .....	5
2	ANITA-IEAF ACTIVATION CODE .....	7
2.1	Main features of the activation code .....	7
2.2	Analytical Method.....	7
3	DATA LIBRARIES .....	9
3.1	Decay, Hazard and Clearance Data library (file “f1”).....	10
3.1.1	Decay data.....	10
3.1.2	Hazard data .....	11
3.1.3	Clearance level data .....	11
3.1.4	Nuclide and Material Clearance Indexes .....	11
3.1.5	Structure of the “f1” file .....	12
3.2	Gamma Library (file “f2”).....	15
3.3	Neutron activation cross section data library (file “lib211”) .....	18
4	HOW TO USE.....	23
4.1	Input/Output Unit-Files Assignments .....	23
4.2	Neutron Fluxes .....	24
4.3	Input Specifications.....	27
4.4	Output Specifications .....	30
4.4.1	Standard Output .....	30
4.4.2	General Inventory Output Data File.....	33
4.4.3	Clearance Index Inventory Output Data File .....	33
4.4.4	Decay gamma sources Output Data File.....	34
4.5	How to run ANITA-IEAF.....	35
4.6	Sample Problems.....	36
4.6.1	Test3 case input.....	36
4.6.2	Test3 case output.....	38
5	ANITA-IEAF VALIDATION.....	48
5.1	Neutron Flux .....	48
5.2	Activation parameters .....	49
5.3	Samples compositions.....	49
5.4	Cooling times .....	50
5.5	Calculated and experimental results comparison.....	51
5.6	Results analysis .....	63
	REFERENCES.....	66

## FIGURE LIST

Figure 1 – ANITA-IEAF activation code block diagram.....	9
Figure 2 – Neutron flux .....	48
Figure 3 – SS-316 specific activity: calculation to experiment ratios (C/E). Main isotope contributors. ....	59
Figure 4 – SS-316 specific activity: calculation to experiment ratios (C/E). Other isotopes. ....	59
Figure 5 – F82H specific activity: calculation to experiment ratios (C/E). Main isotope contributors.....	60
Figure 6 – F82H specific activity: calculation to experiment ratios (C/E). Other isotopes.....	60
Figure 7 – V-alloy specific activity: calculation to experiment ratios (C/E). Main isotope contributors.....	61
Figure 8 – V-alloy specific activity: calculation to experiment ratios (C/E). Other isotopes.....	61
Figure 9 – V-pure specific activity: calculation to experiment ratios (C/E). All isotopes.....	62

## TABLE LIST

Table 1 – Decay processes.....	13
Table 2 – Upper boundaries of the Vitamin-J 42- $\gamma$ energy group structure .....	15
Table 3 – Energy group boundaries of the Vitamin-J +(211-neutron energy group structure) .....	19
Table 4 – List of MT numbers used in ANITA-IEAF package.....	21
Table 5 – Activation parameters.....	49
Table 6 – Composition of samples in weight% .....	49
Table 7 – Cooling times .....	50
Table 8 – SS-316 specific activity- Experimental and calculated results.....	52
Table 9 – F82H specific activity- Experimental and calculated results .....	55
Table 10 – V-alloy specific activity- Experimental and calculated results .....	57
Table 11 – V-pure specific activity- Experimental and calculated results .....	58

 <b>Ricerca Sistema Elettrico</b>	<b>Sigla di identificazione</b>	<b>Rev.</b>	<b>Distrib.</b>	<b>Pag.</b>	<b>di</b>
	ADPFISS-LP1-089	0	L	5	67

## **ANITA-IEAF** **an intermediate energy neutron activation system**

Manuela Frisoni

November 2017

### **1 INTRODUCTION**


ANITA-IEAF is a package (code and libraries) developed in ENEA-Bologna able to assess the activation of materials exposed to neutrons with energies up to 55 MeV. (The identification IEAF results from the first ANITA-IEAF version [1] that used the activation cross section library based on the Intermediate Energy Activation File IEAF-2001 [2]). It is an updating/extension of the ANITA-2000 code package freely distributed at OECD-NEADB [3] and ORNL-RSICC [4], able to handle neutron energies up to 20 MeV, widely used and validated in the past by ENEA [5][6][7][8][9][10].

The ANITA-IEAF package is needed in order to perform neutron activation calculations for some plants as the International Fusion Materials Irradiation Facility (IFMIF) and, more recently, the DEMO Oriented Neutron Source (DONES), that have been proposed as neutron sources to test samples of candidate materials to be used in future fusion power plants. In both these facilities the neutron source is produced through the reaction of 40 MeV deuterons impinging on a liquid lithium target and a considerable amount of neutrons with energies above 20 MeV is produced. The availability of reliable nuclear data and activation codes in the neutron energy range extended over 20 MeV is required in order to perform activation calculations for these devices.

The main component of the ANITA-IEAF package is the activation code ANITA-IEAF that computes the radioactive inventory of a material exposed to neutron irradiation, continuous or stepwise. It traces back to the ANITA code (Analysis of Neutron Induced Transmutation and Activation) [11]. The ANITA-IEAF code provides activity, atomic density, decay heat, biological hazard, clearance index and decay gamma-ray sources versus cooling time. Results are given as for each nuclide as for the material.

The ANITA-IEAF code package is provided with a complete data base allowing to perform calculations for all the elements with the atomic number up to 94. The libraries contained in the code package are:

- 1) Neutron activation data library (file “eaf2010\_lib”), containing the neutron induced cross sections on target nuclides.

 <b>Ricerca Sistema Elettrico</b>	<b>Sigla di identificazione</b>	<b>Rev.</b>	<b>Distrib.</b>	<b>Pag.</b>	<b>di</b>
	ADPFISS-LP1-089	0	L	6	67

- 2) Decay, Hazard and Clearance data library (file “fl1”), containing the quantities describing the decay properties of unstable nuclides.
- 3) Gamma library (file “fl2”), containing the gamma ray spectra emitted by the radioactive nuclei.


The neutron activation cross section data library is based on the EAF-2010 [12] group-wise neutron activation cross section library “eaf\_n\_gxs\_211\_ft\_20010” in the VITAMIN-J+ (211 energy group structure) up to 55 MeV, contained in the EASY-2010 code package [13].

The data contained in the fl1 and fl2 files are based on the JEFF-3.1.1 Radioactive Decay Data Library [14].

Three test cases (both input and output files) are included in the code package.

In this report the characteristics of the libraries contained in the package, the input data specification and the output description, with reference to a representative sample problem, are given.

The validation effort related to the comparison between the code predictions and the activity measurements obtained from the Karlsruhe Isochronous Cyclotron is also presented.

 <b>Ricerca Sistema Elettrico</b>	<b>Sigla di identificazione</b>	<b>Rev.</b>	<b>Distrib.</b>	<b>Pag.</b>	<b>di</b>
	ADPFISS-LP1-089	0	L	7	67

## 2 ANITA-IEAF ACTIVATION CODE

### 2.1 Main features of the activation code

The ANITA-IEAF activation code included in the package computes the radioactive inventory of a material exposed to neutron irradiation, continuous or stepwise. The ANITA-IEAF code provides activity, atomic density, decay heat, biological hazard, clearance index and decay gamma-ray source spectra at shutdown and at different cooling times. It treats all the elements with the atomic number up to 94.

The analytical computational method used by ANITA-IEAF is highly performing as far as the computer time is concerned.

### 2.2 Analytical Method

The calculation method [15] used by the code is summarized in the following.

The neutron irradiation of an atomic species  $A(N,Z)$  gives rise to several possible nuclear reactions whose number increases with increasing the energy of the incident particles. The new atomic species produced by the neutron-induced reactions may be stable or unstable or may be produced in the ground or a metastable state. Unstable nuclei will sooner or later decay into a new state or into a new species of nuclei, which in turn could be stable or decay again. These processes give rise to a decay chain that will end when a stable state is reached.

The time dependence of the concentration of a given nuclide  $N_i$  obeys the following balance equation:


$$\frac{dN_i}{dt} = \text{Formation Rate} - \text{Destruction Rate} - \text{Decay Rate} \quad (1)$$

The ANITA-IEAF code considers radioactive disintegration and neutron induced reactions as the processes appearing on the right-hand side of the Eq. (1). The time rate of change of the concentration for a particular nuclide  $N_i$ , in terms of these phenomena, can be written as:

$$\frac{dN_i}{dt} = \sigma_{r,i-1} N_{i-1} \phi + \lambda'_i N'_i - \sigma_{r,i} N_i \phi - \lambda_i N_i \quad (2)$$

where ( $i= 1\dots I$ ), and

- $\sigma_{r,i-1} N_{i-1} \phi$  is the transmutation rate into  $N_i$  due to the neutron induced reaction  $r$  on the nuclide  $N_{i-1}$ ,

 <b>Ricerca Sistema Elettrico</b>	<b>Sigla di identificazione</b>	<b>Rev.</b>	<b>Distrib.</b>	<b>Pag.</b>	<b>di</b>
	ADPFISS-LP1-089	0	L	8	67

- $\lambda'_i N'_i$  is the rate of formation of  $N_i$  due to the radioactive decay of nuclides  $N'_i$ ,
- $\sigma_{r,i} N_i \phi$  is the destruction rate of  $N_i$  due to all possible neutron induced reactions ( $n,\gamma$  ;  $n,\alpha$  ;  $n,p$  ;  $n,2n$  ;  $n,np$  ; etc.), and
- $\lambda_i N_i$  is the radioactive decay rate of  $N_i$

Considering all the I nuclides of the chain, the Eq. (2) represents a coupled set of homogenous first order linear differential equations with constant coefficients. The ANITA-IEAF code solves this set of equations by the analytical matrix exponential method.

The Eq. (2) can be written in matrix notation as

$$\frac{d\tilde{N}}{dt} = \tilde{A} \tilde{N} \quad (3)$$

where  $\tilde{N}$  is the vector of nuclide concentrations and  $\tilde{A}$  is the transition matrix containing the rate coefficients for radioactive decay and neutron absorption. Eq. (3) has the known solution

$$\tilde{N}(t) = \tilde{N}(0) e^{\tilde{A} t} \quad (4)$$

where  $\tilde{N}(0)$  is the vector of initial nuclide concentrations. The Eq. (4) can be expanded as

$$\tilde{N}(t) = \tilde{N}(0) \sum_{m=0}^{\infty} \frac{(\tilde{A} t)^m}{m!} \quad (5)$$

The Eq. (5) yields a complete solution to the problem. The irradiation is assumed to start at time zero when  $N_1(0)$  is known and  $N_i(0) = 0$  for  $i > 1$ . By defining these initial conditions the solutions of the system of Eq. (2) can be calculated by recurrence relations quite suitable for computer programming.

The particular cases when the decay time of an unstable nucleus of the chain is much longer or shorter than the irradiation time interval are taken into account and treated separately. The Eq. (2) holds during the irradiation time. At the end of this time the Bateman equations are solved describing the naturally occurring radioactive decay chains with the densities, solutions of the system (Eq. 2) at the end of irradiation, as initial conditions. Continuous or multi-steps (up to 2000 burn-dwell intervals) can be considered for the operational scenario. A different level of the irradiation flux can be used for each one of the exposure time steps.

### 3 DATA LIBRARIES

The ANITA-IEAF activation code requires the following data libraries:

- Decay, Hazard and Clearance data library (file “f11”)
- Gamma library (file “f12”)
- Neutron activation cross section data library (file “lib211”)

The schematic block diagram of the data/libraries required by the ANITA-IEAF code is shown in Figure 1.

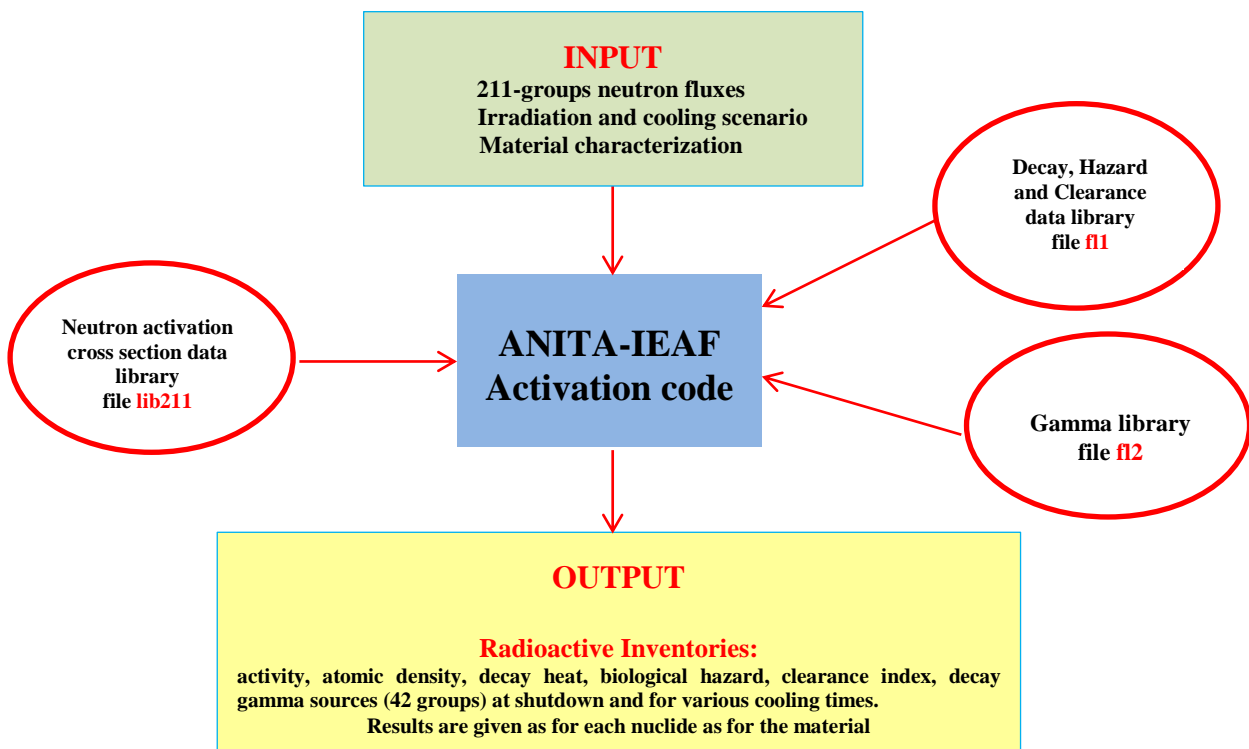



Figure 1 – ANITA-IEAF activation code block diagram



 <b>Ricerca Sistema Elettrico</b>	<b>Sigla di identificazione</b>	<b>Rev.</b>	<b>Distrib.</b>	<b>Pag.</b>	<b>di</b>
	ADPFISS-LP1-089	0	L	10	67

### 3.1 Decay, Hazard and Clearance Data library (file “f11”)

This library contains the information describing the decay properties of unstable nuclides useful for the calculations performed by ANITA-IEAF.

For each nuclide, the decay data, as the decay mode, the decay constant ( $s^{-1}$ ), the total energy (MeV) released in the decay and the energy (MeV) released in the form of gamma or X-rays are provided. Different competitive decay modes are taken into account when contemporary.

The file contains also the hazard data (ALI) for each radionuclide describing its potential biological impact on human beings. The ALI quantities are defined as the Annual Limit of Intake (Bq) by ingestion or inhalation for the public or workers.

The library contains also the clearance level for each radionuclide.

The **f11** file contains data for 3433 nuclides. The description of the data contained in the file and their sources are described in the following.

#### 3.1.1 Decay data


The decay data have been taken from the JEFF-3.1.1 Radioactive Decay Data library [14]. The standard library JEFF-3.1.1 is in ENDF-6 [16] format. The radioactive decay data are given in the section identified by MF=8, MT=457 (in ENDF-6 standard format notation). This section is restricted to single nuclides in their ground state or an isomeric state (a “long lived” excited state of the nucleus). The main purpose of MT=457 is to describe the energy spectra resulting from radioactive decay and give average parameters useful for applications such as decay heat and waste disposal studies, shielding, etc. For each isotope the following decay data are given: nuclide identification, half-life, number of decay modes, fractions of decay in each decay mode (branching ratio), energy released by the decay, gamma-ray intensity and energy spectrum in each decay mode. The standard library contains data for 3853 nuclei, ranging from the neutron (0-nn-1) to roentgenium 272 (111-Rg-272).

In the **f11** file the following basic decay data are included for each unstable nuclide:

- nuclide identification
- decay mode
- decay constant
- total energy released in the decay (MeV) used to calculate decay heat
- energy released in the form of gamma or X-rays (MeV)

For the stable nuclides the isotopic abundances are given taken from Ref. [17].

The **f11** file contains data for the nuclei ranging from the 1-H-1 to 94-Pu-247.

 <b>Ricerca Sistema Elettrico</b>	<b>Sigla di identificazione</b>	<b>Rev.</b>	<b>Distrib.</b>	<b>Pag.</b>	<b>di</b>
	ADPFISS-LP1-089	0	L	11	67

### 3.1.2 Hazard data

The ALI quantities were obtained from the “eaf\_haz\_20100” file contained in the EASY-2010 code package [18]. In the **f11** file used by the ANITA-IEAF code, the ALI values by ingestion for the public are given. A conversion factor of 0.001 (Sv/y) has been adopted to convert the dose coefficients from Ref. 18 to the ALI quantities. The ALI quantity is provided only for the 2006 nuclides contained in the “eaf\_haz\_20100” file.

### 3.1.3 Clearance level data

The **f11** file provides also for each radionuclide the clearance level  $C_L$  (Bq/g). This value allows to establish if a radioactive material can be potentially moved out of the originating facility and recycled.

The safe handling of radioactive waste is recognized as crucial to ensure protection of human health and the environment. IAEA publish regulations on these issues and reference [19] gives information on suggested clearance level values for a set of important radionuclides.

The clearance level data contained in the new **f11** file have been produced by including the information contained in [19].

The clearance levels for the 242 nuclides up to Pu-244 contained in Table 2 of Ref. [19] were included in the file **f11**. The clearance level  $C_L=10$  has been attributed to  $^{40}\text{K}$  as suggested in Table 1 of Ref. [19].

Following the suggestion of Table 1 of Ref. [19], moreover, the clearance level  $C_L=1$  has been attributed to radionuclides of natural origin. The list of the “Radioactive Nuclides in Nature” has been taken from [17].

For any other nuclide the clearance level was calculated by using the following Eq. (6) taken from [20] :

$$C_L = \min \{ 1 / (E_\gamma + 0.1 \times E_\beta) ; ALI_{\text{inhaled}} / 10^3 ; ALI_{\text{ingested}} / 10^5 \} \quad (6)$$


The values of  $E_\gamma$  and  $E_\beta$  in Eq. (6) have been taken from the JEFF-3.1.1 library [14].

The ALI quantities in Eq. (6) have been obtained from the “eaf\_haz\_20100” file of EASY-2010 [18]. The conversion factor of 0.020 (Sv/y) has been adopted to convert the dose coefficients from Ref. [18] to the ALI quantities.

### 3.1.4 Nuclide and Material Clearance Indexes

The Isotope Clearance Index (**ICI**) of a single nuclide is calculated in ANITA-IEAF as:

$$\text{Isotope Clearance Index} = \frac{C_i}{C_{Li}} \quad (7)$$

 <b>Ricerca Sistema Elettrico</b>	<b>Sigla di identificazione</b>	<b>Rev.</b>	<b>Distrib.</b>	<b>Pag.</b>	<b>di</b>
	ADPFISS-LP1-089	0	L	12	67

where  $C_i$  is the specific activity of the radionuclide “i” in the material and  $C_{Li}$  is the clearance level for that radionuclide.

In Eq. (7) activities and clearance levels have units of  $Bq\ g^{-1}$ .

When a material contains several nuclides, the equation given below, and suggested in [20], is used to evaluate in ANITA-EAF the Material Clearance Index (**MCI**) :

$$Material\ Clearance\ Index = \sum_{i=1}^n \frac{C_i}{C_{Li}} \quad (8)$$

If  $MCI \leq 1$  then it is possible to clear the material.

### 3.1.5 Structure of the “f11” file

The structure of the **f11** file used by ANITA-IEAF is described in the following:

**Card 1**      NUCLIB,TITLIB  
(I10,15A4)

where:      NUCLIB: number of nuclides (stable or unstable) contained in the file  
              TITLIB : alphanumeric title

For each nuclide two cards are given:

**Card 2a**      IDNUC, IDEC,  $\lambda_1$ ,  $Q_1$ ,  $G_1$ ,  $\lambda_2$ ,  $Q_2$ ,  $G_2$   
(I7,1X,I2,E10.4,2F10.7,E10.4,2F10.7)

**Card 2b**      IDNUC, IDEC,  $Q_T$ , ALI, CLEAR, SYMB  
(I7,1X,I2,F10.7,2E10.2,1X,A11)

where:

IDNUC      identification of the nuclide=  $Z*10000 + A*10 + M$

Z= atomic number

A= mass number

M= 0,1,2 for the ground state, the first and the second metastable state, respectively

IDEC      identification of the decay type (see Table 1)

0 < IDEC < 10      single decay

10 ≤ IDEC      double decay

“blank”      indicates stable isotopes; in this case “ $Q_1$ ” is the isotopic abundance and  $\lambda$ ,  $Q$ ,  $G$  are zeroes;

=0      indicates naturally occurring very long-lived radioactive

nuclei.  $Q_1$  in this case is their isotopic abundance and the decay parameters are given as  $\lambda_2, Q_2, G_2$ .

$\lambda_1$  decay constant ( $s^{-1}$ )  
 $Q_1$  total energy (MeV) released in the decay (used to calculate the decay heat)  
 $G_1$  energy released (MeV) in the form of X or  $\gamma$  rays

When a nuclide has two decay modes a second set of values  $\lambda_2, Q_2, G_2$  is given. In this case the decay constants  $\lambda_1$  e  $\lambda_2$  were obtained by multiplying the decay constant  $\lambda$  for the branching-ratio of each decay mode while  $Q_2$  e  $G_2$  are equal to  $Q_1$  e  $G_1$  .

When one of the two decay modes has a negligible probability only the dominant mode has been given with branching ratio BR= 1. When more than two decay modes are present only the two most important are considered in the library, with the BR normalised in order to have a total BR=1. These particular cases are outlined by a comment.

$Q_{TOT}$  =  $Q_1$  (MeV)  
ALI is the Annual Limit of Intake (Bq) by ingestion for the public  
CLEAR clearance level ( Bq/g)  
SYMB alphanumeric symbol

IDEC	Type of decay	“Parent nucleus”	“Daughter nuclei”		
1	$\beta^-$	A Z m	A	Z+1	0
2	$\beta^+/\text{EC}$		A	Z-1	0
3	IT <sub>1</sub>		A	Z	0
4	$\alpha$		A-4	Z-2	0
5	IT <sub>2</sub>		A	Z	m-1
10	$\beta^-$		A	Z+1	0
			A	Z+1	1
12	$\beta^-$ and $\beta^+$		A	Z+1	0
			A	Z-1	0
13	$\beta^-$ and IT		A	Z+1	0
			A	Z	0
20	$\beta^+/\text{EC}$		A	Z-1	0
			A	Z-1	1
23	$\beta^+$ and IT		A	Z-1	0
			A	Z	0

Table 1 – Decay processes

An example of the **f11** file (related to some Co isotopes) is given in the following.

\*JEFF-3.1.1 Decay&Hazard&Clearance Data

| Card 1

270540	2	3.587E+00	4.4213428	1.0210000																Card 2a
270540	2	4.4213428	6.67E+07	7.35E-01	27-CO-	54														Card 2b
270541	2	7.806E-03	5.9777899	3.9305599																Card 2a
270541	2	5.9777899	1.09E+05	2.42E-01	27-CO-	54M														Card 2b
270550	2	1.098E-05	2.4436109	2.0070300																Card 2a
270550	2	2.4436109	1.00E+06	1.00E+01	27-CO-	55														Card 2b
270560	2	1.038E-07	3.7138441	3.5916100																Card 2a
270560	2	3.7138441	4.00E+05	1.00E-01	27-CO-	56														Card 2b
270570	2	2.952E-08	0.1435085	0.1252160																Card 2a
270570	2	0.1435085	4.76E+06	1.00E+00	27-CO-	57														Card 2b
270580	2	1.132E-07	1.0105141	0.9762030																Card 2a
270580	2	1.0105141	1.35E+06	1.00E+00	27-CO-	58														Card 2b
270581	3	2.163E-05	0.0240866	0.0018165																Card 2a
270581	3	0.0240866	4.17E+07	1.00E+04	27-CO-	58M														Card 2b
270590			1.																	Card 2a
270590					27-CO-	59														Card 2b
270600	1	4.167E-09	2.6006136	2.5038400																Card 2a
270600	1	2.6006136	2.94E+05	1.00E-01	27-CO-	60														Card 2b
270601	13	2.758E-06	0.0624753	0.0067864	1.101E-03	0.0624753	0.0067864													Card 2a
270601	13	0.0624753	5.88E+08	1.00E+03	27-CO-	60M														Card 2b
270610	1	1.167E-04	0.5633246	0.0969656																Card 2a
270610	1	0.5633246	1.35E+07	1.00E+02	27-CO-	61														Card 2b
270620	1	7.702E-03	3.2399399	1.6002600																Card 2a
270620	1	3.2399399	1.96E+05	5.67E-01	27-CO-	62														Card 2b
270621	13	8.222E-04	3.5220399	1.7611300	8.305E-06	3.5220399	1.7611300													Card 2a
270621	13	3.5220399	2.13E+07	1.00E+01	27-CO-	62M														Card 2b
270630	1	2.530E-02	1.7124330	0.1440830																Card 2a
270630	1	1.7124330	1.23E+06	3.32E+00	27-CO-	63														Card 2b
270640	1	2.310E+00	3.4698150	0.1811650																Card 2a
270640	1	3.4698150	5.56E+07	1.96E+00	27-CO-	64														Card 2b
270650	1	5.776E-01	2.7796230	0.1147330																Card 2a
270650	1	2.7796230	1.22E+07	2.62E+00	27-CO-	65														Card 2b
270660	1	2.975E+00	6.1114502	2.7542801																Card 2a
270660	1	6.1114502	3.57E+07	3.24E-01	27-CO-	66														Card 2b
270670	1	1.631E+00	3.4482501	0.6941000																Card 2a
270670	1	3.4482501	2.70E+07	1.03E+00	27-CO-	67														Card 2b
270680	1	3.483E+00	7.2848501	3.4444201																Card 2a
270680	1	7.2848501	2.56E+07	2.61E-01	27-CO-	68														Card 2b
270681	13	2.166E-01	4.1629400	2.1189699	2.166E-01	4.1629400	2.1189699													Card 2a
270681	13	4.1629400	3.03E+06	4.30E-01	27-CO-	68M														Card 2b
270690	1	3.053E+00	6.6265812	3.3065500																Card 2a
270690	1	6.6265812	2.08E+07	2.75E-01	27-CO-	69														Card 2b

\*only decay type 1 considered\*

### 3.2 Gamma Library (file “fl2”)

This data base contains the gamma ray spectra emitted by the radioactive nuclei in the Vitamin-J 42- $\gamma$  energy group structure given in Table 2.

Energy Group N.	Upper Boundary [eV]
1	5.00E+07
2	3.00E+07
3	2.00E+07
4	1.40E+07
5	1.20E+07
6	1.00E+07
7	8.00E+06
8	7.50E+06
9	7.00E+06
10	6.50E+06
11	6.00E+06
12	5.50E+06
13	5.00E+06
14	4.50E+06
15	4.00E+06
16	3.50E+06
17	3.00E+06
18	2.50E+06
19	2.00E+06
20	1.66E+06
21	1.50E+06
22	1.34E+06
23	1.33E+06
24	1.00E+06
25	8.00E+05
26	7.00E+05
27	6.00E+05
28	5.12E+05
29	5.10E+05
30	4.50E+05
31	4.00E+05
32	3.00E+05
33	2.00E+05
34	1.50E+05
35	1.00E+05
36	7.50E+04
37	7.00E+04
38	6.00E+04
39	4.50E+04
40	3.00E+04
41	2.00E+04
42	1.00E+04

Table 2 – Upper boundaries of the Vitamin-J 42- $\gamma$  energy group structure

The data contained in the library are based on the JEFF-3.1.1 evaluated decay data file (gamma radiation spectra). In the gamma library of ANITA-IEAF in each group the contribution in MeV of the total  $\gamma$  energy emitted is given. The gamma spectra include both the  $\gamma$ -rays spectra and the x-rays and annihilation radiation spectra (photons not arising as transitions between nuclear states) (STYP=0 and STYP=9 in the ENDF-6 standard format). In the library, four cards are given for each nuclide: the first one contains the identification number IDNUC ( $Z*10000+A*10+M$ ), the alphanumeric symbol and the total energy  $E_\gamma$  calculated as the sum over the 42-group values. Then seven cards follow for the 42-group values.

As an example of the structure of the file, the data related to the isotopes from 4-Be-7 to 7-N-13 are given in the following.

```


40070      4-Be- 7                4.98619E-02                9
0.00000E+00 0.00000E+00 0.00000E+00 0.00000E+00 0.00000E+00 0.00000E+00 10
0.00000E+00 0.00000E+00 0.00000E+00 0.00000E+00 0.00000E+00 0.00000E+00 11
0.00000E+00 4.98619E-02 0.00000E+00 0.00000E+00 0.00000E+00 0.00000E+00 12
0.00000E+00 0.00000E+00 0.00000E+00 0.00000E+00 0.00000E+00 0.00000E+00 13
0.00000E+00 0.00000E+00 0.00000E+00 0.00000E+00 0.00000E+00 0.00000E+00 14
0.00000E+00 0.00000E+00 0.00000E+00 0.00000E+00 0.00000E+00 0.00000E+00 15
0.00000E+00 0.00000E+00 0.00000E+00 0.00000E+00 0.00000E+00 0.00000E+00 16
40110      4-Be- 11             1.39541E+00                17
0.00000E+00 0.00000E+00 0.00000E+00 0.00000E+00 0.00000E+00 0.00000E+00 18
0.00000E+00 0.00000E+00 0.00000E+00 0.00000E+00 0.00000E+00 0.00000E+00 19
0.00000E+00 0.00000E+00 0.00000E+00 0.00000E+00 0.00000E+00 0.00000E+00 20
0.00000E+00 0.00000E+00 0.00000E+00 0.00000E+00 0.00000E+00 4.96216E-03 21
7.01184E-01 2.69058E-03 0.00000E+00 0.00000E+00 0.00000E+00 9.33261E-02 22
2.35907E-02 1.24643E-01 0.00000E+00 3.06252E-01 0.00000E+00 1.38760E-01 23
0.00000E+00 0.00000E+00 0.00000E+00 0.00000E+00 0.00000E+00 0.00000E+00 24
50120      5-B - 12             5.68179E-02                25
0.00000E+00 0.00000E+00 0.00000E+00 0.00000E+00 0.00000E+00 0.00000E+00 26
0.00000E+00 0.00000E+00 0.00000E+00 0.00000E+00 0.00000E+00 0.00000E+00 27
0.00000E+00 0.00000E+00 0.00000E+00 0.00000E+00 0.00000E+00 0.00000E+00 28
0.00000E+00 0.00000E+00 0.00000E+00 0.00000E+00 0.00000E+00 0.00000E+00 29
0.00000E+00 0.00000E+00 0.00000E+00 0.00000E+00 0.00000E+00 5.68179E-02 30
0.00000E+00 0.00000E+00 0.00000E+00 0.00000E+00 0.00000E+00 0.00000E+00 31
0.00000E+00 0.00000E+00 0.00000E+00 0.00000E+00 0.00000E+00 0.00000E+00 32
50130      5-B - 13             2.79976E-01                33
0.00000E+00 0.00000E+00 0.00000E+00 0.00000E+00 0.00000E+00 0.00000E+00 34
0.00000E+00 0.00000E+00 0.00000E+00 0.00000E+00 0.00000E+00 0.00000E+00 35
0.00000E+00 0.00000E+00 0.00000E+00 0.00000E+00 0.00000E+00 0.00000E+00 36
0.00000E+00 0.00000E+00 0.00000E+00 0.00000E+00 0.00000E+00 0.00000E+00 37
0.00000E+00 0.00000E+00 0.00000E+00 2.79976E-01 0.00000E+00 0.00000E+00 38
0.00000E+00 0.00000E+00 0.00000E+00 0.00000E+00 0.00000E+00 0.00000E+00 39
0.00000E+00 0.00000E+00 0.00000E+00 0.00000E+00 0.00000E+00 0.00000E+00 40
50140      5-B - 14             5.93628E+00                41
0.00000E+00 0.00000E+00 0.00000E+00 0.00000E+00 0.00000E+00 0.00000E+00 42
0.00000E+00 0.00000E+00 0.00000E+00 0.00000E+00 0.00000E+00 0.00000E+00 43
0.00000E+00 0.00000E+00 0.00000E+00 0.00000E+00 1.36771E-02 0.00000E+00 44
0.00000E+00 3.49440E-02 0.00000E+00 0.00000E+00 0.00000E+00 0.00000E+00 45
0.00000E+00 0.00000E+00 0.00000E+00 0.00000E+00 0.00000E+00 0.00000E+00 46
0.00000E+00 0.00000E+00 5.23946E+00 5.78479E-01 6.97205E-02 0.00000E+00 47
0.00000E+00 0.00000E+00 0.00000E+00 0.00000E+00 0.00000E+00 0.00000E+00 48
60100      6-C - 10             1.74429E+00                49
5.68297E-11 0.00000E+00 0.00000E+00 0.00000E+00 0.00000E+00 0.00000E+00 50
0.00000E+00 0.00000E+00 0.00000E+00 0.00000E+00 0.00000E+00 0.00000E+00 51
0.00000E+00 0.00000E+00 1.02162E+00 0.00000E+00 0.00000E+00 7.07702E-01 52
0.00000E+00 1.49682E-02 0.00000E+00 0.00000E+00 0.00000E+00 0.00000E+00 53
0.00000E+00 0.00000E+00 0.00000E+00 0.00000E+00 0.00000E+00 0.00000E+00 54
0.00000E+00 0.00000E+00 0.00000E+00 0.00000E+00 0.00000E+00 0.00000E+00 55
0.00000E+00 0.00000E+00 0.00000E+00 0.00000E+00 0.00000E+00 0.00000E+00 56
60110      6-C - 11             1.01944E+00                57
4.19710E-10 0.00000E+00 0.00000E+00 0.00000E+00 0.00000E+00 0.00000E+00 58

```

0.00000E+00	0.00000E+00	0.00000E+00	0.00000E+00	0.00000E+00	0.00000E+00	59
0.00000E+00	0.00000E+00	1.01944E+00	0.00000E+00	0.00000E+00	0.00000E+00	60
0.00000E+00	0.00000E+00	0.00000E+00	0.00000E+00	0.00000E+00	0.00000E+00	61
0.00000E+00	0.00000E+00	0.00000E+00	0.00000E+00	0.00000E+00	0.00000E+00	62
0.00000E+00	0.00000E+00	0.00000E+00	0.00000E+00	0.00000E+00	0.00000E+00	63
0.00000E+00	0.00000E+00	0.00000E+00	0.00000E+00	0.00000E+00	0.00000E+00	64
60150	6-C - 15		3.60900E+00			65
0.00000E+00	0.00000E+00	0.00000E+00	0.00000E+00	0.00000E+00	0.00000E+00	66
0.00000E+00	0.00000E+00	0.00000E+00	0.00000E+00	0.00000E+00	0.00000E+00	67
0.00000E+00	0.00000E+00	0.00000E+00	0.00000E+00	0.00000E+00	0.00000E+00	68
0.00000E+00	0.00000E+00	0.00000E+00	0.00000E+00	0.00000E+00	0.00000E+00	69
0.00000E+00	0.00000E+00	0.00000E+00	0.00000E+00	0.00000E+00	0.00000E+00	70
3.60255E+00	0.00000E+00	0.00000E+00	0.00000E+00	5.40143E-04	0.00000E+00	71
5.91552E-03	0.00000E+00	0.00000E+00	0.00000E+00	0.00000E+00	0.00000E+00	72
70120	7-N - 12		1.19062E+00			73
4.19727E-14	0.00000E+00	0.00000E+00	0.00000E+00	0.00000E+00	0.00000E+00	74
0.00000E+00	0.00000E+00	0.00000E+00	0.00000E+00	0.00000E+00	0.00000E+00	75
0.00000E+00	0.00000E+00	1.02121E+00	0.00000E+00	0.00000E+00	0.00000E+00	76
0.00000E+00	0.00000E+00	0.00000E+00	0.00000E+00	0.00000E+00	0.00000E+00	77
0.00000E+00	0.00000E+00	4.82295E-02	0.00000E+00	1.21182E-01	0.00000E+00	78
0.00000E+00	0.00000E+00	0.00000E+00	0.00000E+00	0.00000E+00	0.00000E+00	79
0.00000E+00	0.00000E+00	0.00000E+00	0.00000E+00	0.00000E+00	0.00000E+00	80
70130	7-N - 13		1.02014E+00			81
9.29712E-10	0.00000E+00	0.00000E+00	0.00000E+00	0.00000E+00	0.00000E+00	82
0.00000E+00	0.00000E+00	0.00000E+00	0.00000E+00	0.00000E+00	0.00000E+00	83
0.00000E+00	0.00000E+00	1.02014E+00	0.00000E+00	0.00000E+00	0.00000E+00	84
0.00000E+00	0.00000E+00	0.00000E+00	0.00000E+00	0.00000E+00	0.00000E+00	85
0.00000E+00	0.00000E+00	0.00000E+00	0.00000E+00	0.00000E+00	0.00000E+00	86
0.00000E+00	0.00000E+00	0.00000E+00	0.00000E+00	0.00000E+00	0.00000E+00	87
0.00000E+00	0.00000E+00	0.00000E+00	0.00000E+00	0.00000E+00	0.00000E+00	88

The data given in the gamma library are used in ANITA-IEAF to compute the intensity and the energy distribution of the gamma-rays emitted by the irradiated composition. This gamma-ray source (Photons/cm<sup>3</sup>×s) in the VITAMIN-J 42-γ energy group structure (see Table 2) may be given as input to a radiation transport code to compute the space and energy distribution of the decay gamma-rays and the relative dose equivalent rate.



 <b>Ricerca Sistema Elettrico</b>	<b>Sigla di identificazione</b>	<b>Rev.</b>	<b>Distrib.</b>	<b>Pag.</b>	<b>di</b>
	ADPFISS-LP1-089	0	L	18	67

### 3.3 Neutron activation cross section data library (file “lib211”)

As shown in Figure 1 the ANITA-IEAF code requires a neutron activation cross section data library, defined as “lib211” in binary format, in order to perform the activation calculations.

Actually, the ANITA-IEAF code uses an activation library based on the EAF-2010 [12] group-wise neutron activation cross section library “eaf\_n\_gxs\_211flt\_20010” in the VITAMIN-J+ (211 energy group structure) up to 55 MeV. The library, included in the package (eaf2010\_lib), contains 63349 activation reactions up to Pu-247.

The VITAMIN-J+ (211 energy group structure) is listed in Table 3.

In the ANITA-IEAF code new MT numbers have been introduced, from 151 to 200, the same as in FISPACT code [21], that allow describing reactions with up to 8 emitted particles corresponding to a set of unallocated numbers in the standard ENDF-6 format.

In Table 4, the 85 MT values used in the ANITA-IEAF code are shown. In the Table, in column 3, for each MT, the corresponding reaction label that describes the neutron reaction is given. Each reaction corresponds to a well-defined ZA ( $ZA=Z*1000+A$ ) change with respect to the target nuclide and this  $\Delta(ZA)$  is used in the activation code to create and follow the decay chains.

The format of the multigroup library eaf2010\_lib is the LIBOUT format of the code FOUR ACES (ENEA Bologna), with two additional comment lines for each reaction. For reaction numbers the ENDF-reaction number MT multiplied by 10 has been adopted, with the convention that for the excitation of each isomeric state the reaction number is increased by one. The material numbers, MAT, consist of Z,A and an identifier, LIS, to indicate ground or isomeric target ( $MAT=Z*10000+A*10+LIS$ ). The order of the cross sections of the two libraries is in accordance with increasing Z,A,LIS and MT. The cross section values of each reaction MT are in accordance with decreasing energy of the VITAMIN-J+ group structure.

The eaf2010\_lib library provided in the package is given in card-image format. The MODBIN module must be used for the conversion of the card image file to lib211 in binary format as required by the ANITA-IEAF code.

Table 3 – Energy group boundaries of the Vitamin-J +(211-neutron energy group structure)

Energy Group N.	Upper Boundary [eV]	Energy Group N.	Upper Boundary [eV]
1	5.5000E+07	55	9.0484E+06
2	5.4000E+07	56	8.6071E+06
3	5.3000E+07	57	8.1873E+06
4	5.2000E+07	58	7.7880E+06
5	5.1000E+07	59	7.4082E+06
6	5.0000E+07	60	7.0469E+06
7	4.9000E+07	61	6.7032E+06
8	4.8000E+07	62	6.5924E+06
9	4.7000E+07	63	6.3763E+06
10	4.6000E+07	64	6.0653E+06
11	4.5000E+07	65	5.7695E+06
12	4.4000E+07	66	5.4881E+06
13	4.3000E+07	67	5.2205E+06
14	4.2000E+07	68	4.9659E+06
15	4.1000E+07	69	4.7237E+06
16	4.0000E+07	70	4.4933E+06
17	3.9000E+07	71	4.0657E+06
18	3.8000E+07	72	3.6788E+06
19	3.7000E+07	73	3.3287E+06
20	3.6000E+07	74	3.1664E+06
21	3.5000E+07	75	3.0119E+06
22	3.4000E+07	76	2.8651E+06
23	3.3000E+07	77	2.7253E+06
24	3.2000E+07	78	2.5924E+06
25	3.1000E+07	79	2.4660E+06
26	3.0000E+07	80	2.3852E+06
27	2.9000E+07	81	2.3653E+06
28	2.8000E+07	82	2.3457E+06
29	2.7000E+07	83	2.3069E+06
30	2.6000E+07	84	2.2313E+06
31	2.5000E+07	85	2.1225E+06
32	2.4000E+07	86	2.0190E+06
33	2.3000E+07	87	1.9205E+06
34	2.2000E+07	88	1.8268E+06
35	2.1000E+07	89	1.7377E+06
36	2.0000E+07	90	1.6530E+06
37	1.9640E+07	91	1.5724E+06
38	1.7333E+07	92	1.4957E+06
39	1.6905E+07	93	1.4227E+06
40	1.6487E+07	94	1.3534E+06
41	1.5683E+07	95	1.2874E+06
42	1.4918E+07	96	1.2246E+06
43	1.4550E+07	97	1.1648E+06
44	1.4191E+07	98	1.1080E+06
45	1.3840E+07	99	1.0026E+06
46	1.3499E+07	100	9.6164E+05
47	1.2840E+07	101	9.0718E+05
48	1.2523E+07	102	8.6294E+05
49	1.2214E+07	103	8.2085E+05
50	1.1618E+07	104	7.8082E+05
51	1.1052E+07	105	7.4274E+05
52	1.0513E+07	106	7.0651E+05
53	1.0000E+07	107	6.7206E+05
54	9.5123E+06	108	6.3928E+05


Energy Group N.	Upper Boundary [eV]
109	6.0810E+05
110	5.7844E+05
111	5.5023E+05
112	5.2340E+05
113	4.9787E+05
114	4.5049E+05
115	4.0762E+05
116	3.8774E+05
117	3.6883E+05
118	3.3373E+05
119	3.0197E+05
120	2.9849E+05
121	2.9721E+05
122	2.9452E+05
123	2.8725E+05
124	2.7324E+05
125	2.4724E+05
126	2.3518E+05
127	2.2371E+05
128	2.1280E+05
129	2.0242E+05
130	1.9255E+05
131	1.8316E+05
132	1.7422E+05
133	1.6573E+05
134	1.5764E+05
135	1.4996E+05
136	1.4264E+05
137	1.3569E+05
138	1.2907E+05
139	1.2277E+05
140	1.1679E+05
141	1.1109E+05
142	9.8037E+04
143	8.6517E+04
144	8.2503E+04
145	7.9499E+04
146	7.1998E+04
147	6.7379E+04
148	5.6562E+04
149	5.2475E+04
150	4.6309E+04
151	4.0868E+04
152	3.4307E+04
153	3.1828E+04
154	2.8501E+04
155	2.7000E+04
156	2.6058E+04
157	2.4788E+04
158	2.4176E+04
159	2.3579E+04
160	2.1875E+04

Energy Group N.	Upper Boundary [eV]
161	1.9305E+04
162	1.5034E+04
163	1.1709E+04
164	1.0595E+04
165	9.1188E+03
166	7.1017E+03
167	5.5308E+03
168	4.3074E+03
169	3.7074E+03
170	3.3546E+03
171	3.0354E+03
172	2.7465E+03
173	2.6126E+03
174	2.4852E+03
175	2.2487E+03
176	2.0347E+03
177	1.5846E+03
178	1.2341E+03
179	9.6112E+02
180	7.4852E+02
181	5.8295E+02
182	4.5400E+02
183	3.5358E+02
184	2.7536E+02
185	2.1445E+02
186	1.6702E+02
187	1.3007E+02
188	1.0130E+02
189	7.8893E+01
190	6.1442E+01
191	4.7851E+01
192	3.7267E+01
193	2.9023E+01
194	2.2603E+01
195	1.7604E+01
196	1.3710E+01
197	1.0677E+01
198	8.3153E+00
199	6.4760E+00
200	5.0435E+00
201	3.9279E+00
202	3.0590E+00
203	2.3824E+00
204	1.8554E+00
205	1.4450E+00
206	1.1254E+00
207	8.7643E-01
208	6.8256E-01
209	5.3158E-01
210	4.1399E-01
211	1.0000E-01
212	1.0000E-05

Table 4 – List of MT numbers used in ANITA-IEAF package

Ordering Number	MT	Reaction label	Change in ZA of the target
1	4	(n, n')	0
2	16	(n, 2n)	-1
3	17	(n, 3n)	-2
4	22	(n, n $\alpha$ )	-2004
5	11	(n, 2nd)	-1003
6	23	(n, n3 $\alpha$ )	-6012
7	24	(n, 2n $\alpha$ )	-2005
8	25	(n, 3n $\alpha$ )	-2006
9	28	(n, np)	-1001
10	29	(n, n2 $\alpha$ )	-4008
11	30	(n, 2n2 $\alpha$ )	-4009
12	32	(n, nd)	-1002
13	33	(n, nt)	-1003
14	34	(n, nHe <sup>3</sup> )	-2003
15	35	(n, nd2 $\alpha$ )	-5010
16	36	(n, nt2 $\alpha$ )	-5011
17	37	(n, 4n)	-3
18	41	(n, 2np)	-1002
19	42	(n, 3np)	-1003
20	44	(n, n2p)	-2002
21	45	(n, np $\alpha$ )	-3005
22	102	(n, $\gamma$ )	+1
23	103	(n, p)	-1000
24	104	(n, d)	-1001
25	105	(n, t)	-1002
26	106	(n, He <sup>3</sup> )	-2002
27	107	(n, $\alpha$ )	-2003
28	108	(n, 2 $\alpha$ )	-4007
29	109	(n, 3 $\alpha$ )	-6011
30	111	(n, 2p)	-2001
31	112	(n, p $\alpha$ )	-3004
32	113	(n, t2 $\alpha$ )	-5010
33	114	(n, d2 $\alpha$ )	-5009
34	115	(n, pd)	-2002
35	116	(n, pt)	-2003
36	117	(n, d $\alpha$ )	-3005
37	152	(n, 5n)	-4
38	153	(n, 6n)	-5
39	154	(n, 2nt)	-1004
40	155	(n, t $\alpha$ )	-3006
41	156	(n, 4np)	-1004
42	157	(n, 3nd)	-1004
43	158	(n, nd $\alpha$ )	-3006
44	159	(n, 2np $\alpha$ )	-3006
45	160	(n, 7n)	-6
46	161	(n, 8n)	-7

<b>Ordering Number</b>	<b>MT</b>	<b>Reaction label</b>	<b>Change in ZA of the target</b>
47	162	(n, 5np)	-1005
48	163	(n, 6np)	-1006
49	164	(n, 7np)	-1007
50	165	(n, 4n $\alpha$ )	-2007
51	166	(n, 5n $\alpha$ )	-2008
52	167	(n, 6n $\alpha$ )	-2009
53	168	(n, 7n $\alpha$ )	-2010
54	169	(n, 4nd)	-1005
55	170	(n, 5nd)	-1006
56	171	(n, 6nd)	-1007
57	172	(n, 3nt)	-1005
58	173	(n, 4nt)	-1006
59	174	(n, 5nt)	-1007
60	175	(n, 6nt)	-1008
61	176	(n, 2nHe <sup>3</sup> )	-2004
62	177	(n, 3nHe <sup>3</sup> )	-2005
63	178	(n, 4nHe <sup>3</sup> )	-2006
64	179	(n, 3n2p)	-2004
65	180	(n, 3n2 $\alpha$ )	-4010
66	181	(n, 3np $\alpha$ )	-3007
67	182	(n, dt)	-2004
68	183	(n, npd)	-2003
69	184	(n, npt)	-2004
70	185	(n, ndt)	-2005
71	186	(n, npHe <sup>3</sup> )	-3004
72	187	(n, ndHe <sup>3</sup> )	-3005
73	188	(n, ntHe <sup>3</sup> )	-3006
74	189	(n, nt $\alpha$ )	-3007
75	190	(n, 2n2p)	-2003
76	191	(n, pHe <sup>3</sup> )	-3003
77	192	(n, dHe <sup>3</sup> )	-3004
78	193	(n, He <sup>3</sup> $\alpha$ )	-4006
79	194	(n, 4n2p)	-2005
80	195	(n, 4n2 $\alpha$ )	-4011
81	196	(n, 4np $\alpha$ )	-3008
82	197	(n, 3p)	-3002
83	198	(n, n3p)	-3003
84	199	(n, 3n2p $\alpha$ )	-4008
85	200	(n, 5n2p)	-2006


 <b>Ricerca Sistema Elettrico</b>	<b>Sigla di identificazione</b>	<b>Rev.</b>	<b>Distrib.</b>	<b>Pag.</b>	<b>di</b>
	ADPFISS-LP1-089	0	L	23	67

## 4 HOW TO USE

### 4.1 Input/Output Unit-Files Assignments

The ANITA-IEAF code uses the following 12 input/output unit-files:

- Unit 1 – Decay, hazard and clearance data file, previously described, named “f11”;
- Unit 2 – Gamma file (decay gamma spectra), previously described, named “f12”;
- Unit 3 – Neutron activation cross section data file. This file is used in ANITA-IEAF in binary format as “lib211”. It is obtained from the activation library (eaf2010\_lib) in card-image format by the conversion through the MODBIN module;
- Unit 4 – Input neutron fluxes;
- Unit 5 – Standard input data file;
- Unit 6 – Standard output data file;
- Unit 8 – General inventory output data file;
- Unit 9 – SIGMA-PHI input;
- Unit 10 – SIGMA-PHI output. The files of Unit 9 and Unit 10 are allocation files where the products cross-sections×fluxes (SIGMA-PHI) are stored for successive calculations in order to save computer time (rarely used);
- Unit 11 – Clearance index inventory output data file.
- Unit 12 – Decay gamma sources output data file.

 <b>Ricerca Sistema Elettrico</b>	<b>Sigla di identificazione</b>	<b>Rev.</b>	<b>Distrib.</b>	<b>Pag.</b>	<b>di</b>
	ADPFISS-LP1-089	0	L	24	67

## 4.2 Neutron Fluxes

### input file – Unit 4

This file is named “fl4.211”. It contains the neutron flux spectra obtained by a radiation transport calculation. An arbitrary neutron group structure can be used for the neutron irradiation spectrum. It is internally converted to the standard 211 neutron energy group structure. The format of the file is the following:

#### Card 1

(2I10,A2,10A4)

IPHI        identification of the neutron flux;  
 NG         number of energy groups;  
 STAND     if “blank” or “ST” ( for Standard) then the standard 211 energy group structure  
               is assumed; in all other cases Card 2 has to be given in the file  
 TITLE     will be printed as a label of the neutron spectrum;

#### Card 2

(7E10.5)

NG +1 values of energy boundaries (eV) in decreasing order (only for not standard groups)

#### Card 3

(7E10.5)

NG values of the neutron fluxes ( $n/cm^2 s$ ).


This file may contain as many sets as needed.

The examples related to the two cases are given in the following.

- Example1 : - standard 211 VITAMIN-J+ energy group structure.
- (in this case only Card 1 and Card 3 are given, STAND="blank")

```
40      211  ITER-FEAT  IN BLK01 IG100%      Z 40
0.0000E+000.0000E+000.0000E+000.0000E+000.0000E+000.0000E+000.0000E+000.0000E+000.0000E+000
0.0000E+000.0000E+000.0000E+000.0000E+000.0000E+000.0000E+000.0000E+000.0000E+000.0000E+000
0.0000E+000.0000E+000.0000E+000.0000E+000.0000E+000.0000E+000.0000E+000.0000E+000.0000E+000
0.0000E+000.0000E+000.0000E+000.0000E+000.0000E+000.0000E+000.0000E+000.0000E+000.0000E+000
0.0000E+000.0000E+000.0000E+000.0000E+000.0000E+000.0000E+000.0000E+000.0000E+000.0000E+000
0.0000E+000.0000E+008.0000E-018.0000E-018.0000E-018.0000E-018.0000E-018.0000E-018.0000E-018.0000E-018
8.0000E-011.1075E+131.6450E+121.3511E+122.8791E+112.0290E+112.4519E+111
2.8188E+113.0356E+112.9152E+112.6507E+112.5536E+112.3850E+112.2347E+111
2.2473E+112.3342E+112.3377E+112.3521E+117.8849E+101.5872E+112.4508E+111
2.5353E+112.5984E+112.6980E+112.7769E+112.8801E+113.0088E+116.4485E+111
6.9372E+117.8550E+114.2479E+114.4152E+114.6008E+114.6970E+115.1460E+111
5.4051E+113.9208E+111.0642E+111.0531E+112.0522E+114.3864E+116.7504E+111
6.9569E+117.0763E+117.5315E+118.3326E+118.8412E+119.1036E+119.2874E+111
9.8058E+111.0489E+121.0589E+121.0775E+121.2423E+121.2041E+122.2493E+12
9.2604E+111.4494E+121.2283E+121.3654E+121.3609E+121.3765E+121.5541E+12
1.5127E+121.5107E+121.3194E+121.3559E+121.3356E+121.2448E+121.2330E+12
2.4049E+122.2010E+121.1712E+121.3910E+122.5556E+122.4860E+122.9659E+11
1.0079E+112.0794E+114.9100E+111.0069E+122.0207E+121.0071E+129.8671E+11
9.8020E+118.6880E+117.7289E+119.5321E+111.0513E+128.3429E+118.4604E+11
8.1112E+116.0402E+118.4049E+119.7229E+118.5264E+118.2942E+116.9883E+11
1.5118E+121.7059E+124.7665E+117.0407E+111.0708E+129.5168E+112.0811E+12
7.9677E+111.5959E+121.2840E+121.6384E+127.2497E+115.8725E+112.3162E+11
5.6485E+119.1264E+114.4575E+113.3732E+118.7053E+111.2012E+121.7485E+12
2.4855E+128.8048E+111.0591E+121.9789E+122.0793E+122.0830E+121.3159E+12
9.1594E+118.7589E+117.9516E+113.1864E+112.6974E+115.8759E+116.4222E+11
2.4713E+122.0986E+121.8867E+121.8842E+121.7289E+121.8102E+121.3848E+12
1.9465E+121.7848E+121.7444E+121.5306E+121.7730E+121.7025E+121.6591E+12
1.6350E+121.4760E+121.5345E+121.5342E+121.5146E+121.4871E+121.4503E+12
1.4198E+121.3840E+121.3340E+121.3125E+121.2558E+121.2064E+121.1542E+12
1.0985E+121.0399E+129.7900E+119.1522E+118.4956E+117.8280E+112.2809E+12
2.6475E+12
```




 <b>Ricerca Sistema Elettrico</b>	<b>Sigla di identificazione</b>	<b>Rev.</b>	<b>Distrib.</b>	<b>Pag.</b>	<b>di</b>
	ADPFISS-LP1-089	0	L	26	67

Example2 : - Non- standard energy group structure.  
(in this case Card 1, Card 2 and Card 3 are given, STAND="nn")

```

40          175nnITER-FEAT  IN BLK01 IG100%      Z 40
1.9640E+071.7333E+071.6905E+071.6487E+071.5683E+071.4918E+071.4550E+07
1.4191E+071.3840E+071.3499E+071.2840E+071.2523E+071.2214E+071.1618E+07
1.1052E+071.0513E+071.0000E+079.5123E+069.0484E+068.6071E+068.1873E+06
7.7880E+067.4082E+067.0469E+066.7032E+066.5924E+066.3763E+066.0653E+06
5.7695E+065.4881E+065.2205E+064.9659E+064.7237E+064.4933E+064.0657E+06
3.6788E+063.3287E+063.1664E+063.0119E+062.8651E+062.7253E+062.5924E+06
2.4660E+062.3852E+062.3653E+062.3457E+062.3069E+062.2313E+062.1225E+06
2.0190E+061.9205E+061.8268E+061.7377E+061.6530E+061.5724E+061.4957E+06
1.4227E+061.3534E+061.2874E+061.2246E+061.1648E+061.1080E+061.0026E+06
9.6164E+059.0718E+058.6294E+058.2085E+057.8082E+057.4274E+057.0651E+05
6.7206E+056.3928E+056.0810E+055.7844E+055.5023E+055.2340E+054.9787E+05
4.5049E+054.0762E+053.8774E+053.6883E+053.3373E+053.0197E+052.9849E+05
2.9721E+052.9452E+052.8725E+052.7324E+052.4724E+052.3518E+052.2371E+05
2.1280E+052.0242E+051.9255E+051.8316E+051.7422E+051.6573E+051.5764E+05
1.4996E+051.4264E+051.3569E+051.2907E+051.2277E+051.1679E+051.1109E+05
9.8037E+048.6517E+048.2503E+047.9499E+047.1998E+046.7379E+045.6562E+04
5.2475E+044.6309E+044.0868E+043.4307E+043.1828E+042.8501E+042.7000E+04
2.6058E+042.4788E+042.4176E+042.3579E+042.1875E+041.9305E+041.5034E+04
1.1709E+041.0595E+049.1188E+037.1017E+035.5308E+034.3074E+033.7074E+03
3.3546E+033.0354E+032.7465E+032.6126E+032.4852E+032.2487E+032.0347E+03
1.5846E+031.2341E+039.6112E+027.4852E+025.8295E+024.5400E+023.5358E+02
2.7536E+022.1445E+021.6702E+021.3007E+021.0130E+027.8893E+026.1442E+02
4.7851E+013.7267E+012.9023E+012.2603E+011.7604E+011.3710E+011.0677E+01
8.3153E+006.4760E+005.0435E+003.9279E+003.0590E+002.3824E+001.8554E+00
1.4450E+001.1254E+008.7643E-016.8256E-015.3158E-014.1399E-011.0000E-01
1.0000E-05
0.0000E+000.8000E+000.8000E+000.8000E+000.8000E+000.8000E+000.8000E+00
1.1075E+131.6450E+121.3511E+122.8791E+112.0290E+112.4519E+112.8188E+11
3.0356E+112.9152E+112.6507E+112.5536E+112.3850E+112.2347E+112.2473E+11
2.3342E+112.3377E+112.3521E+117.8849E+101.5872E+112.4508E+112.5353E+11
2.5984E+112.6980E+112.7769E+112.8801E+113.0088E+116.4485E+116.9372E+11
7.8550E+114.2479E+114.4152E+114.6008E+114.6970E+115.1460E+115.4051E+11
3.9208E+111.0642E+111.0531E+112.0522E+114.3864E+116.7504E+116.9569E+11
7.0763E+117.5315E+118.3326E+118.8412E+119.1036E+119.2874E+119.8058E+11
1.0489E+121.0589E+121.0775E+121.2423E+121.2041E+122.2493E+129.2604E+11
1.4494E+121.2283E+121.3654E+121.3609E+121.3765E+121.5541E+121.5127E+12
1.5107E+121.3194E+121.3559E+121.3356E+121.2448E+121.2330E+122.4049E+12
2.2010E+121.1712E+121.3910E+122.5556E+122.4860E+122.9659E+111.0079E+11
2.0794E+114.9100E+111.0069E+122.0207E+121.0071E+129.8671E+119.8020E+11
8.6880E+117.7289E+119.5321E+111.0513E+128.3429E+118.4604E+118.1112E+11
6.0402E+118.4049E+119.7229E+118.5264E+118.2942E+116.9883E+111.5118E+12
1.7059E+124.7665E+117.0407E+111.0708E+129.5168E+112.0811E+127.9677E+11
1.5959E+121.2840E+121.6384E+127.2497E+115.8725E+112.3162E+115.6485E+11
9.1264E+114.4575E+113.3732E+118.7053E+111.2012E+121.7485E+122.4855E+12
8.8048E+111.0591E+121.9789E+122.0793E+122.0830E+121.3159E+129.1594E+11
8.7589E+117.9516E+113.1864E+112.6974E+115.8759E+116.4222E+112.4713E+12
2.0986E+121.8867E+121.8842E+121.7289E+121.8102E+121.3848E+121.9465E+12
1.7848E+121.7444E+121.5306E+121.7730E+121.7025E+121.6591E+121.6350E+12
1.4760E+121.5345E+121.5342E+121.5146E+121.4871E+121.4503E+121.4198E+12
1.3840E+121.3446E+121.3018E+121.2558E+121.2064E+121.1542E+121.0985E+12
1.0399E+129.7900E+119.1522E+118.4956E+117.8280E+112.2809E+122.6475E+12

```

 <b>Ricerca Sistema Elettrico</b>	<b>Sigla di identificazione</b>	<b>Rev.</b>	<b>Distrib.</b>	<b>Pag.</b>	<b>di</b>
	ADPFISS-LP1-089	0	L	27	67

### 4.3 Input Specifications

#### Input File – Unit 5

This file contains the input data defining the problem to be solved. They specify the composition of material, irradiation scenario and cooling steps. The material exposed to neutron irradiation may contain as many elements as required; they are recognised by their chemical symbols.

The input file consists of the following cards:

##### Card 1 (A15)

**INVENT8** name of the general inventory output file.

##### Card 2 (A15)

**INVENT10** name of the clearance index inventory output file.

##### Card 3 (A15)

**SOURCEG** name of the decay gamma sources output file.

##### Card 4 (2I5,2A1,15A4)

**NELE** number of elements in the material;

**IPHI** zone spectrum identification of the flux distribution; read from unit 4; this flux distribution corresponds to the full neutron wall loading.

Other options:

< 0 read SIGMA-PHI from unit 9,

=0 SIGMA-PHI are passed from the previous problem.

**SFISAV** Y or blank, SIGMA-PHI values have to be saved on unit 10 (only if IPHI > 0);

**PRIALL** Y or blank for a complete output, otherwise a reduced output is printed;

**TIT** alphanumeric title1.

##### Card 5 (A72)


**SUBTIT** alphanumeric title2

##### Card 6 (3E10.5,4A4)

**GCM3** density (g/cm<sup>3</sup>) of the material;

**FRACK** (default = 10<sup>-12</sup>);

**VOLTO** volume (cm<sup>3</sup>) of the irradiated region;

 <b>Ricerca Sistema Elettrico</b>	<b>Sigla di identificazione</b>	<b>Rev.</b>	<b>Distrib.</b>	<b>Pag.</b>	<b>di</b>
	ADPFISS-LP1-089	0	L	28	67

**VOLTEX** name of the irradiated region (only if VOLTO > 0).

The input parameter FRACK determines the minimum number of atoms which is not set to zero during the integration. At each step of calculation the “small” branches having atomic density N smaller than the threshold density C are cut, where C is defined as:

$$C = \text{FRACK} * N_0$$

FRACK is given in input and  $N_0$  is the total atomic density of the initial mixture. It is possible to use a parameter value less than  $10^{-12}$  if information on a more wide range of nuclides is required.

**Card 7 (A2,E10.5), for each element (NELE times)**

**SYMELE** chemical symbol of the element (e.g. Fe, Ni, V,...);

**WPERC** weight percent of the element in the mixture.

**Card 8 (3I10)**

**MIRRA** number of irradiation intervals (up to 2000);

The irradiation interval is defined as the pair consisting of a burn interval plus a dwell interval; (for example MIRRA= 1000 means 1000 burn intervals plus 1000 dwell intervals);

if negative, end of file;

**NCT** number of cooling times ( $0 \leq \text{NCT} \leq 30$ ).

**ISEF** not used

**Card 9 (2E10.5) MIRRA times**

**DITAU** burn time interval (s);

**DICOOL** dwell time interval (s).

**Card 10 (7E10.5)**

**COLT(i)** i=1,NCT cooling times (s).


**Card 11 (free format) – control flag for pulsed irradiation**

**NCOST** =0 - the same level of neutron wall loading (i.e. the neutron power load of all the irradiation intervals is equal to the full neutron power load).

=MIRRA (number of irradiation intervals, see card 8) – different level of neutron wall loading (i.e.the neutron power load of some irradiation intervals is different from the full one. This case needs Card 11a).

**Card 11 a (free format)**

**RCONST(MIRRA)** ratio between the neutron wall loading for each irradiation interval


 <b>Ricerca Sistema Elettrico</b>	<b>Sigla di identificazione</b>	<b>Rev.</b>	<b>Distrib.</b>	<b>Pag.</b>	<b>di</b>
	ADPFISS-LP1-089	0	L	29	67

and the full neutron wall loading. When NCOST=0 all the values  
 RCONST(MIRRA) are defined = 1 in the code by default.

Return to Card 8 for a new irradiation or a new problem. On the contrary put MIRRA < 0 in Card  
 12.

**Card 12 (1I10)**

**ENDCARD**      -1.

 <b>Ricerca Sistema Elettrico</b>	<b>Sigla di identificazione</b>	<b>Rev.</b>	<b>Distrib.</b>	<b>Pag.</b>	<b>di</b>
	ADPFISS-LP1-089	0	L	30	67

## 4.4 Output Specifications

### Output files – units 6, 8, 11, 12

The ANITA-IEAF code provides many output data: specific activity, atomic density, specific decay heat, clearance index, ingestion hazard of each nuclide. Moreover it gives total activity, decay heat, contact dose equivalent rate, gamma ray spectra, clearance index and other relevant parameters, for the irradiated material, versus cooling time.

The output data from ANITA-IEAF consist of four distinct files-units :

- standard output;
- general inventory output data file;
- clearance index inventory output data file;
- decay gamma sources output data file.

#### 4.4.1 Standard Output

##### Unit 6

The standard output of ANITA-IEAF provides the following data:

- **Header information**


The header gives a banner version of the program name followed by a box giving the information about the authors.

- **Information from input files**

- number of the nuclides contained in the file fl1(3433) ;
- number of the radionuclides contained in the gamma library fl2 (1355);
- number of the neutron activation reactions (63349 for the neutron activation library based on EAF-2010 data) contained in the file lib211;
- neutron flux spectra read from unit 4 (fl4.211) and total zone flux;
- composition data and nuclear density calculation;
- irradiation scenario and cooling times and sequence of the irradiation step-intervals definition.

- **Total stepwise irradiation material activation data**

- atomic density ( $N/cm^3$ );
- decay heat ( $W/cm^3$ );
- integral decay heat  $H$  ( $J/cm^3$ ). It is the integral decay heat released from time step  $t$  to infinity;
- decay gamma-ray source  $G$  ( $MeV/g \times s$ );

 <b>Ricerca Sistema Elettrico</b>	<b>Sigla di identificazione</b>	<b>Rev.</b>	<b>Distrib.</b>	<b>Pag.</b>	<b>di</b>
	ADPFISS-LP1-089	0	L	31	67

- activity A (Bq/cm<sup>3</sup> and Ci/cm<sup>3</sup>);
- biological hazard  $Y=A/ALI$  (ALI is the Annual limit of Intake (Bq) by ingestion for the public (corresponding to 1mS/y) given in file fl1) (ALI/cm<sup>3</sup>);
- gas production data (appm/y) of H and He;

- **Nuclide radioactive inventory at shutdown and for cooling times**

For each stable nuclide (with  $N > N_0 \times FRACK$ ) the code prints:

- identification;
- atomic density (N/cm<sup>3</sup>);

For each non stable nuclide the code prints:

- identification;
- atomic density (N/cm<sup>3</sup>);
- decay heat (W/cm<sup>3</sup>);
- integral decay heat H (J/cm<sup>3</sup>). It is the integral decay heat released from time step t to infinity;
- decay gamma-ray source G (MeV/g×s);
- activity A (Bq/cm<sup>3</sup> and Ci/cm<sup>3</sup>);
- biological hazard  $Y=A/ALI$  (ALI/cm<sup>3</sup>);
- half life (s)

At the end are printed :

- the total values of all the previous quantities, calculated as the sum of the corresponding values over all the nuclides;
- the composition by element (Atoms/ cm<sup>3</sup>);
- the total gas production data (appm/y) of H and He;
- the energy distribution of the decay gamma-rays. Two columns are given in the VITAMIN-J 42-group energy structure internally used by the ANITA-IEAF code (MeV/cm<sup>3</sup>×s and Photons/cm<sup>3</sup>×s). The decay gamma sources (Photons/cm<sup>3</sup>s) are also printed in rows together with the total number of fotons.


**N.B.** If PRIALL in input is Y or “blank” these quantities are printed for shutdown and for all the NCT cooling times; otherwise they are printed only at shutdown and at the last cooling time.

- **Total radioactive inventory at shutdown and for cooling times**

Four summary tables are given. They contain at shutdown and at all cooling times the following quantities:

First table, total values of:

- contact dose equivalent rate (Sv/h);
- activity (Bq/g , Bq/cm<sup>3</sup> and Ci/cm<sup>3</sup>);
- biological hazard (ALI/cm<sup>3</sup>);

 <b>Ricerca Sistema Elettrico</b>	<b>Sigla di identificazione</b>	<b>Rev.</b>	<b>Distrib.</b>	<b>Pag.</b>	<b>di</b>
	ADPFISS-LP1-089	0	L	32	67

- decay heat ( $\text{W}/\text{cm}^3$ )
- integral decay heat ( $\text{J}/\text{cm}^3$ ).

Second table, total values of:

- activity ( $\text{Bq}/\text{cm}^3$ );
- contact dose equivalent rate ( $\text{Sv}/\text{h}$ );
- biological hazard ( $\text{ALI}/\text{cm}^3$ );
- decay heat ( $\text{W}/\text{cm}^3$ )

Third table, total values of:

- activity ( $\text{Bq}/\text{Kg}$ );
- decay heat ( $\text{KW}/\text{Kg}$ )
- activity ( $\text{Ci}/\text{Kg}$ );
- decay gamma-ray source  $G$  ( $\text{MeV}/\text{g}\times\text{s}$ );

Fourth table, total values of:

- activity ( $\text{Bq}/\text{g}$ );
- contact dose equivalent rate ( $\text{Sv}/\text{h}$ );
- decay heat ( $\text{W}/\text{g}$ )
- Clearance Index

### Remarks:

In the ANITA-IEAF code the contact dose equivalent rate  $D$  is computed with the equation:

$$D=2.5\times 10^{-5} S_m \text{ rem/h}$$


Where  $S_m$  ( $\text{MeV}/\text{g s}$ ), the total decay gamma-ray source of the activated material, is given by:

$$S_m = \frac{1}{\rho} \sum_i A_i G_i$$

$A_i$  = activity of nuclide  $i_{\text{th}}$  ( $\text{Bq}/\text{cm}^3$ );

$G_i$  =  $\text{MeV}/\text{dis}$  of nuclide  $i_{\text{th}}$  given in file fl1;

$\rho$  = ( $\text{g}/\text{cm}^3$ ) density of the material.

 <b>Ricerca Sistema Elettrico</b>	<b>Sigla di identificazione</b>	<b>Rev.</b>	<b>Distrib.</b>	<b>Pag.</b>	<b>di</b>
	ADPFISS-LP1-089	0	L	33	67

#### 4.4.2 General Inventory Output Data File

##### Unit 8

The General Inventory Output Data File is written on unit 8. Its name is defined in input (see “INVENT8”) by the user.

This file contains the radioactive inventories at shutdown and cooling times.

For each nuclide the following quantities are given:

- decay constant ( $s^{-1}$ )
- decay heat ( $W/cm^3$ )
- decay gamma-ray source  $G$  ( $MeV/g \times s$ );
- biological hazard ( $ALI/cm^3$ );
- activity ( $Bq/cm^3$ );

At shutdown and at each cooling time the total values are given, calculated as the sum over all the nuclides. The total values are put in evidence by the characters “XXXXXXXX” in columns 2-8.

#### 4.4.3 Clearance Index Inventory Output Data File

##### Unit 11

The Clearance Index Inventory Output Data File is written on unit 11. Its name is defined in input (see “INVENT10”) by the user.


This file contains the radioactive inventories at shutdown and at different cooling times.

For each nuclide the following quantities are given:

- activity ( $Bq/g$ );
- contact dose equivalent rate ( $Sv/h$ );
- decay heat ( $W/g$ )
- clearance index

At shutdown and at each cooling time the total values are given, calculated as the sum over all the nuclides. The total values are put in evidence by the characters “XXXXXXXX” in columns 2-8 with the corresponding time (s).




 <b>Ricerca Sistema Elettrico</b>	<b>Sigla di identificazione</b>	<b>Rev.</b>	<b>Distrib.</b>	<b>Pag.</b>	<b>di</b>
	ADPFISS-LP1-089	0	L	34	67

#### 4.4.4 Decay gamma sources Output Data File

##### Unit 12

The Decay gamma sources Output Data File is written on unit 12. Its name is defined in input (see “SOURCEG”) by the user.

This file contains the decay gamma sources (Photons/cm<sup>3</sup>×s) in the VITAMIN-J 42 energy group structure (see Table 2), in order of increasing energy, at shutdown and at different cooling times. For each time the total number of photons, summed over the 42 groups, is also provided.

 <b>Ricerca Sistema Elettrico</b>	<b>Sigla di identificazione</b>	<b>Rev.</b>	<b>Distrib.</b>	<b>Pag.</b>	<b>di</b>
	ADPFISS-LP1-089	0	L	35	67

## 4.5 How to run ANITA-IEAF


The ANITA-IEAF code activation package can be installed and run on different LINUX systems. The output files of the test cases included in the package were obtained by running the ANITA-IEAF and MODBIN executable files, compiled through the PGI compiler (pgf77 version 11.10), on CentOS 6.4.

Some information are required to use the ANITA-IEAF for activation calculations.

The user has to know details of the composition of the material to be irradiated by neutrons, the irradiation scenario (the irradiation intervals and the neutron wall loading levels), cooling times and the neutron flux spectrum.

The following steps are needed to run ANITA-IEAF system (after the installation has been performed):

1. process the activation library, eaf2010\_lib file, by MODBIN code to convert from card-image to binary mode; MODBIN is running by interactive mode.
2. the neutron flux file “fl4.211” has to be available from previous neutron transport calculations in the format required by the ANITA-IEAF code;
3. the files fl1 and fl2 must not be changed (always in the working directory);
4. create an input file on the basis of the user’s problem (see “How to use - Input Specifications” § 4.3)
5. run ANITA-IEAF code by the command: `anitaieaf < test_inp > test_out`

 <b>Ricerca Sistema Elettrico</b>	<b>Sigla di identificazione</b>	<b>Rev.</b>	<b>Distrib.</b>	<b>Pag.</b>	<b>di</b>
	ADPFISS-LP1-089	0	L	36	67

## 4.6 Sample Problems

Three sample cases (input and corresponding outputs) are given in the ANITA-IEAF code package. These cases, related to stainless steel irradiation by an ITER neutron flux, are the same as the ANITA-2000 code package. The original fl4.175 file, containing the neutron flux in the VITAMIN-J 175 energy group structure, has been renamed fl4.211 and adapted to be used with the 211 energy group structure of ANITA-IEAF through a “not standard” format (see §4.2). These test cases describe three different irradiation scenarios corresponding to the same integrated fluence on First Wall surface (neutron wall loading  $\times$  burn time).

In the following some details are given for the test3 case.

### 4.6.1 Test3 case input

- This case models the irradiation of 1 cm<sup>3</sup> of AISI 316L(N)-IG, density=7.92 g/cm<sup>3</sup>, in the following irradiation scenario:
  - neutron wall loading 0.013962 MW m<sup>-2</sup> for continuous 5 years burn time;
  - neutron wall loading 0.055849 MW m<sup>-2</sup> for continuous 5 years burn time;
  - neutron wall loading 0.1229 MW m<sup>-2</sup> for continuous 27 days burn time;
  - full neutron wall loading 0.4096 MW m<sup>-2</sup> for last 3 days (pulsed operation scenario) - 21 times: 1 hour burn time, 2.33 hours dwell time, finish with 1 hour burn.
- the composition of AISI 316L(N)-IG contains 30 elements.
- the neutron flux spectrum refers to zone 40 (see §4.2) of the Inboard Blanket of a fusion reactor machine.
- the neutron activation library “eaf2010\_lib” is used.
- test3\_inv is the name chosen for the general inventory output file (INVENT8);
- test3\_clr is the name chosen for the clearance index inventory output file (INVENT10).
- test3\_sg is the name chosen for the decay gamma sources output file (SOURCEG)
- The level of neutron wall loading is different in the various burn time intervals, so the flag NCOST=25 (number of burn time intervals); RCONST represent the ratio between the neutron wall loading of each burn time interval and the full neutron wall loading. For example RCONST(1)=0.013962/0.4096=0.034087 etc.; instead the RCONST values for the pulsed operation are equal 1, because the full neutron wall loading is applied.

The results of the radioactive inventory calculation are printed at shutdown and for 22 cooling times: 1 (s), 5 (m), 30 (m), 1 (h), 3 (h), 5 (h), 10 (h), 1 (d), 3 (d), 7 (d), 30 (d), 90 (d), 1 (y), 3 (y), 10 (y), 30 (y), 50 (y), 100 (y), 1000 (y), 10000 (y), 100000 (y), 1 (My).



#### 4.6.2 Test3 case output

The complete outputs of all the sample cases are included in the package. Some significant parts of the test3 case are presented in this section <sup>1</sup>.

#### Test3 case: Clearance Index Inventory Output Data File (test3\_clr)

The inventory values related only to the isotopes whose contribution is 1% of the total activity, at shutdown and for 50 (y) and 100 (y) cooling times, are given in the following.

```

316LN-IG ACTIVATION FEAT IN BLKT11 EAF-2010 Zone 40          10.08 (y)
      22(Fluxes):ITER-FEAT IN BLK01 IG100%      Z 40
1.00E+00 (cm3) of SS316LNIG

      Bq/g      Sv/h      W/g      Clear Index
Al 28      4.96979E+08  2.21510E+02  2.40476E-04  9.48433E+08
V 52      2.29454E+09  8.30831E+02  9.23632E-04  3.56849E+09
Cr 51      3.21194E+09  2.62661E+01  1.87170E-05  3.21194E+07
Mn 54      8.88829E+08  1.85766E+02  1.19612E-04  8.88830E+09
Mn 56      1.42544E+10  6.09457E+03  5.78063E-03  1.42544E+09
Fe 55      4.65336E+09  1.93242E+00  4.22285E-06  4.65336E+06
Co 57      1.07202E+09  3.35587E+01  2.46459E-05  1.07202E+09
Co 58      1.57456E+09  3.84273E+02  2.54897E-04  1.57456E+09
Co 58m1    1.33990E+09  6.08481E-01  5.17022E-06  1.33990E+05
Co 60      2.92853E+08  1.83314E+02  1.22008E-04  2.92853E+09
Co 60m1    2.07811E+09  3.52572E+00  2.07989E-05  2.07811E+06
Co 61      1.29505E+07  3.13938E-01  1.16871E-06  1.29505E+05
Co 62      1.41846E+07  5.67478E+00  7.36237E-06  2.50170E+07
Co 62m1    1.16039E+07  5.10899E+00  6.54727E-06  1.16039E+06
Mo 99      6.73551E+08  2.49837E+01  5.84941E-05  6.73551E+07
Mo101     3.96551E+08  1.41195E+02  1.24995E-04  3.96551E+07
Tc 97m1    2.88108E+00  6.83990E-09  4.45579E-14  2.88108E-02
XXXXXXXX SHUTDOWN 3.61541E+10  8.41790E+03  8.14001E-03  2.17904E+10

Co 60      4.08439E+05  2.55666E-01  1.70163E-07  4.08439E+06
Ni 59      2.00861E+05  1.27743E-04  2.30600E-10  2.00861E+03
Ni 63      1.69320E+07  0.00000E+00  4.72655E-08  1.69320E+05
Nb 91      2.60109E+05  8.17127E-04  7.68640E-10  3.42249E+03
XXXXXXXX 1.57790E+09  1.80459E+07  2.57939E-01  2.20287E-07  4.35537E+06

Ni 59      2.00770E+05  1.27685E-04  2.30495E-10  2.00770E+03
Ni 63      1.19984E+07  0.00000E+00  3.34934E-08  1.19984E+05
Nb 91      2.47186E+05  7.76527E-04  7.30450E-10  3.25244E+03
XXXXXXXX 3.15570E+09  1.26030E+07  2.48655E-03  3.63162E-08  2.22353E+05

```

<sup>1</sup>


To make easy the understanding of the output data presented in Sect. 4.6.2, some column header and output title have been modified with respect to the actual code output files.

### Test3 case: General Inventory Output Data File (test3\_inv)

The inventory values related only to the isotopes whose contribution is 1% of the total activity , at shutdown and for 50 (y) and 100 (y) cooling times, are given in the following.

316LN-IG ACTIVATION FEAT IN BLKTI1 EAF-2010 Zone 40 10.08 (y)  
 22(Fluxes):ITER-FEAT IN BLK01 IG100% Z 40  
 1.00E+00(cm3) of SS316LNIG

	DECAY CONST (s <sup>-1</sup> )	DECAY HEAT (W/cm3)	GAMMA SOURCE (MeV/g.s)	BIO.HAZARD (ALI/cm3)	ACTIVITY (Bq/cm3)
Al 28	5.15500E-03	1.90457E-03	8.86039E+08	3.61108E+01	3.93607E+09
V 52	3.08500E-03	7.31517E-03	3.32332E+09	2.54521E+02	1.81728E+10
Cr 51	2.89600E-07	1.48239E-04	1.05064E+08	9.67246E+02	2.54386E+10
Mn 54	2.57000E-08	9.47328E-04	7.43063E+08	4.99257E+03	7.03953E+09
Mn 56	7.45600E-05	4.57826E-02	2.43783E+10	2.82237E+04	1.12895E+11
Fe 55	8.03100E-09	3.34450E-05	7.72969E+06	1.21632E+04	3.68546E+10
Co 57	2.95200E-08	1.95196E-04	1.34235E+08	1.78370E+03	8.49043E+09
Co 58	1.13200E-07	2.01879E-03	1.53709E+09	9.23744E+03	1.24705E+10
Co 58m1	2.16300E-05	4.09482E-05	2.43392E+06	2.54484E+02	1.06120E+10
Co 60m1	1.10376E-03	1.64727E-04	1.41029E+07	2.79909E+01	1.64586E+10
Mo 99	2.91960E-06	4.63273E-04	9.99347E+07	3.19432E+03	5.33452E+09
Mo101	7.90700E-04	9.89963E-04	5.64780E+08	1.28717E+02	3.14069E+09
Tc 99m1	3.20412E-05	1.05659E-04	7.41927E+07	1.02056E+02	4.64353E+09
Shutdown		6.44689E-02	3.36716E+10	7.88769E+04	2.86340E+11
Co 60	4.16700E-09	1.34769E-06	1.02267E+06	1.10028E+01	3.23484E+06
Ni 59	2.89000E-13	1.82636E-09	5.10971E+02	1.00052E-01	1.59082E+06
Ni 63	2.18300E-10	3.74343E-07	0.00000E+00	2.01052E+01	1.34102E+08
Nb 91	3.23000E-11	6.08763E-09	3.26851E+03	1.32056E-01	2.06007E+06
	1.57790E+09	1.74467E-06	1.03176E+06	5.64426E+01	1.42923E+08
Ni 59	2.89000E-13	1.82552E-09	5.10738E+02	1.00006E-01	1.59010E+06
Ni 63	2.18300E-10	2.65267E-07	0.00000E+00	1.42470E+01	9.50274E+07
Nb 91	3.23000E-11	5.78516E-09	3.10611E+03	1.25494E-01	1.95771E+06
	3.15570E+09	2.87624E-07	9.94618E+03	3.66478E+01	9.98158E+07

 <b>Ricerca Sistema Elettrico</b>	<b>Sigla di identificazione</b>	<b>Rev.</b>	<b>Distrib.</b>	<b>Pag.</b>	<b>di</b>
	ADPFISS-LP1-089	0	L	40	67

### Test3 case: Decay gamma sources Output Data File (test3\_sg)

The decay gamma sources contained in the test3\_sg file, at shutdown and for 50 (y) and 100 (y) cooling times, are given in the following.

316LN-IG ACTIVATION FEAT IN BLKTI1 EAF-2010 Zone 40

```

At Cooling Time 0.                               Tot.Phot.= 2.7852E+11 Int. 1
3.9347E+10 1.8810E+09 1.1109E+08 6.4019E+07 5.3240E+08 2.8350E+08
2.6459E+07 1.6201E+08 1.3409E+10 1.1876E+09 1.5116E+08 4.8074E+09
9.6292E+07 5.7860E+08 8.0514E+09 1.2277E+09 5.4013E+08 1.1615E+09
1.2374E+11 5.5140E+09 2.4702E+09 1.9232E+10 3.5916E+08 3.5054E+10
1.6068E+10 2.2538E+09 2.0956E+08 4.1568E+05 3.7918E+05 3.2064E+05
1.8067E+05 1.1650E+04 9.6138E+02 2.4380E+04 8.9251E+01 9.6208E+03
1.7187E+02 0.0000E+00 0.0000E+00 0.0000E+00 0.0000E+00 0.0000E+00
At Cooling Time : 50.00 (y)                       Tot.Phot.= 9.1205E+06 Int. 18
8.0962E+05 1.7388E+06 1.0220E+03 8.0229E+03 2.0624E+03 2.1079E+04
4.6943E+03 2.7619E+03 8.8785E-01 1.0516E+03 2.4876E+02 8.3248E+02
8.6674E+02 1.9557E+02 8.2502E+03 2.3821E+01 8.6649E+02 1.6397E+04
2.2283E+04 3.2532E+06 3.2282E+06 7.8454E-03 8.3178E-04 5.4481E+00
3.7241E+01 7.3117E-02 0.0000E+00 0.0000E+00 0.0000E+00 0.0000E+00
0.0000E+00 0.0000E+00 0.0000E+00 0.0000E+00 0.0000E+00 0.0000E+00
0.0000E+00 0.0000E+00 0.0000E+00 0.0000E+00 0.0000E+00 0.0000E+00
At Cooling Time : 100.00 (y)                      Tot.Phot.= 2.4849E+06 Int. 19
7.5461E+05 1.6493E+06 7.5123E+02 6.4195E+03 1.6975E+03 1.0555E+04
2.3487E+03 1.8907E+03 7.6702E-01 8.6638E+02 1.9658E+02 3.5031E+02
7.9738E+02 1.6930E+02 7.8408E+03 2.1306E+01 7.8791E+02 1.6127E+04
2.0805E+04 4.8573E+03 4.5043E+03 7.0185E-03 7.6559E-04 5.4479E+00
5.1962E-02 1.4250E-02 0.0000E+00 0.0000E+00 0.0000E+00 0.0000E+00
0.0000E+00 0.0000E+00 0.0000E+00 0.0000E+00 0.0000E+00 0.0000E+00
0.0000E+00 0.0000E+00 0.0000E+00 0.0000E+00 0.0000E+00 0.0000E+00

```

### Test3 case: Standard Output (test3\_out)

#### Header and library files information

```

*****
* Author: *
* Manuela Frisoni - ENEA Bologna Italy *
* ANITA-IEAF is based on the ANITA code by C.Ponti *
* and S.Stramaccia - CEC JRC Ispra,1989) *
*****

```

The Library \*JEFF-3.1.1 Decay&Hazard&Clearance Data  
contains 3433 Nuclides.

Gamma Data were supplied for 1355 Nuclides.  
316LN-IG ACTIVATION FEAT IN BLKTI1 EAF-2010 Zone 40  
Test3 scenario 25 irradiation steps Zone 40

The Library Activation Library  
contains 63349 Reactions.  
at 211 Groups.

#### Composition Data


DENSITY	7.920 (g/cm3)				
ELEM.	Weight %	AT.WEIGHT	ISO	Rel.Abb.	N/cm3
B	0.0020	10.8200			8.81601E+18
			B 10	0.19900	1.75439E+18
C	0.0225	12.0110	B 11	0.80100	7.06163E+18
					8.93455E+19
N	0.0700	14.0080	C 12	0.98930	8.83895E+19
			C 13	0.01070	9.55997E+17
Al	0.0500	26.9800			2.38337E+20
			N 14	0.99636	2.37469E+20
Si	0.5000	28.0900	N 15	0.00364	8.67547E+17
			Al 27	1.00000	8.83889E+19
P	0.0250	30.9750			8.83889E+19
			Si 28	0.92223	7.82937E+20
S	0.0075	32.0660	Si 29	0.04685	3.97738E+19
			Si 30	0.03092	2.62499E+19
Ti	0.1400	47.9000	P 31	1.00000	3.84945E+19
					1.11554E+19
V	0.0040	50.9500	S 32	0.94990	1.05965E+19
			S 33	0.00750	8.36657E+16
Cr	17.5000	52.0100	S 34	0.04250	4.74105E+17
			S 36	0.00010	1.11554E+15
Mn	1.8000	54.9400	Ti 46	0.08250	1.39400E+20
			Ti 47	0.07440	1.15005E+19
Fe	64.7588	55.8500	Ti 48	0.73720	1.03713E+19
			Ti 49	0.05410	1.02766E+20
			Ti 50	0.05180	7.54153E+18
					7.22091E+18
			V 50	0.00250	3.74443E+18
			V 51	0.99750	9.36107E+15
					3.73507E+18
			Cr 50	0.04345	1.60480E+22
			Cr 52	0.83789	6.97285E+20
			Cr 53	0.09501	1.34465E+22
			Cr 54	0.02365	1.52472E+21
					3.79535E+20
			Mn 55	1.00000	1.56262E+21
					1.56262E+21
					5.53025E+22



			Fe 54	0.05845	3.23243E+21
			Fe 56	0.91754	5.07423E+22
			Fe 57	0.02119	1.17186E+21
			Fe 58	0.00282	1.55953E+20
Co	0.0500	58.9400			4.04603E+19
			Co 59	1.00000	4.04603E+19
Ni	12.2500	58.7100			9.95161E+21
			Ni 58	0.68077	6.77476E+21
			Ni 60	0.26223	2.60961E+21
			Ni 61	0.01140	1.13438E+20
			Ni 62	0.03635	3.61701E+20
			Ni 64	0.00926	9.21022E+19
Cu	0.3000	63.5400			2.25187E+20
			Cu 63	0.69150	1.55717E+20
			Cu 65	0.30850	6.94702E+19
Nb	0.0100	92.9100			5.13342E+18
			Nb 93	1.00000	5.13342E+18
Mo	2.5000	95.9500			1.24270E+21
			Mo 92	0.14530	1.80564E+20
			Mo 94	0.09150	1.13707E+20
			Mo 95	0.15840	1.96843E+20
			Mo 96	0.16670	2.07157E+20
			Mo 97	0.09600	1.19299E+20
			Mo 98	0.24390	3.03093E+20
			Mo100	0.09820	1.22033E+20
Ta	0.0010	180.9500			2.63579E+17
			Ta180	0.00012	3.16295E+13
			Ta181	0.99988	2.63547E+17
Zr	0.0020	91.2200			1.04571E+18
			Zr 90	0.51450	5.38016E+17
			Zr 91	0.11220	1.17328E+17
			Zr 92	0.17150	1.79339E+17
			Zr 94	0.17380	1.81744E+17
			Zr 96	0.02800	2.92798E+16
Sn	0.0020	118.7000			8.03616E+17
			Sn112	0.00970	7.79508E+15
			Sn114	0.00660	5.30387E+15
			Sn115	0.00340	2.73230E+15
			Sn116	0.14540	1.16846E+17
			Sn117	0.07680	6.17177E+16
			Sn118	0.24220	1.94636E+17
			Sn119	0.08590	6.90307E+16
			Sn120	0.32580	2.61818E+17
			Sn122	0.04630	3.72074E+16
			Sn124	0.05790	4.65294E+16
W	0.0010	183.8600			2.59407E+17
			W180	0.00120	3.11289E+14
			W182	0.26500	6.87429E+16
			W183	0.14310	3.71212E+16
			W184	0.30640	7.94824E+16
			W186	0.28430	7.37495E+16
K	0.0005	39.1000			6.09906E+17
			K 39	0.93258	5.68787E+17
			K 40	0.00012	7.13590E+13
			K 41	0.06730	4.10479E+16
Ag	0.0002	107.8800			8.84216E+16
			Ag107	0.51839	4.58369E+16
			Ag109	0.48161	4.25847E+16
Cd	0.0002	112.4100			8.48583E+16
			Cd106	0.01250	1.06073E+15
			Cd108	0.00890	7.55239E+14
			Cd110	0.12490	1.05988E+16
			Cd111	0.12800	1.08619E+16
			Cd112	0.24130	2.04763E+16
			Cd113	0.12220	1.03697E+16
			Cd114	0.28730	2.43798E+16
			Cd116	0.07490	6.35589E+15
Sb	0.0005	121.7600			1.95855E+17
			Sb121	0.57210	1.12049E+17
			Sb123	0.42790	8.38064E+16
Ba	0.0005	137.3600			1.73612E+17
			Ba130	0.00106	1.84029E+14
			Ba132	0.00101	1.75348E+14
			Ba134	0.02417	4.19620E+15
			Ba135	0.06592	1.14445E+16

			Ba136	0.07854	1.36355E+16
			Ba137	0.11232	1.95001E+16
			Ba138	0.71698	1.24476E+17
Tb	0.0005	158.9300			1.50049E+17
			Tb159	1.00000	1.50049E+17
Ir	0.0005	192.2000			1.24076E+17
			Ir191	0.37300	4.62802E+16
			Ir193	0.62700	7.77954E+16
Pb	0.0008	207.2100			1.84140E+17
			Pb204	0.01400	2.57796E+15
			Pb206	0.24100	4.43778E+16
			Pb207	0.22100	4.06950E+16
			Pb208	0.52400	9.64895E+16
As	0.0005	74.9200			3.18304E+17
			As 75	1.00000	3.18304E+17
	100.0000				

The four summary tables listing the *total material inventory at shutdown and for cooling times* are presented in the following.

 <b>Ricerca Sistema Elettrico</b>	<b>Sigla di identificazione</b>	<b>Rev.</b>	<b>Distrib.</b>	<b>Pag.</b>	<b>di</b>
	ADPFISS-LP1-089	0	L	44	67

### First summary table

316LN-IG ACTIVATION FEAT IN BLKT11 EAF-2010 Zone 40  
 Test3 scenario 25 irradiation steps Zone 40

ITER-FEAT IN BLK01 IG100% Z 40

Time	D(Sv/h)	Bq/g	Bq/cm3	Ci/m3	ALI/cm3	WATT/cm3	JOULE/cm3
zero	8.418E+03	3.615E+10	2.863E+11	7.739E+06	7.888E+04	6.447E-02	3.633044E+05
1.0 (s)	8.411E+03	3.610E+10	2.859E+11	7.727E+06	7.839E+04	6.439E-02	3.633043E+05
5.0 (m)	7.497E+03	3.255E+10	2.578E+11	6.967E+06	7.295E+04	5.580E-02	3.632891E+05
30.0 (m)	6.361E+03	2.808E+10	2.224E+11	6.011E+06	6.855E+04	4.630E-02	3.632211E+05
1.0 (h)	5.642E+03	2.595E+10	2.055E+11	5.555E+06	6.514E+04	4.080E-02	3.631470E+05
3.0 (h)	3.681E+03	2.101E+10	1.664E+11	4.496E+06	5.590E+04	2.601E-02	3.629237E+05
5.0 (h)	2.544E+03	1.813E+10	1.436E+11	3.881E+06	5.046E+04	1.745E-02	3.627805E+05
10.0 (h)	1.355E+03	1.493E+10	1.182E+11	3.195E+06	4.460E+04	8.502E-03	3.625849E+05
1.0 (d)	9.240E+02	1.322E+10	1.047E+11	2.830E+06	4.182E+04	5.234E-03	3.623116E+05
3.0 (d)	8.660E+02	1.225E+10	9.702E+10	2.622E+06	3.993E+04	4.765E-03	3.614906E+05
7.0 (d)	8.213E+02	1.143E+10	9.055E+10	2.447E+06	3.811E+04	4.418E-03	3.599326E+05
30.0 (d)	7.088E+02	9.509E+09	7.531E+10	2.035E+06	3.442E+04	3.759E-03	3.519200E+05
90.0 (d)	5.311E+02	7.326E+09	5.802E+10	1.568E+06	2.904E+04	2.815E-03	3.351177E+05
1.0 (y)	2.698E+02	4.778E+09	3.784E+10	1.023E+06	1.964E+04	1.435E-03	2.892977E+05
3.0 (y)	1.429E+02	2.545E+09	2.016E+10	5.449E+05	1.161E+04	7.628E-04	2.250260E+05
10.0 (y)	4.943E+01	4.716E+08	3.735E+09	1.010E+05	3.139E+03	2.629E-04	1.256136E+05
30.0 (y)	3.551E+00	2.826E+07	2.238E+08	6.049E+03	2.085E+02	1.917E-05	6.719399E+04
50.0 (y)	2.579E-01	1.805E+07	1.429E+08	3.863E+03	5.644E+01	1.745E-06	6.276047E+04
100.0 (y)	2.487E-03	1.260E+07	9.982E+07	2.698E+03	3.665E+01	2.876E-07	6.190710E+04
1000.0 (y)	1.333E-03	4.476E+05	3.545E+06	9.581E+01	3.507E+00	1.435E-08	6.027675E+04
10000.0 (y)	6.918E-04	2.202E+05	1.744E+06	4.714E+01	4.226E-01	6.661E-09	5.796727E+04
100000.0 (y)	7.622E-05	8.545E+04	6.767E+05	1.829E+01	6.362E-02	1.355E-09	5.022967E+04
1.0 (My)	5.157E-07	4.589E+02	3.635E+03	9.823E-02	1.317E-03	3.001E-11	4.301894E+04

### Second summary table

316LN-IG ACTIVATION FEAT IN BLKTI1 EAF-2010 Zone 40  
 Test3 scenario 25 irradiation steps Zone 40  
 For a volume of 1.0000E+00 (cm3) of SS316LNIG :

Time	Becquerel	Sv/h	ALI	Watt
zero	2.863E+11	8.418E+03	7.888E+04	6.447E-02
1.0 (s)	2.859E+11	8.411E+03	7.839E+04	6.439E-02
5.0 (m)	2.578E+11	7.497E+03	7.295E+04	5.580E-02
30.0 (m)	2.224E+11	6.361E+03	6.855E+04	4.630E-02
1.0 (h)	2.055E+11	5.642E+03	6.514E+04	4.080E-02
3.0 (h)	1.664E+11	3.681E+03	5.590E+04	2.601E-02
5.0 (h)	1.436E+11	2.544E+03	5.046E+04	1.745E-02
10.0 (h)	1.182E+11	1.355E+03	4.460E+04	8.502E-03
1.0 (d)	1.047E+11	9.240E+02	4.182E+04	5.234E-03
3.0 (d)	9.702E+10	8.660E+02	3.993E+04	4.765E-03
7.0 (d)	9.055E+10	8.213E+02	3.811E+04	4.418E-03
30.0 (d)	7.531E+10	7.088E+02	3.442E+04	3.759E-03
90.0 (d)	5.802E+10	5.311E+02	2.904E+04	2.815E-03
1.0 (y)	3.784E+10	2.698E+02	1.964E+04	1.435E-03
3.0 (y)	2.016E+10	1.429E+02	1.161E+04	7.628E-04
10.0 (y)	3.735E+09	4.943E+01	3.139E+03	2.629E-04
30.0 (y)	2.238E+08	3.551E+00	2.085E+02	1.917E-05
50.0 (y)	1.429E+08	2.579E-01	5.644E+01	1.745E-06
100.0 (y)	9.982E+07	2.487E-03	3.665E+01	2.876E-07
1000.0 (y)	3.545E+06	1.333E-03	3.507E+00	1.435E-08
10000.0 (y)	1.744E+06	6.918E-04	4.226E-01	6.661E-09
100000.0 (y)	6.767E+05	7.622E-05	6.362E-02	1.355E-09
1.0 (My)	3.635E+03	5.157E-07	1.317E-03	3.001E-11

### Third summary table

316LN-IG ACTIVATION FEAT IN BLKTI1 EAF-2010 Zone 40  
 Test3 scenario 25 irradiation steps Zone 40

Time	Bq/Kg	KW/Kg	Ci/Kg	MeV/g*s
zero	3.615E+13	8.140E-03	9.771E+02	3.367E+10
1.0 (s)	3.610E+13	8.130E-03	9.756E+02	3.364E+10
5.0 (m)	3.255E+13	7.046E-03	8.796E+02	2.999E+10
30.0 (m)	2.808E+13	5.846E-03	7.590E+02	2.544E+10
1.0 (h)	2.595E+13	5.151E-03	7.014E+02	2.257E+10
3.0 (h)	2.101E+13	3.285E-03	5.677E+02	1.473E+10
5.0 (h)	1.813E+13	2.203E-03	4.900E+02	1.017E+10
10.0 (h)	1.493E+13	1.073E-03	4.034E+02	5.421E+09
1.0 (d)	1.322E+13	6.608E-04	3.573E+02	3.696E+09
3.0 (d)	1.225E+13	6.017E-04	3.311E+02	3.464E+09
7.0 (d)	1.143E+13	5.579E-04	3.090E+02	3.285E+09
30.0 (d)	9.509E+12	4.746E-04	2.570E+02	2.835E+09
90.0 (d)	7.326E+12	3.555E-04	1.980E+02	2.125E+09
1.0 (y)	4.778E+12	1.811E-04	1.291E+02	1.079E+09
3.0 (y)	2.545E+12	9.631E-05	6.880E+01	5.714E+08
10.0 (y)	4.716E+11	3.320E-05	1.275E+01	1.977E+08
30.0 (y)	2.826E+10	2.421E-06	7.638E-01	1.420E+07
50.0 (y)	1.805E+10	2.203E-07	4.877E-01	1.032E+06
100.0 (y)	1.260E+10	3.632E-08	3.406E-01	9.946E+03
1000.0 (y)	4.476E+08	1.811E-09	1.210E-02	5.333E+03
10000.0 (y)	2.202E+08	8.410E-10	5.952E-03	2.767E+03
100000.0 (y)	8.545E+07	1.710E-10	2.309E-03	3.049E+02
1.0 (My)	4.589E+05	3.789E-12	1.240E-05	2.063E+00

### Fourth summary table

316LN-IG ACTIVATION FEAT IN BLKTI1 EAF-2010 Zone 40  
 Test3 scenario 25 irradiation steps Zone 40

Time	Bq/g	Sv/h	W/g	Cl Index
zero	3.615E+10	8.418E+03	8.140E-03	2.179E+10
1.0 (s)	3.610E+10	8.411E+03	8.130E-03	2.176E+10
5.0 (m)	3.255E+10	7.497E+03	7.045E-03	1.845E+10
30.0 (m)	2.808E+10	6.361E+03	5.846E-03	1.644E+10
1.0 (h)	2.595E+10	5.642E+03	5.151E-03	1.618E+10
3.0 (h)	2.101E+10	3.681E+03	3.284E-03	1.567E+10
5.0 (h)	1.813E+10	2.544E+03	2.203E-03	1.539E+10
10.0 (h)	1.493E+10	1.355E+03	1.073E-03	1.509E+10
1.0 (d)	1.322E+10	9.240E+02	6.608E-04	1.493E+10
3.0 (d)	1.225E+10	8.660E+02	6.016E-04	1.475E+10
7.0 (d)	1.143E+10	8.213E+02	5.579E-04	1.453E+10
30.0 (d)	9.509E+09	7.088E+02	4.746E-04	1.363E+10
90.0 (d)	7.326E+09	5.311E+02	3.555E-04	1.177E+10
1.0 (y)	4.778E+09	2.698E+02	1.811E-04	7.012E+09
3.0 (y)	2.545E+09	1.429E+02	9.631E-05	2.823E+09
10.0 (y)	4.716E+08	4.943E+01	3.320E-05	7.898E+08
30.0 (y)	2.826E+07	3.551E+00	2.421E-06	5.698E+07
50.0 (y)	1.805E+07	2.579E-01	2.203E-07	4.355E+06
100.0 (y)	1.260E+07	2.487E-03	3.632E-08	2.224E+05
1000.0 (y)	4.476E+05	1.333E-03	1.811E-09	7.548E+04
10000.0 (y)	2.202E+05	6.918E-04	8.410E-10	3.591E+04
100000.0 (y)	8.545E+04	7.622E-05	1.710E-10	5.852E+03
1.0 (My)	4.589E+02	5.157E-07	3.789E-12	2.443E+02

## 5 ANITA-IEAF VALIDATION

ANITA-IEAF predictions were compared with the activity measurements obtained from the Karlsruhe Isochronous Cyclotron [22][23].

In this experiment a saturation thick target of natural lithium was irradiated with 40 MeV deuterons.

The resulting neutron spectrum and yield were measured by multi-foil activation.

Samples of two different steels, SS-316 and F82H, pure vanadium and a vanadium alloy were activated in the neutron field. These are structural materials of interest in fusion technology. For each sample, the specific activities of many radio nuclides, (Bq/kg), were determined by gamma spectrometry.

The details of the experimental set-up, taken from [22], (i.e. material composition, irradiation time, neutron flux, etc.) used in the ANITA-IEAF input in order to model the experiment, are given in the following.

### 5.1 Neutron Flux

The Centre position neutron flux of [22], in the 211 energy group structure, was used in the ANITA-IEAF calculations (see Figure 2). It resembles very closely the IFMIF neutron spectrum.

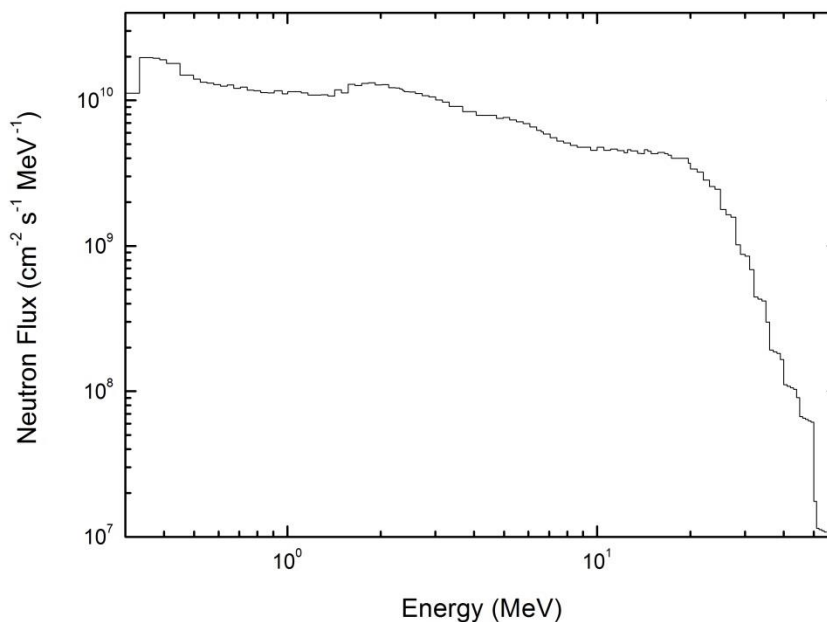


Figure 2 – Neutron flux

## 5.2 Activation parameters

The activation parameters are given in Table 5.

<b>Material</b>	<b>Neutron Flux density <math>\Phi(\text{cm}^{-2} \text{s}^{-1})</math></b>	<b>Irradiation time (s)</b>
SS-316	4.10 E11	7525
F82H	4.14 E11	7525
V- alloy	4.22 E11	7525
V- pure	4.27 E 11	7525

Table 5 – Activation parameters

## 5.3 Samples compositions

The sample compositions in weight% are given in the following Table 6.

<b>Element</b>	<b>SS-316</b>	<b>F82H</b>	<b>V-alloy</b>	<b>V-pure</b>
<b>B</b>	0.0002	0.0002	0.0005	0.0005
<b>C</b>		0.09	0.0045	0.0027
<b>N</b>		0.008	0.011	0.013
<b>O</b>			0.037	0.041
<b>Mg</b>			0.001	0.001
<b>Al</b>	0.05	0.003	0.020	0.025
<b>Si</b>	0.4	0.11	0.034	0.017
<b>P</b>		0.002	0.003	0.003
<b>S</b>		0.002	0.001	0.001
<b>Ti</b>	0.15	0.01	4.1	
<b>V</b>		0.16	91.8483	99.8658
<b>Cr</b>	17.5	7.70	3.9	
<b>Mn</b>	1.8	0.16		
<b>Fe</b>	65.1648	89.7467	0.021	0.016
<b>Co</b>	0.03	0.005		
<b>Ni</b>	12.3	0.02		
<b>Cu</b>	0.1	0.01	0.005	0.005
<b>Nb</b>	0.005	0.0001	0.0087	0.004
<b>Mo</b>	2.5	0.003	0.005	0.005
<b>Ta</b>		0.02		
<b>W</b>		1.95		

Table 6 – Composition of samples in weight%




## 5.4 Cooling times

The measurements on the activated samples were performed at different cooling times ranging from about 1 hour up to 150 days. They are given in the following Table 7.

<b>SS316</b>	<b>F82H</b>
5965 s $\approx$ 1.7 h	4173 s $\approx$ 1.2 h
18848 s $\approx$ 5.2 h	18011 s $\approx$ 5 h
93333 s $\approx$ 1.1 d	92043 s $\approx$ 1.1 d
178860 s $\approx$ 2.1 d	158665 s $\approx$ 1.8 d
432539 s $\approx$ 5 d	424416 s $\approx$ 4.9 d
2520240 s $\approx$ 29.2 d	2922060 s $\approx$ 33.8 d
12962640 s $\approx$ 150 d	13036200 s $\approx$ 150.9 d
<b>V-alloy</b>	<b>V-pure</b>
5477 s $\approx$ 1.5 h	4983 s $\approx$ 1.4 h
17189 s $\approx$ 4.8 h	16396 s $\approx$ 4.6 h
90710 s $\approx$ 1 d	90001 s $\approx$ 1 d
417962 s $\approx$ 4.8 d	412474 s $\approx$ 4.8 d
2254080 s $\approx$ 26.1 d	3100500 s $\approx$ 35.9 d
13341780 s $\approx$ 154.4 d	13146900 s $\approx$ 152.2 d

Table 7 – Cooling times

 <b>Ricerca Sistema Elettrico</b>	<b>Sigla di identificazione</b>	<b>Rev.</b>	<b>Distrib.</b>	<b>Pag.</b>	<b>di</b>
	ADPFISS-LP1-089	0	L	51	67

## 5.5 Calculated and experimental results comparison

The results of the comparison between the measured activities and the corresponding ANITA-IEAF predictions are given in Table 8 to Table 11 for SS-316 and F82H steels, V-alloy and V-pure respectively.

For each nuclide at the various cooling times these quantities are given :

- experimental activity
- experimental uncertainty
- ANITA-IEAF calculated activity
- percentage respect to the total activity (calculated by ANITA-IEAF)
- calculation-to-experiment C/E ratio

N.B In the tables the cooling times are in seconds for sake of comparison with the experimental values of FZKA 6764 Report.

The C/E ratios calculated as averages over more than one cooling time for each nuclide are shown in Figure 3 to Figure 9.

The error bars ( $1 \sigma$ ) account for the experimental uncertainties only.

For SS-316, F82H steels and V-alloy samples the C/E ratios of the main contributors to the total activity are shown separately, while for V-pure the C/E values of all the nuclides are given together.

**Table 8 – SS-316 specific activity- Experimental and calculated results**

Isotope product	Cooling time	Experimental data		ANITA-IEAF calculation		C/E
		Specific activity	Uncertainty	Specific activity	Percentage of the total activity	
		s	Bq/kg	± %	Bq/kg	
<b>Sc-46</b>	178860	5.33E+04	54	1.25E+05	1.47E-02	2.34
	2520240	5.72E+04	13	9.95E+04	3.43E-02	1.74
	12962640	2.20E+04	18	3.66E+04	4.05E-02	1.66
<b>Sc-48</b>	93333	3.37E+06	13	3.90E+06	2.19E-01	1.16
	178860	1.57E+06	9	2.67E+06	3.16E-01	1.70
	432539	6.55E+05	14	8.74E+05	1.68E-01	1.33
<b>V-48</b>	93333	1.04E+06	14	1.43E+06	8.03E-02	1.38
	178860	1.08E+06	9	1.38E+06	1.63E-01	1.28
	432539	9.03E+05	9	1.22E+06	2.36E-01	1.36
	2520240	3.41E+05	6	4.29E+05	1.48E-01	1.26
<b>Cr-48</b>	178860	1.05E+05	25	1.59E+05	1.88E-02	1.51
<b>Cr-49</b>	5965	2.22E+08	35	1.77E+08	5.02E-01	0.80
<b>Cr-51</b>	18848	3.14E+08	27	3.01E+08	1.86E+00	0.96
	93333	2.91E+08	5	2.95E+08	1.65E+01	1.01
	178860	2.78E+08	5	2.87E+08	3.40E+01	1.03
	432539	2.58E+08	5	2.67E+08	5.14E+01	1.03
	2520240	1.38E+08	5	1.46E+08	5.03E+01	1.06
	12962640	6.83E+06	5	7.09E+06	7.84E+00	1.04
<b>Mn-52</b>	18848	1.14E+07	40	1.11E+07	6.83E-02	0.97
	93333	1.01E+07	6	1.03E+07	5.80E-01	1.02
	178860	7.72E+06	5	9.22E+06	1.09E+00	1.19
	432539	5.38E+06	5	6.42E+06	1.24E+00	1.19
	2520240	2.74E+05	6	3.21E+05	1.11E-01	1.17
<b>Mn-54</b>	18848	2.68E+07	33	2.03E+07	1.25E-01	0.76
	93333	1.82E+07	5	2.03E+07	1.14E+00	1.11
	178860	1.73E+07	5	2.02E+07	2.39E+00	1.17
	432539	1.71E+07	5	2.01E+07	3.87E+00	1.17
	2520240	1.59E+07	5	1.90E+07	6.56E+00	1.20
	12962640	1.22E+07	5	1.46E+07	1.61E+01	1.19
<b>Mn-56</b>	5965	2.61E+10	5	2.76E+10	7.84E+01	1.06
	18848	9.60E+09	5	1.06E+10	6.53E+01	1.10
	93333	3.83E+07	5	4.10E+07	2.30E+00	1.07
<b>Fe-52</b>	93333	3.41E+05	50	1.48E+06	8.29E-02	4.34
<b>Fe-59</b>	178860	3.50E+05	18	3.68E+05	4.35E-02	1.05
	2520240	2.33E+05	10	2.41E+05	8.31E-02	1.04
	12962640	3.21E+04	39	3.67E+04	4.06E-02	1.14
<b>Co-55</b>	93333	2.30E+06	16	1.70E+06	9.52E-02	0.74
	178860	5.81E+05	10	6.64E+05	7.85E-02	1.14
<b>Co-56</b>	93333	2.54E+06	21	2.89E+06	1.62E-01	1.14
	178860	2.82E+06	5	2.87E+06	3.39E-01	1.02
	432539	2.67E+06	7	2.80E+06	5.40E-01	1.05
	2520240	2.12E+06	5	2.27E+06	7.84E-01	1.07
	12962640	7.22E+05	5	7.70E+05	8.51E-01	1.07

*Table 7 – SS-316 specific activity- Experimental and calculated results (continued)*

Isotope product	Cooling time	Experimental data		ANITA-IEAF calculation		C/E
		Specific activity	Uncertainty	Specific activity	Percentage of the total activity	
		s	Bq/kg	± %	Bq/kg	
<b>Co-57</b>	18848	2.19E+07	39	2.16E+07	1.34E-01	0.99
	93333	2.08E+07	6	2.22E+07	1.24E+00	1.07
	178860	2.03E+07	5	2.25E+07	2.66E+00	1.11
	432539	2.01E+07	5	2.29E+07	4.41E+00	1.14
	2520240	1.91E+07	5	2.17E+07	7.49E+00	1.14
	12962640	1.41E+07	5	1.60E+07	1.77E+01	1.13
<b>Co-58</b>	18848	5.71E+07	16	6.03E+07	3.72E-01	1.06
	93333	7.18E+07	5	7.87E+07	4.41E+00	1.10
	178860	7.36E+07	5	8.19E+07	9.68E+00	1.11
	432539	7.13E+07	5	8.03E+07	1.55E+01	1.13
	2520240	5.53E+07	5	6.34E+07	2.19E+01	1.15
	12962640	1.70E+07	5	1.94E+07	2.15E+01	1.14
<b>Co-60</b>	178860	2.35E+05	15	2.25E+05	2.66E-02	0.96
	432539	2.88E+05	27	2.25E+05	4.33E-02	0.78
	2520240	2.60E+05	6	2.23E+05	7.68E-02	0.86
	12962640	2.23E+05	6	2.13E+05	2.36E-01	0.96
<b>Co-61</b>	5965	1.04E+08	34	2.48E+08	7.04E-01	2.39
<b>Ni-56</b>	93333	1.32E+06	17	4.04E+05	2.27E-02	0.31
	178860	1.21E+06	7	3.61E+05	4.27E-02	0.30
	432539	9.21E+05	11	2.58E+05	4.97E-02	0.28
<b>Ni-57</b>	5965	2.59E+08	27	3.40E+08	9.63E-01	1.31
	18848	2.49E+08	23	3.17E+08	1.96E+00	1.27
	93333	1.72E+08	21	2.13E+08	1.19E+01	1.24
	178860	9.44E+07	21	1.34E+08	1.59E+01	1.42
	432539	2.70E+07	21	3.45E+07	6.63E+00	1.28
<b>Y-87m</b>	178860	1.25E+05	28	6.14E+04	7.25E-03	0.49
<b>Y-87</b>	178860	1.80E+05	19	9.50E+04	1.12E-02	0.53
<b>Y-88</b>	12962640	1.05E+04	34	1.77E+04	1.96E-02	1.69
<b>Zr-86</b>	178860	1.16E+05	23	2.97E+03	3.51E-04	0.03
<b>Zr-88</b>	2520240	2.28E+04	60	3.88E+04	1.34E-02	1.70
<b>Zr-89</b>	93333	1.71E+06	18	2.22E+06	1.24E-01	1.30
	178860	1.29E+06	5	1.80E+06	2.12E-01	1.39
	432539	7.68E+05	11	9.63E+05	1.85E-01	1.25
<b>Zr-97</b>	178860	5.44E+06	21	1.05E+05	1.25E-02	0.02
<b>Nb-90</b>	93333	7.55E+06	8	4.82E+06	2.70E-01	0.64
	178860	1.73E+06	6	1.63E+06	1.93E-01	0.94
<b>Nb-92m</b>	93333	1.39E+06	31	2.47E+06	1.39E-01	1.78
	178860	1.82E+06	11	2.31E+06	2.73E-01	1.27
	432539	1.79E+06	9	1.89E+06	3.64E-01	1.06
	2520240	2.89E+05	7	3.63E+05	1.25E-01	1.26

*Table 8– SS-316 specific activity- Experimental and calculated results (continued)*

Isotope product	Cooling time	Experimental data		ANITA-IEAF calculation		C/E
		Specific activity	Uncertainty	Specific activity	Percentage of the total activity	
		s	Bq/kg	± %	Bq/kg	
<b>Nb-95</b>	93333	5.90E+05	37	7.08E+05	3.97E-02	1.20
	178860	4.88E+05	8	7.08E+05	8.37E-02	1.45
	432539	5.36E+05	17	6.96E+05	1.34E-01	1.30
	2520240	3.29E+05	6	4.69E+05	1.62E-01	1.42
	12962640	4.09E+04	19	5.57E+04	6.16E-02	1.36
<b>Nb-95m</b>	178860	9.39E+05	13	6.30E+05	7.45E-02	0.67
<b>Nb-96</b>	93333	5.36E+06	9	7.26E+06	4.07E-01	1.35
	178860	2.28E+06	5	3.58E+06	4.24E-01	1.57
	432539	3.37E+05	25	4.42E+05	8.52E-02	1.31
<b>Mo-90</b>	178860	1.45E+04	55	2.21E+04	2.62E-03	1.53
<b>Mo-93m</b>	93333	1.85E+06	18	1.79E+06	1.00E-01	0.97
	178860	7.26E+04	35	1.62E+05	1.91E-02	2.23
<b>Mo-99</b>	93333	4.84E+07	7	5.12E+07	2.87E+00	1.06
	178860	3.21E+07	6	3.99E+07	4.71E+00	1.24
	432539	1.57E+07	7	1.90E+07	3.66E+00	1.21
<b>Tc-99m</b>	18848	5.69E+07	16	2.97E+07	1.83E-01	0.52
	93333	4.45E+07	5	4.67E+07	2.62E+00	1.05
	178860	3.08E+07	5	3.84E+07	4.55E+00	1.25
	432539	1.54E+07	5	1.84E+07	3.55E+00	1.20
	2520240	2.24E+04	47	4.15E+04	1.43E-02	1.85

**Table 9 – F82H specific activity- Experimental and calculated results**

Isotope product	Cooling time	Experimental data		ANITA-IEAF calculation		C/E
		Specific activity	Uncertainty	Specific activity	Percentage of the total activity	
		s	Bq/kg	± %	Bq/kg	
<b>Sc-46</b>	158665	4.13E+04	44	2.05E+04	8.54E-03	0.50
	2922060	3.56E+04	10	1.57E+04	1.16E-02	0.44
	13036200	1.44E+04	15	5.97E+03	9.40E-03	0.41
<b>Sc-47</b>	92043	7.17E+05	20	1.44E+06	4.59E-01	2.01
	158665	6.78E+05	12	1.23E+06	5.13E-01	1.82
	424416	3.59E+05	20	6.53E+05	2.98E-01	1.82
<b>Sc-48</b>	92043	2.06E+06	11	1.68E+06	5.35E-01	0.82
	158665	1.35E+06	5	1.26E+06	5.23E-01	0.93
	424416	5.00E+05	10	3.89E+05	1.78E-01	0.78
<b>V-48</b>	92043	3.53E+05	32	6.59E+05	2.09E-01	1.87
	158665	5.57E+05	16	6.41E+05	2.67E-01	1.15
	424416	3.55E+05	13	5.65E+05	2.58E-01	1.59
	2922060	1.25E+05	6	1.61E+05	1.19E-01	1.29
<b>Cr-48</b>	158665	7.81E+04	30	8.66E+04	3.61E-02	1.11
<b>Cr-49</b>	4173	3.14E+08	28	1.35E+08	3.04E-01	0.43
<b>Cr-51</b>	92043	1.42E+08	5	1.46E+08	4.63E+01	1.03
	158665	1.37E+08	5	1.43E+08	5.96E+01	1.04
	424416	1.27E+08	5	1.32E+08	6.05E+01	1.04
	2922060	6.00E+07	4	6.42E+07	4.72E+01	1.07
	13036200	3.31E+06	5	3.43E+06	5.40E+00	1.04
<b>Mn-52</b>	92043	1.13E+07	6	1.42E+07	4.51E+00	1.26
	158665	1.02E+07	5	1.30E+07	5.42E+00	1.27
	424416	7.13E+06	5	8.90E+06	4.06E+00	1.25
	2922060	1.73E+05	6	2.48E+05	1.82E-01	1.43
<b>Mn-54</b>	92043	1.80E+07	5	2.10E+07	6.67E+00	1.17
	158665	1.76E+07	5	2.10E+07	8.74E+00	1.19
	424416	1.78E+07	5	2.08E+07	9.52E+00	1.17
	2922060	1.65E+07	4	1.95E+07	1.44E+01	1.18
	13036200	1.27E+07	4	1.51E+07	2.37E+01	1.19
<b>Mn-56</b>	4173	4.08E+10	5	4.39E+10	9.85E+01	1.08
	18011	1.45E+10	5	1.56E+10	9.81E+01	1.08
	92043	5.71E+07	6	6.26E+07	1.99E+01	1.10
	158665	2.70E+05	11	4.36E+05	1.82E-01	1.61
<b>Fe-52</b>	92043	5.39E+05	22	2.11E+06	6.71E-01	3.92
	158665	1.09E+05	18	4.49E+05	1.87E-01	4.12
<b>Co-55</b>	92043	1.01E+06	22	2.83E+03	8.99E-04	2.80E-03
	158665	6.65E+05	9	1.36E+03	5.67E-04	2.05E-03
<b>Co-56</b>	158665	7.52E+05	8	4.75E+03	1.98E-03	0.01
	424416	7.20E+05	13	4.64E+03	2.12E-03	0.01
	2922060	5.74E+05	5	3.61E+03	2.65E-03	0.01
	13036200	2.04E+05	7	1.26E+03	1.99E-03	0.01
<b>Co-57</b>	2922060	3.91E+04	13	3.63E+04	2.67E-02	0.93
	13036200	3.69E+04	16	2.69E+04	4.24E-02	0.73

*Table 9 – F82H specific activity- Experimental and calculated results (continued)*

Isotope product	Cooling time	Experimental data		ANITA-IEAF calculation		C/E
		Specific activity	Uncertainty	Specific activity	Percentage of the total activity	
		s	Bq/kg	± %	Bq/kg	
<b>Co-58</b>	158665	1.74E+05	17	1.81E+05	7.56E-02	1.04
	424416	1.68E+05	28	1.79E+05	8.17E-02	1.06
	2922060	1.12E+05	7	1.35E+05	9.90E-02	1.20
	13036200	3.76E+04	18	4.29E+04	6.75E-02	1.14
<b>Co-60</b>	2922060	1.40E+04	16	5.03E+02	3.70E-04	0.04
	13036200	7.05E+03	30	4.83E+02	7.59E-04	0.07
<b>Ni-57</b>	158665	2.51E+05	24	2.46E+05	1.02E-01	0.98
<b>Tc-99m</b>	158665	4.57E+04	40	4.92E+04	2.05E-02	1.08
<b>Ta-182</b>	424416	1.31E+05	13	3.51E+04	1.60E-02	0.27
<b>Ta-183</b>	92043	1.05E+06	20	8.54E+05	2.71E-01	0.81
	158665	1.02E+06	18	7.69E+05	3.20E-01	0.75
	424416	7.88E+05	29	5.05E+05	2.31E-01	0.64
<b>Ta-184</b>	92043	7.10E+05	44	9.25E+05	2.94E-01	1.30
	158665	9.81E+04	52	2.12E+05	8.83E-02	2.16
<b>W-187</b>	92043	4.60E+06	17	1.87E+06	5.93E-01	0.41
	158665	2.83E+06	7	1.09E+06	4.55E-01	0.39

**Table 10 – V-alloy specific activity- Experimental and calculated results**

Isotope product	Cooling time	Experimental data		ANITA-IEAF calculation		C/E
		Specific activity	Uncertainty	Specific activity	Percentage of the total activity	
		Bq/kg	± %	Bq/kg	%	
	s					
<b>Ca-47</b>	417962	1.09E+06	18	7.32E+05	1.38E-01	0.67
	2254080	5.06E+04	15	2.85E+04	4.65E-02	0.56
<b>Sc-43</b>	5477	3.85E+07	26	1.33E+06	5.34E-02	0.03
<b>Sc-44</b>	5477	1.92E+07	21	2.82E+07	1.13E+00	1.47
	17189	1.62E+07	18	1.66E+07	8.44E-01	1.03
<b>Sc-44m</b>	417962	4.43E+05	28	3.94E+05	7.45E-02	0.89
<b>Sc-46</b>	5477	4.00E+06	72	4.55E+06	1.83E-01	1.14
	17189	6.05E+06	47	4.54E+06	2.31E-01	0.75
	90710	4.09E+06	27	4.51E+06	3.24E-01	1.10
	417962	4.97E+06	6	4.37E+06	8.26E-01	0.88
	2254080	4.40E+06	4	3.67E+06	5.98E+00	0.83
	13341780	1.47E+06	4	1.27E+06	7.69E+00	0.86
<b>Sc-47</b>	5477	4.87E+08	5	7.58E+08	3.05E+01	1.56
	17189	5.36E+08	5	7.37E+08	3.74E+01	1.38
	90710	4.46E+08	5	6.18E+08	4.44E+01	1.39
	417962	2.05E+08	5	2.83E+08	5.35E+01	1.38
	2254080	1.92E+06	7	3.56E+06	5.81E+00	1.86
<b>Sc-48</b>	5477	9.72E+08	5	9.79E+08	3.94E+01	1.01
	17189	1.04E+09	5	9.30E+08	4.72E+01	0.89
	90710	7.30E+08	5	6.72E+08	4.83E+01	0.92
	417962	1.70E+08	5	1.59E+08	3.00E+01	0.93
	2254080	3.08E+04	11	4.84E+04	7.90E-02	1.57
<b>V-48</b>	2254080	2.12E+06	4	1.47E+06	2.40E+00	0.69
	13341780	1.94E+04	24	5.62E+03	3.40E-02	0.29
<b>Cr-49</b>	5477	5.89E+07	15	4.54E+07	1.83E+00	0.77
<b>Cr-51</b>	5477	8.00E+07	37	6.56E+07	2.64E+00	0.82
	17189	6.98E+07	27	6.54E+07	3.32E+00	0.94
	90710	8.74E+07	16	6.40E+07	4.59E+00	0.73
	417962	6.16E+07	5	5.82E+07	1.10E+01	0.94
	2254080	3.55E+07	4	3.42E+07	5.58E+01	0.96
	13341780	1.38E+06	5	1.38E+06	8.36E+00	1.00
<b>Mn-52</b>	2254080	9.50E+03	25	1.54E+02	2.51E-04	0.02
<b>Nb-92m</b>	2254080	3.85E+04	10	3.56E+04	5.81E-02	0.93



Table 11 – V-pure specific activity- Experimental and calculated results

Isotope product	Cooling time	Experimental data		ANITA-IEAF calculation		C/E
		Specific activity	Uncertainty	Specific activity	Percentage of the total activity	
		s	Bq/kg	± %	Bq/kg	
<b>Ca-47</b>	412474	1.11E+06	18	4.49E+05	1.04E-01	0.40
	3100500	4.53E+03	36	3.88E+03	1.79E-02	0.86
<b>Sc-46</b>	412474	3.01E+06	8	1.78E+06	4.13E-01	0.59
	3100500	2.31E+06	4	1.38E+06	6.36E+00	0.60
	13146900	8.47E+05	4	5.26E+05	3.44E+00	0.62
<b>Sc-47</b>	4983	4.99E+08	5	6.54E+08	3.56E+01	1.31
	16396	4.80E+08	5	6.36E+08	3.97E+01	1.33
	90001	3.98E+08	5	5.34E+08	4.38E+01	1.34
	412474	1.84E+08	5	2.47E+08	5.73E+01	1.34
	3100500	2.08E+05	7	4.08E+05	1.89E+00	1.96
<b>Sc-48</b>	4983	9.38E+08	5	9.51E+08	5.17E+01	1.01
	16396	9.01E+08	5	9.04E+08	5.65E+01	1.00
	90001	6.56E+08	5	6.54E+08	5.36E+01	1.00
	412474	1.52E+08	4	1.58E+08	3.66E+01	1.04
<b>V-48</b>	412474	6.10E+06	4	3.77E+06	8.75E-01	0.62
	3100500	1.33E+06	24	9.78E+05	4.52E+00	0.74
	13146900	9.14E+03	33	6.30E+03	4.12E-02	0.69
<b>Cr-51</b>	412474	1.05E+07	10	3.67E+03	8.51E-04	3.49E-04
	3100500	4.33E+06	4	1.68E+03	7.78E-03	3.89E-04
	13146900	2.33E+05	11	9.18E+01	6.00E-04	3.94E-04
<b>Nb-92m</b>	3100500	6.53E+03	27	8.74E+03	4.04E-02	1.34

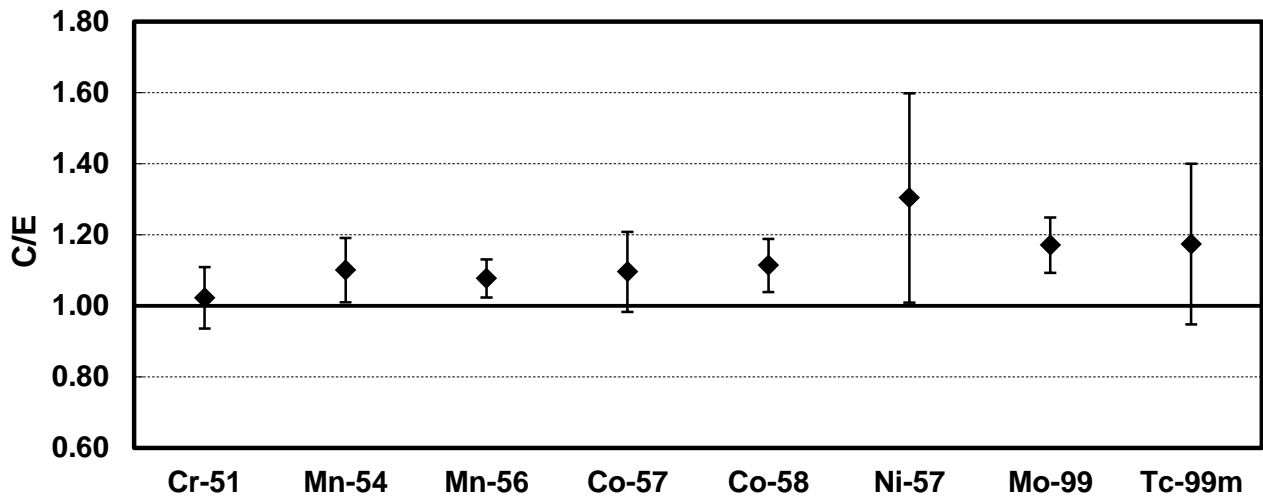


Figure 3 – SS-316 specific activity: calculation to experiment ratios (C/E). Main isotope contributors.

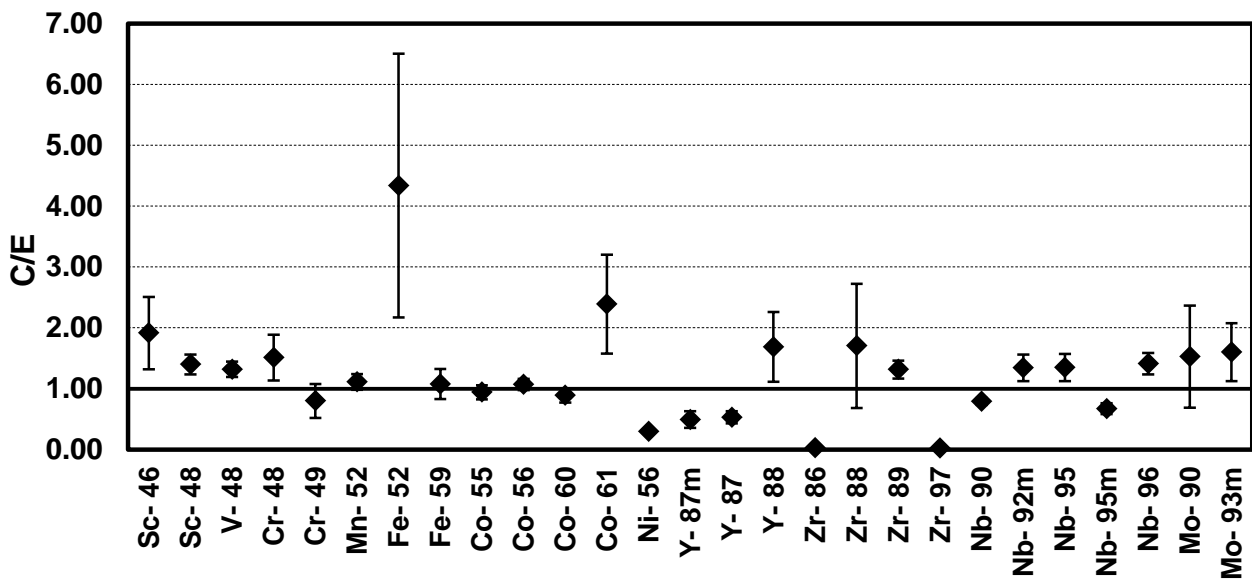


Figure 4 – SS-316 specific activity: calculation to experiment ratios (C/E). Other isotopes.

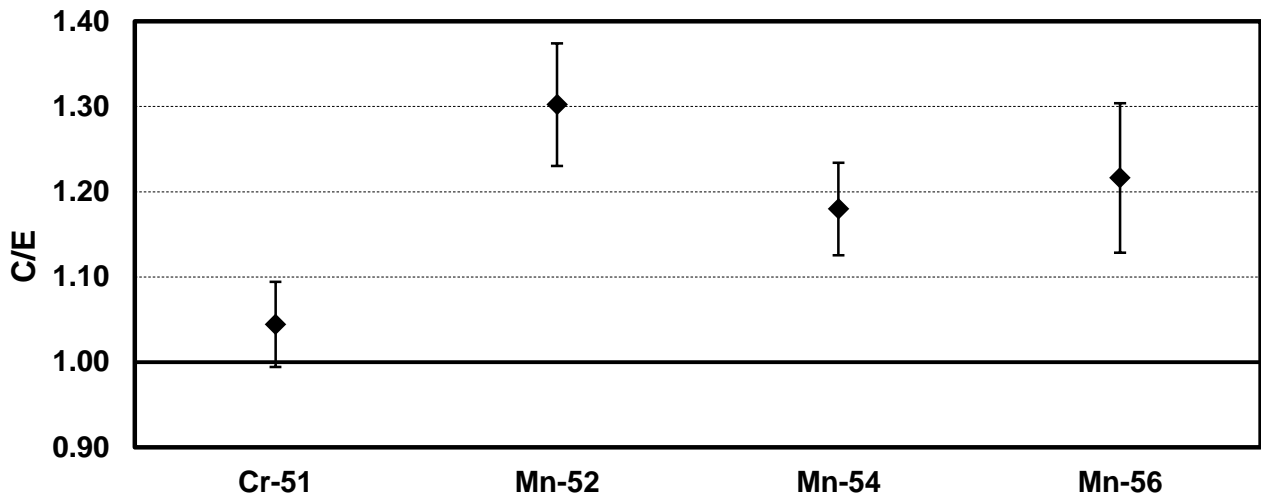


Figure 5 – F82H specific activity: calculation to experiment ratios (C/E). Main isotope contributors.

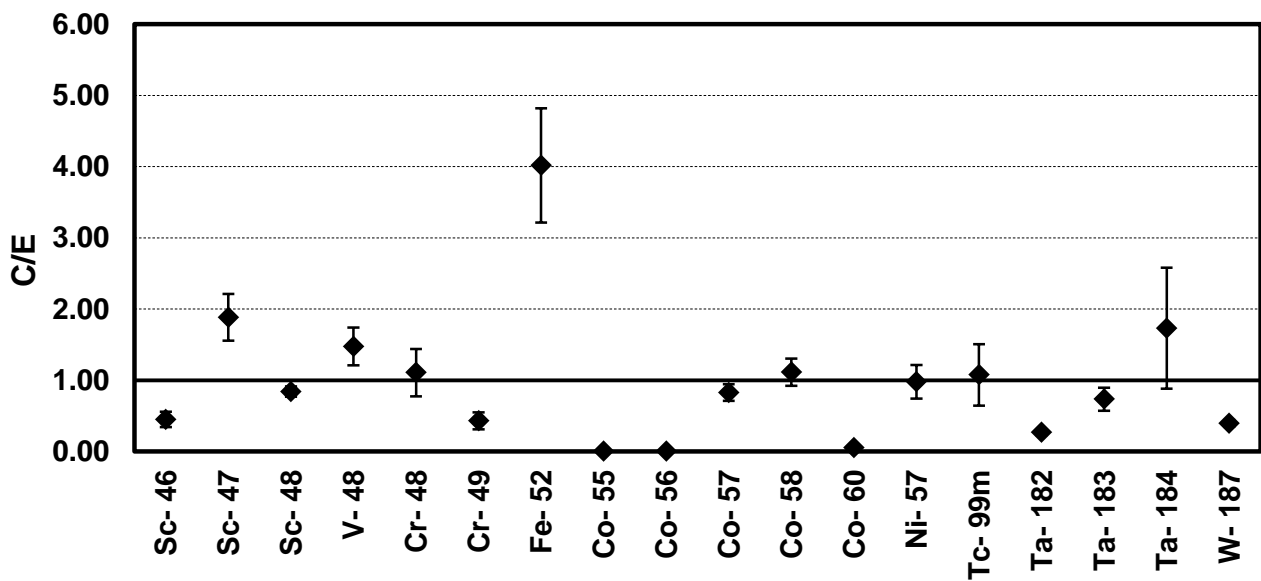


Figure 6 – F82H specific activity: calculation to experiment ratios (C/E). Other isotopes.

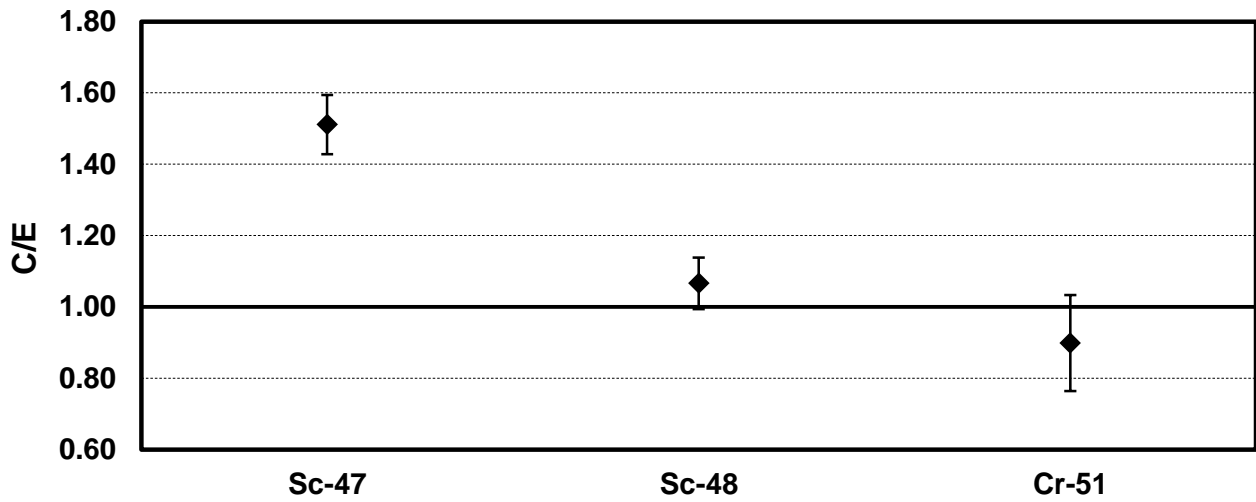


Figure 7 – V-alloy specific activity: calculation to experiment ratios (C/E). Main isotope contributors.

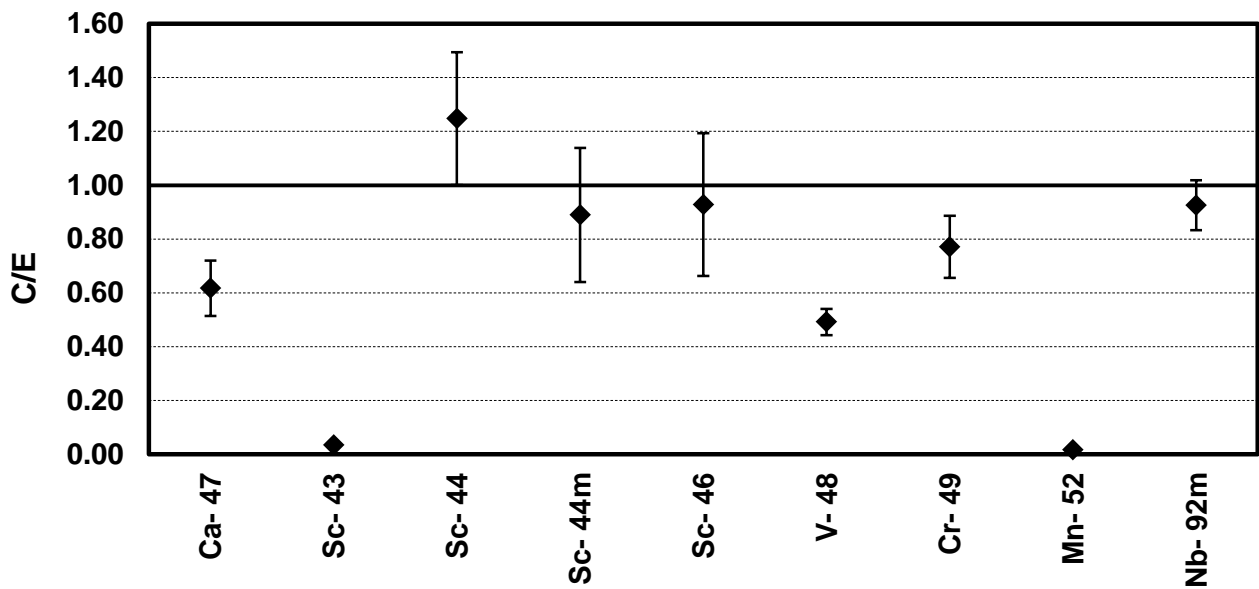


Figure 8 – V-alloy specific activity: calculation to experiment ratios (C/E). Other isotopes.

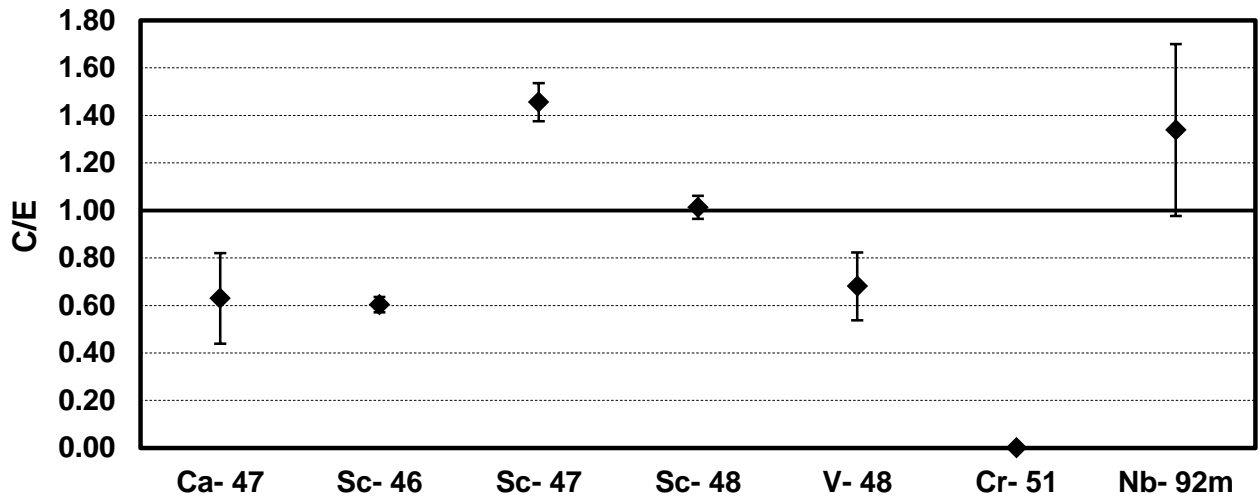


Figure 9 – V-pure specific activity: calculation to experiment ratios (C/E). All isotopes.

## 5.6 Results analysis

In this section the results analysis related to the comparison between the ANITA-IEAF predictions and the activity measurements obtained from the Karlsruhe Isochronous Cyclotron is presented. The comparison is performed for samples of two different steels, SS-316 and F82H, pure vanadium and a vanadium alloy.

From such a validation work the following detailed information can be drawn.

### SS-316

- For the irradiated SS-316 steel sample, 35 isotopes have been analyzed. Among the measured nuclides the main contributors to the total activity are: Cr-51, Mn-54, Mn-56, Co-57, Co-58, Ni-57, Mo-99 and Tc-99m. The corresponding C/E values are shown in Figure 3.
- Cr-51: is an important contributor, up to 50% , for all the cooling times considered. The agreement between experimental and calculated activities is quite good (discrepancies within 6%).
- Mn-54: its contribution is not relevant, 0.1%, in the first two hours of cooling time where the discrepancy is large (24%). The importance of Mn-54 increases up to 16.1% at the last cooling time considered. The corresponding C/E values show discrepancies within 20%.
- Mn-56: is the most important contributor to the total activity, from 65% to 78%, up to 6 hours of cooling time. The measured values and the ANITA-IEAF predictions, in terms of C/E, show a very good agreement. For all the cooling times the discrepancies are lower than 10%.
- Co-57: is an important activation contributor, up to 17.7% at 150 days of cooling time. The measured values and the ANITA-IEAF predictions, in terms of C/E, show a good agreement. For all the cooling times the discrepancies are lower than 15%.
- Co-58: this nuclide becomes significant after 1 day of cooling time; its contribution grows up to 22% after 29 days of cooling time. The C/E discrepancies are always within 15%.
- Ni-57: is an important product in the first 5 days (half-life $\approx$ 36h); its contribution increases from 1% at the first cooling time up to about 16% at 2.1 days. The discrepancies range from 24% to 42%.
- Mo-99: its contribution is about 4% from 1 to 5 days of cooling time. The C/E values show discrepancies up to 24%.
- Tc-99m: its contribution is about 4% in the range between 1 and 5 days of cooling time. For these times the C/E values show discrepancies within 25%. The largest discrepancies are found at the cooling times where its contribution is negligible.

- The average C/E values of Cr-51, Co-57, Tc-99m show a good agreement within the error bars. The discrepancies are within 20% for all the isotopes except for Ni-57. In general the calculations predict an overestimation of the experimental results.
- The other less important nuclides show larger discrepancies as, mainly, Sc-46 (C/E=1.91), Co-61 (C/E=2.39), Fe-52 (C/E=4.34), Zr-86 (C/E=0.03) and Zr-97 (C/E=0.02) (see Figure 4).

## F82H

- For the irradiated F82H steel sample, 22 isotopes have been analysed. The main isotope contributors to the total activity are: Cr-51, Mn-52, Mn-54 and Mn-56. The corresponding C/E values are reported in Figure 5.
- Cr-51: is an important contributor, up to 60%, for all the cooling times. The discrepancies between experimental and calculated activities are within 7%, showing a very good agreement.
- Mn-52: its contribution is relevant up to 5 days of cooling time; the discrepancies between experimental and calculated activities are large, up to 43%, showing an overestimation of the experimental results.
- Mn-54: its contribution increases from about 7% at the first cooling time up to 23.7% at 150 days. The corresponding C/E values show discrepancies up to 19%.
- Mn-56: is the most important contributor to the total activity, 98%, up to 5 hours of cooling time. For these times the C/E values show discrepancies within 10%. The largest discrepancy, about 60%, is found at the cooling time where its contribution is negligible (lower than 0.2%).
- the average C/E value of Cr-51 only shows a good agreement within the error bars with a discrepancy lower than 10%. The biggest discrepancy is found for Mn-52 (30%). In general the calculations predict an overestimation of the experimental results.
- The other less important nuclides show larger discrepancies as, mainly, Fe-52 (C/E=4.0), Co-55 (C/E=2.4E-03), Co-56 (C/E=0.01) and Co-60 (C/E=0.05) (see Figure 6).

## V-alloy

- For the irradiated V-alloy sample, 12 isotopes have been analyzed. The main isotope contributors to the total activity are: Sc-48, Cr-51 and Sc-47. The corresponding C/E values are reported in Figure 7.
- Sc-48: is the most important contributor to the total activity up to 5 days of cooling time. At these times the C/E values show a good agreement, discrepancies within 11%, between experimental and calculated results. The largest discrepancy, greater than 50%, is found at 26 days of cooling time where its contribution is negligible (lower than 0.1%).

- Cr-51: is an important contributor, up to 56%, for all the cooling times. The biggest discrepancy between experimental and calculated activities is found at 1 day cooling time where the discrepancy grows up to 27%. The calculated values are in general underestimate with respect to the experimental data.
- Sc-47: is an important contributor, up to about 54%, for all the cooling times considered. The discrepancies between experimental and calculated activities are up to 86%, showing an overestimation of the calculated results with respect to the experimental ones.
- The average C/E values of the previous nuclides show discrepancies within 20% except for Sc-47.
- For the other less important nuclides the major discrepancies are found for Sc-43 and Mn-52. All the experimental results are underestimated except for Sc-44 (see Figure 8).

### V-pure

- For the irradiated V-pure sample, 7 isotopes have been analyzed. The main isotope contributors to the total activity are: Sc-48, Sc-47 and Sc-46. The pure-Vanadium C/E values for all the isotopes are reported in Figure 9.
- Sc-48: is the most important contributor, up to 56%, to the total activity for all the cooling times considered. The C/E values show a very good agreement, discrepancies within 4%, between experimental and calculated results.
- Sc-47: is an important contributor, up to 57%, up to 5 days of cooling time. The agreement between experimental and calculated activities is rather poor. The calculated results show a general overestimation of the experimental values.
- Sc-46: contributes up to 6% to the total activity. The calculated activities show an underestimation, up to 40%, of the experimental ones.
- For the other nuclides the agreement between experimental and calculated activities is rather poor. In particular, for Cr-51, the calculated results show a huge underestimation of the experimental values.



## REFERENCES

- 
- [1] D.G. Cepraga, M. Frisoni, G. Cambi, ANITA-IEAF: a code package for performing fusion material transmutation and activation analysis induced by intermediate energy neutrons, *Fusion Engineering and Design* 69 (2003) 719-722.
- [2] U.Fischer, D.Leichtle,U.v.Mollendorff and I.Schmuck, ZZ-IEAF-2001, Intermediate Energy Activation File, NEA-1656/01.
- [3] D.G. Cepraga, G. Cambi, M. Frisoni, G.C. Panini, ANITA-2000, OECD NEA Data Bank NEA-1638, 22 November 2000.
- [4] D.G. Cepraga, G. Cambi, M. Frisoni, G.C. Panini, ANITA-2000, RSICC CCC-693, January 2002.
- [5] D.G. Cepraga, G. Cambi, M. Frisoni, ANITA-2000 Activation Code Package. Part I - Manual, ENEA ERG-FUS/TN-SIC TR 16/2000, November 2000.
- [6] D.G. Cepraga, G. Cambi, M. Frisoni, ANITA-2000 Activation Code Package. Part II : Code validation, ENEA FUS-TN-SA-SE-R-020, June 2001.
- [7] D.G. Cepraga, E. Menapace, A. Musumeci, G. Cambi, M. Frisoni, Validation of activation and decay data libraries with respect to integral decay heat experiments, EFF-DOC-654, JEFF/EFF/EAF Meeting, NEA Head Quarter, Paris, September 14-15, 1998.
- [8] D.G. Cepraga, G. Cambi, M. Frisoni, ANITA-2000 photon and electron decay heat validation based on FNG-Frascati experimental data and comparison with EASY-99 results, EFDA Task No. TW1-TSS-SEA5, Milestone 3, Final Report, ENEA FUS-TN-SA-SE-R-65, December 2002.
- [9] G. Cambi, D.G. Cepraga, M. Frisoni, L. Manzana, F. Carloni, M.L. Fiandri, Anita-2000 activation code package: clearance assessment of ITER activated materials, Proc. of the 19th Symposium on Fusion Engineering SOFE, Atlantic City, NJ, USA, January 22-25, 2002, pp. 44-47, IEEE Catalog No. 02CH37231C, ISBN 0-7803-7075-9 - U.S.A. 2002.
- [10] D.G. Cepraga, G. Cambi, M. Frisoni, D. Ene, ANITA-2000 activation code package development and validation. Part 2: a) Gamma source calculation with Anita-2000-D, b) Sn discrete ordinate method and MCNP dose rate calculation, c) Experimental-calculated results comparison, EFDA Task No. TW1-TSS-SEA5 Milestone D2, Final Report, ENEA FUS-TN-SA-SE-R-64, December 2002.
- [11] C. Ponti and S. Stramaccia, ANITA: Analysis of Neutron Induced Transmutation and Activation, EUR 12622 EN report, 1989.
- [12] J.-Ch. Sublet, L. W. Packer, J. Kopecky, R. A. Forrest, A. J. Koning and D. A. Rochman, The European Activation File: EAF-2010 neutron-induced cross section library, CCFE-R (10) 05.
- [13] EASY-2010 OECD NEA Data Bank NEA-1564/13, 16 December 2011.
- [14] M.A. Kellet, The JEFF-3.1.1 Decay Data Library, JEFDOC-1188, June 2007.
- [15] C. Ponti, Calculation of radioactive decay chains produced by neutron irradiation, EUR 9389, 1984.
- [16] ENDF-6 Formats Manual, Data Formats and Procedures for the Evaluated Nuclear data File ENDF/B-VI and ENDF/B-VII, CSEWG Document ENDF-102, Report BNL-90365-2009, Edited by M.Herman and A Trkov, June 2009.
- [17] J.K. Tuli, Nuclear Wallet Cards (8th Edition), National Nuclear Data Centre, October 2011.
- [18] L.W.Packer and J.-Ch.Sublet, The European Activation File: EAF-2010 biological, clearance and transport libraries, EASY Documentation Series, CCFE-R(10) 04, March 2010.
- [19] Application of the Concepts of Exclusion, Exemption and Clearance, IAEA Safety Standard Series No. RS-G-1.7, IAEA Vienna, 2004.
- [20] IAEA, Clearance levels for radionuclides in solid materials – Application of exemption principles, IAEA-TECDOC-855, IAEA, Vienna, January 1996.
- [21] R. A. Forrest, FISPACT-2007:User manual, EASY Documentation Series UKAEA FUS 534.

- 
- [22] U.von Mollendorff, F.Maekawa, H.Giese, H.Feuerstein, A Nuclear Simulation Experiment for the International Fusion Materials Irradiation Facility (IFMIF), FZKA 6764, October 2002.
- [23] M.Frisoni, ANITA-IEAF activation code package – updating of the decay and cross section data libraries and validation on the experimental data from the Karlsruhe Isochronous Cyclotron, presented at the 13th International Conference on Radiation Shielding (ICRS-13) & 19th Topical Meeting of the Radiation Protection & Shielding Division of the American Nuclear Society -2016 (RPSD-2016), 3-6 October 2016, Paris, EPJ Web of Conferences 153, 07002 (2017)